PETROCHEMICAL CHARACTERIZATION OF DOLERITES AND THEIR INFLUENCE ON COAL IN THE WITBANK HIGHVELD COALFIELD, SOUTH ARICA

By

Johannes Jochemus du Plessis

DEGREE OF MASTER OF SCIENCE

In the faculty of Natural Science,
University of the Free State,
Bloemfontein,
South Africa

August 2008

Supervisor: Prof. W.A. van der Westhuizen

ABSTRACT

A study was firstly conducted on the mineralogy and geochemistry of the dolerites, secondly on sedimentological controls (syngenetic) on coal deposition and diagenesis to gain a better understanding of the environment of the coal deposition and thirdly, the metamorphic influence of dolerite intrusions (epigenetic) on coal. The Ogies Dyke is the only intrusion found in the study area at Optimum Colliery. The absence of dolerite sill intrusions in this area made it possible to study coal deposition and diagenesis. It was to investigate the behaviour of a 20m thick bifurcating dolerite sill (the Witbank sill) and its associated metamorphic influence which occurs in the other Koornfontein, Bank and Goedehoop Collieries. The most prominent structure, the Ogies Dyke, forms the northern limit of the study area and forms a very important part of the geochemical and mineralogical study.

Thin section investigations revealed the involvement of plagioclase in both the Witbank and Sasolburg dolerite fractionation assemblages indicates that the fractionation processes must have occurred within the crust although within different depths. The absence of pyroxene phenocrysts in the B5 sill (Sasolburg) indicates that the fractionation took place at a pressure significantly higher than that at which the plagioclase and olivine microphenocrysts have formed. The high percentage olivine in the B4 sill (Sasolburg) indicates that these two sills originated from different magma sources. Plagioclase microphenocrysts in the B5 sill as oppose to the macrophenocrysts of the B4 sill concludes that the fractionation processes of the B5 sill must have happened deeper within the crust.

This study engage with dolerites that crystallised rapidly, intermediately and slowly as the crystal sizes are directly related to magma cooling. Fine crystalline dolerites like the chilled margins and bifurcations tend to be more susceptible for alteration as opposed to the medium and coarse crystalline dolerites. The 40m thick, fine crystalline B4 sill has undergone the most alteration comparing to the B5 sill, Witbank sill and the Ogies Dyke. The differences identified during this study distinguish the Sasolburg dolerites from the Witbank sill and the Ogies Dyke.

X-ray fluorescence techniques were used to analyse the dolerite samples from the study area. All the dolerites are falling in the “basic” group. The B4 – Sasol dolerite sill is a high-MgO (picritic) basalt while the rest are basalts. The chilled margins of the bifurcations have an arithmetic mean of 4.89% MgO and the Ogies Dyke has 4.9% MgO and can be classified as evolved basalts. Lower MgO and Ni values in the Witbank bifurcations comparing to the Witbank sill indicate that the bifurcations are more evolved.

The basaltic and evolved basalts can further be divided into low and intermediate K_2O concentrations. A higher K_2O concentration is placing the Ogies Dyke in the intermediate-K_2O group whilst the Witbank sill (interior and chilled margins), and the Witbank bifurcations (interior and the chilled margins) are all falling in the low-K_2O group. Two of the Witbank bifurcations (interior) having intermediate-K_2O concentrations and are associated with the Ogies Dyke. The picritic B4 sill (Sasol) is also classified as a low- K_2O dolerite. Considering K_2O and MgO element concentrations the samples are falling in three categories, from evolved to picritic with the majority in the basaltic field.

Borehole information was used to conduct isopach and isopleth maps of the pre-Karoo topography, floor elevation and thickness distribution, coal parameters and statistical data of various coal seams to underpin the sedimentological controls (syngenetic) on coal deposition and diagenesis The undulated platform onto which the No. 2 Upper Coal Seam formed at the Optimum study area had a major influence on coal grade. Thicker coals were deposited in the lower lying areas while they were thinning towards palaeohigh areas. Significant values indicate that the thinner coals are higher in ash (air-dry), lower in VM (daf), lower in CV MJ/kg (air-dry) and higher in relative density comparing to the coals deposited in the lower lying areas of the palaeovalley.

Lithological descriptions from boreholes and structural interpretations in geological cross-sections revealed the presence of a green 20m thick, bifurcating dolerite sill that intruded into the Vryheid formation of the Karoo Supergroup. It is associated with ±20m displacement and metamorphism on coal which is putting major constraints on coal mining in general.

The metamorphic influence of the coal is largely restricted to the width of the contact aureole. The nature of the aureole depends on the geometry, variation in thickness and bifurcation of the sill. It is also found that the metamorphic contact aureole is much more extensive in the displaced and uplifted coal seams comparing to those beneath the sill.

Moisture (ash-free) of the proximate analyses, volatile matter (daf), CV (daf) and approximated ash yield (AD) isopleth maps show that the dolerite sill caused a localised increase in rank. Areas of high moisture (proximate analyses moisture content) correspond to devolatilised areas, which are higher in ash and therefore having lower CV’s and are adjacent to known intrusions.

TABLE OF CONTENTS

CHAPTER 5

LIST OF FIGURES

CHAPTER 1

CHAPTER 2

CHAPTER 3

CHAPTER 4

CHAPTER 5

LIST OF TABLES

CHAPTER 1

CHAPTER 3

CHAPTER 4

CHAPTER 5

CHAPTER 1

INTRODUCTION

1.1 How this work fits into Coaltech 2020

Coaltech 2020 is a collaborative research programme among various coal owners in South Africa which is aimed at providing the needed technology that should improve productivity and reduce the costs of coal mining in general (Beukes, 2000).

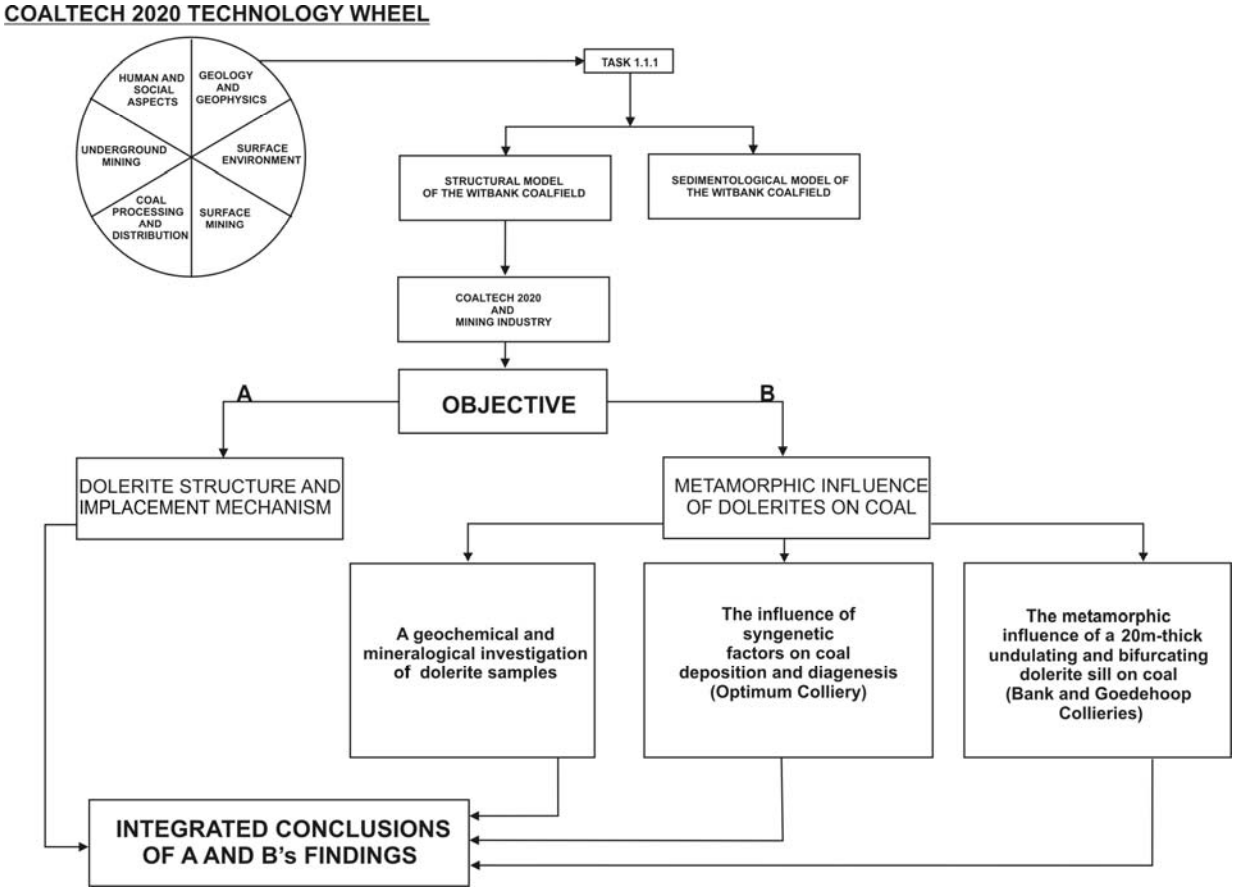

Figure 1.1 ***A flow diagram that indicates how the structural analysis of dolerite intrusions in the Witbank Coalfield fits into Coaltech 2020, and more specifically, the 3 stages followed in this work, which is B, to quantify the metamorphic influence of the dolerite intrusions on coal.***

The Coaltech 2020 Research Programme comprises a technological wheel which is grouped into six project areas, i.e. geology and geophysics, underground mining, surface environment, coal processing and distribution, surface mining and human and social aspects (Figure 1.1).

The focus of the Geological and Geophysical Working Group is on the Northern Witbank-Highveld Coalfield. The main objective of this working group is to concentrate on the remaining resources and reserves by evaluating critical geotechnical factors associated with previously mined areas, which could affect the potential exploitation of the remaining reserves and to improve 2D seismic surveys to the point where these will become an essential feature in coal-mine planning and the selection of optimal mine layouts (Beukes, 2000).

An integrated sedimentological and structural project (A and B in Figure 1.1) was planned to facilitate the identification of geological features that have an impact on mining and constitutes Task 1.1.1 of the Geological and Geophysical working group (Figure 1.1). As dolerite intrusions are merely the structures with which coal mining in the south-eastern Witbank Coalfield are confronted, a need existed to investigate the metamorphic influence of such magmatic intrusions on coal (B in Figure 1.1). To address this need, a methodology comprising three stages was followed, i.e.:

1. A mineralogical and geochemical investigation was performed on dolerite samples that were collected during underground mine visits at the Bank, Goedehoop and Koornfontein Collieries (chapter 3).
2. A dolerite-free area was selected in order to investigate the influence of syngenetic factors on coal deposition and diagenesis (study area at Optimum Colliery) (chapter 4).
3. An area where a 20m thick dolerite sill displaced and uplifted coal seams was investigated with geochemical and mineralogical techniques in order to quantify its associated metamorphic influence on coal rank (study areas at Bank, Goedehoop and Koornfontein Collieries) (chapter 5).

The above three stages were followed by an integration between A and B's findings as they are inseparable. Throughout A and B various aspects reinforced each other, and their findings together will conclude the structural part of Task 1.1.1 of the Geological and Geophysical Working Group, Coaltech 2020.

This structural project is aimed at casting light on the geometry, intrusion mechanism and metamorphic influence of dolerite intrusions in the south-eastern part of the Witbank Coalfield.

1.2 General geology

Coal deposits in the Witbank Coalfield occur within the Vryheid Formation, Ecca Group, Karoo Supergroup. The Vryheid Formation is described as consisting essentially of sandstones, shales and subordinate coal beds (Table 1.1).

Coal deposition in the Witbank Coal Basin was mainly controlled by the undulating glaciated Pre-Karoo topography (Smith, 1990). Thicker peat accumulations were developed in the deeper basins, while thinner accumulations occur in smaller subsidiary basins (Smith, 1990). The seams that are normally found in the Witbank Coal Basin are numbered 1, 2, 3, 4 and 5. Coal seams normally thin out towards smaller palaeo-ridges and eventually pinch out against main palaeohighs (Smith, 1990).

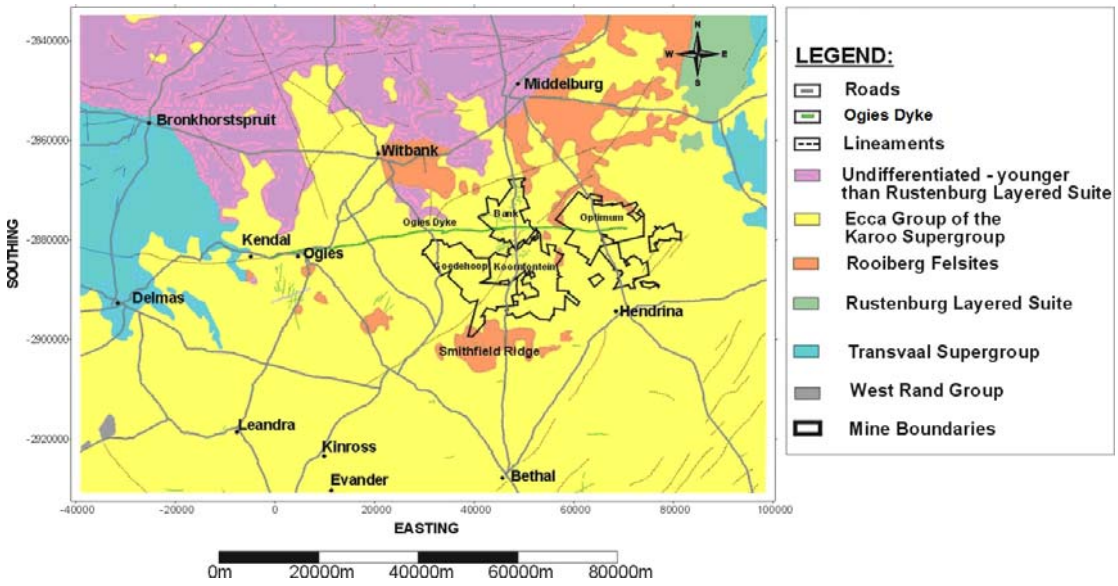

Figure 1.2 Geological and geographical setting of study area (modified from Henckel, 2001).

During the initial stages of Gondwana fragmentation, dolerite dykes and sills intruded the Karoo Supergroup (White, 1997). In the Witbank Coalfield, the sediments occurring above dolerite sills were displaced and uplifted in the direction of dip approximately equal to the thickness of the dolerite. Therefore, sediments occurring underneath the sills remain undisturbed. Dolerite dykes in the Witbank Coalfield are caused with minimal vertical displacement.

The heat emanating from these intrusions (Jurassic Times, Table 1.1) accelerated metamorphism and depleted the volatile constituents of the coal seams. A simplified stratigraphic column for the Karoo Supergroup in the northern portion of the main Karoo basin is presented in Table 1.1.

Table 1.1 Simplified stratigraphic column of the Karoo Supergroup in the northern portion of the main Karoo basin (SACS, 1980).

Period (Age)	Group	Formation	Rock Types
Jurassic (150 my)		**Drakensberg**	**Basaltic lava**
Triassic (195 my)		Clarens	Fine-grained sandstone
		Elliot	Red sandstone, mudstone
		Molteno	Sandstone, subordinate coal
Permian (225 my)	Beaufort	Tarkastad	Sandstone, shale
		Estcourt	Sandstone, shale, subordinate coal
	Ecca	Volksrust	Shale, sandstone, subordinate coal
		Vryheid	**Sandstone, shale, coal**
		Pietermaritzburg	Shale
Upper Carboniferous (285 my)		Dwyka	Tillite, varved shale

1.3 Pre-volcanic period

Prior to Karoo volcanism, a long period of marginal and yoked basin sedimentation that lasted from the Upper Carboniferous through to the early Jurassic, formed the Karoo Basin (Eales *et al*., 1984).

The basement of this sedimentary succession consists of various rock formations of varying ages over much of southern Africa (Eales *et al*., 1984). The succession records a sedimentary sequence with a palaeo-climatical change from glacial through temperate to dry desert (Cadle *et al*., 1993). The base of the sedimentary rocks represent a Permo-Carboniferous glaciation (Dwyka Tillite Formation) followed by a yoked basinal and marine phase (Ecca Group), and finally by a period of terrestrial sedimentation with increasing aridity (Beaufort Group, Molteno, Elliot and Clarens Formations) (Tankard *et al*., 1982).

Remnant glacial valleys, formed by the northward retreat of Dwyka ice sheets, reflect the major directions of ice movement (Tankard *et al*., 1982). These features of the pre-Karoo topography controlled the later sedimentation and to some extent, peat deposition (Cairncross and Cadle, 1987).

The coal deposits of the Karoo Basin in South Africa are contained within the 80-250 m thick coarse fluviodeltaic sequence designated the Vryheid Formation, which constitutes part of the Ecca Group of the Karoo Supergroup (Cairncross, 1989). Several mineable seams of bituminous coal, anthracite and torbanite are present in the Vryheid Formation (Cairncross, 1989).

The Vryheid Formation is a deposit of facies that hosts the main coal seams in the different coalfields of South Africa (Cadle *et al*., 1993). This sedimentary succession was deposited during the Early Permian following the Late Carboniferous Dwyka ice age. Plant assemblages of the Early Permian attest to a cool, temperate climatic regime. In the northern parts of the basin, the lowermost coal seams sometimes directly overlie the Dwyka diamictite or Pre-Karoo basement (Cairncross, 1989). Coal associated with the above glaciogenic succession consisted predominantly of regressive fluviodeltaic facies assemblages (Cairncross, 1989).

The coalfields in the northern and northeastern parts of the main Karoo Basin are restricted to a stable tectonic setting suitable for peat accumulation (Cairncross, 1989).

1.4 Structural background

During the Jurassic period dolerite dykes and sills intruded the Karoo Supergroup during a period of extensive magmatic activity that took place over almost the entire South African subcontinent during the initial stages of Gondwana fragmentation (Chevallier et al., 2001). These dykes and sills represent the roots and feeders of the extrusive Drakensberg Formation that are dated ± 180 my during (Duncan et al., 1997; Fitch and Miller, 1984 and Richardson, 1984), and this is one of the largest outpourings of flood basalt in the world.

Dolerite dykes and sills are the localised intrusive features of this magmatic episode in the Witbank Coalfield. The most prominent magmatic feature is the Ogies Dyke (± 15m - thick), which has an east-west strike from Ogies in the west to the Optimum and Arnot Collieries in the east (Smith, 1990). Du Plessis (2001) found that dolerite sills are absent north of the Ogies Dyke, even though dolerite dykes appear to be a common feature of the area, south of the Ogies Dyke where only sills with dyke and sill-like bifurcations are present. It was also found that the major dolerite sill (20m thick) in the

south-eastern part of the Witbank Coalfield transects the sedimentological units (Du Plessis, 2001).

1.5 Study objective

The objective of this work was first to understand the mineralogy and geochemistry of the dolerites, secondly to gain a better understanding of the environment of the coal deposition i.e. the sedimentological controls (syngenetic) on coal deposition and diagenesis, and thirdly, the metamorphic influence of dolerite intrusions (epigenetic) on coal.

The Ogies Dyke is the only intrusion found in the study area at Optimum. The absence of dolerite sill intrusions in this area made it possible to study coal deposition and diagenesis. Another aim was to investigate the behaviour of a 20m thick bifurcating dolerite sill and its associated metamorphic influence which occurs in the other Koornfontein, Bank and Goedehoop Collieries. The most prominent structure, the Ogies Dyke, forms the northern limit of the study area and forms a very important part of the geochemical and mineralogical study of this work.

The main ***objective*** of this work is to synthesize interpretations from subsurface data in order to fingerprint the behaviour of dolerite intrusions and its associated metamorphic influence on coal.

CHAPTER 2

METHODOLOGY

2.1 Selection of study areas

Four collieries were selected in the south-eastern part of the Witbank Coalfield. The Koornfontein and Goedehoop Collieries are the southern-most collieries, and are located just north of the so-called Smithfield Ridge, a palaeohigh mainly of Bushveld felsitic rocks, which forms the divide between the Witbank and Highveld Coalfields (Figure 1.2) (Smith, 1990). The Bank and Optimum Collieries are positioned further to the north while the Optimum Colliery forms the eastern limit of the selected area (Figure 1.2). The major Ogies Dyke, which strikes east-west for ~ 100 km, cuts through the Bank and Optimum Collieries (Smith and Whittaker, 1986).

During a visit to each colliery, an area "to be investigated" was selected in consultation with the mine geologist. The areas that were selected at Bank, Koornfontein and Goedehoop Collieries were based on the presence of complex dolerite structures. Mined-out areas allowed sampling of dolerite and thermally altered coal. The Optimum Colliery were selected due to the presence of the Ogies Dyke and also to investigate the influence of the sedimentary environment on the coal distribution and quality i.e. grade and type.

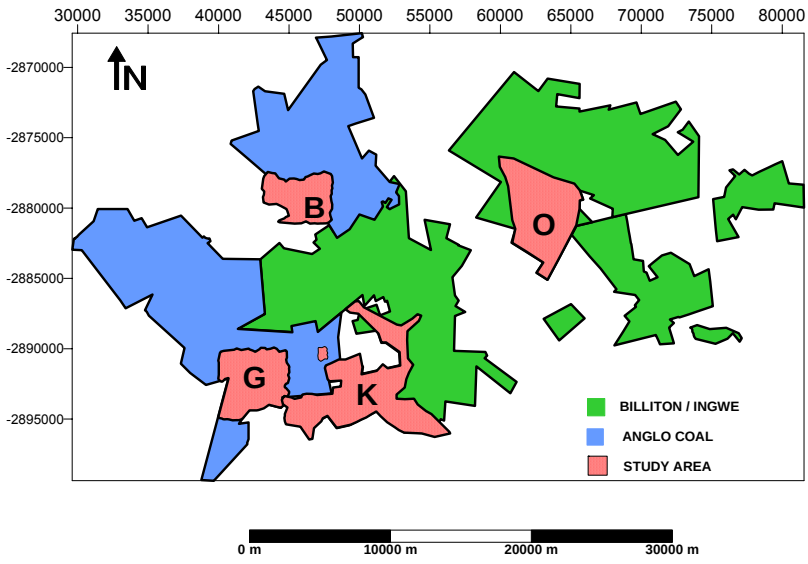

Figure 2.1 Map showing the 4 areas selected for this study where B=Bank, G=Goedehoop, K=Koornfontein and O=Optimum Collieries.

2.2 Data acquisition from study areas

The main sources of data for these studies is borehole logs and air-dry raw coal analysis from ±1551 boreholes that were drilled in the study areas and indicated in Figure 2.1. Some of the boreholes are several decades old, while the most recent ones were drilled early in 2001. Only a few of the boreholes penetrated the pre-Karoo basement as drilling was normally stopped at the base of the No. 2 Coal Seam.

The Borehole data comprise of:

1. LO29 coordinates are transposed and a constant of –1 applied to the X and Y values.
2. Collar elevation.
3. Lithological descriptions.
4. Air-dry raw coal analyses.

All these data were received in electronic format on compact discs from the mines (air-dry raw coal analyses were in spreadsheet (MS Office X-Cell) format and borehole lithology descriptions in text format).

Borehole data were used to establish depositional models for the different study areas. North-south, east-west geological cross-sections have been drawn by Du Plessis (2001) over principal areas in order to understand the geometry of dolerite sills and also its intrusion mechanism. A vertical scale of 1:1000 and horizontal scale of 1:667 were used for the construction of the geological cross-sections (Figures. 4.4; 4.18; 4.22; 4.26; 4.30 and 4.38) Geological cross-sections revealed a better understanding of the spatial relationship of coal seams and dolerite sill structures. It also shed light on areas where coal seams show devolatilisation.

To investigate the metamorphic influence of dolerite intrusions, samples of the main sill, bifurcations and coal in the contact aureole were collected at selected localities to investigate their relationship with the extent of coal metamorphism and coal seam displacement. Underground intersections of the Ogies Dyke were inaccessible due to flooding. A road cut between the towns Middelburg and Bethal exposed the Ogies Dyke, and allowed sampling. Dolerite sampling was carried out mainly to perform mineralogical and geochemical characterisation and to compare with the results of

analysis performed on various other dolerites in the South African coalfields. Samples of the No. 2 Coal Seam (1 bench) adjacent to dolerite intrusions, were collected to investigate the metamorphic influence on the inorganic geochemistry and mineralogy of thermally altered coal. A visit to the Koornfontein Colliery coincided with exploration drilling and enabled borehole core sampling.

2.3 Lithological descriptions based on boreholes.

Lithological descriptions were used to draw geological cross-sections whilst the proximate analyses, calorific values and relative densities of coal seams supplemented the structural interpretation of the dolerite sill.

2.4 Air-dry raw coal analyses

Raw coal analyses on an air-dry basis comprise proximate analyses (in percentages), calorific values (in MJ/kg) and relative densities. The proximate analysis is expressed in terms of volatile matter (VM), ash, moisture and fixed carbon of air-dry coal. Proximate analyses are carried out on a routine basis in most coal laboratories. All the values are reported to the nearest 0.1%.

The values of many coal parameters are not absolute, but are empirically determined under standard conditions specified by institutions such as the SABS (South African Bureau of Standards) and ISO (International Organisation for Standardisation) (Snyman, 1998). To obtain comparable values, it is necessary to adhere strictly to the conditions specified for the determination of various coal parameters (Snyman, 1998).

Moisture content is the percentage mass loss of air-dry coal when heated at temperatures between 105–110ºC. All coals are porous, irrespective of the compression and compaction they had undergone during burial (Snyman *et al*., 1983). Pores vary in diameter, and are accessible to molecules of water vapour and gas such as methane. H_2O molecules are readily absorbed on internal and external coal surfaces (Snyman *et al*., 1983). A distinction must be made between free (surface) moisture and inherent moisture of coal (Snyman *et al*., 1983):

a) surface moisture is present on the external surfaces of coal, or in the joints, and

b) inherent moisture occurs in the pores of coal.

For proximate analysis, the moisture content is determined on air-dry coal, and is regarded as the inherent moisture (Snyman et al., 1983). Changes in relative humidity will cause changes in the inherent moisture content and will also influence calorific value, other values of the proximate analyses and the ultimate analyses (Snyman et al., 1983).

The possible influence of clay minerals should be kept in mind when the inherent moisture content is considered as a parameter for coal characterisation as it also depends on mineralogical composition and mineral matter (Snyman et al., 1983).

Ash content of coal is the solid residue remaining after complete combustion. A small proportion is derived from the original inorganic mineral matter present in the biomass (Snyman et al., 1983). Mineral phases present in coal mainly comprise quartz, clay minerals (kaolinite, illite and also interstratified illite and montmorillonite), carbonate minerals (calcite, dolomite, siderite and ankerite) and sulphides (pyrite and marcasite) (Snyman et al., 1983). With the exception of quartz, all these minerals are decomposed during high temperature combustion (Snyman et al., 1983).

To determine ash content, a sample of air-dry coal is heated in air to 500ºC and then to 815ºC at a specified rate and maintained at this temperature until constant mass is attained (Snyman et al., 1983). This two-stage heating cycle allows dissociation of sulphide minerals and venting of sulphur compounds before carbonate minerals lose carbon dioxide; otherwise, SO_3 will be returned in the ash as calcium sulphate.

Volatile Matter in coal is driven off when air-dry coal is heated at 900ºC for 7 minutes, under standard conditions, in the absence of air (Snyman et al., 1983). Organic VM consists mainly of tar, light oils and hydrocarbon gases, containing variable amounts of oxygen, nitrogen and sulphur, derived from the decomposition of the organic substance of coal (Snyman et al., 1983).

At the high temperatures specified for the test, all the clay minerals present in the coal lose their hydroxyl groups in the form of H_2O vapour; carbonate minerals dissociate into carbon dioxide and the appropriate basic oxides, while pyrite loses some of its sulphur in the form of sulphurous gas (Snyman et al., 1983). Strictly speaking, the VM content should therefore be corrected for the contribution of the inorganic volatiles (Snyman et al., 1983). Such a correction requires an accurate estimate of the mineral matter, which

is normally not available. Dissociation of inorganic minerals contributes from 5% for low-ash highly-volatile coal to about 60 % for low-ash, low-volatile coal to the VM content (Snyman et al., 1983).

Calculation of the ***fixed carbon*** content of coal requires the prior determination of its moisture, ash and volatile matter contents. Fixed carbon equals the sum of the moisture, ash and volatile matter contents subtracted from 100 (Snyman et al., 1983).

To determine the ***calorific value*** (CV), a known mass of air-dry coal is burned under standard conditions in an oxygen atmosphere contained in a bomb (Snyman et al., 1983). CV of coal is determined by the temperature rise of the water in the calorimeter vessel, and the mean effective heat capacity of the system (Snyman et al., 1983). The results are expressed in megajoules per kilogram of coal.

Interrelationships between some of the coal properties discussed above are illustrated by means of a Seyler diagram (Figure 2.2).

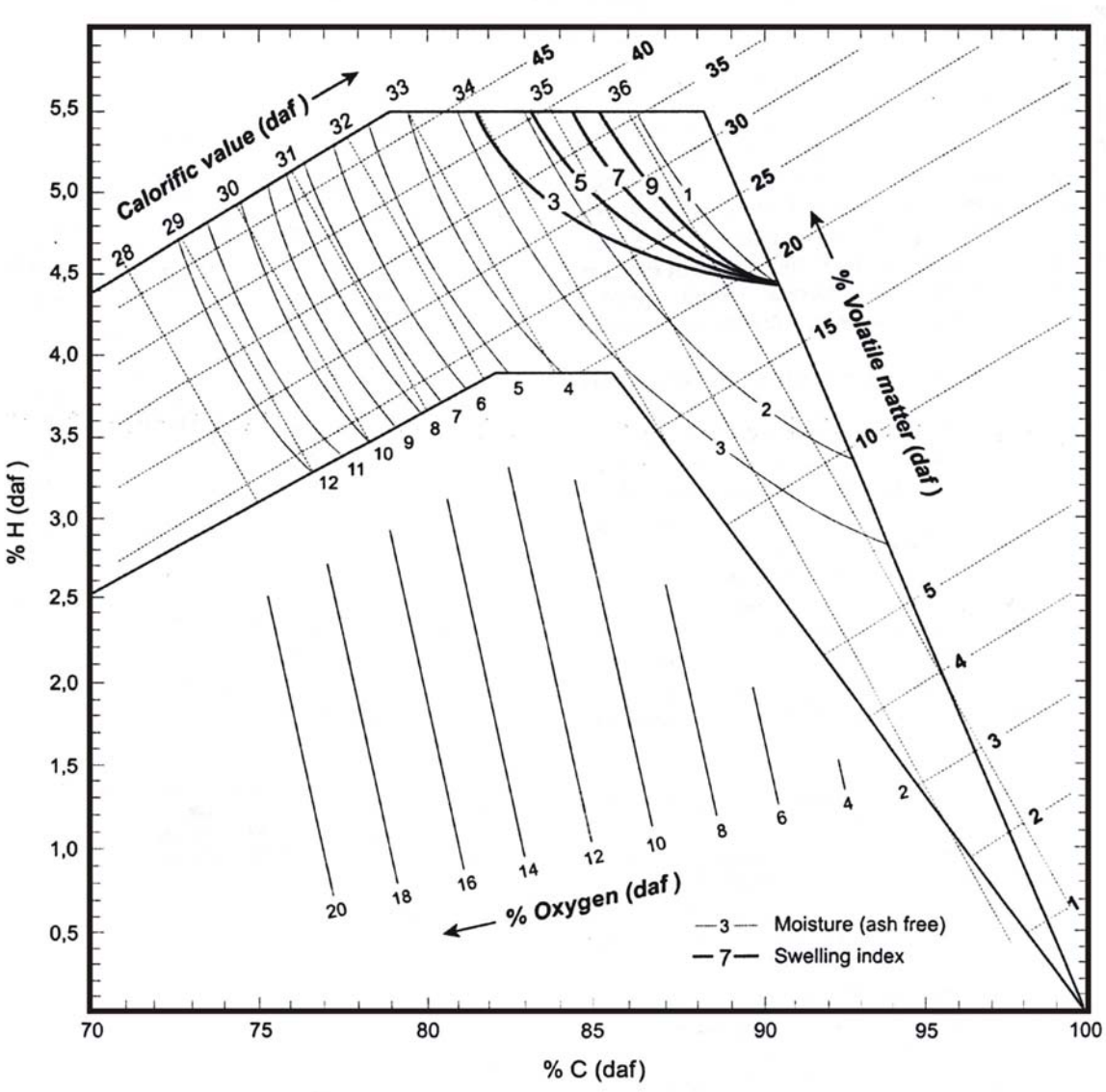

Figure 2.2 The Seyler diagram that illustrates interrelationships of coal properties adapted for South African humic coals (Snyman, 1996).

2.5 Data assimilation and presentation

Borehole data and raw coal analyses needed to be assimilated and integrated into a meaningful database. Normally coal properties like CV (MJ/kg) (air-dry) and VM (air-dry) ***(K in equation 1)*** are calculated on a dry ash-free (daf) and moisture (air-dry) ***(K in equation 2)*** on an ash-free basis, i.e.

1) $K_{(daf)} = (K \times 100) \div (100 - \%\ moisture - \%\ ash)$

2) $K_{(ash\text{-}free)} = (K \times 100) \div (100 - \%\ ash)$

Each proximate analysis (air-dry basis) was received with a CV and a relative density. As the proximate analysis is made up of moisture, VM, ash and fixed carbon, the proportion relative density (using equation 3) and CV (using equation 4) for each can be calculated i.e.

3) Relative density (M) = (M ÷ 100) × relative density (of the raw coal analysis)

4) CV (M) = (M ÷ 100) × CV (of the raw coal analysis)

Where *M* = air dry VM, ash, moisture and CV.

This sampling method necessitated the calculation of the weighted average for various coal parametres illustrated in the following equation where numbers 1 and 2 indicate sample units:

6) Weighted Average (N) =

$$((\text{thickness}_1 \times \text{relative density}_1 \times N_1)+(\text{thickness}_2 \times \text{relative density}_2 \times N_2)) \div ((\text{thickness}_1 \times \text{relativedensity}_1)+(\text{thickness}_2 \times \text{relative density}_2))$$

In equation 6, $N_{1 \text{ and } 2}$ equal a specific air-dry raw coal parameter and Weighted Average (N) the recalculated (air-dry or daf basis) parameter.

Data from the raw coal analyses, the seam thickness and elevations were imported and processed using Surfer 7. Statistical analyses of the processed data were carried out using Surfer 7. Isopach and contour maps were produced using Kriging as the gridding method. Kriging is a geostatistical gridding technique that has proven useful and is popular in many fields. This method produces visually appealing maps from irregularly spaced data. Kriging attempts to express trends so that, for example, high points might be connected along a ridge rather than isolated by bull's-eye type contours. Kriging is a very flexible gridding method. It accepts the kriging defaults to produce an accurate grid of the data. Within Surfer, kriging can be an exact interpolator, depending on the specified parameters. It incorporates anisotropy and underlying trends in an efficient and natural manner.

2.6 Coal parameters

Coal can be classified independently in terms of grade, type and rank. Briefly, ***grade*** of coal is related to the quantity of inorganic material accumulated during the depositional stage of coal formation when clastic material were deposited simultaneously with plant material; ***type*** of coal is determined by the nature of the original plant material and the degree of alteration during the diagenetic stage of coal formation while the ***rank*** of coal is the degree of metamorphism after burial by younger sediments. Hence the increase in rank is quite often accelerated by igneous intrusions that partially carbonised the coal (Snyman, 1998).

Maceral composition (type) depends on the environmental conditions during peat deposition, while carbon content, CV and VM content are partly dependent on the maceral composition, and partly on both the degree of regional coalification and local metamorphism by igneous intrusions.

Only the No. 2 and 4 Lower seams were utilized for this study, as they are the only seams extending over the entire study area. However, the No. 4L Coal Seam is poorly developed in some of the areas and was therefore omitted. Various recalculated and other air-dry parameters are used to determine the rank of the above-mentioned coal seams in thermally altered as well as non-thermally altered areas.

2.7 Sampling of dolerite

A total of 26 samples of dolerite sills, dyke and sill-like bifurcations from major sills were collected during mine visits to the Bank, Goedehoop and Koornfontein Collieries in the southeastern part of the Witbank Coalfield. A road cutting between Middelburg and Bethal exposed the Ogies Dyke where it was sampled. Dolerite samples for comparison (the B4 and B5 dolerite sills which will be discussed in Chapter 3) were also collected during a visit to the Block 13 exploration project of SASOL.

Dolerite bifurcations sampled vary from 1.5m to 3m in thickness. The 20m-thick sill was sampled at the Goedehoop and Bank Collieries. Unfortunately, the underground workings did not allow ideal sampling, for example, the 20m thick dolerite sill could only be sampled at one chilled margin as well as the bulk of the sill.

Sampling was conducted in a manner to minimize contamination – weathered surfaces were kept to a minimum. Sample powders were prepared at the Department of Geology, University of the Free State. The following procedure was undertaken during sample preparation:

1. Samples were broken into fragments using a pre-cleaned tungsten-carbide jaw crusher.
2. Hand picked fragments was milled to a powder using a carbon-steel mill.
3. All possible precautions were taken to prevent contamination of the samples.

2.8 Analyses of dolerites

All dolerite samples were prepared for petrographical investigation, for X-ray fluorescence (XRF) spectrometry and powder X-ray diffraction (XRD) analyses at the University of the Free State.

The H_2O^- and LOI (loss of ignition) were determined at 110ºC and 1000ºC respectively. Fusion discs were prepared by mixing 0.28g sample powder with 0.02g $NaNO_3$ and 1.5g spectroflux 105 before being melted at 980ºC and made into fusion discs according to the technique of Norrish and Hutton (1969). Major elements analysed included SiO_2; Al_2O_3; TiO_2; Fe_2O_3 (total iron); MnO; MgO; CaO; Na_2O and P_2O_5 Table 3.3). Trace element concentrations and sodium were determined on pressed powder pellets: approximately 10g of powder from each sample was mixed with 6 drops of binding agent moviol and pressed into pellets with a boric acid backing (Table 3.4). Trace elements analysed included Sc, V, Cr, Co, Ni, Cu, Zn, Rb, Sr, Y, Zr, Nb and Ba.

H_2O^- and LOI were determined by gravimetric techniques after a silica crucible containing 2g of sample was ignited at 1000ºC for 6 hours. The weight loss obtained was used to calculate the LOI. Corrections were applied for line overlap, matrix effects and dead time. Calibration was done on the spectrometer using a set of international standards.

X-ray diffraction (XRD) analyses were also carried out on dolerite samples using a Siemens D5000 diffractometer.

CHAPTER 3

PETROGRAPHY, MINERALOGY AND GEOCHEMISTRY OF THE DOLERITES

3.1 Introduction

The dolerites investigated intruded into the coal-bearing Vryheid Formation (of the Ecca Group, Karoo Supergroup) in the southeastern part of the Witbank Coalfield. According to Smith and Whittaker (1986) the main trends of these intrusions in the Witbank Coalfield are east, northeast and north. The Ogies Dyke is the most prominent structure in the Witbank Coalfield, which has a strike distance of ±100km east west, extending from Ogies in the west to south of the Arnot Colliery in the east (Smith and Whittaker, 1986) (Figure 3.1).

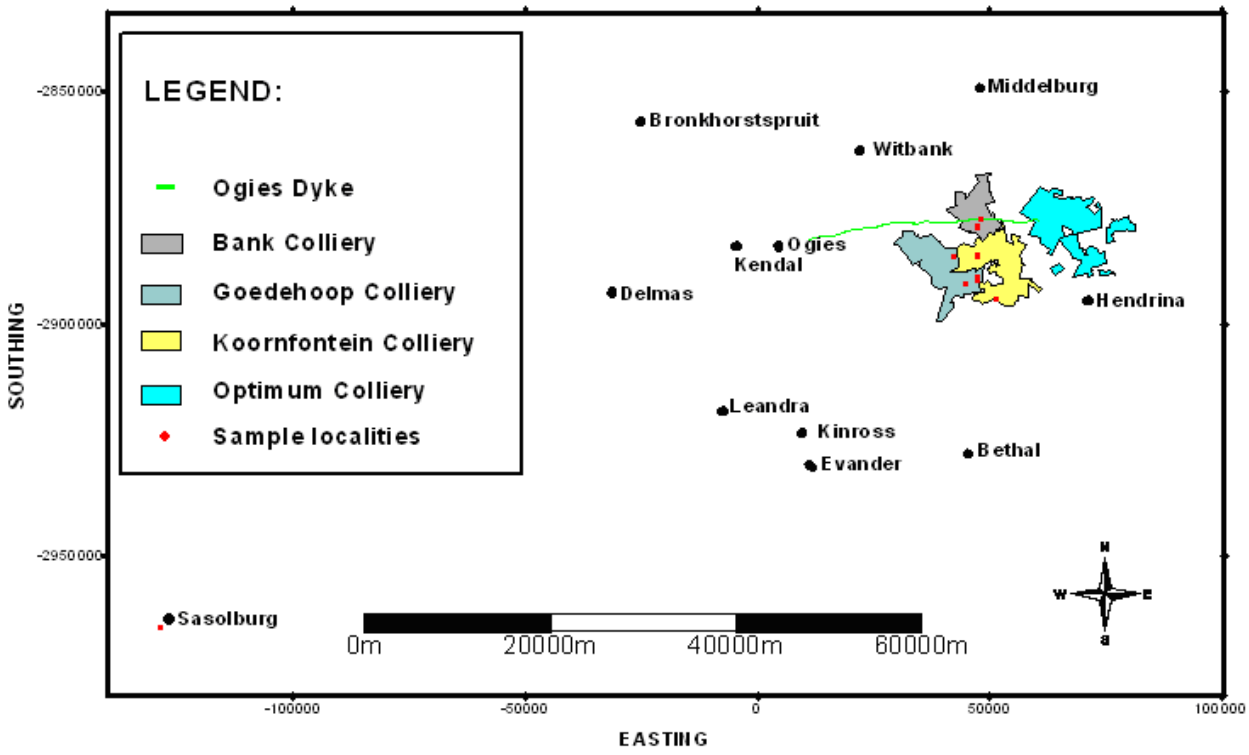

Figure 3.1 Locality map of the dolerite sampling positions (the scale of the map cause cluttering of the sample points particularly in the Bank, Goedehoop and Koornfontein Colliery areas)

3.2 Sampling

Samples of the 20m thick dolerite sill (Samples K8, K10, G2, G3, G5, K5, K6, K7, K9, BNK1, BNK2 and BNK3 in Table 3.1) and its bifurcations (Samples, G4, G1, K1, K2, K3, K4, K11, GI,

GII, GIII and K12 in Table 3.1) were collected underground from the Bank, Goedehoop and Koornfontein Collieries in the southeastern part of the Witbank Coalfield.

Table 3.1 Localities and Descriptions of dolerite samples

LOCALITIES AND DESCRIPTIONS OF DOLERITE SAMPLES											
DOLERITE SAMPLE NUMBER	Sample locality	Geometry						Dolerite Thickness	Colour	Grain size	Alteration
		Sill		Dyke		Bifurcations					
		Chilled margin	Interior	Chilled margin	Interior	Chilled margin	Interior				
OD1	Ogies Dyke				✓			15m	Green	Medium	Highly altered
G3	Goedehoop Colliery	✓						20m	Green	Fine	Altered
GII	Goedehoop Colliery						✓	1.4m	Light green	Fine	Altered
G4	Goedehoop Colliery						✓	2m	Light green	Fine	Altered
G1	Goedehoop Colliery						✓	2m	Light green	Fine	Altered
K1	Koornfontein Colliery						✓	2m	Light green	Fine	Altered
K2	Koornfontein Colliery						✓	2m	Light green	Fine	Altered
K3	Koornfontein Colliery						✓	2m	Light green	Fine	Altered
K4	Koornfontein Colliery						✓	2m	Light green	Fine	Altered
K11	Koornfontein Colliery						✓	2m	Light green	Fine	Altered
K8	Koornfontein Colliery	✓						20m	Green	Fine	Altered
K10	Koornfontein Colliery	✓						20m	Green	Fine	Altered
GI	Goedehoop Colliery					✓		1.4m	Whitish green	Fine	Highly altered
GIII	Goedehoop Colliery					✓		1.4m	Whitish green	Fine	Highly altered
K12	Koornfontein Colliery					✓		0.5m	Whitish green	Fine	Highly altered
G2	Goedehoop Colliery		✓					20m	Green	Medium	Unaltered
G5	Goedehoop Colliery		✓					20m	Green	Medium	Unaltered
K5	Koornfontein Colliery		✓					20m	Green	Medium	Unaltered
K6	Koornfontein Colliery		✓					20m	Green	Medium	Unaltered
K7	Koornfontein Colliery		✓					20m	Green	Medium	Unaltered
K9	Koornfontein Colliery		✓					20m	Green	Medium	Unaltered
B4 FS	Sasolburg		✓					48m	Green	Coarse	Unaltered
B5 FS	Sasolburg		✓					40m	Green	Fine	Altered
BNK1	Bank Colliery		✓					20m	Green	Medium	Unaltered
BNK2	Bank Colliery		✓					20m	Green	Medium	Unaltered
BNK3	Bank Colliery		✓					20m	Green	Medium	Unaltered

An exposure in a road cut between Middelburg and Bethal permitted sampling of the Ogies Dyke (Sample OD1 in Table 3.1). Dolerite samples (B4 and B5 dolerite sills) were also collected ±30km southwest of Sasolburg (Block 13 exploration project of SASOL) (Samples B4

FS and B5 FS in Table 3.1). These samples were collected for comparison with the Witbank Coalfield dolerites.

3.3 Background

According to Duncan et al., (1984) variation in composition is convenient to distinguish between different types of Karoo igneous rocks, such as those that would give rise to different rock types and subtle variation by the minor and trace constituents in the rocks. SiO_2 (weight % on a volatile free basis) has been chosen as the variable on which the Karoo igneous rocks are divided into basic, intermediate and acid rocks (Duncan et al., 1984). The TAS classification diagram of Le Maitre et al., (1989) is intended for common unaltered volcanic rocks. The analyses should be anhydrous and recalculated to 100 %.

It was suggested by Eales et al., (1984) that compositional differences between basaltic magma types could be due to differences in one or more of the following:

1) Variation of the mantel composition in either a lateral or a vertical fashion.
2) The degree of partial melting.
3) The degree of fractional crystallization.
4) Contamination processes.

According to De Oliveira (1997) the differences between the 4 dolerite types on the Majuba Colliery (south eastern Transvaal) are due to mantle source heterogeneities, which could be derived from reasonable differentiation patterns (with values of ±7% MgO). The distinctive features of the dolerites at the Majuba Colliery could apparently not be related to crustal contamination (De Oliveira, 1997). Eales et al., (1984) observed that the geological, petrographical as well as the major, trace element and isotopic compositions of the Karoo basalts suggested that crustal contamination of the magmas has been minimal. Eales et al., (1984) also suggested that the geochemical grouping seen throughout the Karoo basin must be a consequence of mantle composition variation from north to south.

3.4 Petrographical investigation of dolerites.

3.4.1 Dolerite samples.

(i) 20m thick dolerite sill (Witbank Coalfield)

In thin section it was observed that biotite display evidence of slight chloritisation, and the olivines some serpentinisation. Brown iddingsite show negligible alteration. Phenocrysts found in these rock samples include olivine, plagioclase and augite pyroxene. The groundmass is fine grained with magnetite, pyrite and ilmenite frequently present.

Olivine phenocrysts (0.5–2.75mm) show euhedral and subhedral morphologies in Figure 3.2. Euhedral plagioclase phenocrysts and microphenocrysts are commonly present as laths and needles intergrowing ophitic and sub-ophitic with augite (Figure 3.3). The pyroxene crystals are nodular microphenocrysts.

Opaque minerals, magnetite and ilmenite are commonly found as phenocrysts (Figures 3.4 and 3.5). Occasional flakes of biotite, serpentine and iddingsite are fine grained accessory minerals.

The samples from the interior of the Witbank sill indicate that the sill is a medium crystalline dolerite (Table 3.1). These crystals formed during intermediate cooling of the magma. Further investigation show that the chilled margins and the bifurcations are fine crystalline (Table 3.1). In this case the crystallisation of the magma must have happened rapidly.

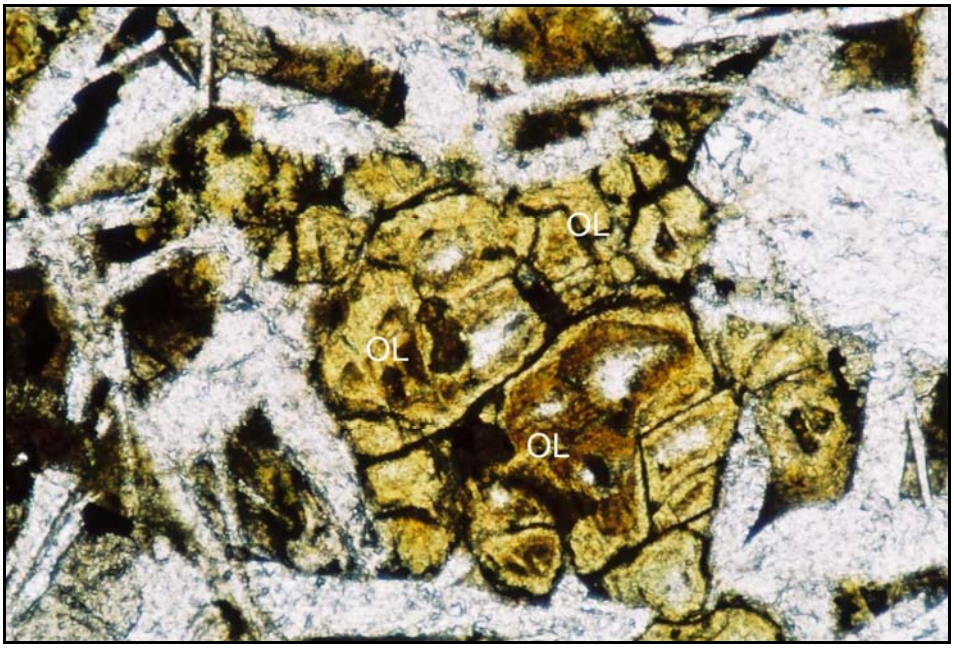

Figure 3.2 Olivine (OL) crystal enclosed by pyroxene and plagioclase (open nicols, 10X, W.O.F. = 2.8mm).

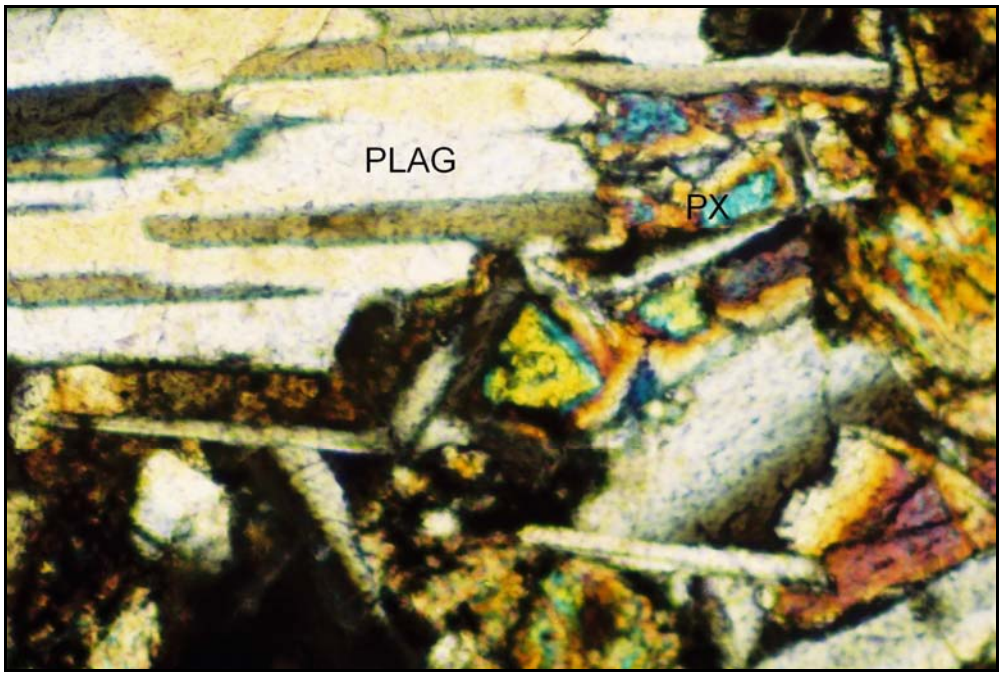

Figure 3.3 Ophitic and sub-ophitic intergrowth textures between plagioclase (PLAG) and pyroxene (PX) and opaque minerals (crossed nicols, 10X, W.O.F. = 2.8mm).

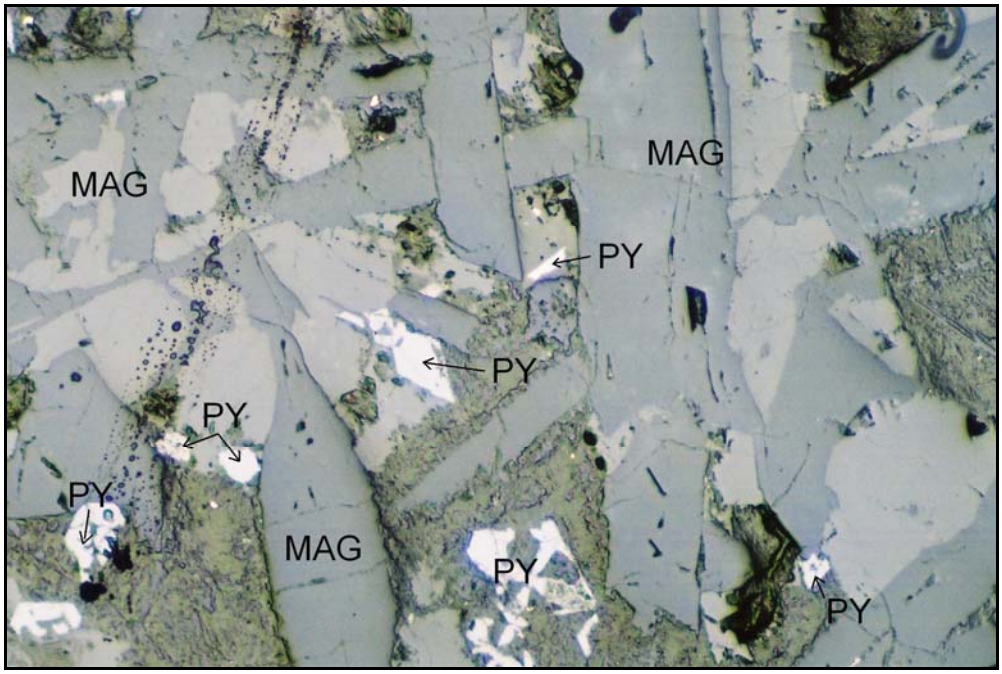

Figure 3.4 Magnetite (MAG) and pyrite (PY) (open nicols, 10X, W.O.F. = 2.8mm)

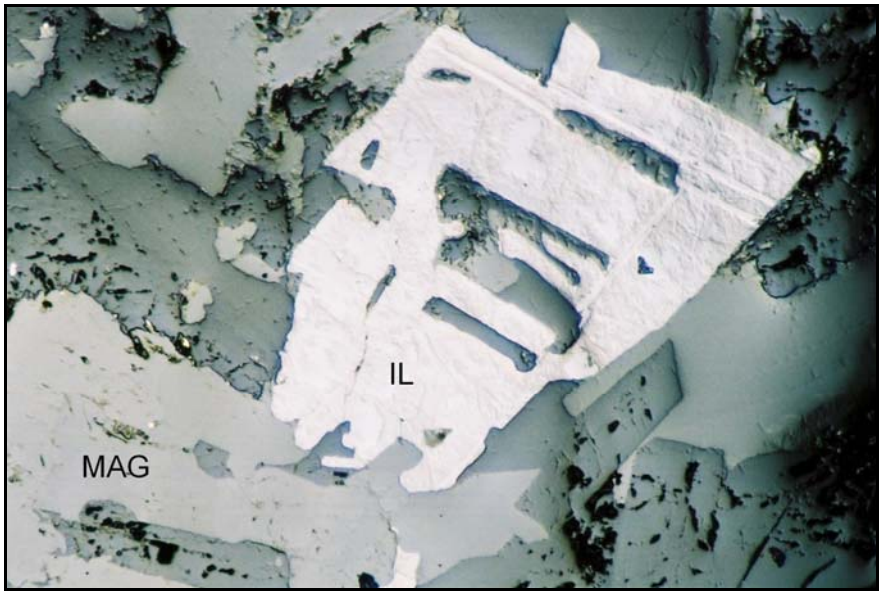

Figure 3.5 Magnetite (MAG) and ilmenite (IL) (open nicols, 10X, W.O.F. = 2.8mm)

(ii) 15m thick Ogies Dyke (Witbank Coalfield)

Thin sections of the Ogies Dyke show pyroxene and plagioclase phenocrysts. The Ogies Dyke mainly constitute augite and ca plagioclase.

Ophitic and sub-ophitic intergrowth textures between the plagioclase and pyroxene crystals are commonly found (Figure 3.6).

Accessory biotite in Figure 3.7 is showing minor chloritisation. Phenocrysts of magnetite and ilminite are associated with a fine crystalline groundmass (Figure 3.8).

Thin section investigation of the Ogies Dyke show that it is a medium crystalline dolerite (Table 3.1). This indicates that the crystals must have formed during an intermediate cooling process.

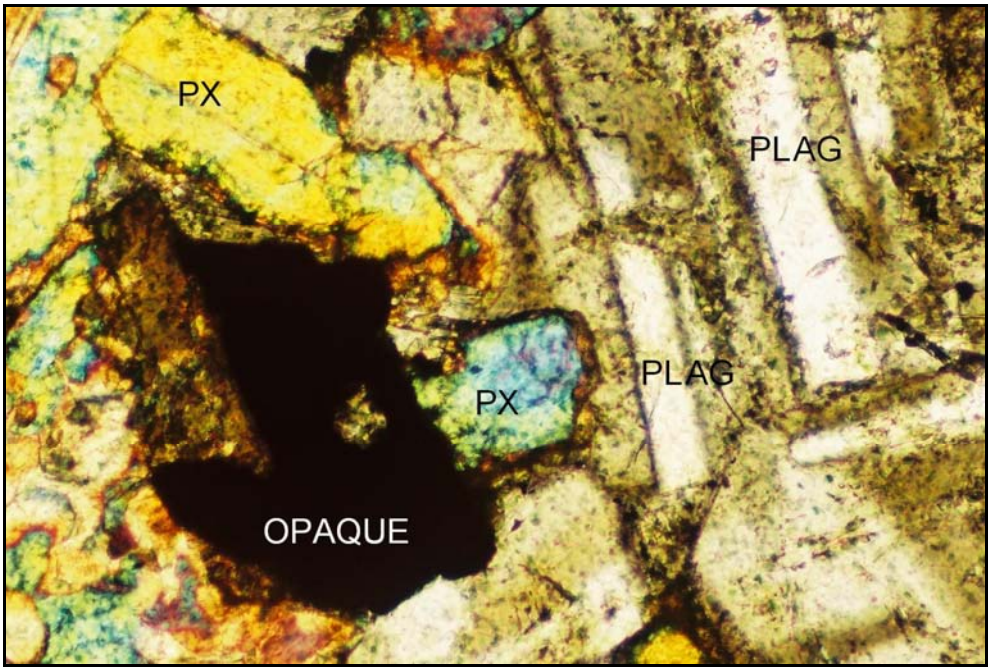

Figure 3.6 ***Ophitic and sub-ophitic intergrowth textures between plagioclase (PLAG) and pyroxene (PX); opaque minerals (crossed nicols, 10X, W.O.F. = 2.8mm)***

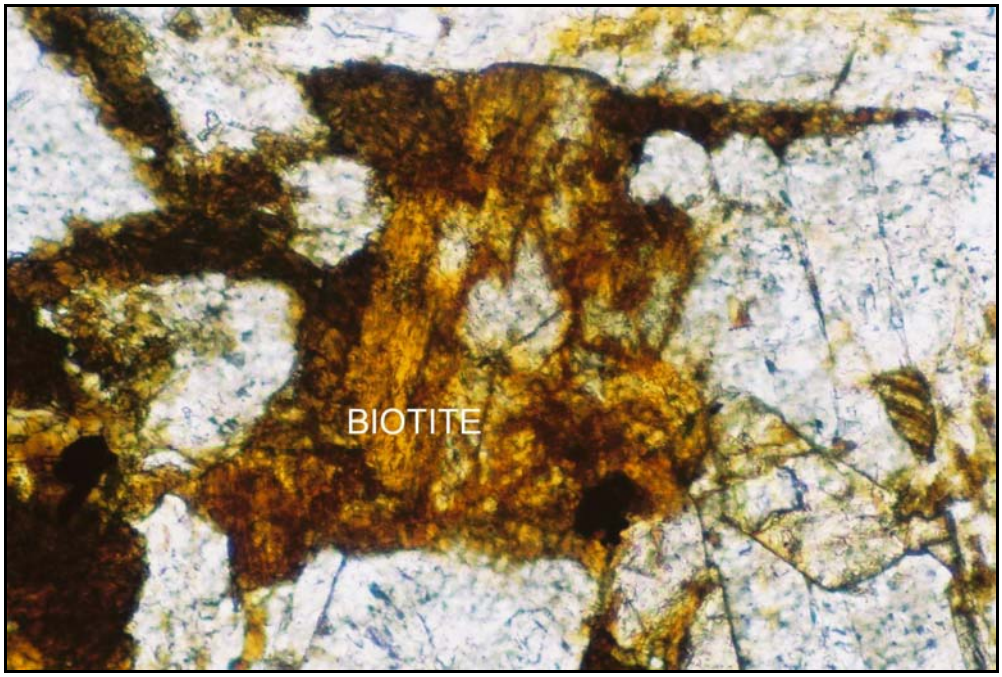

Figure 3.7 Biotite showing negligible chloretization on its edges (open nicols, 10X, W.O.F. = 2.8mm)

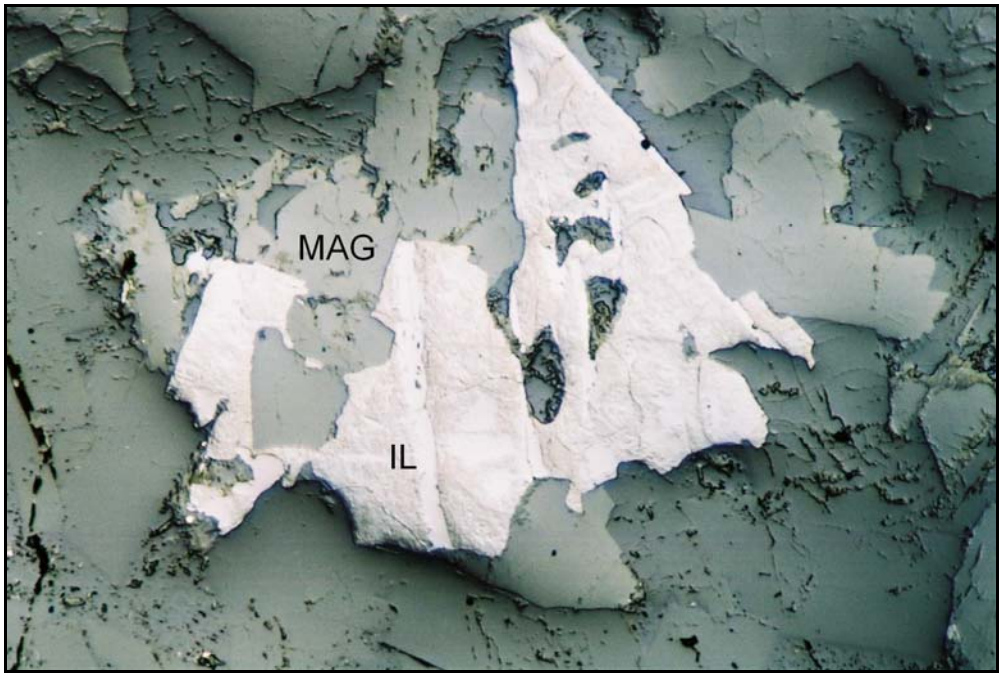

Figure 3.8 Magnetite (MAG) and ilmenite (IL) (open nicols, 10X, W.O.F. = 2.8mm)

(iii) 60 m thick B4 sill (Sasolburg)

A microscopic investigation of a thin section reveals that macrophenocrysts of augite pyroxene and olivine crystals and also microphenocrysts of antigorite and plagioclase are present (Figure 3.9).

Olivine and augite are classified as the main minerals and antigorite and plagioclase are the minor minerals in these samples (Figure 3.10). The phenocrysts have distinctly euhedral and subhedral morphologies.

The investigation also revealed that this is a coarse crystalline dolerite that formed during slow cooling of the magma (Table 3.1).

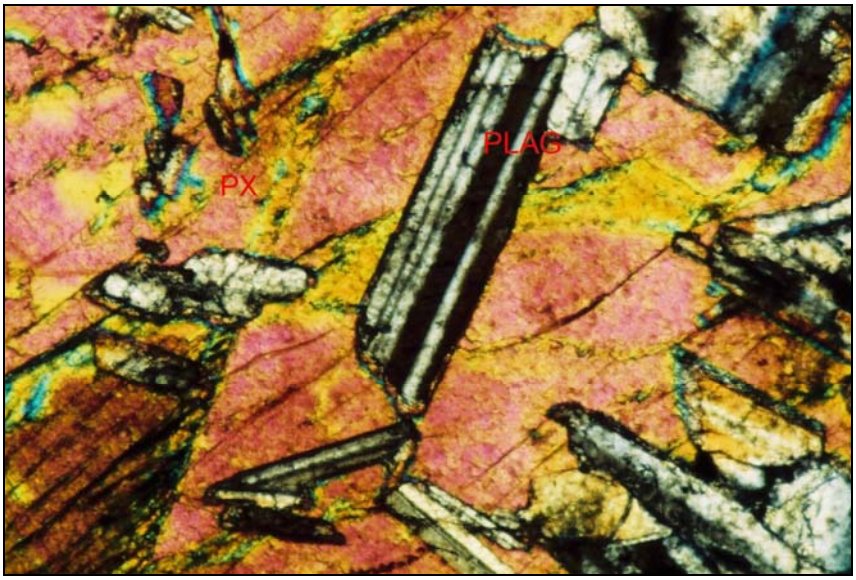

Figure 3.9 Ophitic intergrowth textures between pyroxene (PX) and plagioclase (PLAG) crystals (crossed nicols, 10X, W.O.F. = 2.8mm).

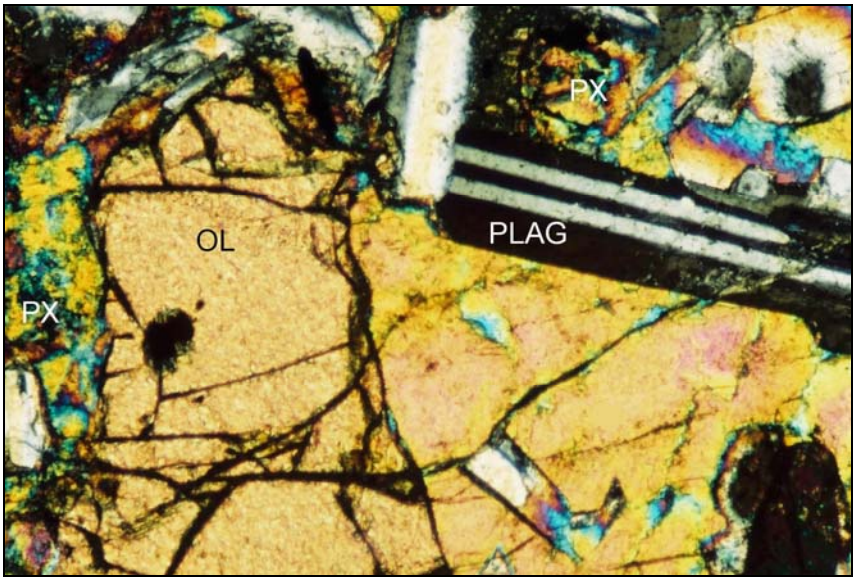

Figure 3.10 ***Ophitic intergrowth textures between pyroxene (PX) and plagioclase (PLAG) crystals and olivine (OL) macrophenocrysts (crossed nicols, 10X, W.O.F. = 2.8mm).***

(iv) 60 m thick B5 sill (Sasolburg)

A microscopic investigation revealed that microphenocrysts of plagioclase and altered microphenocrysts of olivine are the main minerals. Biotite and serpentine have been indentified as the accessory minerals (Figure 3.11).

This investigation further revealed that this sill is a fine crystalline dolerite. The crystals must have formed during rapid crystallisation of the magma (Table 3.1).

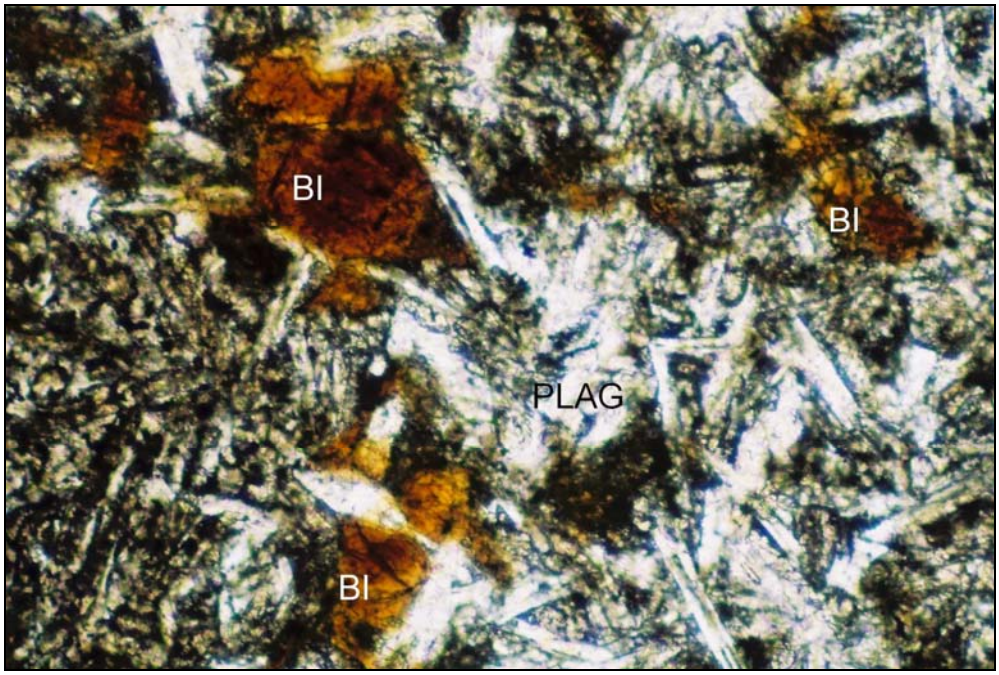

Figure 3.11 Flakes of biotite enclosed in a fine grained plagioclase / carbonate groundmass (open nicols, 10X, W.O.F. = 2.8mm).

Conclusions

It is clear from Table 3.2 that the dolerites from the study area are distinctively different in terms of their mineral content, geometry, thickness, grain size, and alteration.

Mineral content - Involvement of plagioclase in both the Witbank and Sasolburg dolerite fractionation assemblages indicates that the fractionation processes must have occurred within the crust (Eales et al., 1984). However the plagioclase phenocrysts in the Witbank dolerites as opposed to the microphenocrysts in the Sasolburg dolerites indicate that crystallization must have happened at different depths within the crust (Eales et al., 1984).

Table 3.2 Detail summary of the physical and petrographic characteristics of dolerites

Interior samples								
Descriptions	**Locality**	**Geometry (Green = Dolerite; Black = coal seams; Yellow = Karoo sediments**		**Thickness**	**Colour**	**Grain size**	**Alteration**	**Petrography**
Sill	Witbank Coalfield		Undulating/bifurcating - transgressing horizontal bedding of Karoo sediments	20 m	Green	Medium crystalline	Fresh	Phenocrysts: olivine, plagioclase, augite pyroxene Ore Minerals: magnetite, pyrite, and ilminite Accessory: biotite and iddingsite
Ogies Dyke	Witbank Coalfield		Sub-vertical - perpendicular to horizontal bedding of Karoo sediments	15 m	Green	Medium to fine crystalline	Highly altered	Phenocrysts: bytownite plagioclase, augite pyroxene Ore Minerals: magnetite and ilminite Accessory: biotite
B4	Sasolburg		Horizintal - follow horizontal bedding planes of Karoo sediments	48 m	Green	Coarse crystalline	Fresh	Macrophenocrysts: augite pyroxene and olivine (>20%) Microphenocrsists: antigorite and plagioclase
B5	Sasolburg		Horizintal - follow horizontal bedding planes of Karoo sediments	40 m	Green	Fine crystalline	Altered	Microphenocrysts: plagioclase and olivine Accessory: biotite and serpentine

Fractionation in the Sasolburg dolerites must have occurred at higher temperatures and therefore deeper within the crust as oppose to the Witbank dolerites. Olivine phenocrysts identified in the Witbank sill is absent in the Ogies Dyke.

The absence of pyroxene phenocrysts in the B5 sill indicates that the fractionation took place at a pressure significantly higher than that at which the plagioclase and olivine microphenocrysts have formed. The high percentage olivine in the B4 sill indicates that these two sills originated from different magma sources. Plagioclase microphenocrysts in the B5 sill as oppose to the macrophenocrysts of the B4 sill concludes that the fractionation processes of the B5 sill must have happened deeper within the crust (Eales et al., 1984).

Geometry – Geological cross-sections in chapter 5 depict representative information where the domal and basin-shaped Witbank sill transgressed the coal seams (Table 3.2). This sill was intersected during exploration drilling and underground mining at the Bank, Goedehoop and Koornfontein Collieries. The overall extent of the sill is unknown to the author.

The Ogies Dyke is a sub-vertical intrusion striking over a distance of ~ 100km. The Karoo sediments have not been displaced during the intrusion of the Ogies Dyke (Table 3.2).

The B4 and B5 dolerite sills are massive horizontal intrusions that follow the horizontal bedding of the Karoo sediments (Table 3.2). The overall extent of these sills is unknown by the author.

Thickness – The Witbank sill is 20m thick and either widens or bifurcates when intersecting the coal seams. The Ogies Dyke ends in the west with a circular shape where the intrusion widened while the rest of the dyke has a thickness of 15m. The B4 and B5 sills have thicknesses of 48m and 40m respectively and are classified as massive sills in this study.

Grain size – Both the Ogies Dyke and the Witbank sill are medium crystalline while the B4 sill is coarse and the B5 sill is fine crystalline. This study engage with dolerites that crystallised rapidly, intermediately and slowly as the crystal sizes are directly related to magma cooling.

Alteration – Fine crystalline dolerites like the chilled margins and bifurcations tend to be more susceptible for alteration as opposed to the medium and coarse crystalline dolerites. The 40m thick, fine crystalline B4 sill has undergone the most alteration comparing to the B5 sill, Witbank sill and the Ogies Dyke.

The differences identified during thin section investigations, geometry and thickness distinguish the Sasolburg dolerites from the Witbank sill and the Ogies Dyke. The rest of chapter 3 focus on the geochemical differentiation between these dolerites while chapters 4 and 5 are fingerprinting the influences of these intrusions especially on the coal sediment layers.

3.5 Jointing and alteration of the dolerites

Nearly all the dolerite samples obtained from chilled margins and bifurcations suffered some degree of jointing, which appears to be related to their cooling history. Samples collected from narrow dolerite bifurcations are generally more intensely jointed as opposed to wider bifurcations.

Dolerite samples collected adjacent to coal tend to have a higher frequency of jointing than those adjacent to sandstones and shales. Rapid cooling of the bifurcations and chilled margins results in more frequent joint patterns than in the interior of the dolerites.

The degree of alteration is closely linked to the degree of jointing. Jointing, which facilitates easy movement of groundwater through rocks will result in more rapid alteration. Dolerite samples collected adjacent to coal are microcrystalline and has undergone carbonate alteration. The matrix is light grey to grey in colour due to the considerable amount of carbona and is called “white trap” (Kisch and Taylor, 1966), while some of the samples have been silicified as well.

In the coal/dolerite contact zone, injections of coal into dolerite and dolerite stringers into the coal are commonly found at the investigated areas. According to Hagelskamp (1987), dolerites that intruded coal are usually wider in the coal than in the floor and the roof and also tend to bifurcate into the coal. Hagelskamp (1987) also states that this irregular bulging within the coal is attributed to plasticity and shrinkage of the coal due to the loss of volatiles and moisture. Helgeson (1979) states that the association of sulphides with altered wall rocks is a manifestation of the chemical link between the precipitation of ore minerals in hydrothermal veins and their associated wall rock alteration. Exchange reactions occurring between the silicate wall rock and an aqueous electrolyte solution are essentially acid, in which the acidic solution is neutralized by the basic wall rock (Rose and Burt, 1979). Precipitation and dissolution of metal complexes depend on the change in activity of different ions in the fluid, which will affect the solubility of the metal. Meyer and Hemley (1967) stated that the most common cations involved in alteration reactions are K^{+}, Na^{+}, Ca^{2+}, Mg^{2+}, Fe^{2+} and Al^{3+}.

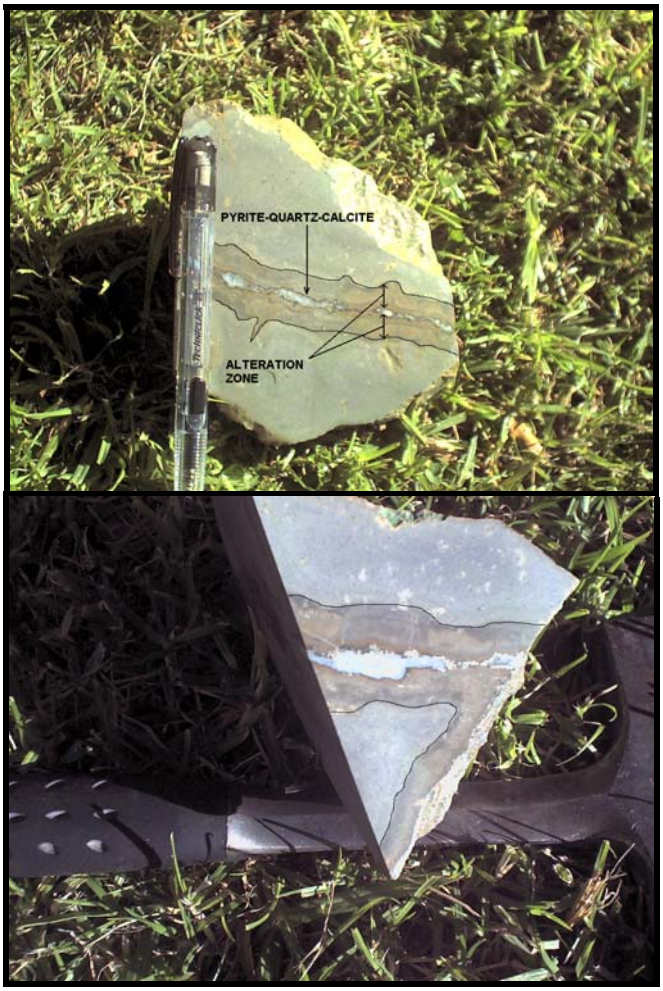

Figure 3.12 Dolerite samples from the Koornfontein Colliery containing mineralised veins containing quarts and calcite. A distinctive zoning pattern along these veins can be recognised.

According to Whitelaw (1998) alteration zones where the H^+/Mg^{++} ratio is at a minimum, the most common minerals to crystallize are pyrite and calcite. It was observed during the present study that dolerite samples contain veins filled with pyrite, quartz and calcite (Figure 3.12). The change in chemistry of the fluid over time would result in a zoning pattern of different alteration types (Whitelaw, 1998). Dolerite samples collected from the Koornfontein Colliery had similar zoning patterns (Figure 3.12).

Hagelskamp (1987) collected a dolerite sample 100 m above the coal seam which didn't show any signs of endometamorphism by the coal while the dolerite sample collected adjacent to coal was altered to the so called "white trap". Petrographically the top samples (100m above the coal seam) contained euhedral glomeroporphyritic labradorite phenocrysts in a matrix dominated by pyroxene, with variable amounts of opaque minerals and trace quantities of quartz (Hagelskamp,1987). The "white trap" dolerite contained fewer of the larger feldspar phenocrysts (than the unaffected dolerite), but numerous agglomerations of smaller feldspar needles (Hagelskamp, 1987). The "white trap" dolerite consisted almost completely out of matrix material and is contaminated with slithers and specks of carbonaceous material. Siderite appeared to be the most abundant carbonate mineral (Hagelskamp, 1987). This was also found during the present investigation.

Dolerite samples from a borehole intersection were used to investigate dolerite alteration. This borehole intersected an 11,72m thick dolerite sill with sandstone contacts above and below as well as bifurcations from the major sill, which intruded into the No. 2 Coal Seam. According to structural interpretations of geological sections through Koornfontein (Du Plessis, 2001), all the dolerite material intersected in this borehole are from the same source. The main objective of this investigation was to compare alteration between the major sill (with sandstone contacts) and the bifurcations (with coal contacts). A sample (K9 in Figures 3.13 and 3.14) was collected from the interior of the sill and indicated minimum alteration after a thin section investigation. This sample was compared with K8 and K10 (taken from the upper and lower chilled margins of the major sill) as well as samples K11 and K12 (Figures 3.13 and 3.14). XRD and XRF analyses were conducted on these 5 samples in order to investigate their mineralogical alteration and also to provide information on the differences in element concentrations (Tables 3.3, 3.5 and 3.7).

Alteration, carbonisation and silicification were detected in sample K9 due to the accessory quantities quartz, siderite, clinochlore, talc and kaolinite (Table 3.5). Higher quantities of montmorillonite, quartz, and biotite were identified in samples K8 and K10 (Table 3.5). Rapid cooling of the chilled margins resulted in the fine crystals and indicated a high degree of

weathering and alteration. When comparing Samples K9 with K11 and K12 no major mineralogical differences were identified, except that Samples K11 and K12 don't have any montmorillonite, biotite and talc (Table 3.5).

On a local base Samples K11 and K12 are both having low MgO and Ni concentrations as oppose to Samples K8, K9 and K10. Higher Fe_2O_3 concentrations were detected in the sill (Samples K8, K9 and K10) comparing to the bifurcations (Samples K11 and K12). It is a direct correlation with the Fe-sulphide mineral (pyrite) and the magnetic mineral (magnetite) concentrations.

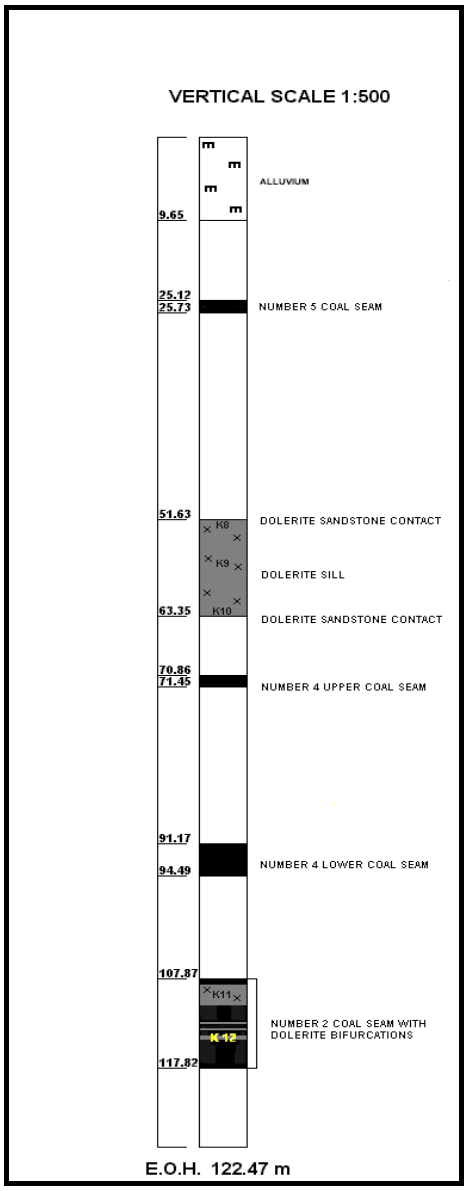

Figure 3.13 A stratigraphic column of a borehole drilled on the farm Dunbar/Koornfontein Colliery. The column shows the intersected coal seams and the 20m-thick bifurcating dolerite sill.

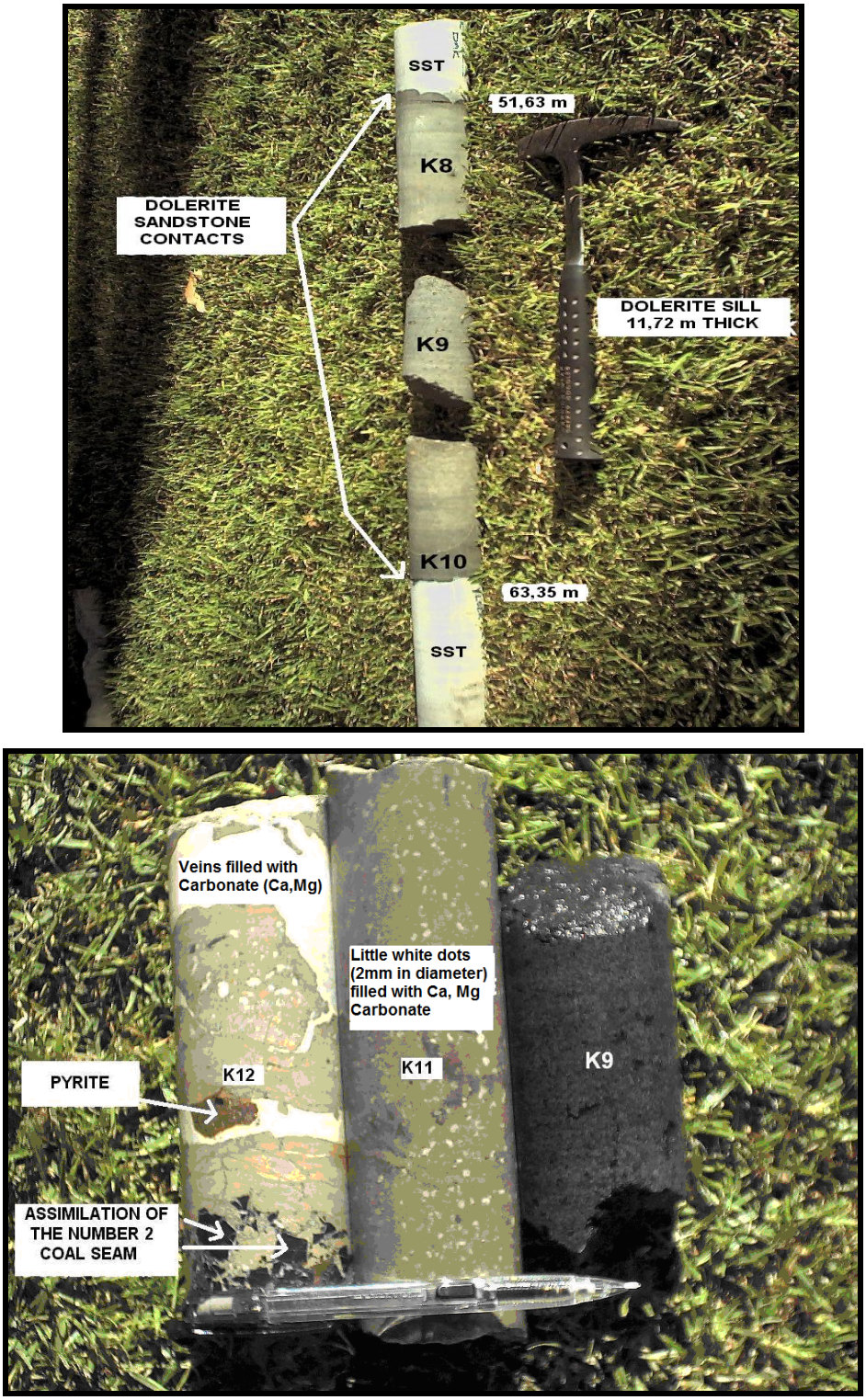

Figure 3.14 Photographs of dolerite samples collected from the borehole column in Figure 3.13. Note the pyrite in Sample K12.

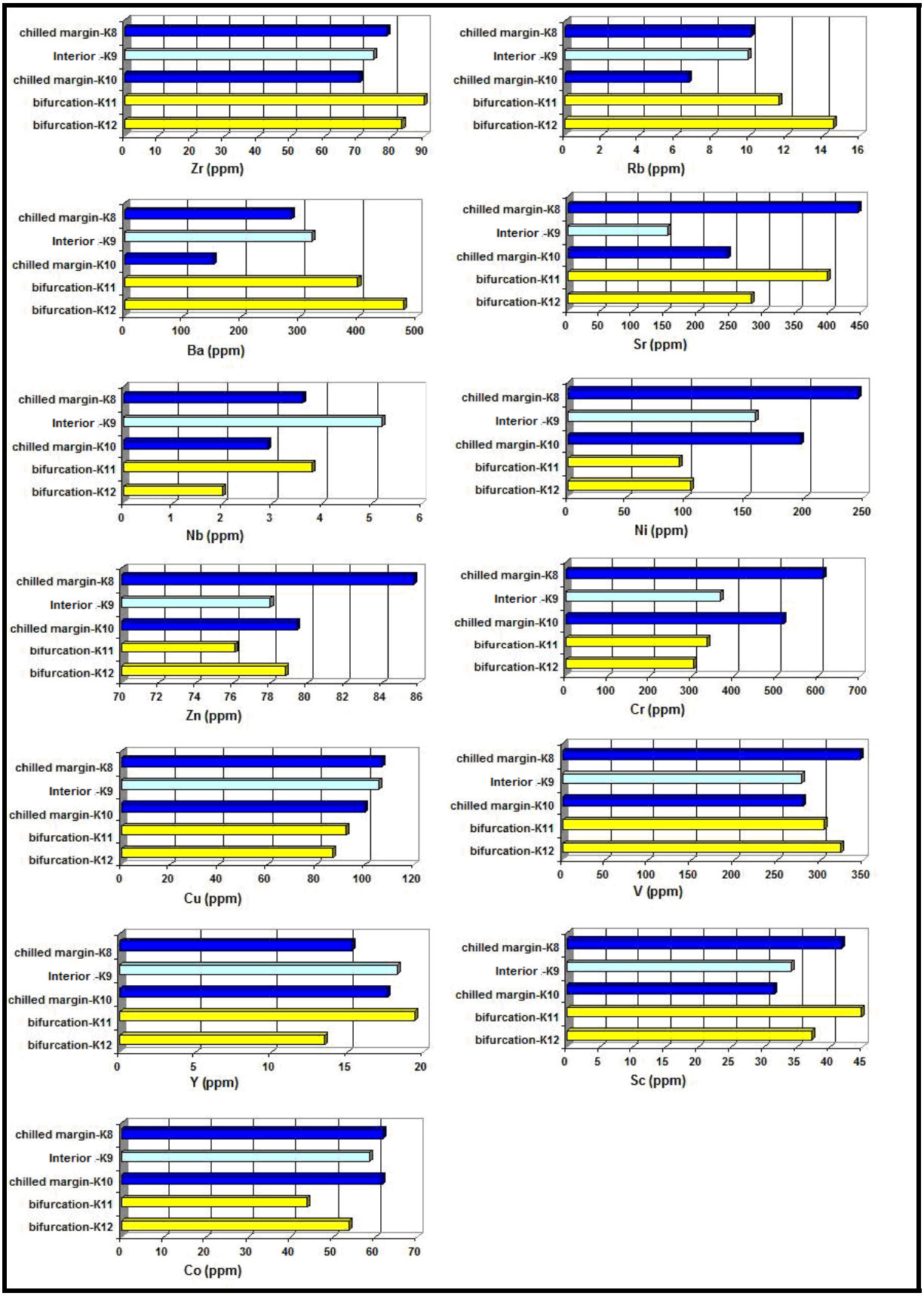

Figure 3.15 ***A comparison of trace element concentrations of sample K9 with K8 and K10 of the chilled margins and K11 and K12 of the bifurcations in the No. 2 Coal Seam.***

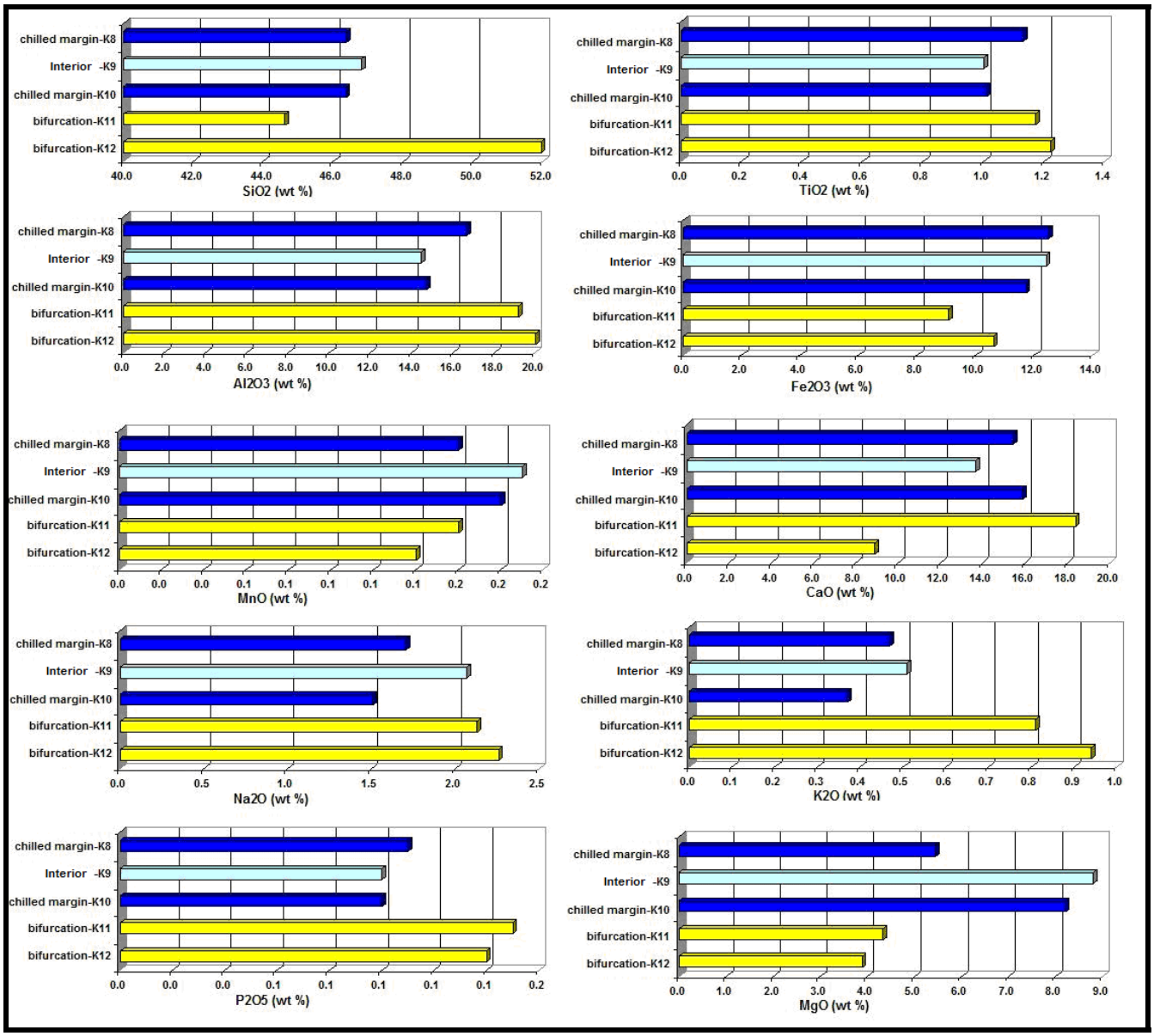

Figure 3.16 A comparison between major element concentrations of sample K9 with K8 and K10 of the chilled margins and K11 and K12 of the bifurcations in the No. 2 Coal Seam.

Sample K 12 is containing the highest percentage SiO_2 (Figure 3.16) which could be due to the assimilation of sandstone. As sandstone generally contain feldspar, heavy minerals and apatite, its assimilation by the dolerite can be confirmed with the higher Al_2O_3, K_2O (feldspar) and TiO_2 (heavy minerals) and P_2O_5 (apatite).

The two bifurcations (Samples K11 and K12) are showing a constant correlation when comparing K, Rb, Ni, V, Cr, Co, and Fe_2O_3. It is evident from these correlations that the dolerite only assimilated sandstone and is not contaminated with other rocks as well.

Table 3.3 Major oxide data of the dolerites sampled at the Goedehoop, Koornfontein, Bank Collieries, the Ogies Dyke and the B4 and B5 dolerites in the Free State Coalfield (Sasolburg). All the data is anhydrous and recalculated to 100%. Loss of Ignition (LOI) and H_2O^- values are also shown in the table.

Weight %	GI	GII	GIII	G1	G2	G3	G4	G5	OD1
SiO2 %	36.96	48.16	49.93	38.35	47.76	46.74	47.67	44.91	50.77
TiO2 %	1.35	1.14	1.32	1.11	0.97	1.09	1.01	1.22	1.51
Al2O3 %	18.25	16.95	19.74	17.55	15.41	17.11	14.79	17.36	13.54
Fe2O3%	7.76	9.7	5.56	10.19	11.93	9.24	11.67	10.22	14.42
MnO %	0.17	0.15	0.11	0.17	0.18	0.4	0.22	0.17	0.21
MgO %	7.2	4.38	3.58	5.55	7.63	4.15	6.98	3.92	4.9
CaO %	25.22	16.8	15.79	24.85	13.6	19.38	14.9	19.37	9.94
Na2O %	2.3	2.18	2.61	1.68	1.95	1.51	2.15	2.13	2.76
K2O %	0.56	0.39	0.49	0.46	0.46	0.26	0.48	0.53	1.78
P2O5 %	0.23	0.16	0.87	0.11	0.11	0.12	0.12	0.16	0.17
TOTAL	100	100	100	100	100	100	100	100	100
H2O	0.83	0.85	1.93	1.23	0.47	0.66	0.47	0.65	0.61
LOI	17.37	9.43	12.13	16.72	1.28	10.09	3.52	13.54	0.34

Weight %	B4 FS	B5 FS	KI	K2	K3	K4	K5	K6	K7
SiO2 %	45.5	48.3	44.54	45.27	43.47	40.68	49.36	44.91	40.24
TiO2 %	0.83	1.18	1	1.67	1.37	1.4	1.35	1.25	1.32
Al2O3 %	13.24	14.88	15.47	26.14	20.34	16.38	18.01	17.56	18.21
Fe2O3%	11.67	11.53	11.18	10.79	12.44	19.25	9.55	12.98	18.89
MnO %	0.18	0.18	0.19	0.14	0.23	0.28	0.16	0.18	0.22
MgO %	14.11	7.26	5.97	4.68	4.94	5.24	2.78	3.52	5.68
CaO %	11.97	12.95	19.42	7.63	13.49	13.65	15.07	16.84	12.43
Na2O %	2.08	2.68	1.74	1.36	1.8	1.67	2.15	1.98	1.95
K2O %	0.33	0.87	0.4	2.14	1.72	1.23	1.38	0.6	0.88
P2O5 %	0.09	0.17	0.1	0.19	0.2	0.2	0.2	0.18	0.18
TOTAL	100	100	100	100	100	100	100	100	100
H2O	0.67	0.29	0.76	2.88	1.43	0.97	0.98	0.87	0.92
LOI	0.3	0.19	10.59	12.35	16.06	15.56	11.54	12.02	15.32

Weight %	K8	K9	K10	K11	K12	BNK1	BNK2	BNK3
SiO2 %	46.37	46.8	46.36	44.62	51.93	45.16	45.58	46.46
TiO2 %	1.13	1	1.01	1.17	1.22	1.04	1	1.03
Al2O3 %	16.68	14.45	14.7	19.18	19.99	16.06	15.49	15.17
Fe2O3%	12.48	12.4	11.71	9.07	10.61	12.63	12.13	12.17
MnO %	0.16	0.19	0.18	0.16	0.14	0.19	0.18	0.18
MgO %	5.45	8.79	8.2	4.33	3.89	7.46	8.92	8.34
CaO %	15.44	13.69	15.86	18.39	8.9	14.76	14.22	14.08
Na2O %	1.71	2.07	1.51	2.13	2.26	2.06	1.94	1.98
K2O %	0.47	0.51	0.37	0.81	0.94	0.55	0.45	0.48
P2O5 %	0.11	0.1	0.1	0.15	0.14	0.12	0.1	0.11
TOTAL	100	100	100	100	100	100	100	100
H2O	1.05	0.29	1.39	0.6	0.66	0.42	0.38	0.43
LOI	9.59	0.88	3.33	12.45	11.63	6.03	1.4	1.2

Table 3.4 Trace element data of the dolerites sampled at the Goedehoop, Koornfontein, Bank Collieries, the Ogies Dyke and the B4 and B5 dolerites sill in the Free State Coalfield (SASOL – BLOCK 13).

ppm	GI	GII	GIII	G1	G2	G3	G4	G5	OD1	B4 FS	B5 FS	KI	K2
Zr	80.2	79.8	66.1	70.8	80.7	77.3	85.4	80.5	153.3	59.5	101.6	68.3	99.3
Rb	8.4	6.5	12	13.7	11.7	2.9	11.3	9.7	64.3	7.3	17.8	9.6	65.8
Ba	494.6	753.6	482.3	241.7	164.6	174.6	200.6	649.1	320	119	251.2	513	1084.9
Sr	620.6	490	579	391.5	165.2	283.5	252.7	632.5	192.2	160.2	198.3	473.4	487
Nb	4.2	4.5	2.8	5.1	6.2	4.3	8	6.6	15.1	3.3	8.6	5.2	3.5
Ni	70	81.1	67	239.2	142.7	193.1	79.1	83.8	43.8	397.9	106.3	194.2	307.4
Zn	77.5	82	76.7	90	81.5	85.2	76.3	83.2	108.5	76	82.9	79.3	112.6
Cr	304.2	283.5	346	504.6	308.2	549.4	296.3	298.6	42.6	899.4	312.2	471	937.4
Cu	85.9	83.1	86.2	107.4	106.9	110.5	81.4	82.3	165.2	78.9	91.9	103.9	161
V	284.4	266.8	313	297.7	231.3	322.2	266.9	277	352.2	211.6	266	270.5	514.1
Y	22.4	23.8	23.8	18.1	21.5	20	23.4	24.7	41.6	14	25.8	19.3	21.2
Sc	42.1	37.5	40	37.2	33	41.5	40.9	40.6	36.6	30.9	33.3	34.2	58.1
Co	37	42.7	32	50.4	51	47.9	49.9	44.9	52.6	64.1	47.3	51.2	87.4

ppm	K3	K4	K5	K6	K7	K8	K9	K10	K11	K12	BNK1	BNK2	BNK3
Zr	100.1	110.2	117.8	99.1	104.4	78.6	74.6	70.3	89.9	83.2	77.8	76.4	75.6
Rb	48.8	34.4	32.5	17.9	21	10.1	9.9	6.7	11.6	14.5	13.1	9.5	11.3
Ba	1223.8	828.5	914.9	850.3	645.6	286.5	320.3	153.3	398.9	476.7	452.8	232.9	183.9
Sr	617.4	504.5	786.7	560.4	443.3	442.8	154.1	244.6	396.7	281.2	178	157	165.7
Nb	7.4	12	6.1	6.7	9	3.6	5.2	2.9	3.8	2	5	6.4	4.9
Ni	80.1	70.7	80.5	67.2	65.5	244.7	158.2	196	94	103.6	163.5	160.8	150.2
Zn	94.9	98.7	95.1	86.3	101.2	85.7	78	79.4	76.1	78.8	80.9	79.1	74.3
Cr	315.6	230.6	333.2	274.4	303.7	611.1	367.9	516.4	336.6	304.7	345.3	341.5	320.2
Cu	97.7	114.5	103.8	98.6	103.7	106.7	105.6	99.7	92.3	86.8	101	102.8	101.4
V	333.1	303.2	349.1	298.3	325.2	346	278.6	279.7	304.7	323.6	279.1	260.8	256.3
Y	27.8	31.1	25.3	24.1	33.8	15.3	18.3	17.6	19.4	13.5	19.2	19.9	20
Sc	46.9	38.8	46.9	34.8	42.1	41.8	34.2	31.5	44.8	37.2	36.3	30	27.9
Co	57	59.2	49.7	48.1	62.7	61.9	58.6	61.5	43.8	53.8	56.8	52.3	55.1

3.6 Major and trace element classification of the dolerites of the south-eastern Witbank Coalfield.

Major element oxide and the trace element data of 26 samples are presented and discussed in this section and have been obtained by X-ray fluorescence spectrometry (XRF). This technique is described in section 2.8.

Statistical parameters pertaining to the samples are presented in Tables 3.6 to 3.9.

The original data used for the compilation of these tables was calculated on a volatile free basis so that major oxides total 100%. All the data used for calculating these averages are contained in Tables 3.3 (major oxides) and 3.4 (trace elements).

Major oxides and trace element distributions are presented as Harker diagrams with SiO_2 as the abscissa (Figures 3.18 A/B and 3.19 A/B). As it has been the case in many studies of igneous rocks, SiO_2 has been chosen as the variable on which to make the most fundamental division.

This conventional classification technique is one in which rocks with less than 56% (weight % on a volatile-free basis) are termed “basic”, those with 56-63% are termed “intermediate” and those with more than 63% are termed “acid”. These divisions are convenient for the discussion of Karoo Igneous rocks since the majority fall into either the “basic” or “acid” groups when this classification is used (Duncan et al., 1984).

Table 3.5 Semi-quantitative X-ray diffraction analyses of the dolerites sampled at the Goedehoop, Koornfontein, Bank Collieries, the Ogies Dyke and the B4 and B5 dolerites in the Free State Coalfield (Sasol – Block 13).

XX = DOMINANT (> 40%)
X = MAIN (±10-50%)
x = MINOR (±2-10%)
xx = ACCESSORY (±1-2%)

DOLERITE SAMPLE NUMBER	MONTMORILLONITE	BYTOWNITE	QUARTZ	SIDERITE	BIOTITE	ILLITE	CLINOCHLORE	PYRITE	TALC	KAOLINITE	DOLOMITE
OD1	xx	X	X		x		xx			xx	
G1	x	XX	X				X	xx			
G2	x	XX	xx				X		x		
G3	xx	XX	X		x		xx			xx	
G4	xx	XX	X		x		X		x	xx	
G5		XX	X	xx			X				
GI	x	X	xx				xx				X
GII	x	XX	X				X				
GIII	x	XX	X				X				
K1	x	XX	X	X	x	x	xx			X	
K2		X	xx	X	x	x	x			xx	
K3	x	X	xx	X	x	x	xx			xx	
K4	x	X	X	X	x	x	xx	xx		x	
K5	x	X	X	xx			xx	x			
K6		XX	X	X	x		xx			x	
K7	x	X	xx	X	x		xx			x	
K8	x	XX	X		x		xx		x	x	
K9		XX	x	xx			xx		x	x	
K10	x	XX	X	x	x		xx		x	x	
K11		XX	X	X			xx				
K12		X	X	xx			xx			X	
B4 FS	x	XX	xx	x	x		x			x	
B5 FS		XX	X	x			xx			x	
BNK1	x	XX	x				x				
BNK2	x	X	xx				x				
BNK3	x	X	xx				x				

Witbank Sill

The Fe_2O_3 enrichment with progressive decrease in SiO_2 can be explained by the phases containing magnetite and ilmenite (Figure 3.18). Interior samples are depleted in Cr and Ni whereas the chilled margins are enriched (Figure 3.19 and 3.21). Crystallisation of olivine and chromitite cumulates within the chilled margins proof that the interior of the sill in its present position was subject to further differentiation (Henning, 1995). The chilled margins are higher in CaO as oppose to the interior samples which is due to carbonates and is called “white trap” (Kisch and Taylor, 1966).

Table 3.6 Standard deviations (S.D.), Variances (Var) and the arithmetic mean (Mean) for the major oxides, trace elements and a selected set of element ratios of the interior and chilled margins of the Witbank sill.

Sill - Interior					Sill - Chilled margins				
Variable	S.D.	Var	Mean	N	Variable	S.D.	Var	Mean	N
SiO2	2.86	8.2	45.91	7	SiO2	0.88	0.8	45.86	5
TiO2	0.16	0.0	1.10	7	TiO2	0.10	0.0	1.14	5
Al2O3	1.45	2.1	16.11	7	Al2O3	1.16	1.3	16.68	5
Fe2O3	2.87	8.2	12.81	7	Fe2O3	1.56	2.4	11.33	5
MnO	0.02	0.0	0.19	7	MnO	0.10	0.0	0.22	5
MgO	2.19	4.8	7.09	7	MgO	1.90	3.6	5.05	5
CaO	0.87	0.7	13.98	7	CaO	1.89	3.6	17.38	5
Na2O	0.08	0.0	2.01	7	Na2O	0.28	0.1	1.77	5
K2O	0.35	0.1	0.67	7	K2O	0.13	0.0	0.45	5
P2O5	0.04	0.0	0.13	7	P2O5	0.03	0.0	0.13	5
Zr	17.18	295.2	86.76	7	Zr	10.74	115.4	81.16	5
Rb	8.41	70.7	15.57	7	Rb	5.53	30.6	9.46	5
Ba	277.71	77121.1	416.43	7	Ba	310.96	96694.8	422.76	5
Sr	241.48	58313.7	292.86	7	Sr	168.80	28492.9	432.76	5
Nb	1.41	2.0	6.11	7	Nb	1.74	3.0	4.82	5
Ni	40.88	1671.2	131.63	7	Ni	77.36	5984.4	156.96	5
Zn	9.90	98.1	84.30	7	Zn	2.80	7.9	83.96	5
Cr	22.59	510.3	331.43	7	Cr	153.30	23500.0	449.98	5
Cu	2.13	4.5	103.60	7	Cu	10.83	117.4	99.56	5
V	40.95	1677.2	282.91	7	V	29.35	861.3	304.64	5
Y	5.45	29.7	22.57	7	Y	4.07	16.5	20.34	5
Sc	6.70	44.9	35.77	7	Sc	4.63	21.5	38.04	5
Co	4.59	21.1	55.17	7	Co	8.17	66.7	52.86	5
Zr/Nb	2.66	7.1	14.46	7	Zr/Nb	4.93	24.4	18.21	5
Zr/Y	0.47	0.2	3.89	7	Zr/Y	0.68	0.5	4.07	5
Ba/Rb	7.96	63.3	25.81	7	Ba/Rb	19.26	370.9	45.17	5
Ba/Sr	0.57	0.3	1.55	7	Ba/Sr	0.39	0.2	0.89	5
Ba/Zr	2.15	4.6	4.51	7	Ba/Zr	3.14	9.9	4.95	5
Rb/Sr	0.01	0.0	0.06	7	Rb/Sr	0.01	0.0	0.02	5
Ni/Co	0.76	0.6	2.41	7	Ni/Co	1.20	1.4	2.89	5
Cr/Ni	1.09	1.2	2.80	7	Cr/Ni	0.68	0.5	3.12	5

3.6.1 Witbank Bifurcations

Slightly lower Fe_2O_3 enrichment within the bifurcations does not dissociate them from the Witank sill and can also be explained by the sulphide phases (pyrite) containing iron. The chilled margins are higher in CaO as oppose to the interior samples which is due to carbonates and is related to “white trap”.

Table 3.7 Standard deviations (S.D.), Variances (Var) and the arithmetic mean (Mean) for the major oxides, trace elements and a selected set of element ratios of the interior and chilled margins of the Witbank bifurcations.

Bifurcations - Interior					Bifurcations - Chilled Margins				
Variable	S.D.	Var	Mean	N	Variable	S.D.	Var	Mean	N
SiO2	3.30	10.9	44.10	8	SiO2	6.64	44.0	46.27	3
TiO2	0.23	0.1	1.23	8	TiO2	0.06	0.0	1.30	3
Al2O3	3.64	13.3	18.35	8	Al2O3	0.77	0.6	19.33	3
Fe2O3	3.20	10.3	11.79	8	Fe2O3	2.07	4.3	7.98	3
MnO	0.05	0.0	0.19	8	MnO	0.02	0.0	0.14	3
MgO	0.90	0.8	5.26	8	MgO	1.64	2.7	4.89	3
CaO	5.06	25.6	16.14	8	CaO	6.69	44.7	16.64	3
Na2O	0.29	0.1	1.84	8	Na2O	0.16	0.0	2.39	3
K2O	0.67	0.5	0.95	8	K2O	0.20	0.0	0.66	3
P2O5	0.04	0.0	0.15	8	P2O5	0.32	0.1	0.41	3
Zr	0.00	0.0	100.00	8	Zr	7.46	55.6	76.50	3
Rb	14.78	218.4	87.98	8	Rb	2.50	6.3	11.63	3
Ba	22.02	484.8	25.21	8	Ba	7.48	55.9	484.53	3
Sr	380.08	144459.4	655.63	8	Sr	151.15	22845.3	493.60	3
Nb	106.69	11382.6	451.65	8	Nb	0.91	0.8	3.00	3
Ni	2.84	8.1	6.19	8	Ni	16.59	275.3	80.20	3
Zn	91.34	8343.2	143.23	8	Zn	0.87	0.7	77.67	3
Cr	12.86	165.3	88.74	8	Cr	19.59	383.7	318.30	3
Cu	228.38	52156.0	421.95	8	Cu	0.37	0.1	86.30	3
V	25.31	640.6	105.16	8	V	16.56	274.1	307.00	3
Y	81.91	6708.4	319.63	8	Y	4.56	20.8	19.90	3
Sc	4.53	20.5	23.01	8	Sc	2.01	4.0	39.77	3
Co	7.62	58.0	42.30	8	Co	9.32	86.9	40.93	3
Zr/Nb	14.19	201.3	55.20	8	Zr/Nb	9.72	94.5	28.10	3
Zr/Y	6.63	44.0	16.27	8	Zr/Y	1.44	2.1	4.17	3
Ba/Rb	0.51	0.3	3.86	8	Ba/Rb	10.95	119.9	43.98	3
Ba/Sr	33.75	1139.1	38.10	8	Ba/Sr	0.42	0.2	1.11	3
Ba/Zr	0.58	0.3	1.36	8	Ba/Zr	0.66	0.4	6.40	3
Rb/Sr	3.58	12.8	7.23	8	Rb/Sr	0.02	0.0	0.03	3
Ni/Co	0.04	0.0	0.05	8	Ni/Co	0.09	0.0	1.97	3
Cr/Ni	1.31	1.7	2.54	8	Cr/Ni	0.92	0.8	4.15	3

Zr and Ni can be used in a compatible-incompatible element plot (Figure 3.17) to constrain the processes and composition of the source material (Henning, 1995). Using the reasoning of Henning (1995) it is clear from Figure 3.17 that a process of fractional crystallisation must have been present in the Witbank sill and the Witbank bifurcations.

There is a distinctive pattern amongst various element associations when comparing the interior and the chilled margins of the bifurcations (Table 3.7). It is evident that Ni, Cr and V are depleted in the interior sample and enriched in the chilled margins. Whereas Fe, Mn, Mg; Zr, Nb, Y; Rb, Sr; and Cu, Zn are enriched in the interior and depleted in the chilled margins. Hence the geochemical variations which indicate that magma flow continued in the interior after the chilled margins crystallized or the other way around. The present study did not focus in more detail on within flow variations of the magma.

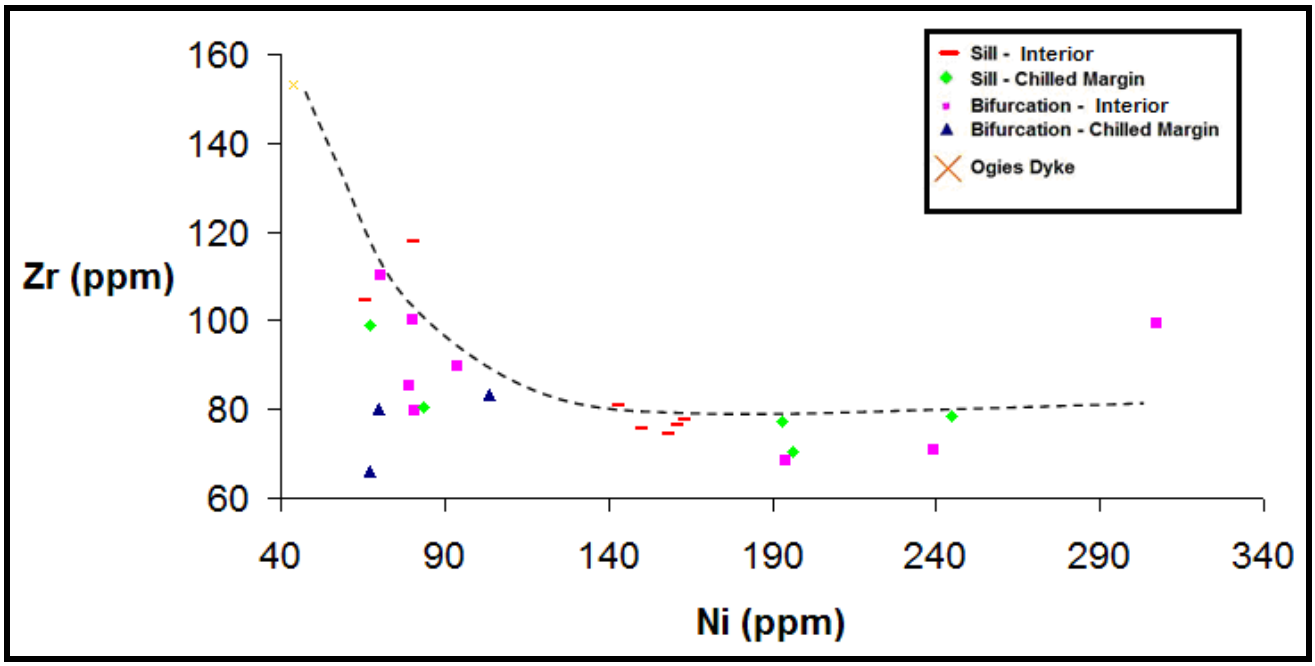

Figure 3.17 Zr vs Ni plot for the Sill interior and chilled margins, the Bifurcation interior and chilled margins as well as the Ogies Dyke.

3.6.2 Ogies Dyke

Abundances in TiO_2, K_2O, Zr, Nb, Zn, Cu, V, Y and poor Cr and Al_2O_3 concentrations geochemically dissociate the Ogies Dyke from the rest of the dolerites in the present study (Harker plots in Figures 3.18A/B, 3.29A/B; Histograms in Figures 3.20, 3.21 and 3.22). Significant low Ba/Rb, Ni/Co and Cr/Ni rations indicates magma source heterogeneity.

3.6.3 B4 and B5 sills – Sasol (Block 13)

The **B4 sill** compare with the Witbank sill in terms of SiO_2 content, although extremely higher in Ni, Cr and MgO dissociating this dolerite from the rest (Harker plots in Figures 3.18A/B, 3.29A/B; Histograms in Figures 3.20, 3.21 and 3.22). Ni is fractionated in the olivine and Cr

must be fractionated in chromitite bearing minerals although not identified in thin section. Extremely low TiO_2, Al_2O_3, CaO, Zr, Zn, Cu, V and Y concentrations also dissociate this dolerite from the rest (Harker plots in Figures 3.18A/B, 3.29A/B; Histograms in Figures 3.20, 3.21 and 3.22)

In terms of the Harker plots in Figures 3.18A/B, 3.29A/B and the Histograms in Figures 3.20, 3.21 and 3.22 the **B5 sill** (Sasol – Block 13) is overall geochemical very similar to the Witbank sill and the Witbank bifurcations.

Table 3.8 Standard deviations (S.D.), Variances (Var) and the arithmetic mean (Mean) for the major oxides, trace elements and a selected set of element ratios of the B4 and B5 sills (Sasol - Block 13).

B4 and B5									
Variable	S.D.	Var	Mean	N	Variable	S.D.	Var	Mean	N
SiO2	2.0	3.9	46.9	2	Zn	4.9	23.8	79.5	2
TiO2	0.2	0.1	1.0	2	Cr	415.2	172401.9	605.8	2
Al2O3	1.2	1.3	14.1	2	Cu	9.2	84.5	85.4	2
Fe2O3	0.1	0.0	11.6	2	V	38.5	1479.7	238.8	2
MnO	0.0	0.0	0.2	2	Y	8.3	69.6	19.9	2
MgO	4.8	23.5	10.7	2	Sc	1.7	2.9	32.1	2
CaO	0.7	0.5	12.5	2	Co	11.9	141.1	55.7	2
Na2O	0.4	0.2	2.4	2	Zr/Nb	4.4	19.3	14.9	2
K2O	0.4	0.1	0.6	2	Zr/Y	0.2	0.0	4.1	2
P2O5	0.1	0.0	0.1	2	Ba/Rb	1.5	2.4	15.2	2
Zr	29.8	886.2	80.6	2	Ba/Sr	0.4	0.1	1.0	2
Rb	7.4	55.1	12.6	2	Ba/Zr	0.3	0.1	2.2	2
Ba	93.5	8738.4	185.1	2	Rb/Sr	0.0	0.0	0.1	2
Sr	26.9	725.8	179.3	2	Ni/Co	2.8	7.8	4.2	2
Nb	3.7	14.0	6.0	2	Cr/Ni	0.5	0.2	2.6	2
Ni	206.2	42515.3	252.1	2					

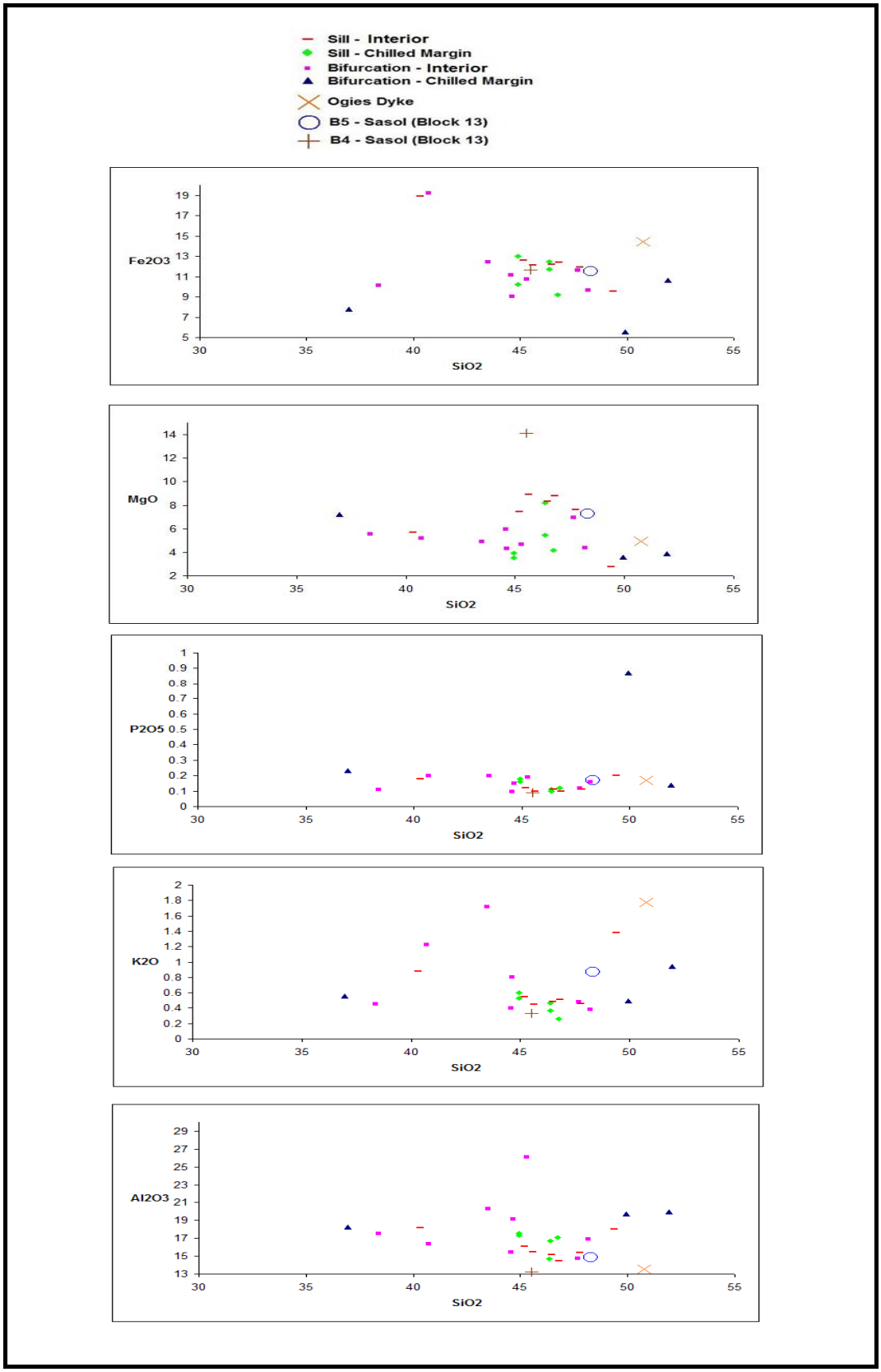

Figure 3.18A Harker diagrams of major elements (%) vs SiO_2 (%). All data in these diagrams is normalized to 100% on a volatile free basis.

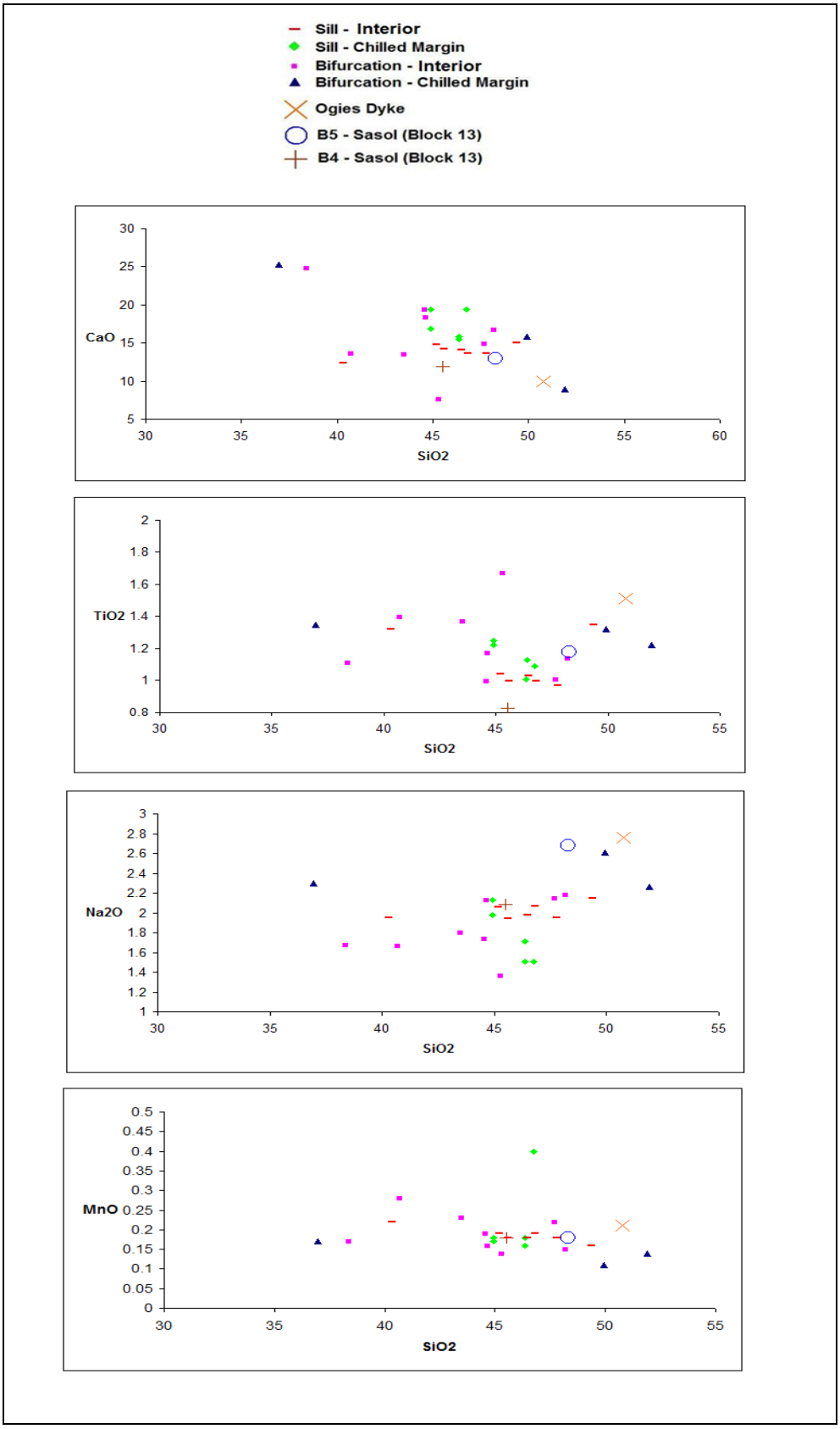

Figure 3.18B Harker diagrams of major elements (%) vs SiO_2 (%). All data in these diagrams is normalized to 100% on a volatile free basis.

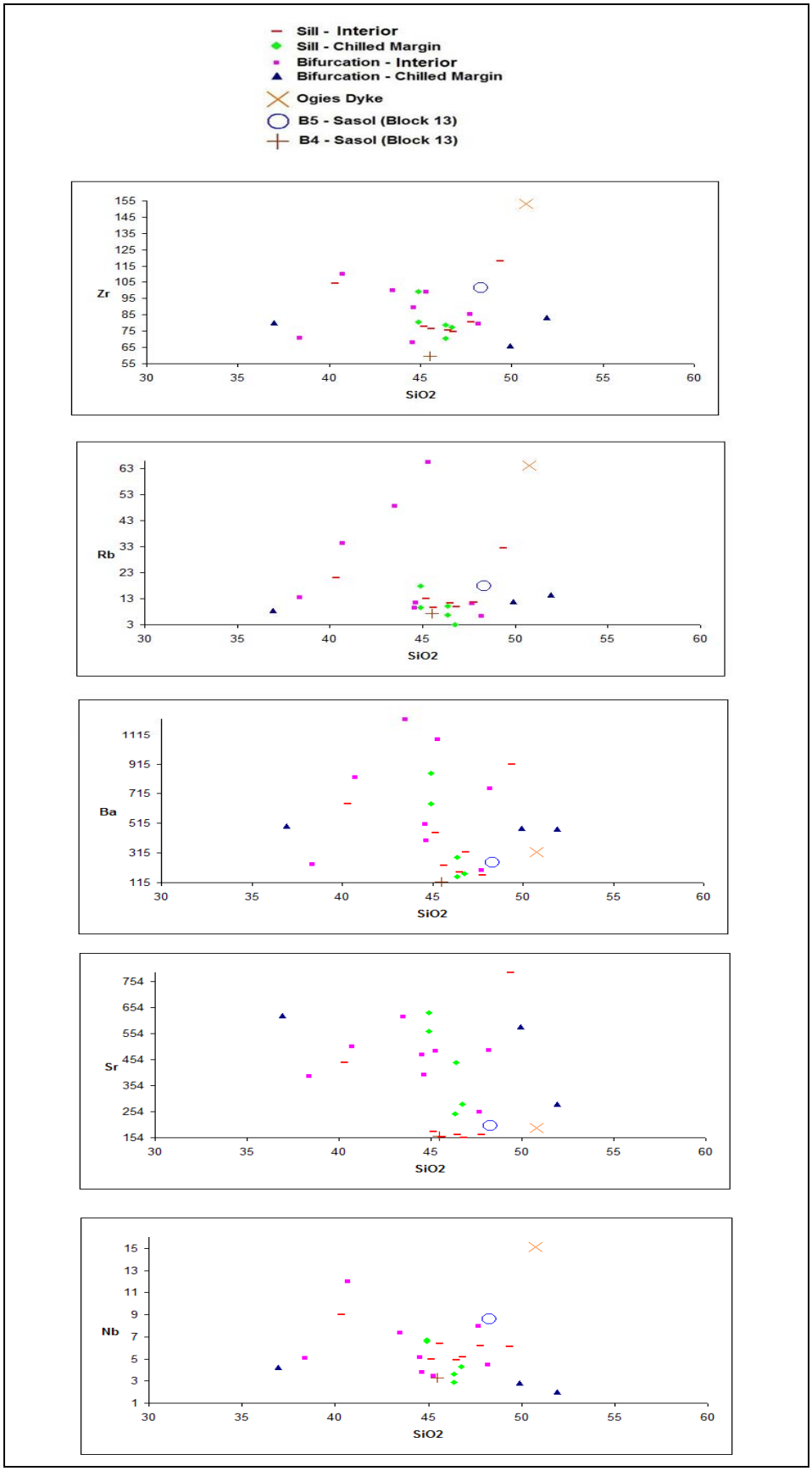

Figure 3.19A Harker diagrams of trace elements (ppm) vs SiO_2 (%). SiO_2 in these diagrams is normalized to 100% on a volatile free basis.

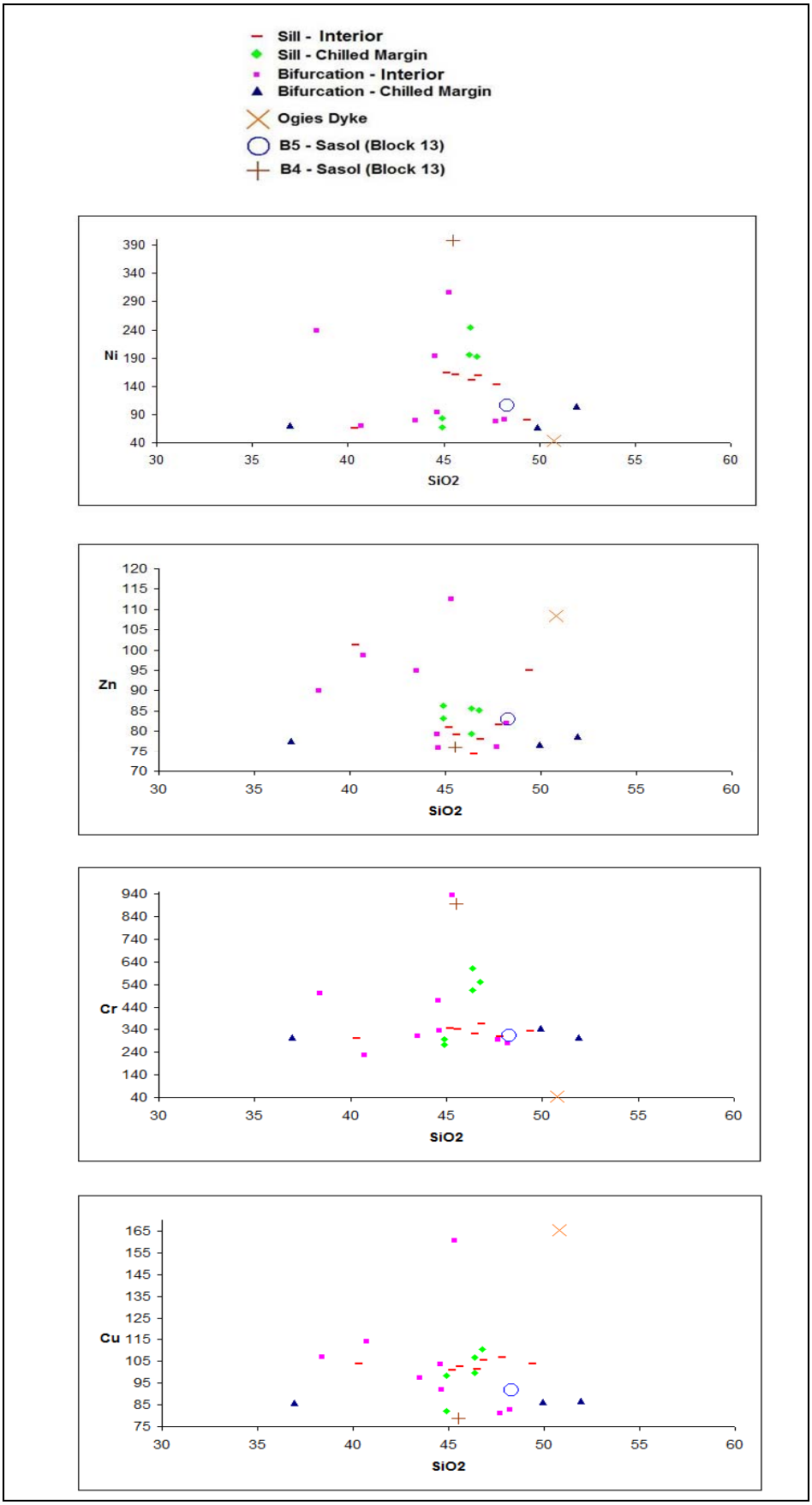

Figure 3.19B Harker diagrams of trace elements (ppm) vs SiO_2 (%). SiO_2 in these diagrams is normalized to 100% on a volatile free basis.

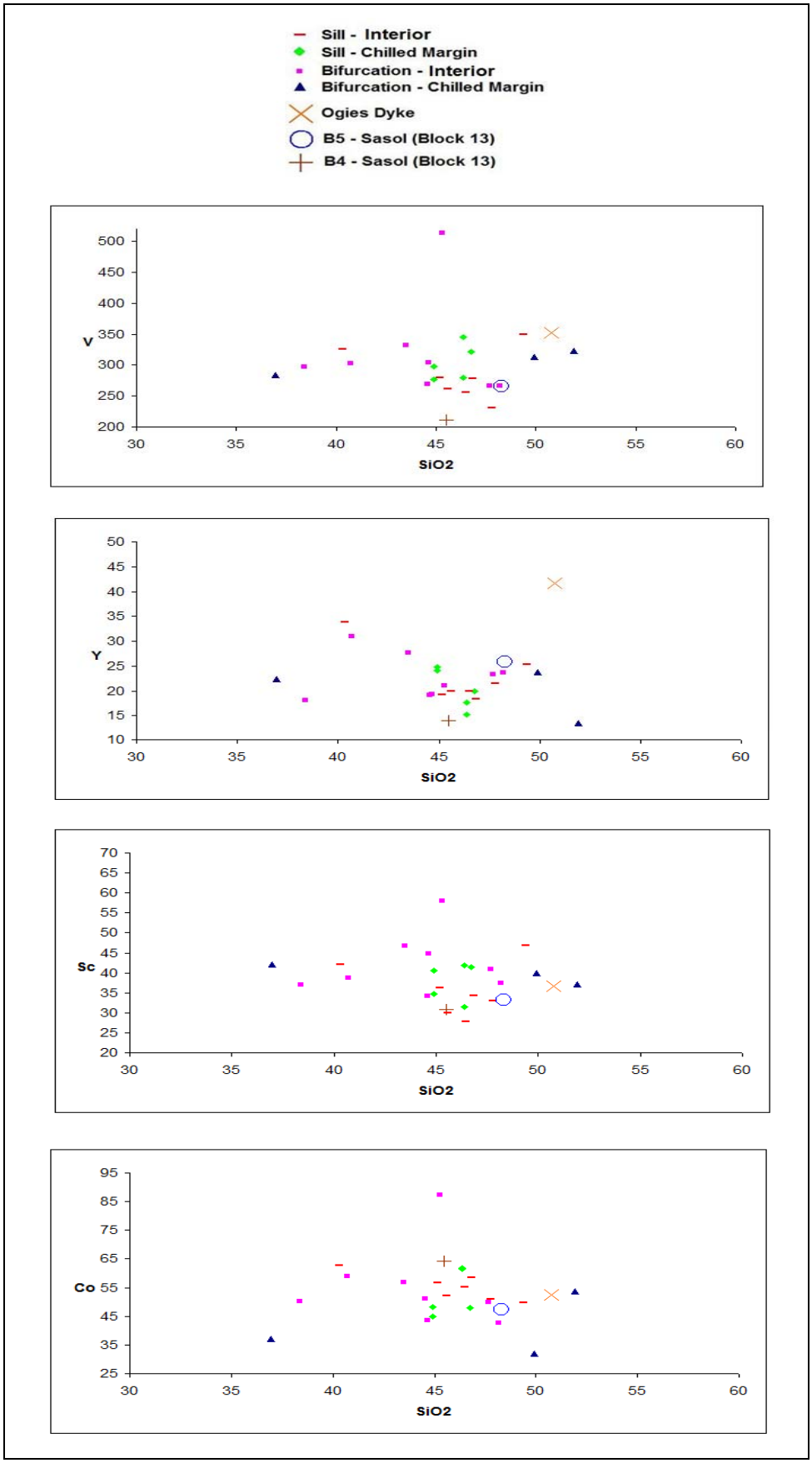

Figure 3.19C Harker diagrams of trace elements (ppm) vs SiO_2 (%). SiO_2 in these diagrams is normalized to 100% on a volatile free basis.

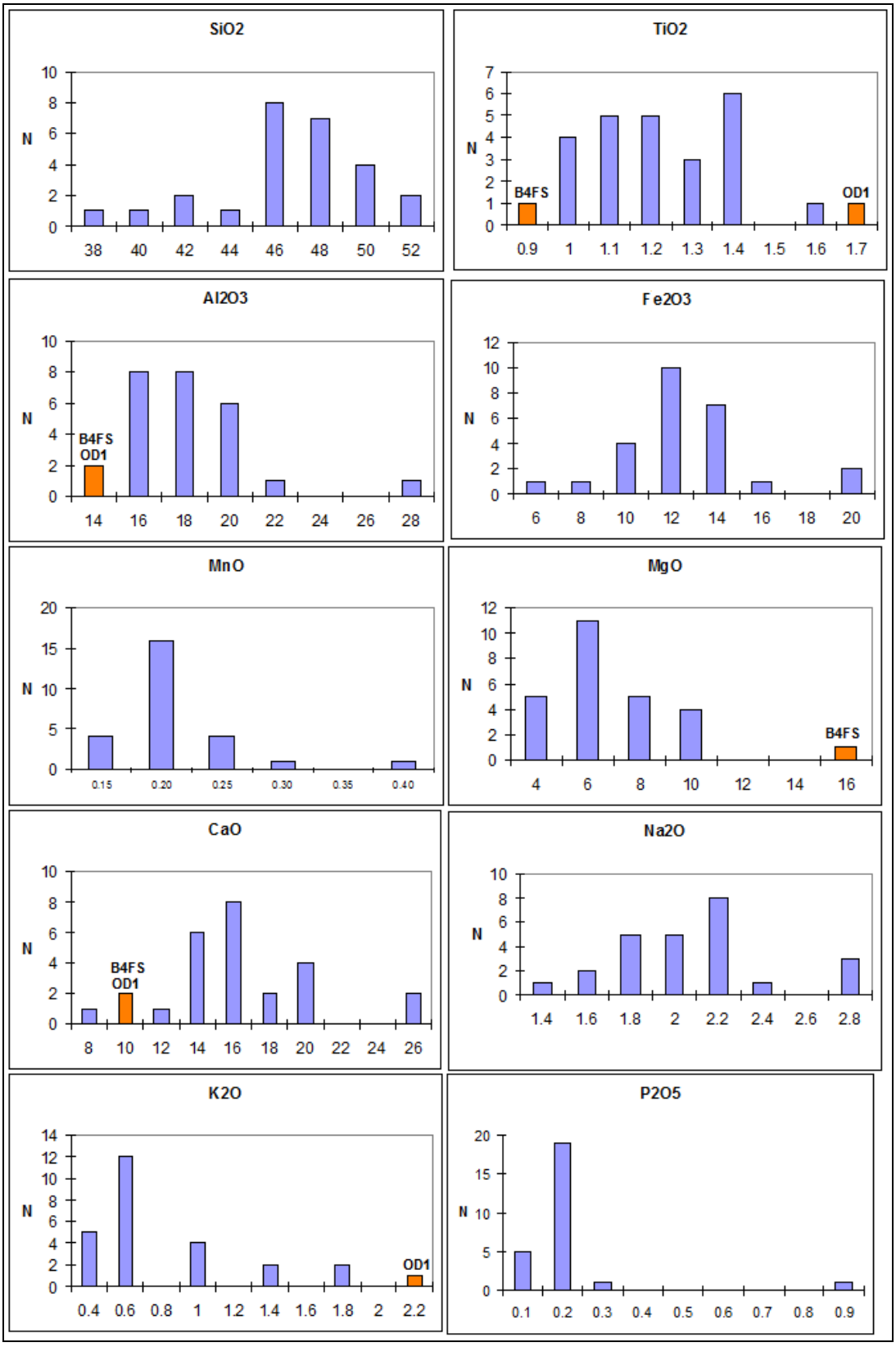

Figure 3.20 Histograms to show the variation in major element concentrations (weight %) of the dolerites (N=26; analyses are from the data in Tables 3.3 and 3.4).

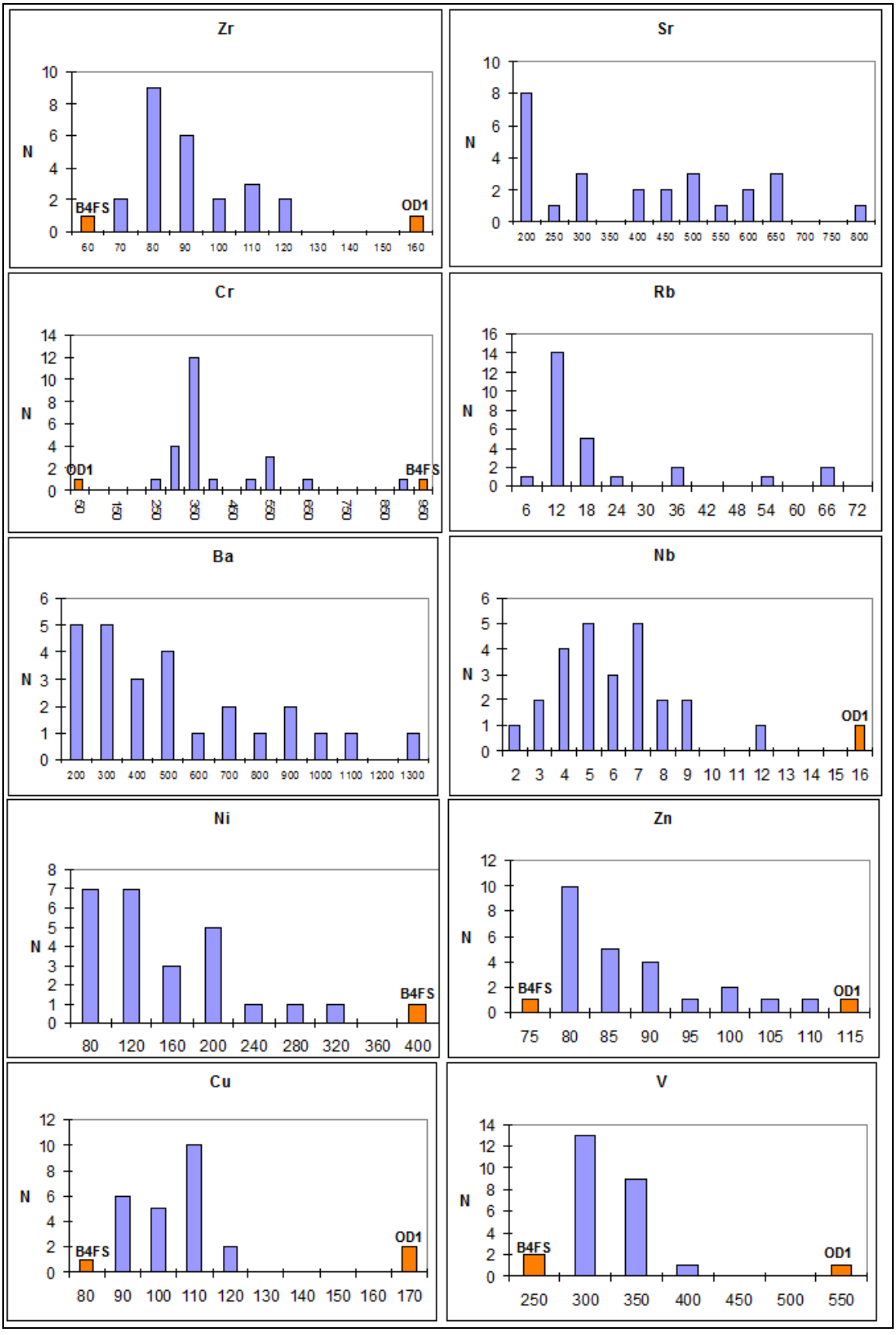

Figure 3.21 Histograms to show the variation in trace element concentrations (ppm) of the dolerites (N=26; analyses are from the data in Tables 3.3 and 3.4).

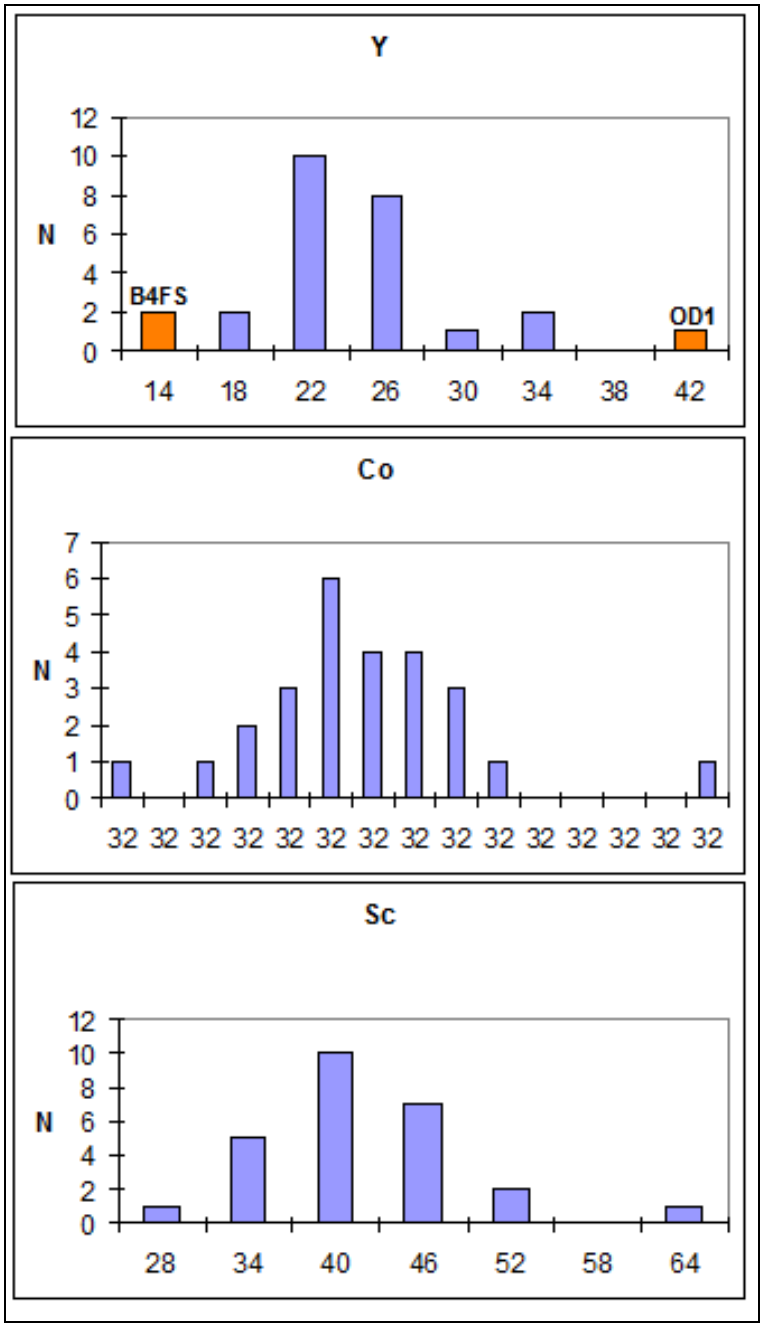

Figure 3.22 Histograms to show the variation in trace element concentrations (ppm) of the dolerites (N=26; analyses are from the data in Tables 3.3 and 3.4).

3.7 Conclusions

When the classification technique of Duncan et al. (1984) is applied all the dolerites in this study are falling in the “basic” group. Bristow and Cox (1984) noted a natural division within the basic volcanics into those of □9% MgO, termed high-MgO or picritic basalts, and those of □9% MgO, termed as basalts. Their additional subdivision at 5% MgO (with Mafic rocks with □5% MgO termed “evolved”. The B4 – Sasol dolerite sll is a high-MgO (picritic) basalt while the rest are

basalts. The chilled margins of the bifurcations have an arithmetic mean of 4.89% MgO and the Ogies Dyke has 4.9% MgO and can be classified as evolved basalts. Lower MgO and Ni values in the Witbank bifurcations comparing to the Witbank sill indicate that the bifurcations are more evolved.

The basaltic and evolved basalts can further be divided into low and intermediate K_2O concentrations. A higher K_2O concentration is placing the Ogies Dyke in the intermediate-K_2O group whilst the Witbank sill (interior and chilled margins), and the Witbank bifurcations (interior and the chilled margins) are all falling in the low-K_2O group. Two of the Witbank bifurcations (interior) having intermediate-K_2O concentrations and are associated with the Ogies Dyke. The picritic B4 sill (Sasol) is also classified as a low- K_2O dolerite.

Considering K_2O and MgO element concentrations the samples are falling in three categories, from evolved to picritic with the majority in the basaltic field (Figure 3.23).

I – Intermediate K_2O, low MgO (evolved)

II – Low K_2O, intermediate MgO (basaltic)

III – Extremely low K_2O, High MgO (picritic)

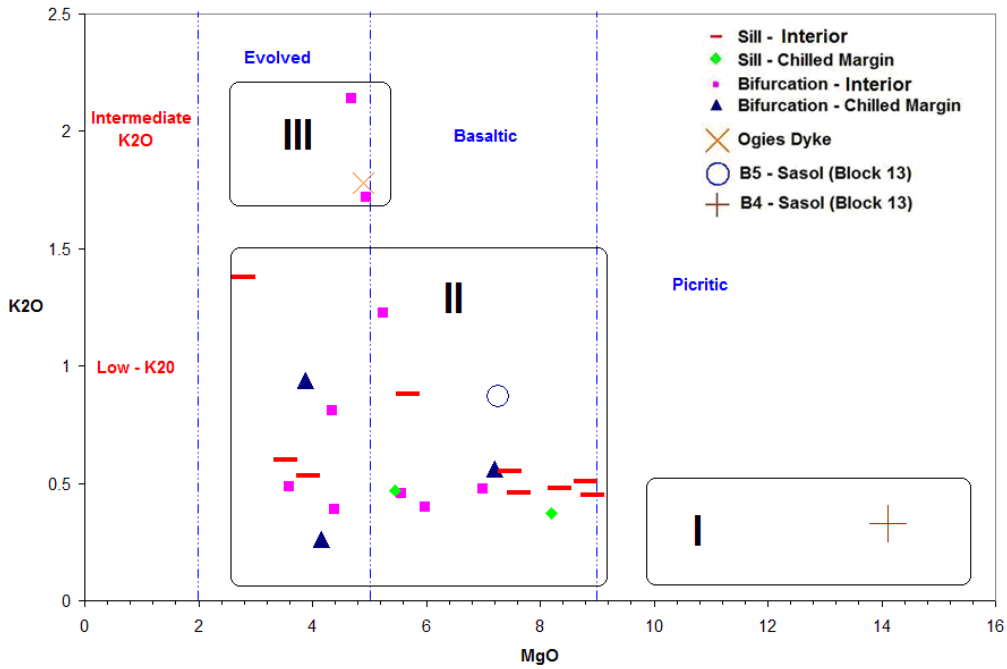

Figure 3.23 MgO vs K_2O diagram indicating the sub-division of the basic dolerites. These sub-divisions are named I (evolved), II (basaltic) and III (picritic).

CHAPTER 4

THE INFLUENCE OF SYNGENETIC FACTORS ON COAL DEPOSITION AND DIAGENESIS

4.1 General coal sedimentological aspects in the south-eastern Witbank Coalfield

Coal deposits in the south-eastern part of the Witbank Coalfield are contained within a clastic sequence designated to the Vryheid Formation, Ecca Group, Karoo Supergroup. Deposition took place during the Early Permian following the Late Carboniferous Dwyka ice age. Palaeoclimate initially influenced depositional environments. The lowermost depositional stages comprise glaciofluvial outwash braided-plain deposits overlying minor deltaic and glaciolacustrine fill. Plant assemblages of the Early Permian attest to a cool climatic regime during deposition of the peat layers, which today comprise the lower-most coals that overlie the Dwyka Formation conformably and in places pre-Karoo basement unconformably (Cairncross, 1989).

The structural history of the Witbank Coalfield suggests that sediments accumulated in a moderately slowly subsiding basin in which transgressive and regressive sedimentation patterns occurred (Table 4.1) (Cadle et al., 1989).

Five coal seams (Figure 4.1) present in the Witbank Coalfield are contained in a 90m thick sequence (Vryheid Formation), consisting predominantly of sandstone with subordinate siltstone and mudstone (Snyman, 1998).

Cairncross and Cadle (1987) established a genetic subdivision for the Vryheid Formation in the east Witbank Coalfield. They identified three sequences comprising depositional events, each defined by a progradational phase, a aggradational phase and a transgressive phase constituting the 90m thick stratigraphic succession. The No. 2, 4 and 5 seam sequences are each terminated by one or more coal seams (Table 4.1, Cairncross and Cadle, 1987).

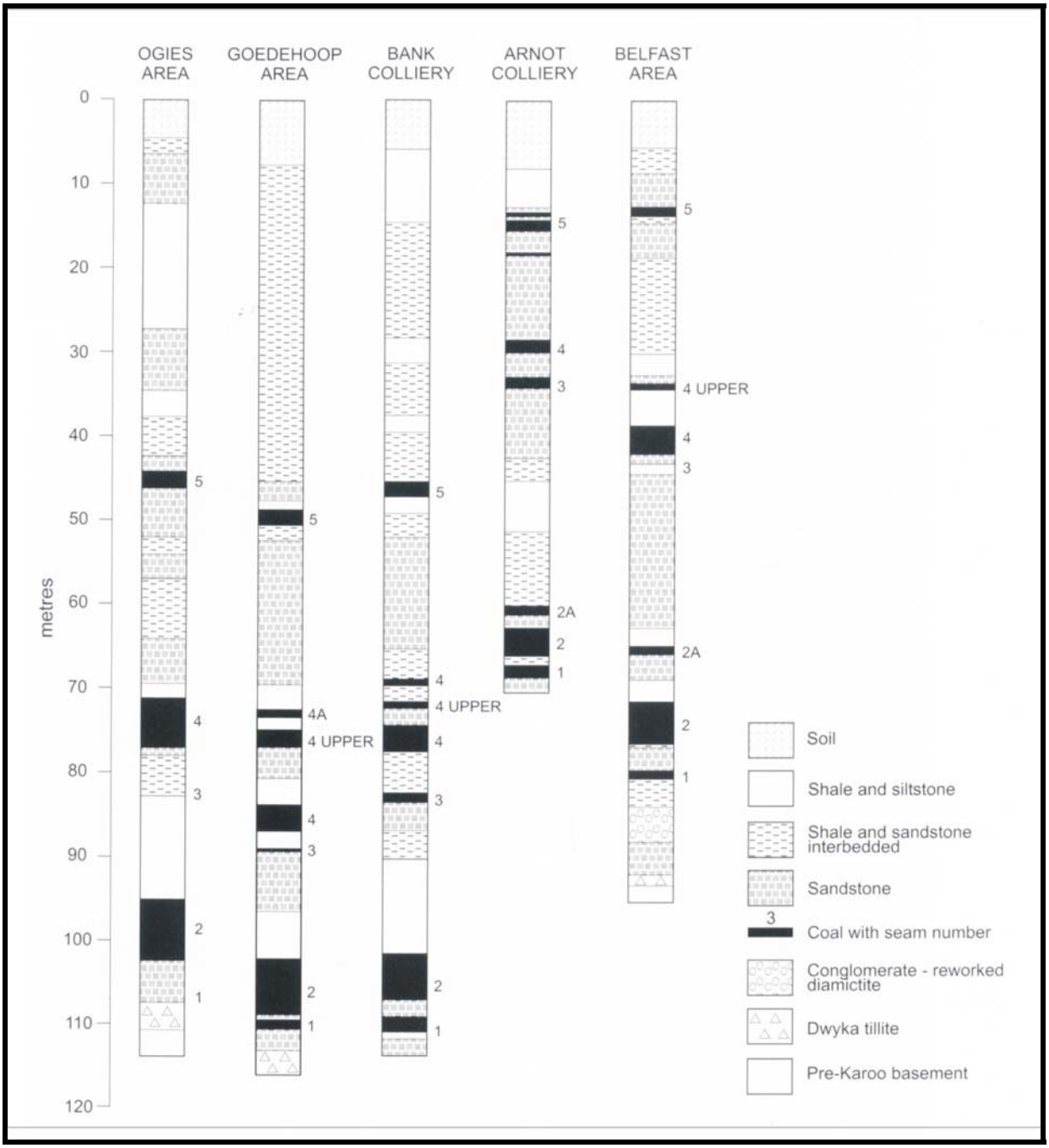

Figure 4.1 Typical stratigraphic columns in the Witbank Coalfield (Smith and Whittaker, 1986).

The lowermost sequence comprises the strata interval between the pre-Karoo basement or Dwyka Formation and the top of the No. 2 Coal Seam (Table 4.1, Cairncross and Cadle, 1987). The No. 4 sequence, which ranges from the top of the No. 2 Coal Seam to the top of the No. 4 Coal Seam, is a succeeding upward-coarsening sequence (Table 4.1, Cairncross and Cadle, 1987).

Table 4.1 Genetic Sequences of the Witbank Coalfield (Cairncross and Cadle, 1987).

	Sequence	From	To	Facies
Upward fining 	No. 5 Seam	Roof of No. 4 Seam	Roof of No. 5 Seam	No 5. Seam
				Interbedded siltstones
				Cross-bedded sandstone
				Cross-bedded granules
				Massive granules
Upward coarsening 	No. 4 Seam	Roof of No. 2 Seam	Roof of No. 4 Seam	No. 4 Seam
				Braided bed-load channel system
				No. 3 Seam
				Fine to Medium grained cross-bedded sandstone
				Interlaminated siltstone sandstone
				Micaceous bioturbated siltstone
				Carbonaceous siltstone
Upward fining and then coarsening 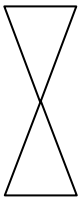	No. 2 Seam	Basement	Roof of No. 2 Seam	No. 2 Seam
				Sandstone
				No. 1 Seam
				Subordinate carbonaceous siltstone
				Sandstone
				Cross-bedded sandstone
				Massive granules

Anastomosed channel deposits within the No. 2 Coal Seam pose some of the most severe underground mining problems and varying coal quality (Cairncross, 1986). These channel deposits a) removed coal by scouring, b) cause loss of tonnages along channel flanks where the seam shows multiple splits and interfingers with channel clastics, c) have thin coal which overlays abandoned channel fill sequences (caused by loading and differential compaction of coal), d) and lower grade coal qualities (Cairncross, 1986).

Cairncross (1986) also found that coal deposits in elevated areas can have higher ash content than stratigraphic equivalent parts of the seam in adjacent lower-lying areas and interpreted that this resulted from partial aerobic oxidation of the peat which caused higher inherent ash concentrations.

Le Blanc Smith (1980) found overall vertical coal seam quality deterioration from the bottom to the top. The basal portions are typically bright; vitrinite rich coal that grade upwards into dull inertinite rich coal, which may indicate a greater degree of exposure

and oxidation upward in seams (Cairncross and Cadle, 1987). It may also be the effect of carbonaceous matter, together with clastic mineral matter, that has been washed in from higher ground. Le Blanc Smith (1980) observed an increase in ash and a decrease in volatile matter and calorific value from the bottom to the top of the coal seams. At the close of peat-forming periods, suspended clastic material sediment was gradually introduced into the swamp by transgressing basinal waters to form a argillaceous layer on top of the carbonaceous matter which could probably be the reason for the increase in ash content (Cairncross, 1989).

The palaeotopography directly controlled sedimentation patterns with the thickest and lowermost coals located in the palaeovalleys (Cairncross, 1989). These coals thin and eventually pinch out against relatively steep valley flanks and palaeohighs (Cairncross, 1989). Coals deposited above abandoned glaciogenic deposits occur in association with lobate deltaic and bed-load fluvial sequences in contrast to younger peat (Cairncross, 1989).

Cadle et al. (1989) defined banding of the No. 2 Coal Seam, using borehole logs and proximate analyses from 15 collieries. They found that internal banding of the No. 2 Coal Seam could be correlated with the underlying pre-Karoo topography. Six bands exist in areas of thickest No. 2 Coal Seam that coincide with palaeo depressions. Where the No. 2 Coal Seam thins out over basement highs, only the No's 2, 3 and 4 bands exist (Cadle et al., 1989) (Figures 4.2 and 4.3). No's 1, 5 and 6 are restricted to thicker seam portions in the palaeovalleys. In Figure 4.3 bands 1, 3 and 5 are associated with bright coal (low ash values, high calorific values and a high volatile matter content), compared to bands 2, 4 and 6, which are associated with dull coal (high ash values, low calorific values and less volatile matter content) (Cadle et al., 1989).

Cadle et al. (1989) listed the following pre-requisites for the formation of low ash, high grade coal:

1. Abundant plant material;
2. a suitable depository;
3. sustained water levels in the swamp to prevent peat degradation;
4. and rapid covering of peat by sediment after peat accumulation in order to prevent oxidation and to enhance preservation after burial.

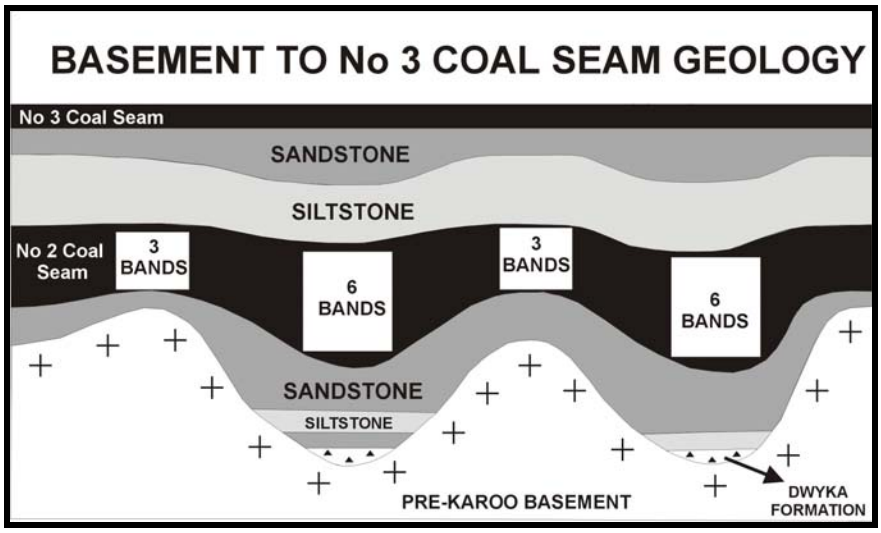

Figure 4.2 Generalized cross-section between basement and No. 3 Coal Seam (Cadle et al., 1989).

Sustained water levels (point 3 above) probably resulted from high peat accumulation rates where peat may have formed above the water level. This younger peat then protects older formations against oxidation. Such protected peat normally has low ash content as no clastic mineral matter could be washed in.

"*Coal quality"* is specified by three independent variables, namely, grade (% ash after combustion), type (maceral and micro lithotype composition) and rank (the degree of metamorphism). For example, a high-grade coal (low ash) may be a low-grade coking coal due to its low vitrinite contents or its subordinate rank. Furthermore, as a sedimentological control on the grade of coal, it may be of interest to quantify the energy conditions under which settling of particles of different diameters will take place (Figure 4.4).

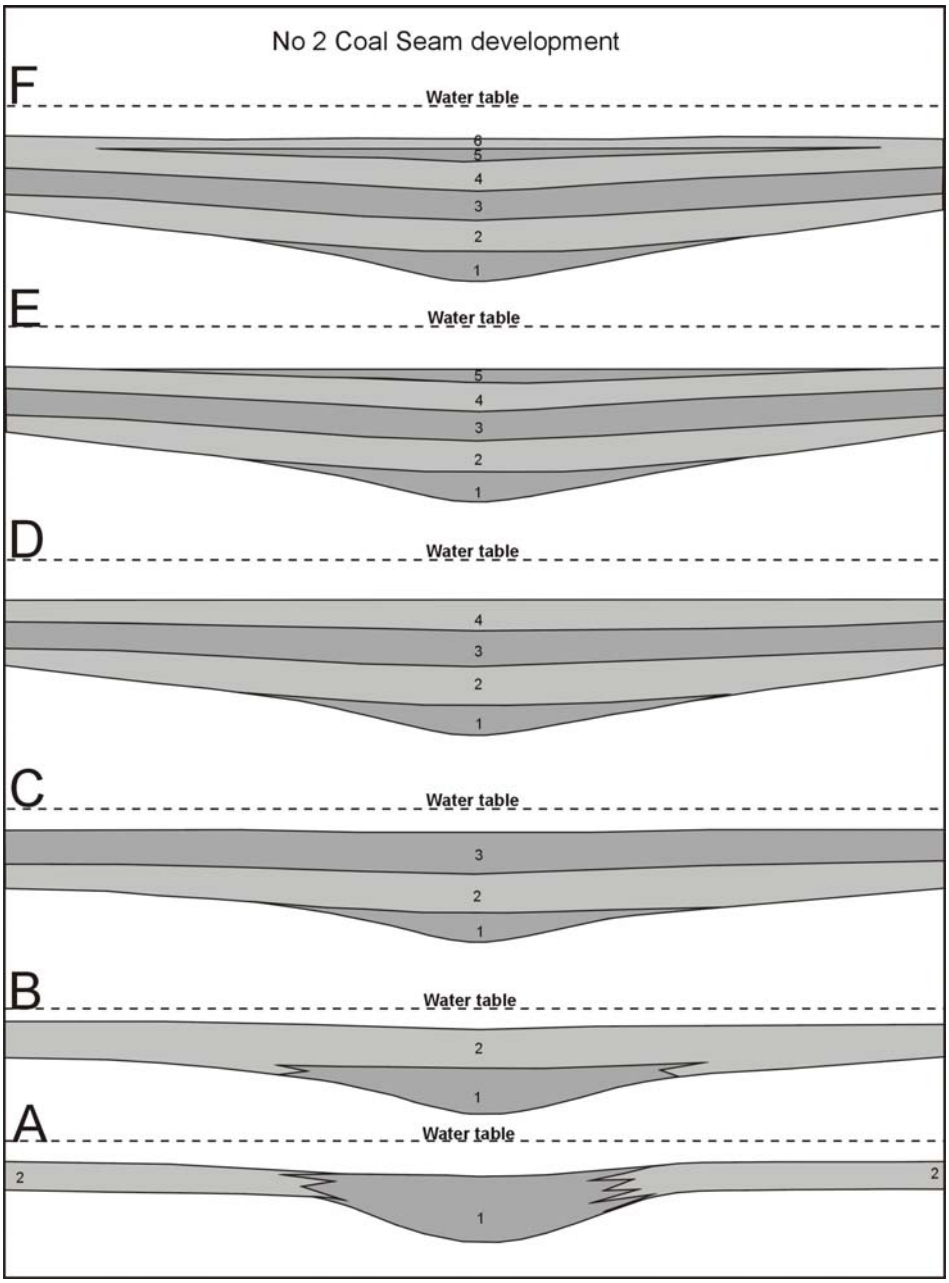

Figure 4.3 Development of in–seam banding during peat accumulation of the No. 2 Coal Seam (Cadle et al., 1989).

Clastic quartz and clay mineral grains associated with inertodetrinite (i.e. occurring in dull coal) are generally less than 0.03 mm, so that a water velocity of less than 3 meter/h is necessary for them (and the associated inertodetrinite precursors at diameter of about 0.04-0.06 mm) to settle. The associate silicate rocks (sandstones and siltstones/shales) would require minimum velocities of 3.5 to 120 and even 180 times that for the relevant grains to settle. Vitrinite precursors probably formed in stagnant water (velocity <0.18 m/h) as they contain colloidal illite as main silicate mineral.

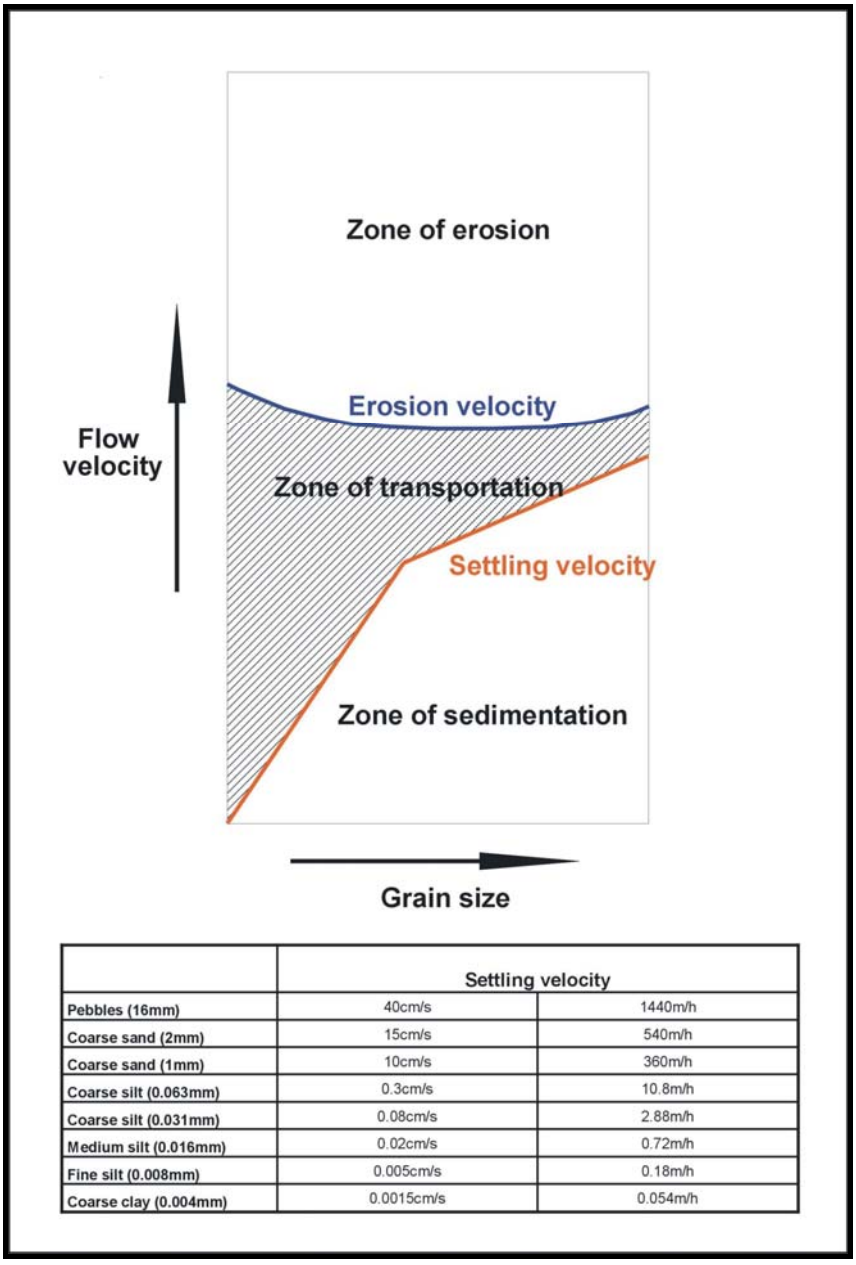

	Settling velocity	
Pebbles (16mm)	40cm/s	1440m/h
Coarse sand (2mm)	15cm/s	540m/h
Coarse sand (1mm)	10cm/s	360m/h
Coarse silt (0.063mm)	0.3cm/s	10.8m/h
Coarse silt (0.031mm)	0.08cm/s	2.88m/h
Medium silt (0.016mm)	0.02cm/s	0.72m/h
Fine silt (0.008mm)	0.005cm/s	0.18m/h
Coarse clay (0.004mm)	0.0015cm/s	0.054m/h

Figure 4.4 ***A diagram of flow velocity against grain size to quantify the energy conditions under which settling of particles of different diameters will take place (settling velocities of different diameters in table underneath diagram) (*Snyman, 2001*).***

Thus, the depositional history of the immediate floor rocks of the coal seam only set the stage for peat formation. The topography of the landscape at the time of peat formation and the climate (dry periods, floods etc.) probably were of greatest importance in

determining type and grade of the coal. Considering the rate of peat formation (about 5 mm/year), stable sedimentation conditions were required for tens of thousands of years, in contrast to a crevasse splay deposit which may form within days as a result of severe flooding.

Cadle et al. (1989) concluded that the No. 2 Coal Seam overlies coarse-grained sandstone deposited by bed-load dominated fluvial systems, and is in turn overlaid by a subregional upward coarsening regressive deltaic sequence. The entire No. 2 Coal Seam sequence overlies an undulating pre-Karoo floor, which has a significant effect on sedimentation patterns (Cadle et al., 1989).

All the economic coal seams in South Africa are confined to specific geographic localities within a restricted stratigraphic interval (Cairncross, 1989). Limited geographical and geological distribution of the coal bearing succession stems primarily with the following regional controls, a) intracratonic setting, b) palaeotopography of basement beneath the coal sequence, c) palaeo-depositional environments that were governed by tectonic and palaeoclimatic factors (Cairncross, 1989).

4.2 Study area – Optimum Colliery

A total number of 293 boreholes have been drilled in the study area (32.9 km^2) at Optimum Colliery (Figure 2.1). None of the boreholes intersected any dolerite with a drill spacing of one borehole per 0.112 km^2. The only dolerite present in the study area is the 15-m thick Ogies Dyke (not to scale on the isopach and isopleth maps to follow), which forms the northern limit of the area that is not associated with any vertical displacement.

4.2.1 Pre-Karoo topography

Seventy five boreholes intersected the pre-Karoo topography at the Optimum study area. These boreholes were used to compile a structure contour map of the elevation in metres above mean sea level (MAMSL) (Figure 4.4) and three-dimensional models of the pre-Karoo topography (Figure 4.5). The thickness map extends over a surface of 30.6 km^2. The boreholes are concentrated along the western side of the north-south

palaeovalley. The details of the contour map and three-dimensional models can thus be questioned.

Deposition of the Ecca Group was preceded by Permo-Carboniferous Dwyka ice age during which the subcontinent was covered by continental ice sheets (Cadle et al., 1990). These ice sheets sculptured the rugged pre-Karoo topography, illustrated in Figure 4.5, prior to deposition of the Ecca Group (Cadle et al., 1990).

The palaeovalley is more or less 5000-m wide with relatively steep flanks to the east (about 20:1000) and the west (about 13:1000) (Figure 4.5). Borehole logs did not contain any detailed lithological descriptions of the pre-Karoo rocks; however, the pre-Karoo rocks in the vicinity of the Optimum Colliery have been described as Rooiberg felsites (Henckel, 2001). Smith (1990) described pre-Karoo rocks at the Optimum Colliery mostly as felsitic and rhyolitic rocks of the Selons River and Damwal Formations (Rooiberg Group) and less frequently as diabase and granites (Rashoop Suite).

Melt water discharged from the north and north-east retreat of the ice sheets (Stratten, 1968; Crowell and Frakes, 1975) served to rework unconsolidated till, as well as to introduce coarse, gravel detritus into the northern basin areas (Cadle et al, 1990). Tillite and overlying glaciogenic strata can, however, be absent, in which case the lowermost coals (No. 1 and 2 Coal Seams) directly overlie the pre-Karoo basement (Cairncross and Hobday, 1985). The lowermost coals originated as a direct result of vegetation proliferation and peat swamp encroachment over the moribund alluvial plains (Cadle et al, 1990). A high water table enhanced peat accumulation and preservation, as the lowermost coals are the thickest and the most widespread in the region (Cadle et al, 1990).

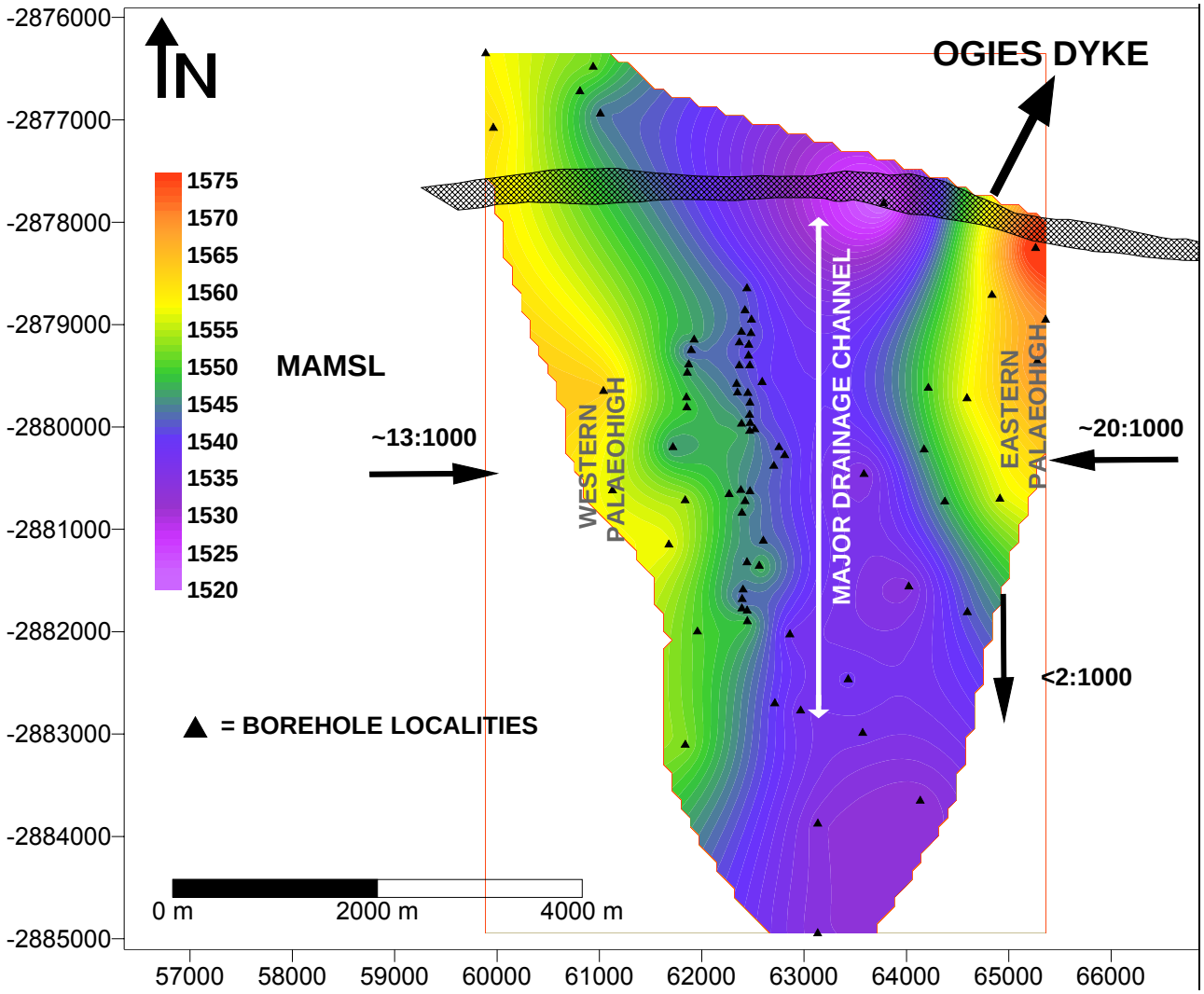

Figure 4.5 *Contour map of the pre-Karoo topography in the vicinity of the Optimum Colliery (contours in metres above mean sea level=MAMSL).*

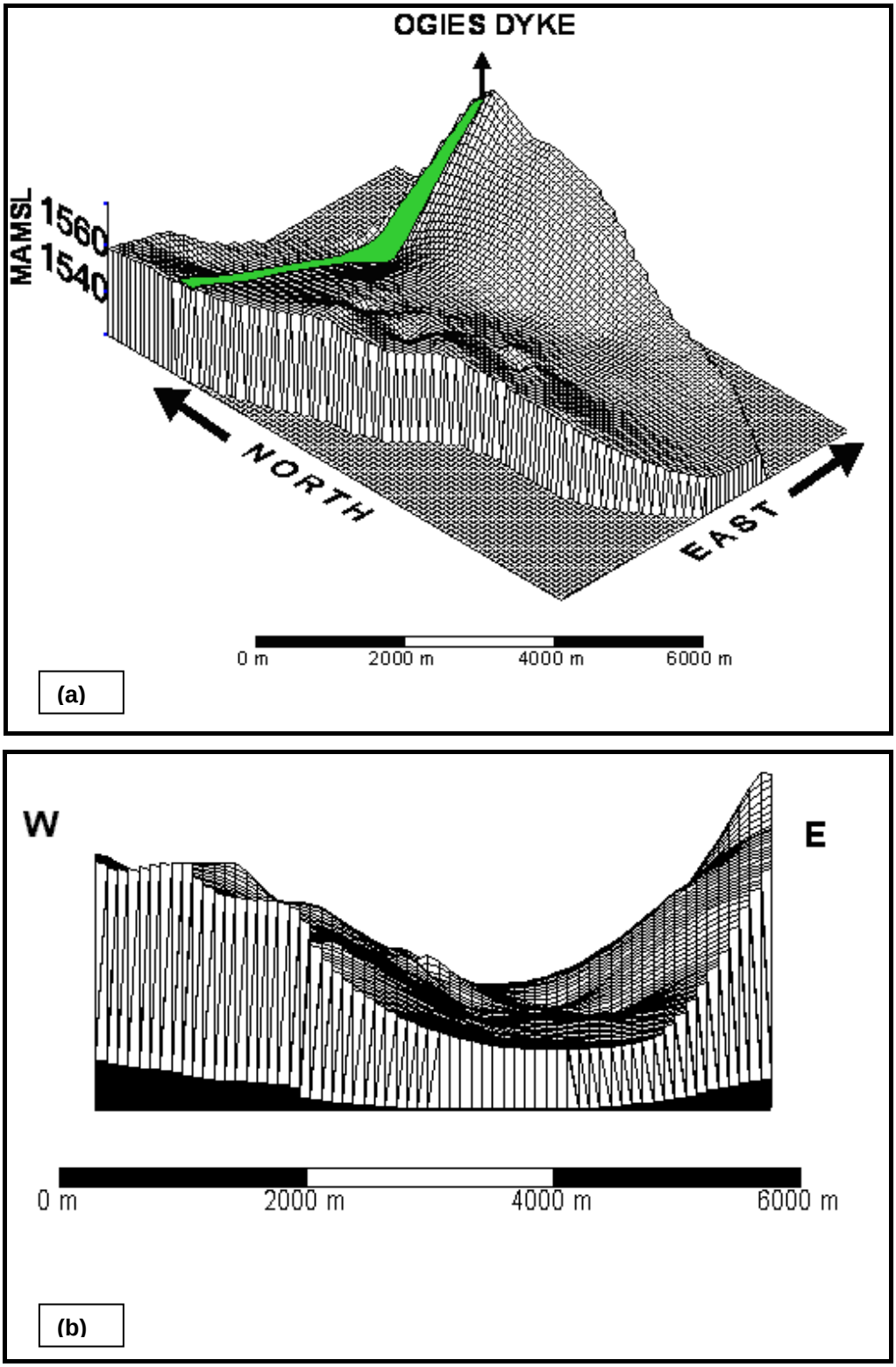

Figure 4.6 ***Three-dimensional models of the pre-Karoo topography at the Optimum Colliery. (a) Perspective image looking north-east (the green line only indicates the position of the Ogies Dyke), (b) northerly view along the valley axis.***

4.2.2 No. 2 Coal Seam

4.2.2.1 Floor elevation (MAMSL) and thickness distribution.

Detailed stratigraphic subdivisions of the No. 2 Coal Seam north-east of Optimum Colliery have been done by Cairncross (1986) (Table 4.2). The No. 2 Coal Seam contains several clastic partings; therefore he subdivided it into the 2 Lower, 2 Upper and the uppermost 2 A. Three splits of the No. 2 Coal Seam also exist in the study area at Optimum Colliery, but they are called the 2 A, 2 Lower and the 2 Upper (Table 4.2). The No. 2 Upper Coal Seam is the thickest split and is also well developed throughout the entire study area at Optimum and therefore used for this study.

Table 4.2 Comparison between stratigraphic subdivisions of the No. 2 Coal Seam in the eastern part of the Witbank Coalfield.

No. 2 Coal Seam	Cairncross (1986)	Optimum
	Uppermost 2A	2 Upper
	2 Upper	2 Lower
	2 Lower	2A

The floor elevation of the No. 2 Upper Coal Seam was contoured in 1 m intervals (Figure 4.6). A reasonable match exists between the pre-Karoo topography (Figures 4.5 and 4.6) and the contour map (Figure 4.7). However, it should be mentioned here that the platforms onto which the various coal seams have developed were followed by burial that resulted in the present floor elevations.

The south-western limit of the Optimum reserve area (which is the western limit of the study area) is formed by a ± 15m-thick dolerite sill (Smith, 1990). This dolerite sill was not intersected in any borehole drilled in the study area; thus, no displacement allowance in the contouring was necessary.

Small-scale depressions in the underlying pre-Karoo basement in the Witbank Coalfield are filled with isolated deposits of Dwyka tillite (Cadle et al., 1989). A regional braided channel deposited sand and gravel over a broad alluvial plain which provided the platform upon which the No. 1 and 2 Coal Seams accumulated (Cadle et al., 1989). Again it should be mentioned that the present undulating coal seam floor elevations and thicknesses resulted from post burial events. Coal seams display 20-35% and the clastic sedimentary rocks 60-90% of its original thicknesses (Cadle et al., 1989).

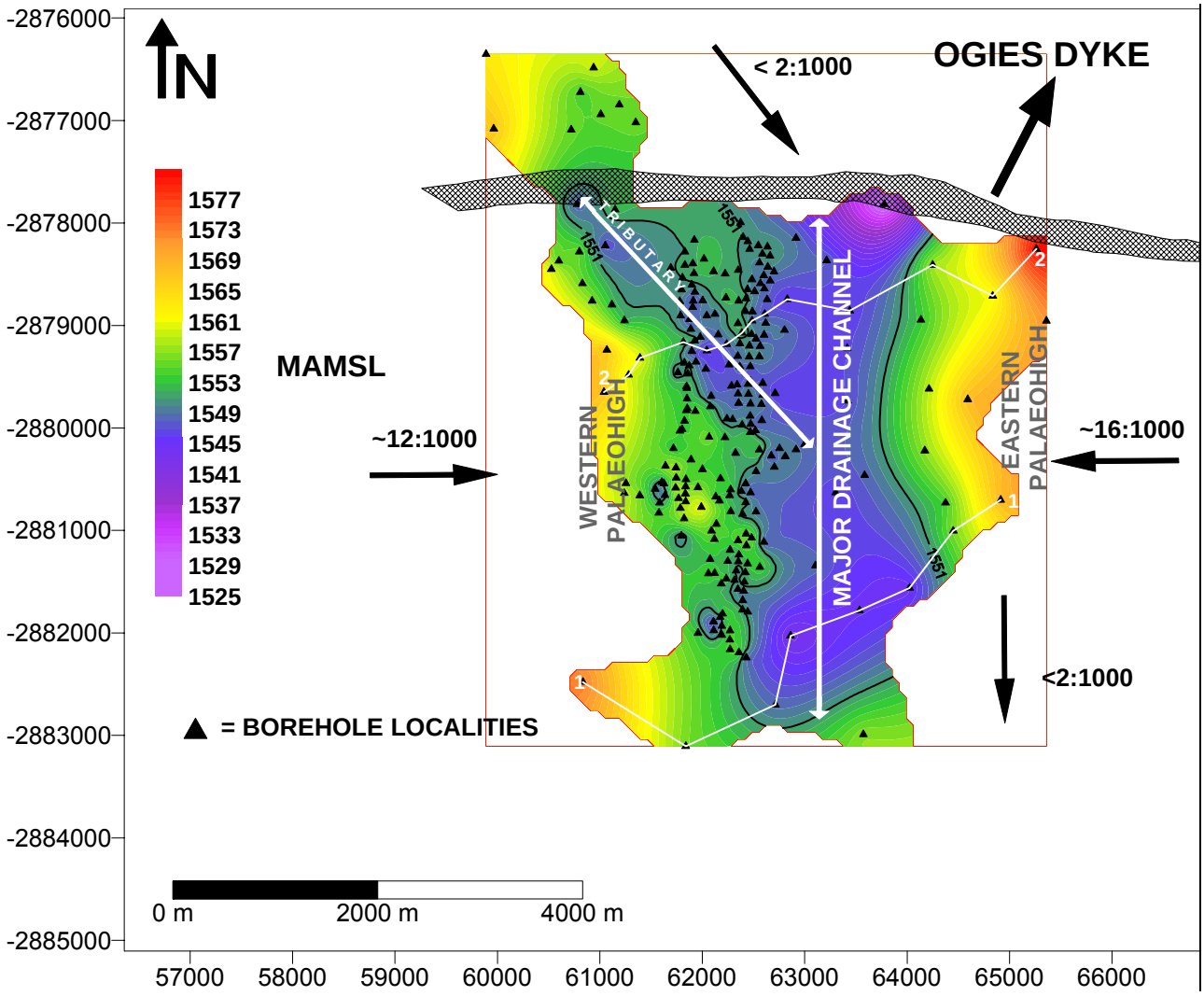

Figure 4.7 ***Contour map of the floor elevation of the No. 2 Upper Coal Seam at the Optimum Colliery study area (contours in MAMSL). The two white east-west lines indicate the geological cross-sections in Figures 4.12 and 4.13. The 1551 MAMSL contour is shown as a solid line.***

The 1551 MAMSL contour in Figure 4.7 is a solid line to delineate the major north-south drainage channel. Borehole data indicates that a north-west, south-east trending tributary of the main palaeo-channel is also present.

Due to the clastic sediments forming the floor of the No. 2 Upper Seam, the pre-Karoo topography has been evened out, so that the main palaeovalley and the tributary channel have slopes of less than 2:1000, whereas the eastern and western valley flanks have slopes of about 16:1000 and 12:1000 respectively. However, the valley flanks of

the pre-Karoo topography (Figure 4.5) are still outlived by the floor structure of the No. 2 Upper Coal Seam.

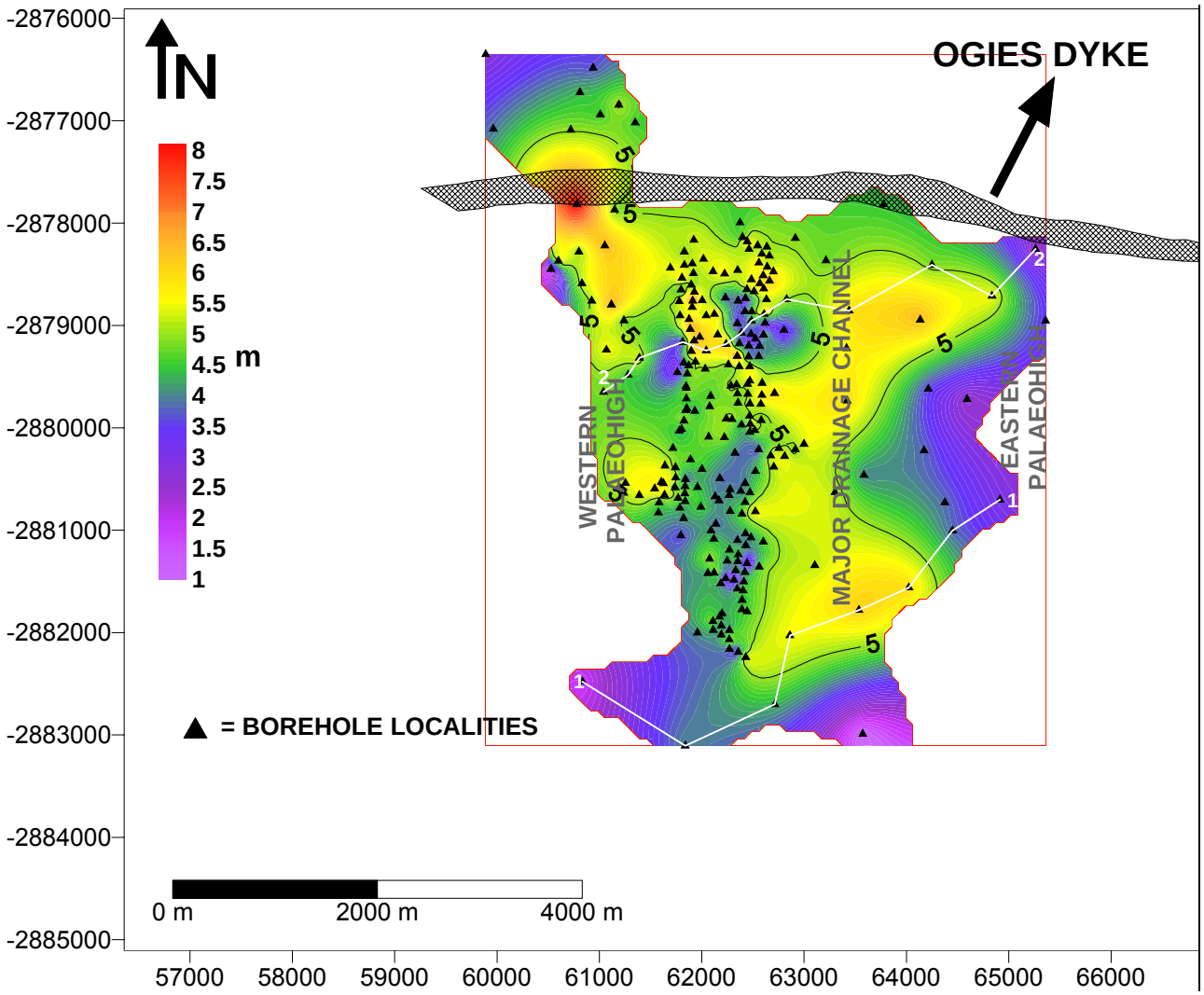

Figure 4.8 ***Isopach map of the No. 2 Upper Coal Seam in the Optimum Colliery study area. The two white east-west lines indicate the geological cross-sections in Figures 4.12 and 4.13. The 5m isopach is shown as a solid line.***

The isopach map of the No. 2 Upper Coal Seam shows considerably thicker coal in the main palaeovalley and in the tributary channel, compared the eastern and western high lying areas (Figure 4.8). Bright coal represents only about 10% of the original peat thickness, whereas in the case of dull coal (rich in inertodetrinite, i.e. fairly strongly oxidised peat detritus) the compaction figure may be about 50-60% (Snyman, 2001). The high Volatile Matter of the coal on especially the eastern palaeohigh (Figure 4.13) suggests that many of these “thin coals” may actually be vitrinite-rich (i.e. bright to semi-

bright) so that coal thicknesses of 1-3m may in fact represent thicknesses of 10-30m peat, whereas the thick coal in the northwest (>7m) may be dull (ea 20% VM), representing a peat thickness of about 11-14m.

A total of 248 boreholes intersected the No. 2 Upper Coal Seam in the Optimum study area. A correlation coefficient of only –0.42 between floor elevation and thickness of the No. 2 Upper Coal Seam was found (Figure 4.11). The following reasons could have resulted in the low correlation coefficient, namely:

- The highly irregular distribution of boreholes obviously favours the western portion of the north-south palaeovalley and the adjoining valley side (Figure 4.7).

- The non-uniform compaction of peat to coal, which is about 90% in the case of bright coal and about 40-50% in the case of dull coal. Shaly coal (>40% ash) probably has a compaction figure similar to dull coal (Figure 4.10).

- Also, probably at the time of peat formation, the underlying sediments had not yet undergone complete compaction and lithification, so that the floor of the peat might have been without undulations, except for the pre-Karoo highs not covered by younger sediments, i.e. the present floor topography and coal thickness were superimposed by compaction after peat formation (Figure 4.10).

Therefore it was decided to concentrate in on a larger scale by drawing two geological cross-sections (Section 1 and 2 in Figures 4.12 and 4.13).

The thickest No. 2 Upper Seam was intersected in the north-west corner (just south of the Ogies Dyke) (Figure 4.8) with a thickness of 8.34 m in the northern end of the north-west, south-east tributary. Its analyses yield 27,1% ash (air-dry), 1.27 % moisture (air-dry), 14.2 % VM (air-dry), 57.3 % fixed carbon (air-dry) and a CV of 24.02 MJ/kg. The fairly high ash content and thick coal suggest that the thickest peat accumulation occurred in low lying areas.

In Figure 4.8 the 5 m isopach is shown bold to separate thick coal accumulation (>5m thick coal) and thin coal accumulation (<5m thick coal). This 5m isopach was digitized and overlain on a three-dimensional model of the No. 2 Upper Coal Seam floor elevation so that the grey area in Figure 4.9 delineates coal of ≥5m thick. Thicker peat not only occurs in the palaeovalley but tends to be present on the valley flanks or palaeohigh areas as well (Figure 4.10).

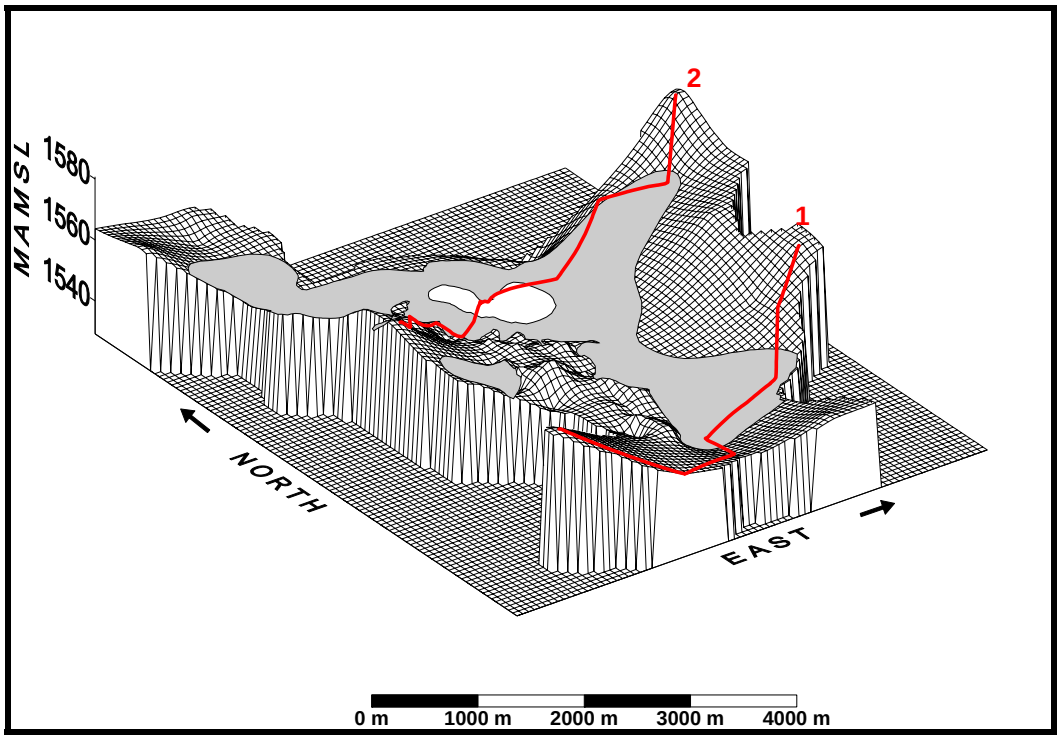

Figure 4.9 ***Three-dimensional model of the floor elevation in MAMSL of the No. 2 Upper Coal Seam, Optimum Colliery study area. The grey area indicates a coal thickness of >5m. The two red east-west lines indicate the geological cross-sections in Figures 4.12 and 4.13.***

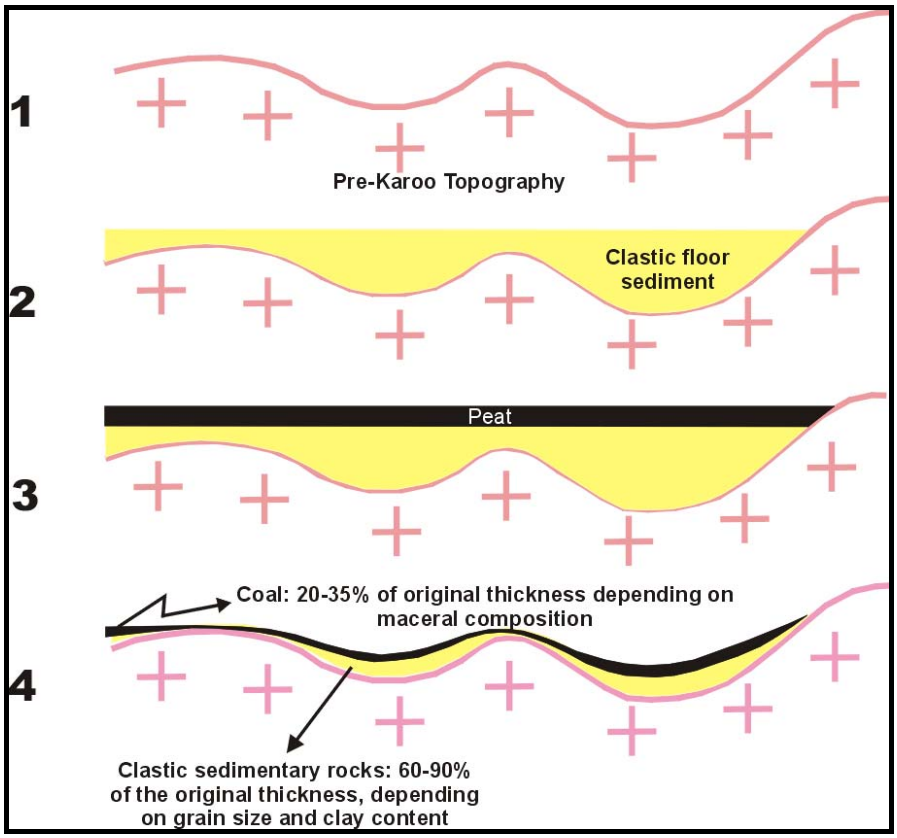

Figure 4.10 ***Four stages indicating how burial could have influenced the compaction of peat and clastic sedimentary rocks (*Snyman, 2001*).***

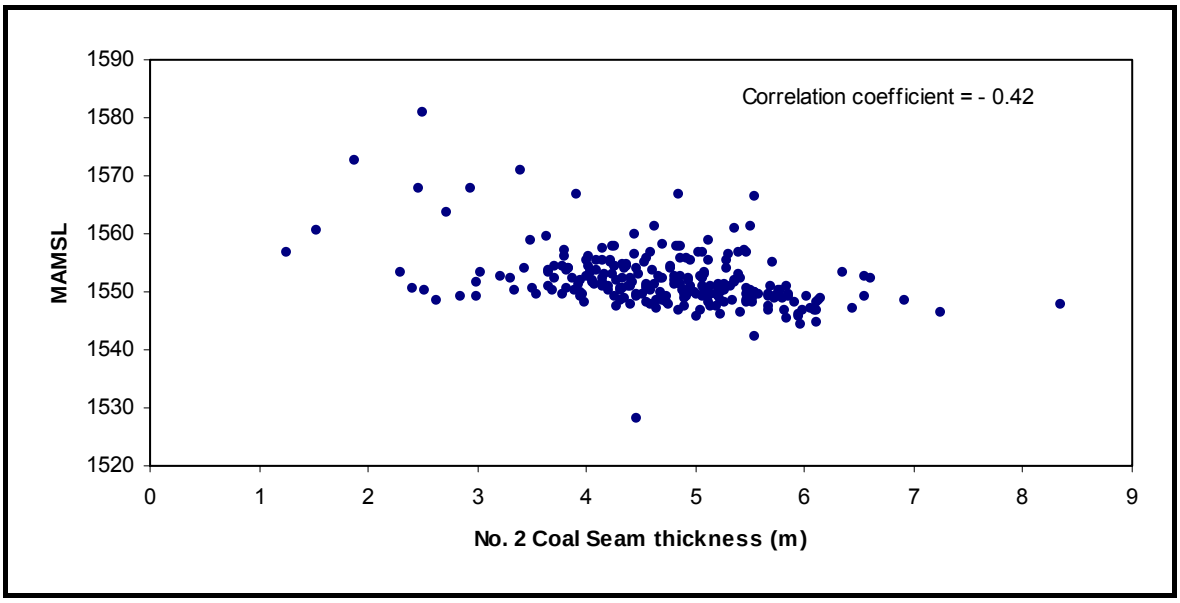

Figure 4.11 ***Correlation between No. 2 Upper Coal Seam thickness (m) and its floor elevation (MAMSL).***

4.2.2.2 Geological cross-sections

Two geological cross-sections show the floor elevation in MAMSL and thickness of the No. 2 Upper Coal Seam in Figures 4.12 and 4.13. Correlation coefficients between thickness, floor elevation and various coal quality parameters were calculated for both sections.

Section 1:

Geological cross-section 1 is based on eight boreholes, and indicates floor elevation in MAMSL and coal thickness (Figure 4.12).

The correlation coefficients between various coal parameters are given in Table 4.2, where significant values are shown in red. Significant values indicate that coals deposited on the valley flanks are thinner, higher in ash (air-dry), lower in VM (daf), lower in CV MJ/kg (air-dry), higher in relative density in contrast with coals deposited in the lower-lying areas of the palaeovalley.

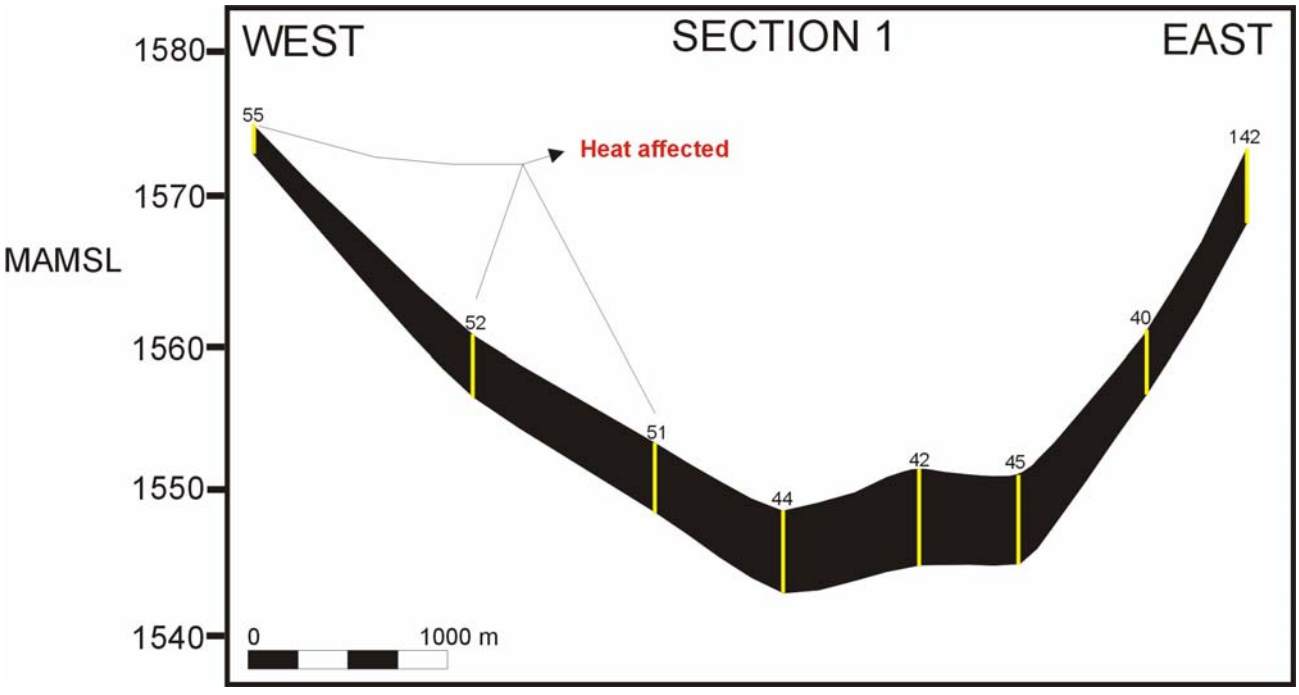

Figure 4.12 Geological cross-section showing the floor elevation in MAMSL and thickness (m) of the No. 2 Upper Coal Seam. The yellow lines and above numbers indicate borehole localities and names respectively.

Table 4.3 Correlation coefficients for Section 1.

	Thickness (m)	Floor Elevation (MAMSL)	Relative Density	Calorific Value (air-dry)	Fixed Carbon (air-dry)	Ash (air-dry)	Moisture (ash-free)	Volatile Matter (dry,ash-free)
Thickness (m)	1.00							
Floor elevation (MAMSL)	**-0.79**	1.00						
Relative density	**-0.68**	**0.75**	1.00					
Calorific value (air-dry)	0.59	**-0.81**	**-0.92**	1.00				
Fixed carbon (air-dry)	-0.30	-0.13	-0.15	0.47	1.00			
Ash (air-dry)	**-0.63**	**0.83**	**0.95**	**-0.97**	-0.34	1.00		
Moisture (ash-free)	-0.27	0.25	0.36	-0.51	-0.48	0.29	1.00	
Volatile matter (dry,ash-free)	**0.73**	-0.40	-0.47	0.16	**-0.79**	-0.29	0.22	1.00
Average	4.5	1554.1	1.55	23.19	52.6	25.7	3.7	26.3

Figure 4.12 proves that the coal pinch out towards the valley flanks. Higher ash values in the elevated areas have been explained by Cairncross (1986) and Cadle et al. (1989) by assuming that shallower water levels which resulted in a lower preservation potential of the peat material has led to a relative increase in ash values (Figure 4.16).

Some of the correlations correspond with the findings of Cadle et al. (1989) where the lower-lying coals contained low ash values, high CVs and a high VM content. However a dolerite sill intrusion west of the section devolatilised the coal in boreholes 51, 52 and 55 and also lowered the CV as a result of oxidation of the coal by groundwater associated with the dolerite.

Section 2:

Geological cross-section 2 is situated north of Section 1 and is based on 14 boreholes. Figure 4.13 only indicates floor elevation in MAMSL and coal thickness across the same north-south trending palaeovalley and also across the tributary from the north-west.

In Section 2 the No. 2 Upper Coal Seam has a more irregular floor elevation compared to Section 1. Figure 4.13 shows that the thickest coal was formed in the lower-lying areas and that the coal is thinning towards elevated areas.

The correlation coefficients between various coal parameters, based on data used for Section 2, are given in Table 4.4. Once again significant correlation coefficients are shown in red. Only seam thickness is significantly negatively correlated with floor elevation, although the correlation is poorer than for Section 1 (-0.66 compared with –0.79). In general the same tendencies are present in the samples of Section 2 as in Section 1, but at a much lower order of significance (Table 4.5).

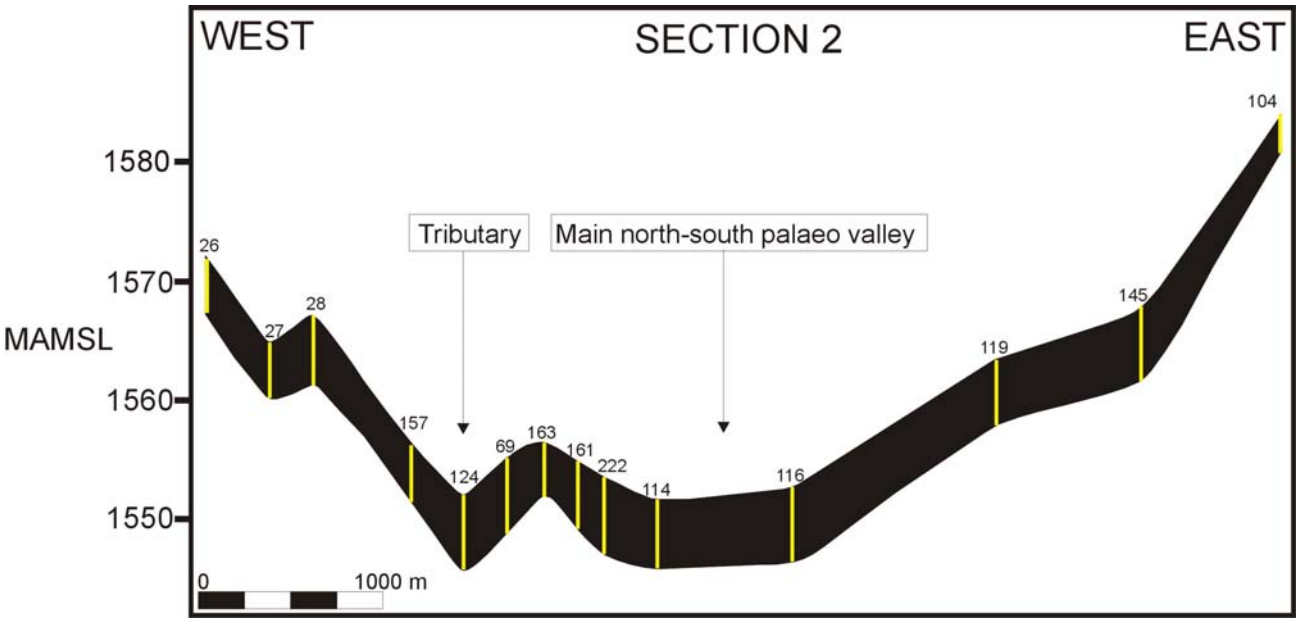

Figure 4.13 Geological cross-section showing the floor elevation in MAMSL and thickness (m) of the No. 2 Upper Coal Seam. The yellow lines and above numbers indicate borehole localities and names respectively.

Table 4.4 Correlation coefficients for Section 2.

	Thickness (m)	Floor Elevation (MAMSL)	Relative Density	Calorific Value (air-dry)	Fixed Carbon (air-dry)	Ash (air-dry)	Moisture (ash-free)	Volatile Matter (dry,ash-free)
Thickness (m)	1.00							
Floor elevation (MAMSL)	**-0.60**	1.00						
Relative density	0.05	0.55	1.00					
Calorific value (air-dry)	-0.17	-0.48	**-0.90**	1.00				
Fixed carbon (air-dry)	0.04	-0.44	**-0.74**	**0.80**	1.00			
Ash (air-dry)	0.13	0.48	**0.89**	**-0.98**	**-0.87**	1.00		
Moisture (ash-free)	0.48	-0.48	-0.27	0.45	0.52	-0.51	1.00	
Volatile matter (dry,ash-free)	-0.39	0.15	0.00	0.00	**-0.59**	0.13	-0.36	1.00
Average	4.9	1555.3	1.54	23.26	47.6	24.7	3.5	34.4

Table 4.5 Geographical variations of coal parametres to the topography of the No. 2 Upper Coal Seam.

	Parametres	Palaeohigh	Palaeolow	Correlation coefficient
Section 1 (in the South)	**Seam Thickness**	Thin	Thick	-0.79
	Relative density	High	Low	0.75
	Calorific value (air-dry)	Low	High	-0.81
	Ash (air-dry)	High	Low	0.83
Section 2 (in the North)	**Seam Thickness**	Thin	Thick	-0.60
	Relative density	High	Low	0.55
	Calorific value (air-dry)	Low	High	-0.48
	Ash (air-dry)	High	Low	0.48

The controlling factors during the deposition and diagenesis of the plant material in the south and the north of this study area (Optimum Colliery) may have been the same although differences in the degree of intensity exists (Table 4.5).

The differences in correlation coefficients between relative density and fixed carbon (air-dry) for Sections 1 and 2 (respectively –0.15 and –0.74) and between ash content (air-

dry) and fixed carbon (air-dry) (respectively –0.34 and –0.87) can be explained by the fact that ash content and relative density are a first approximation. Both ash content and relative density are functions of one independent coal classification variable, namely coal grade. Whereas fixed carbon depends on all three independent classification parameters, namely coal grade, type and rank. Even in its simplest form, fixed carbon depends on the content of moisture, ash and VM, e.g. at the same d.a.f. VM content:

Fixed carbon = 100 – (3% moisture +20% ash + 25% VM) = 52%
And fixed carbon = 100 – (3% moisture + 35% ash + 21% VM) = 41%

Therefore if VM could remain constant, fixed carbon would be inversely proportional to the ash content.

4.2.2.3 Geographical variations of various coal parameters in the No. 2 Upper Coal Seam – Optimum Colliery

Before attempting to generate the relevant isopleth maps, statistical correlations of the data are presented (Tables 4.7and 4.8) as they may facilitate the discussion that follows. In these tables significant correlation coefficients are shown in red. A distinction was made between coal with more than 28% VM (daf) (222 boreholes) and coal with less then 28% VM (daf) (26 boreholes). These latter samples were regarded as being partly devolatilised by dolerite, especially in the north-western and south-eastern portions of the study area. The relative high negative correlation coefficients between VM (daf) and relative density and also between VM (daf) and ash content (respectively –0.58 and –0.44) (Table 4.6) suggest that this may indeed be the case, as secondary carbonate minerals commonly have been precipitated in degasification pores of heat-affected coal.

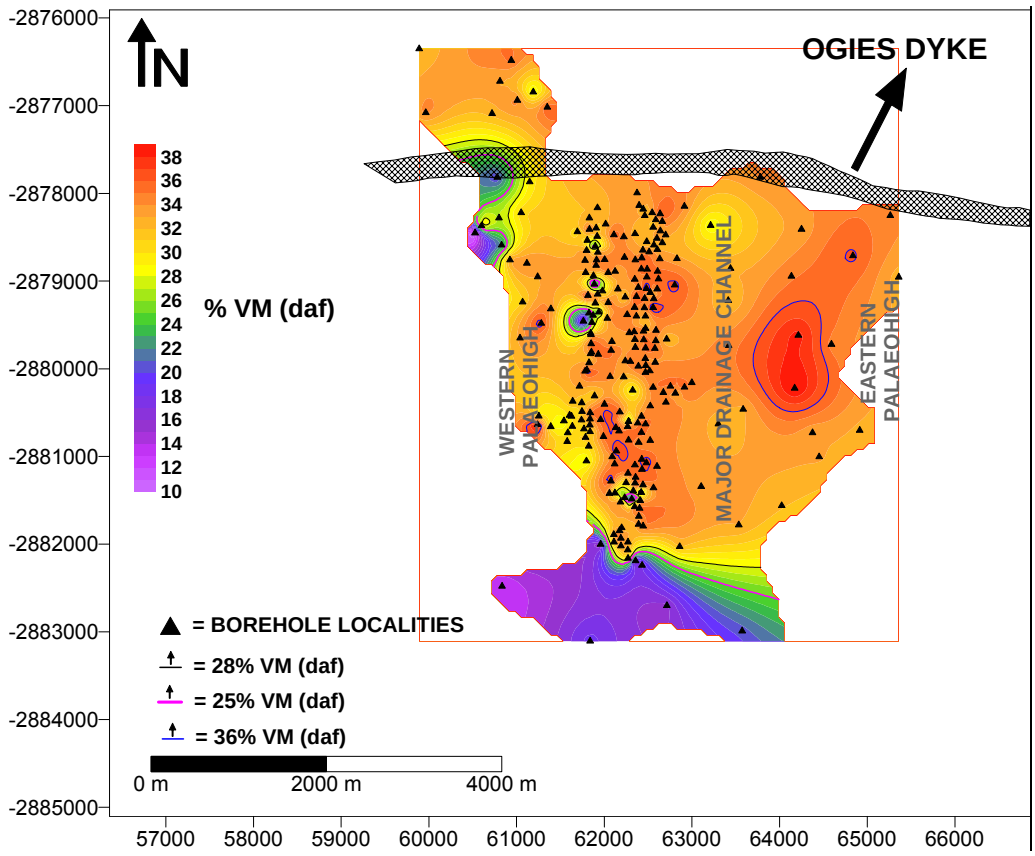

Figure 4.14 Isopleth map of the VM content (daf) of the coal in the No. 2 Upper Coal Seam.

Volatile matter Content:

The volatile matter content of coal is of great importance during many technological applications (Hagelskamp, 1987):

- It contributes to pore-formation and swelling due to degasification during carbonisation of coking coals.
- It is responsible for the coal gas used for household and industrial heating, produced by carbonisation in gas factories.
- It contributes to flame stability in combustion processes, especially in pulverised coal used for power generation.

Stach et al., (1982) have found that VM is dependent on maceral composition and results from peat preservation, which is controlled by depositional environments. In low-rank coals, VM is an indication of type rather than rank.

No dolerites were intersected during drilling in the study area, but Smith (1990) reported a green olivine-rich dolerite sill to the west of this area which caused the coal

devolatilisation delineated by the 28% VM (daf) contour in Figure 4.14. In this area a displacement of ±10 m is indicated by elevation differences of the floor of the seams which is in agreement with the average thickness of the sill (11.25 m) (Smith, 1990). A broad zone of 600m devolatilisation only in the extreme west part of the Optimum Colliery is associated with the Ogies Dyke running east-west (Smith, 1990)

This broad zone which narrows eastwards terminates in a roughly circular zone, 1.3 km in diameter, where all the coal is devolatilised (Smith, 1990). The study area at Optimum is located approximately 5 km west of this circular shape of the Ogies Dyke. The coal from only one borehole on the far western vicinity of the Ogies Dyke (Figure 4.14) is strongly devolatilised (±15VM daf), but this can also be related to the nearby sill to the west. However, some of the high volatile matter values coincide with relatively high ash values (Figure 4.17) close to the Ogies Dyke. Values of more than 36% VM (daf) are delineated by the blue contour line in Figure 4.14. According to Harvey and Dillon (1985) in the Illinois coal seams with such high volatile matter, the contents probably represent underlying crevasse, levee or channel deposits that allowed higher plant density to grow, due to more nutrient supply and stable rooting ground. The higher water level would have provided better preservation conditions which probably resulted in higher contents of vitrinite, which has a higher VM content than inertinites of the same rank (Stach et al., 1982). Coals with an extremely high VM (daf) content of more than 38% represent deep water depositional areas of a swamp where an increased accumulation of alginite could have led to the formation of torbanite or boghead coal (Hagelskamp, 1987). None of the lithotype descriptions of the seam intersected in the boreholes in Figure 4.14 revealed the presence of torbanite.

The Calorific Value and Ash Content:

The maceral composition and its VM content have a great influence on the CV of coal (Hagelskamp, 1987). Ash dilutes the coal and therefore, all properties dependent on the elemental composition, volatile matter, fixed carbon and CV will increase as the ash content decreases. The CV (air-dry) (Figure 4.15) and CV (daf) (Figure 4.18) correlates negatively with the ash distribution in Figure 4.16. In Tables 4.6 and 4.7, the correlation coefficient between CV MJ/kg (air-dry) and % Ash (air-dry) are –0.96 and –0.98 respectively.

Table 4.6 ***Correlation coefficients for coal containing >28 % Volatile Matter (daf), Optimum Colliery (222 boreholes). Significant correlations are bold and in red.***

	Thickness (m)	Elevation (MAMSL)	Relative Density	Calorific Value (air-dry)	Fixed Carbon (air-dry)	Ash (air-dry)	Moisture (ash-free)	Volatile Matter (dry,ash-free)
Thickness (m)	1.00							
Elevation (MAMSL)	-0.40	1.00						
Relative Density	0.19	-0.09	1.00					
Calorific Value (air-dry)	-0.15	0.09	**-0.92**	1.00				
Fixed Carbon (air-dry)	0.03	0.06	**-0.78**	**0.83**	1.00			
Ash (air-dry)	0.12	-0.06	**0.91**	**-0.96**	**-0.89**	1.00		
Moisture (ash-free)	0.11	-0.10	0.09	-0.09	0.05	-0.05	1.00	
Volatile Matter (dry,ash-free)	-0.31	0.01	-0.07	0.06	-0.47	0.02	-0.26	1.00

Table 4.7 ***Correlation coefficients for coal containing ≤ 28 % Volatile Matter (daf), Optimum Colliery (26 boreholes). Significant correlations are bold and in red.***

	Thickness (m)	Elevation (MAMSL)	Relative Density	Calorific Value (air-dry)	Fixed Carbon (air-dry)	Ash (air-dry)	Moisture (ash-free)	Volatile Matter (dry,ash-free)
Thickness (m)	1.00							
Elevation (MAMSL)	-0.53	1.00						
Relative Density	-0.33	0.13	1.00					
Calorific Value (air-dry)	0.31	-0.11	**-0.94**	1.00				
Fixed Carbon (air-dry)	0.10	0.08	**-0.72**	**0.86**	1.00			
Ash (air-dry)	-0.24	0.08	**0.92**	**-0.98**	**-0.87**	1.00		
Moisture (ash-free)	-0.39	0.16	0.57	**-0.73**	**-0.65**	**0.65**	1.00	
Volatile Matter (dry,ash-free)	0.39	-0.35	-0.58	0.45	-0.04	-0.44	-0.30	1.00

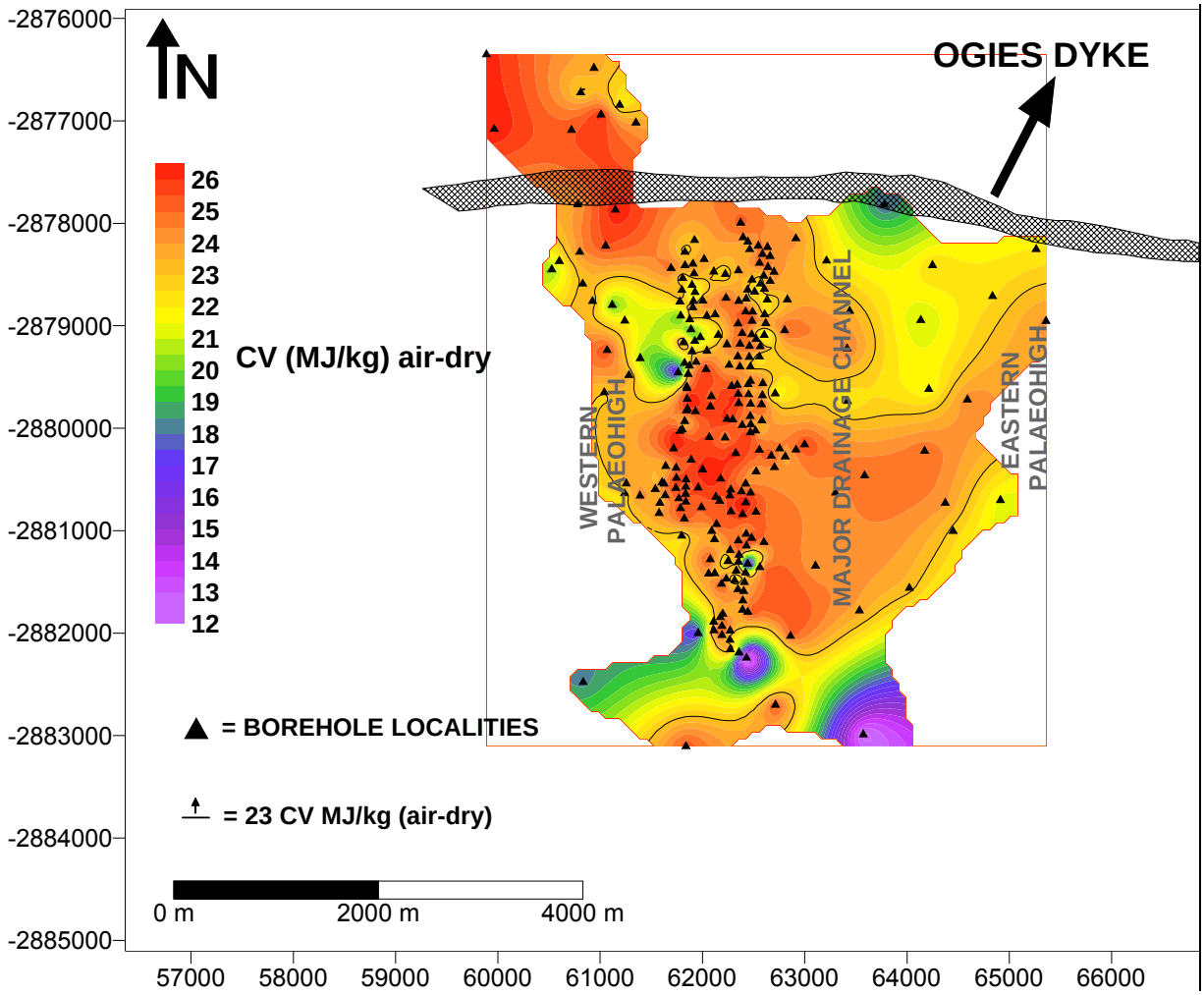

Figure 4.15 Isopleth map of the CV MJ/kg (air-dry) of the coal in the No. 2 Upper Coal Seam.

These correlations, however, proved an inverse relationship between CV and ash content. Ash content which dilutes the organic substance of coal, originates from the inorganic mineral matter in coal (Hagelskamp, 1987).

In Figure 4.17 the 25% ash contour is shown as a solid line to delineate areas of > 25% ash. These high ash areas were digitized and overlain onto the isopach map in Figure 4.19 where the thick coal (>5m) coincides with areas of low ash (<25%) coal. Higher ash concentrations are found in the southern part of the area and also in parts of the western and eastern palaeohighs. In Figure 4.20, flow directions based on thickness distribution and ash content, are indicated by the blue and orange arrows. The blue arrows represent areas of > 25% ash (air-dry) and the orange arrows areas of < 25%

ash (air-dry). These flows carried mineral matter that was filtered out by plant growth on the valley flanks of the swamp (the dark green areas in Figure 4.16), resulting in higher ash coals compared to coals in the lower-lying areas.

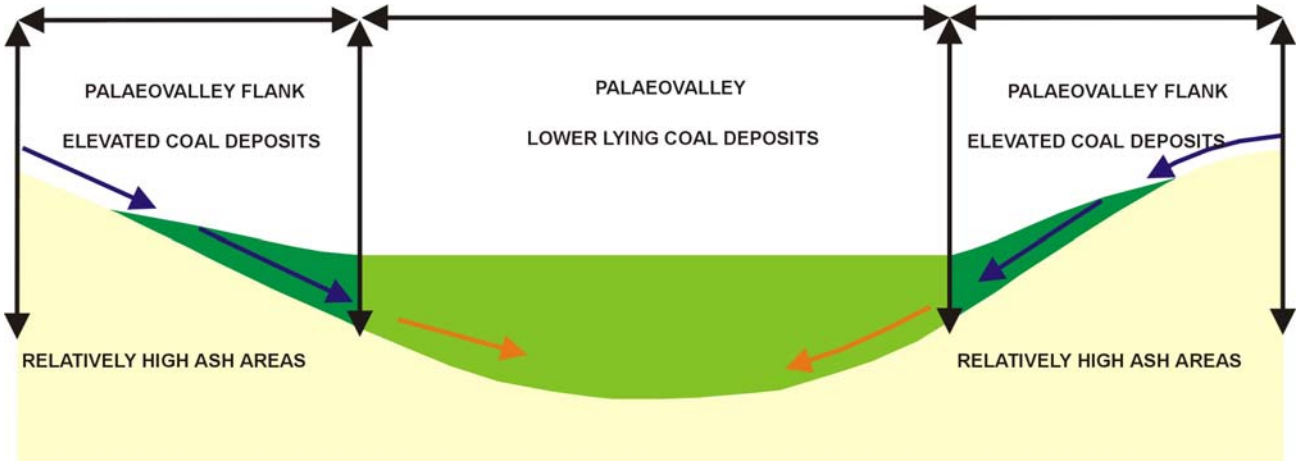

Figure 4.16 ***A schematic diagram to illustrate the probable reason for the coal ash distribution in the No. 2 Upper Coal Seam at the Optimum study area. The blue arrows indicate coal deposits with a relative high ash (air-dry) content of > 25%, and the orange arrows coal deposits with a relative low ash (air-dry) content of < 25%.***

285 analyses from the study area at Optimum, only 23 are below 18% ash and only 19 are above 30% ash with the bulks between 18 and 30%. Dull coals identified in borehole core are generally related to the high ash values, which, however, cannot be ascribed to specific layers of inorganic sedimentary rocks.

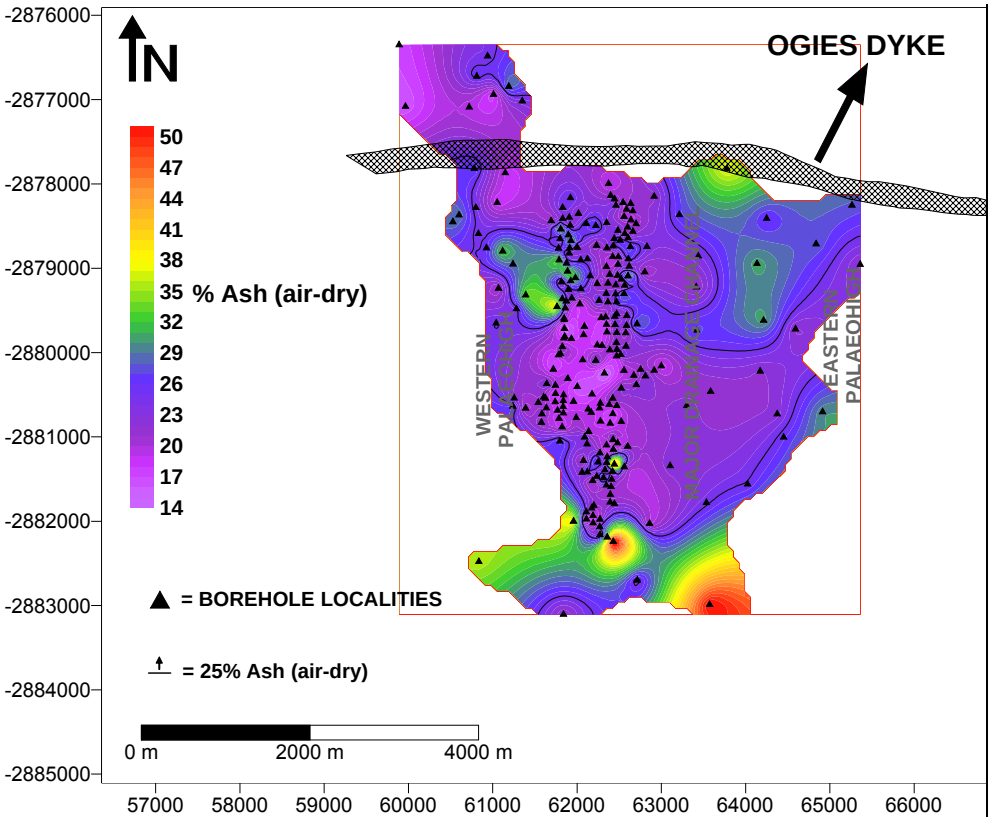

Figure 4.17 Isopleth map of ash (air-dry) of the coal in the No. 2 Upper Coal Seam.

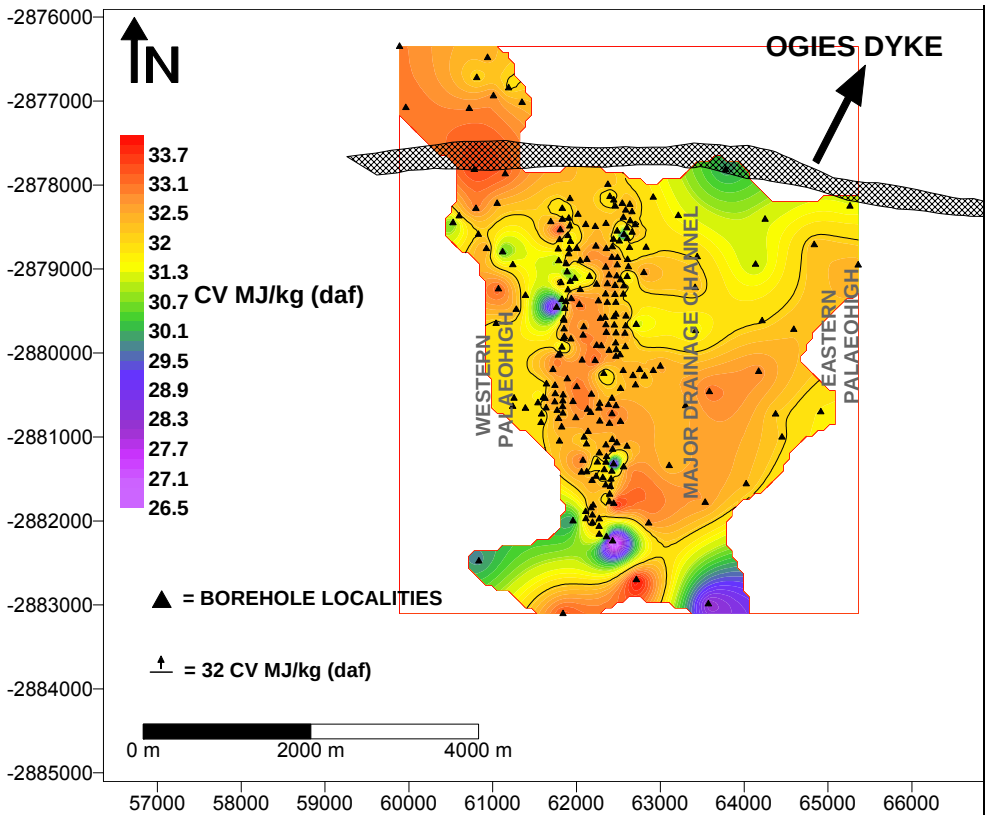

Figure 4.18 Isopleth map of the CV MJ/kg (daf) of the coal in the No. 2 Upper Coal Seam.

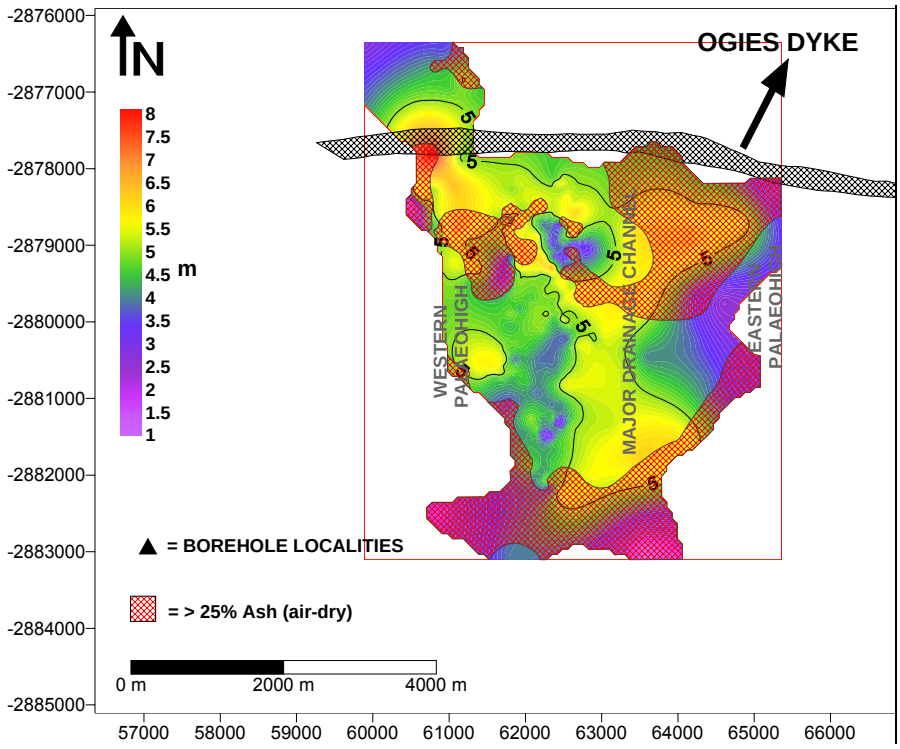

Figure 4.19 ***Areas of > 25% ash superimposed onto an isopleth map of the No. 2 Upper Coal Seam.***

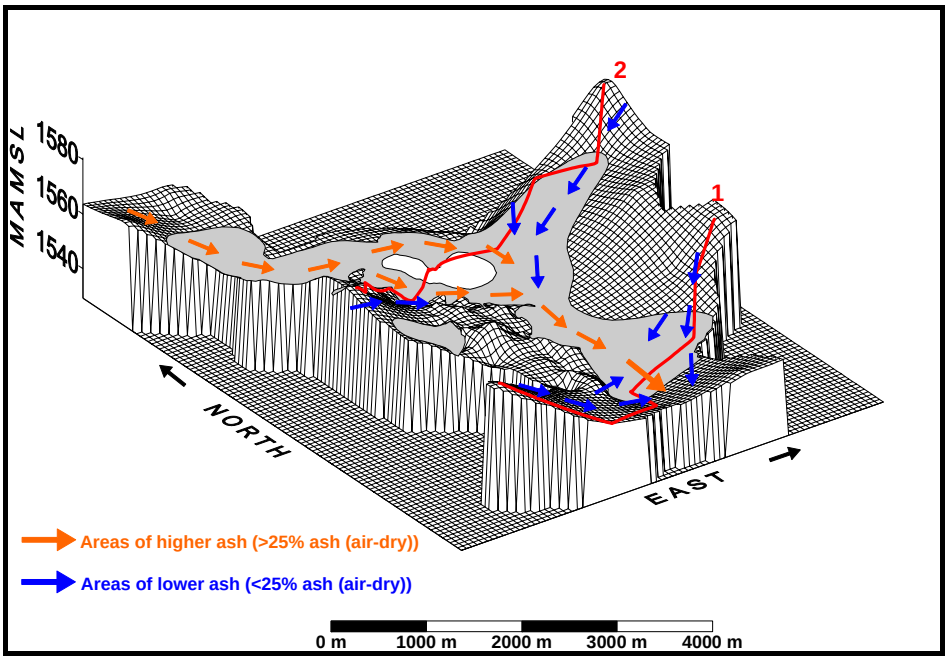

Figure 4.20 ***Probable flow directions shown by the blue and orange arrows on the model of Figure 4.8. The blue arrows represent areas of > 25 % ash (air-dry) and the orange arrows areas of < 25 % ash (air-dry). Sections 1 and 2 from Figures 4.12 and 4.13 are indicated by the red lines.***

The Relative Density and Fixed Carbon Content

Correlation coefficients (Tables 4.6 and 4.7) exist between relative densities, CV (air-dry), fixed carbon (air-dry) and ash (air-dry). Both CV (air-dry) and fixed carbon (air-dry) have an inverse relationship with relative density. It is not only the correlation coefficients that show meaningful relationships; correspondences have also been found between the various isopleth maps (compare Figures 4.21, 4.15, 4.17, 4.18 and 4.22). Higher density coals have lower CV's, lower fixed carbon contents, and higher ash contents. In tables 4.6 and 4.7, fixed carbon (air-dry) show significant correlations with relative density (-0.78), CV MJ/kg (air-dry) (0.83), ash (air-dry) (-0.89) and to some extent with moisture (ash-free) (-0.65). These correlations revealed that there is an inverse relationship between fixed carbon (air-dry) and relative density, ash (air-dry) and moisture (ash-free). Ash content does not only diminish the CV of coal, as mentioned before, but also the fixed carbon content, according to its inverse relationship with ash. Its correlation with moisture will be discussed in the following paragraph.

The above correlations can be explained by the mineral matter content in coal which dilutes its organic substance. Therefore, as mentioned before, all the properties that depend on the organic substance will increase as the mineral matter content decrease.

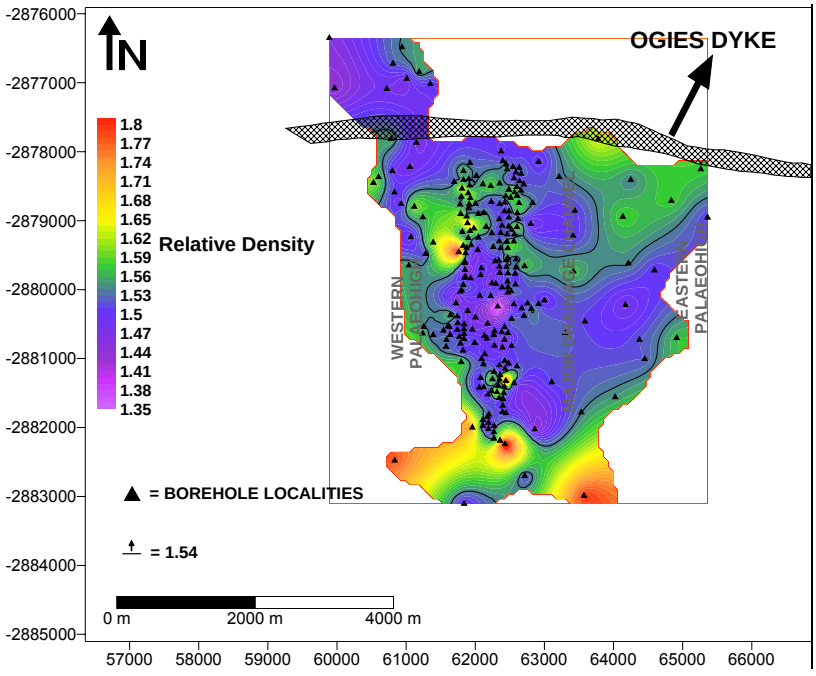

Figure 4.21 Isopleth map of the relative density of the coal in the No. 2 Upper Coal Seam.

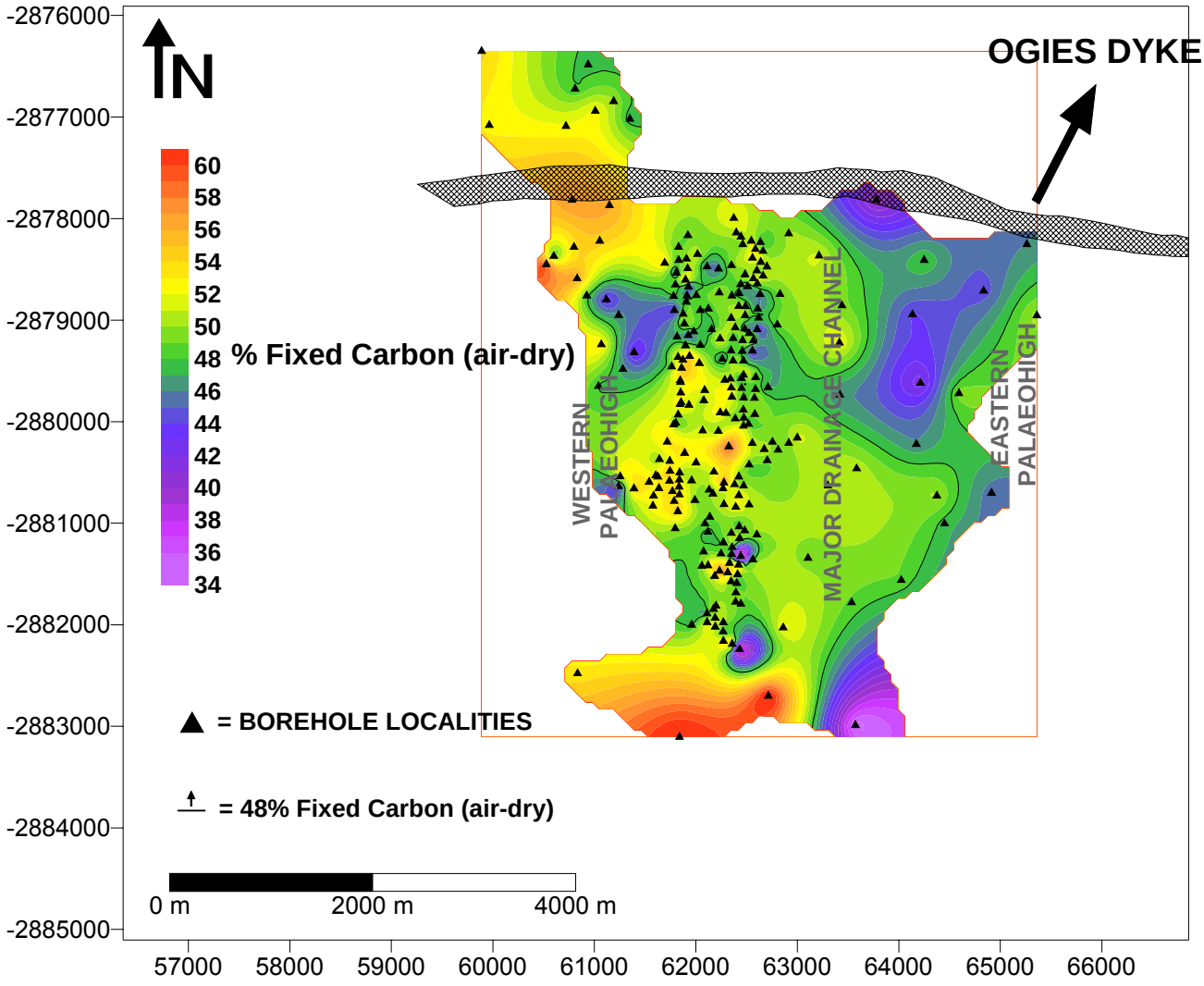

Figure 4.22 ***Isopleth map of fixed carbon (air-dry) of the coal in the No. 2 Upper Coal Seam.***

The Moisture Content:

Moisture content on an ash-free basis shows significant correlations with CV MJ/kg (air-dry), relative density, ash (air-dry) and fixed carbon (air-dry) in Table 4.6.

The 5 % moisture (ash-free) contour is shown as a solid line in Figure 4.23 to delineate these areas of high moisture. Correlations are only found in the devolatilised areas, therefore a relationship with dolerite activity. The higher values of ±9% shown in Figure 4.23 can be explained by a larger internal surface area of the coal due to the presence of pores resulted from the mechanical effect of the intrusion, which would facilitate the adsorption of moisture.

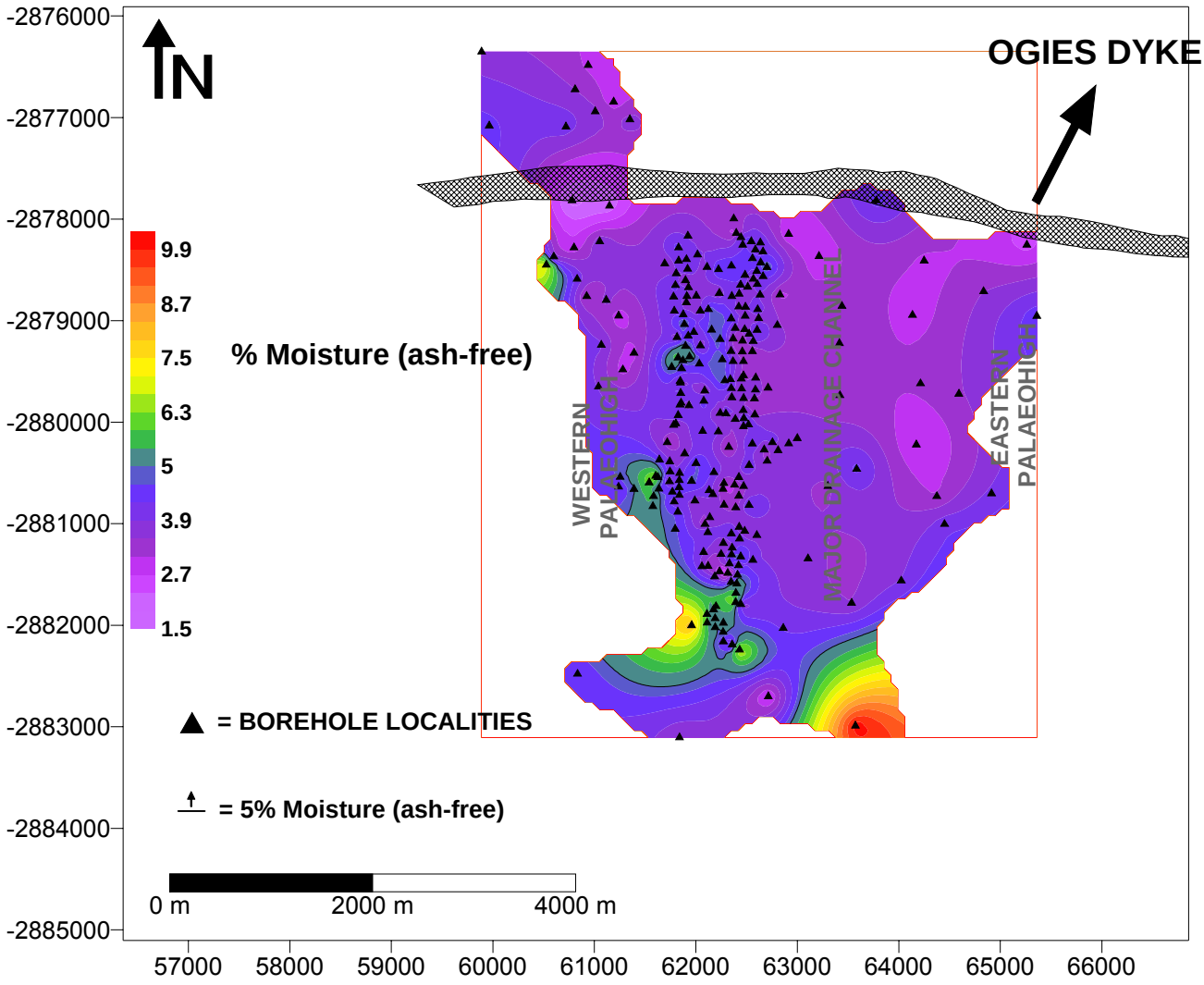

Figure 4.23 An Isopleth map of the ash-free moisture content of the coal in the No. 2 Upper Coal Seam.

4.2.2.4 Conclusions

This chapter by no means emphasizes the sedimentology of coal, but it merely focuses on various coal grade controls in a “dolerite-free” area, and also, to some extent, the metamorphic influence of the Ogies Dyke that bounds the northern portion of this area.

The undulated floor onto which the No. 2 Upper Coal Seam formed at the Optimum study area had a major influence on coal grade. Thicker coals were deposited in the lower lying areas while they were thinning towards palaeohigh areas. Significant values indicate that the thinner coals are higher in ash (air-dry), lower in VM (daf), lower in CV

MJ/kg (air-dry) and higher in relative density comparing to the coals deposited in the lower lying areas of the palaeovalley.

A decrease in VM to the south and western border of the study area can be associated with the nearby dolerite sill as reported by Smith (1990). According to various authors, the Ogies Dyke is responsible for intense coal devolatilisation in the extreme east part; however, in this area it was not found to be the case. The area of intense devolitilisation indicates a rather continuous flow of magma as appose to this area where no such influence was found.

CHAPTER 5

AFFECT OF THE DOLERITE INTRUSIONS ON COAL OF THE VRYHEID FORMATION IN THE WITBANK AND HIGHVELD COALFIELD.

5.1 Literature review

Coal affected by intrusions occurs in most coalfields throughout the world. Snyman and Barclay (1989) investigated the coalification of South African coal concluding that the rank of coal metamorphosed by dolerite intrusions is related to the ratio proposed by *D/T* of Blignaut (1952), where *D* is the distance between the coal and the intrusive and *T* the thickness of the intrusive. As the contact aureoles were generally very narrow, they concluded that the aureoles were largely controlled by the low thermal diffusivity of the coal and associated rocks at the time of intrusion. According to Blignaut (1952), South African dolerite intrusions affected coal seams over a distance equal to their thickness. This is still *"a rule of thumb"* in South African coal geology. Du Toit (1954), however mentions a specific case where a 4.8 m thick dolerite has a contact aureole of 90 m wide. In this case all the coalification stages were present: from bituminous coal, through semi-anthracite and anthracite, to ash at the contact.

Kisch and Taylor (1966) did a mineralogical study of the metamorphism caused by a porphyritic intrusion in a coal seam of medium-volatile bituminous rank in the Collinsville Coal Measures, Eastern Queensland, Australia. The intrusive itself is altered to "white trap", consisting mainly of albite, kaolinite, chalcedony, ankerite, siderite, calcite and leucoxene. Close to the contact, the coal had been converted to natural coke. They concluded that a temperature of not more than 760ºC had been attained during the intrusion.

Crelling and Dutcher (1968) studied a thermally altered coal seam below a lamprophyric sill in the Purgatoire River of Colorado. Micrinoids and fusinoids (macrinite and fusinite in modern nomenclature) are common, with the cell cavities of the fusinoids filled with calcite. The sulphur distribution apparently has no relationship to the intrusion, but there was a change in the ash (higher) and volatile matter (lower) values closer to the intrusion. Considering various techniques, they concluded that temperatures greater

than 600ºC at the top to less than 375ºC at the base were attained during the igneous intrusion.

According to Varga and Horvath (1986), under-sea-bed volcanic activity in the Mecsek bituminous coal basin, dolerite veins in the coal seams exerted a strong metamorphic influence. The metamorphism resulted in a thermal contact alteration to natural coke and semicoke of varying metamorphic intensity. The quality and characteristics of the coal have been adversely affected by the metamorphism.

At the Twistdraai Colliery, Secunda Coalfield, Hagelskamp (1987) found that the metamorphic influence of dolerite intrusions on the quality of coal is similar to analogous occurrences around the world. Distinct metamorphic aureoles are recognised on account of petrographic and chemical parameters.

Thorpe et al., (1998) have studied the change in magnetic properties of coal intruded by an igneous dyke in the Dutch Creek Mine, Colorado. Magnetic measurements were taken on natural coke and coal samples at various distances from the dyke to characterise the nature and distribution of Fe-bearing phases. The magnetic measurements supported the geochemical data which indicated that magmatic fluids moved along the coal bed as a high temperature gas pulse. Reducing gas derived from the coal penetrated further and produced a high temperature zone just ahead of the magmatic fluids. Metallic iron found in this zone is the principal cause of the high magnetism.

Merrit (1990) studied the thermal alteration and rank variation of coals in the Matanuska field, south central Alaska. He concluded that the importance of studying coal-intrusive relationships stems mainly from the economic ramification and commercial coal mining. The physical and qualitative constraints to economic mineability must be studied on a case-by-case basis.

5.2 The metamorphic influence of a 20m thick undulating and bifurcating dolerite sill.

The dolerite sill has been intersected during surface diamond drilling at the Bank, Goedehoop and Koornfontein Collieries (Figure 2.1). Geological cross-sections, isopleth and isopach maps from the Bank study area will introduce this part of the study.

Subsequently, the chemical characteristics of the coal which resulted from the thermal influence of the sill will be outlined.

Du Plessis (2001), used borehole data from the Bank study area to draw north-south, east-west geological cross-sections over principal areas at the Bank study area. The cross-sections revealed insight into the spatial relationship between coal seam and dolerite sill structures. The Karoo strata occurring above this domal and basin-shaped dolerite sill have been displaced and uplifted in the direction of dip by an amount approximately equal to its thickness (20m).

Contour maps of present and palaeofloor elevations and thickness variation of the different coal seams were compiled in order to gain a better understanding of the depositional environment prior to dolerite intrusions (Figure 5.5 A and B). It was considered that thicker peat accumulated in palaeovalleys, narrows towards and eventually pinches out against palaeoridges. The main channel axes and pre-Karoo ridges could thus be identified. In addition, the pre-Karoo topography has been postulated as information on the Pre-Karoo rocks is sparse. Dry ash-free (daf) volatile matter, calorific value (CV), ash content and displacement of the coal seams assist in the interpretation of dolerite sill structures using geological cross-sections. Maps containing intersection lines between dolerite sill structures and coal seams were superimposed onto contour maps of various coal parameters which assisted in quantifying the metamorphic effect of dolerite intrusions on coal.

During underground mine visits, it was noted at dolerite/coal seam intersections that the dolerite either widens or bifurcates within the seam. It was also evident that the dolerite becomes microcrystalline at this point of contact and is associated with a light grey matrix. According to Kish and Taylor (1966), dolerite intrusions in coal contain considerable amounts of carbonate minerals that form the so-called “white trap”. Contact planes between dolerite and coal are filled with calcite, quartz and sulphide minerals. The geometry of the contact aureole extends as far as intrusion-related jointing extend. The interior of this 20m thick dolerite sill is dark green and porphyritic; however, the chilled margins are light grey and microcrystalline. The sharp contacts between the sill and sandstones observed from borehole core indicate that the sediments were consolidated at the time of intrusion. The geometry of the sill defines pre-existing jointing structures which were favoured by the magma intrusion. Such phenomena are also reported by Hagelskamp (1987).

5.3 Study area – Bank Colliery

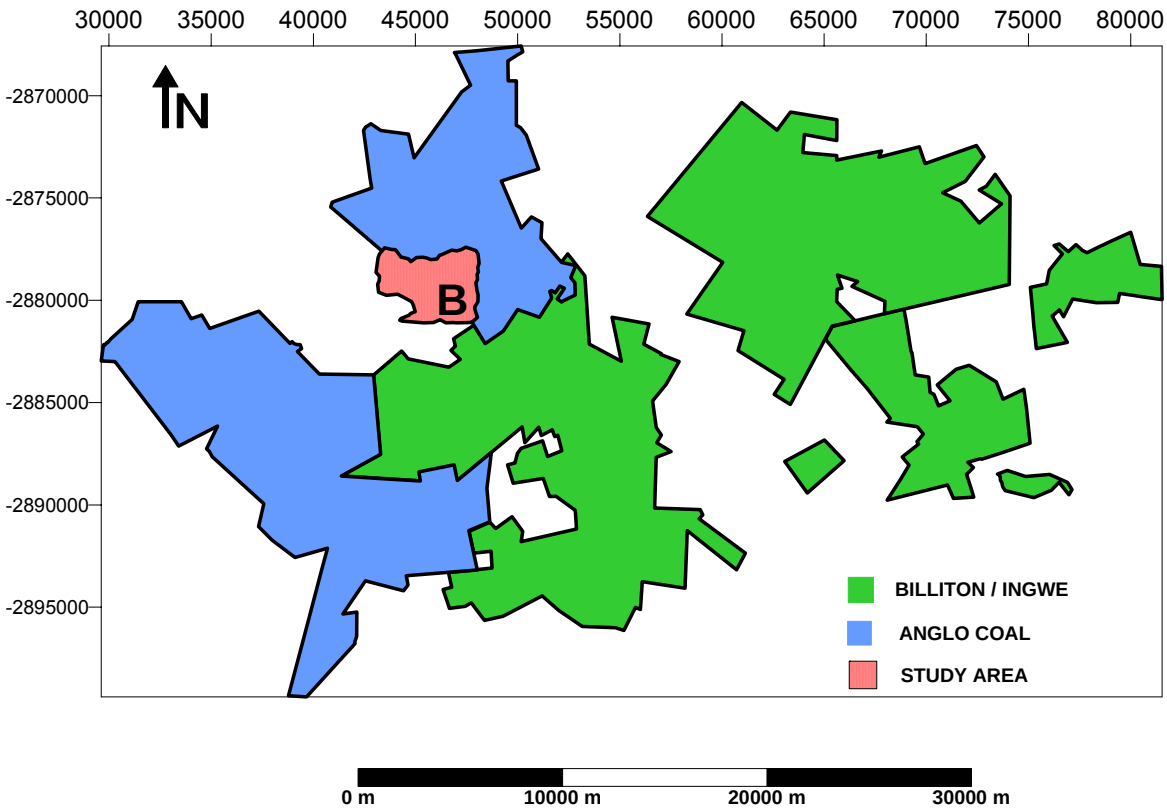

Figure 5.1 Map of the study area (marked B) at Bank Colliery.

A total number of 467 boreholes have been drilled in the study area at Bank Colliery (13.5km^2) (Figure 5.1) resulting in an average of one borehole per 0.028km^2. The 15m thick Ogies Dyke (thickness is not to scale on the maps to follow) forms the northern limit of the area (Figure 5.2) and is not associated with vertical displacement in the study areas.

5.3.1 Geological cross-sections

Geological cross-sections (Figure 5.2) depict the most representative geological information where the sill transgressed the coal seams (No's 2, 4L and 5) (Du Plessis, 2001). The sections were selected on the basis of sill and coal seam intersections. Intersection lines between the sill and the No's 2, 4L and 5 Coal Seams are shown in Figure 5.2, hence the apparent strike and down-dip of the sill. The No. 2 Coal Seam has been reconstructed by removing the dolerite sill (Figures 5.3 A and B) (Du Plessis, 2001). Cross-sections are located on either valley flanks or valley ridges (Figures 5.3 A and B).

To avoid repetition, the results of the proximate analyses are not discussed in detail. Only trends are outlined. Fixed carbon content is not dealt with as it is determined by difference.

Six coal parameters, i.e. ash content, moisture (ash-free), calorific value (air-dry), relative density, volatile matter (daf) and inferred %RoV (max) (reflectance) which was calculated from the Seyler classification system (Snyman, 1996), are used to characterise the coal in Section 21 (Figure 5.2). Following this, only ash content, moisture (ash-free) and VM (daf) are used in the rest of the section discussions. Combined graphs of the actual relationship between the coal seams (indicated by the black lines on the graphs), the dolerite sill (indicated by the green lines on the graphs) and the coal parameters will be combined to quantify dolerite metamorphism (for example Figure 5.5). Each cross-section is discussed separately. The interpretation is corroborated by the section itself, the coal and dolerite lithological descriptions from the borehole logs, the combined graphs and also the reconstructed isopach and contour maps in Figures 5.3 A and B. In some of the sections where a sparseness of representative raw coal data defies a reasonable interpretation, the No. 4L Coal Seam or both the No. 4L and No. 2 Coal Seams are used together, to reveal insight into the heat that emanated from the sill. However, in such instances it must be kept in mind that the 2 coal seams will react differently from the metamorphic influence from the dolerite sill.

In addition, Figure 5.2 depicts the intersection lines (apparent strike and down-dip direction) between the main sill and the No's 2, 4L and 5 Coal Seams from where their spatial relationship can be observed. This map provides the third dimension of the interpreted sill of the two-dimensional geological cross-sections. The investigation of the contact metamorphism in section-view will be followed in plan-view to define a spatial metamorphic influence of the sill. The main objective is to synthesize all the available data from the geological cross-sections and isopach plans to define the influence of the dolerite sill.

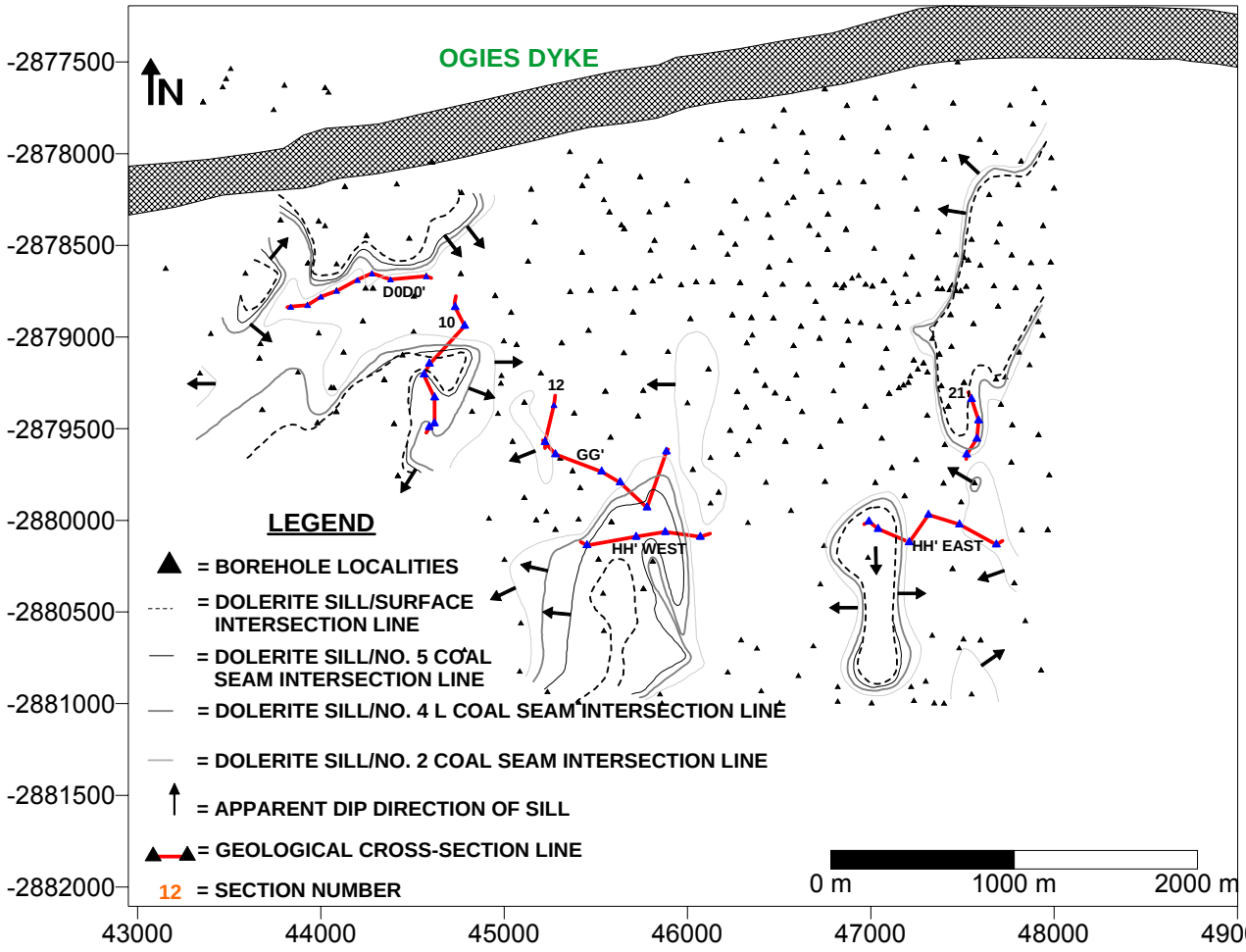

Figure 5.2 A map of the Bank study area indicating geological cross-sections (red lines). Thickness of the Ogies Dyke is not to scale (Du Plessis, 2001).

5.3.1.1 Section 21 (Figure 5.4)

All the boreholes in Section 21 (Figure 5.3) have intersected the 20m thick bifurcating dolerite sill. The sill is light grey to blue in colour; with chilled contacts and contains abundant calcite veins. Coal seams above the sill are intensely fractured and associated with slickensides. Abundant calcite and pyrite mineralisation on joints and cleats are also associated with slickensides. Borehole logs reveal that bifurcations are light grey in colour, fine crystalline, carbonaceous and with uneven top and bottom contacts. The lithological descriptions of the various coal seams intersected in Section 21 are summarised in Table 5.1. Only general trends associated with the dolerite sill are outlined in the next paragraphs.

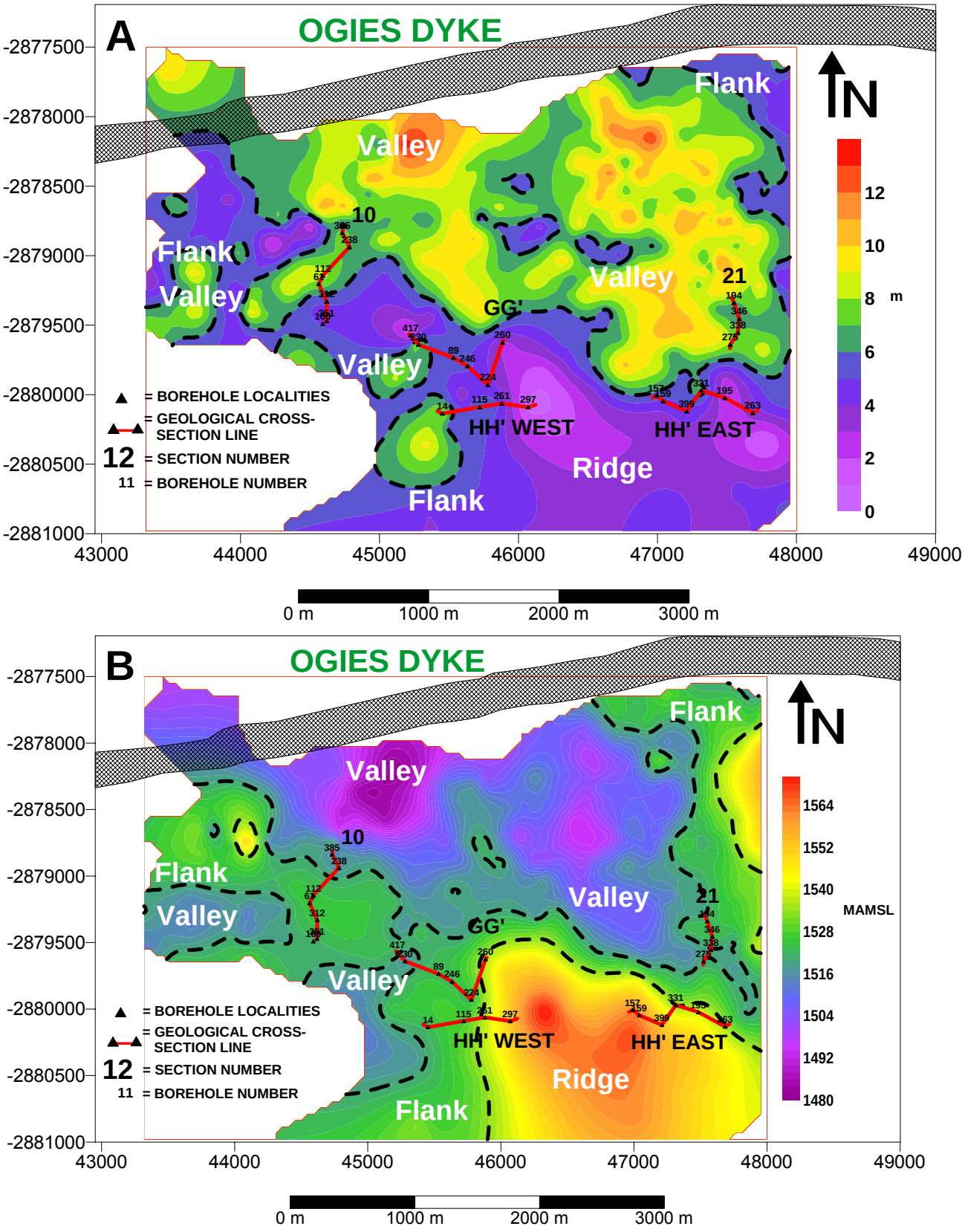

Figure 5.3 *A:* *Reconstructed isopach map of the No. 2 Coal Seam.*

B: *Reconstructed contour map in MAMSL of the No. 2 Coal Seam (Bank Colliery study area) (Du Plessis, 2001).*

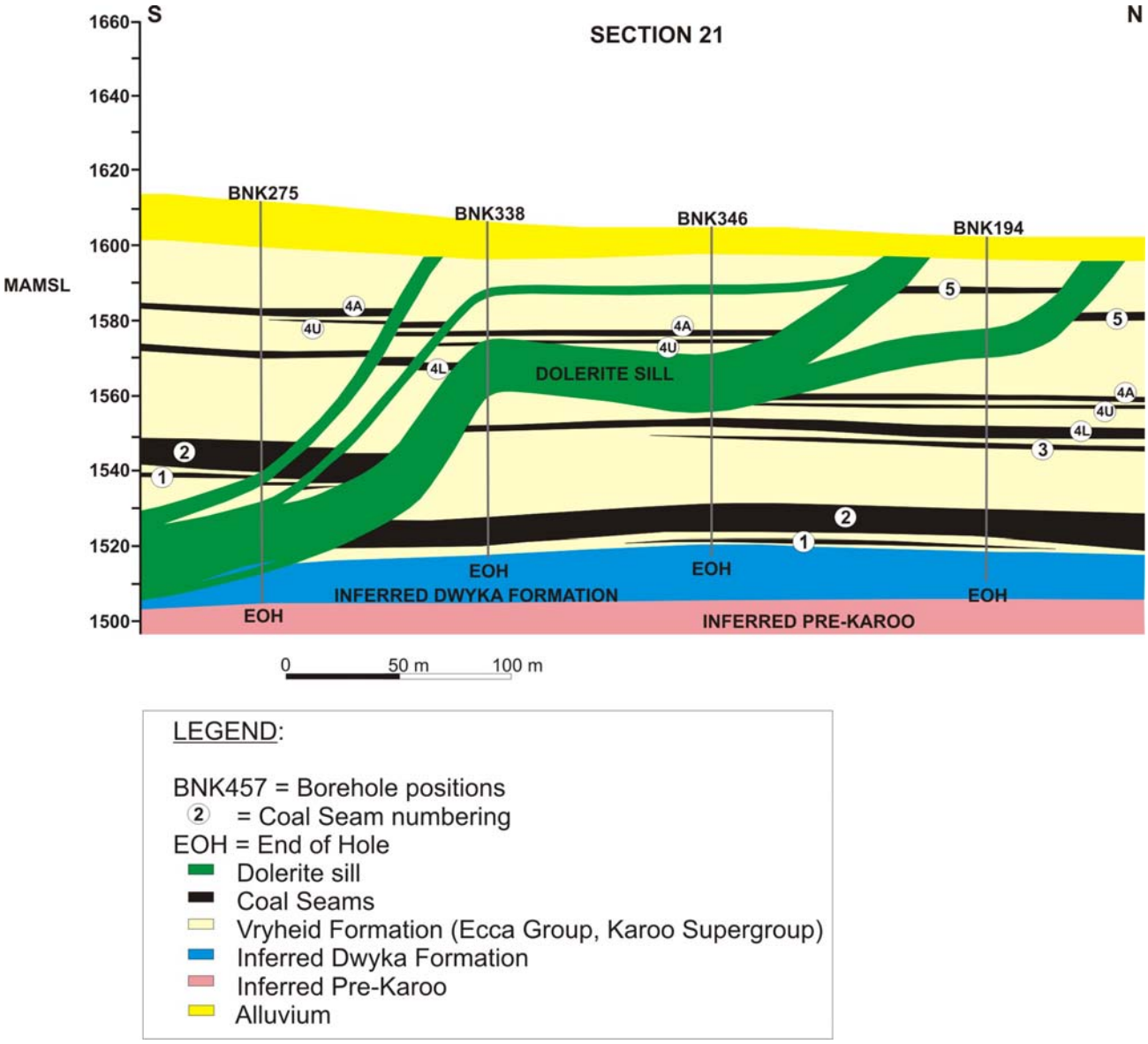

Figure 5.4 ***A geological cross-section showing the interpretation of a dolerite sill structure (Du Plessis, 2001). See locality of section in Figure 5.2 and 5.3 indicated by the number 21 on the plan..***

No's 2, 4L and 4A Coal Seams have been completely devolatilised by the sill (Borehole BNK275). The broken core obtained from these coal seams indicates a shearing effect from the dolerite sill. The occurrence of calcite and pyrite veins is also related to the intrusion. Where the sill adopted a steeper angle (adopting a dyke-like character), it was associated with bifurcation (between boreholes BNK275 and BNK338). All the sediments above the sill have been displaced by ±20m.

Only the top of the No. 2 and bottom of the No. 4L Coal Seams have been devolatilised by the sill (borehole BNK338). Slickensides within the coal seams resulted from friction along small scale fault planes. No's 4L, 4U and 4A Coal Seams have been devolatilised and sheared by the sill (borehole BNK346).

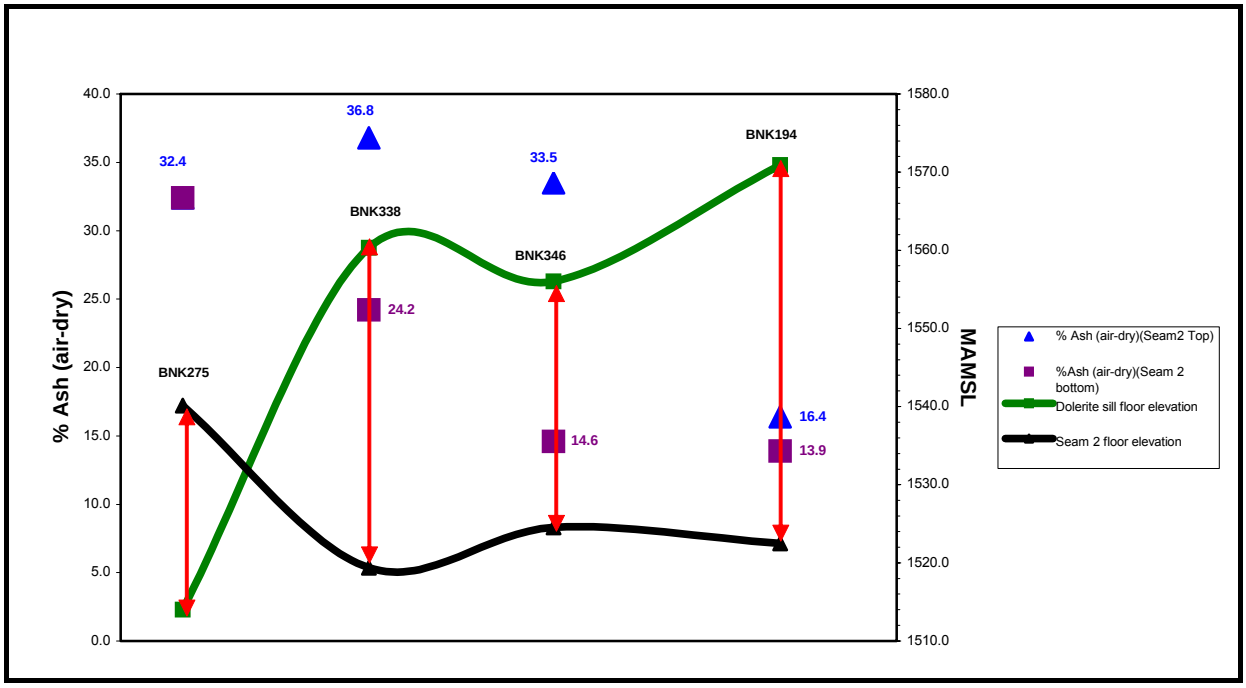

Figure 5.5 ***A combined graph of the actual relationship between the No. 2 Coal Seam and the sill, as well as the ash content variation in the top (blue triangles) and bottom (purple squares) of the No. 2 Coal Seam (Section 21). The red lines indicate the vertical distance between the sill and the No. 2 Coal Seam.***

When the sill intruded at a steeper angle (between boreholes BNK346 and BNK194), it was associated with bifurcation (borehole BNK194). The poor core recovery at the No. 5 Coal Seam can certainly be linked to the shearing effect of the sill. Only slight devolatilisation in the No. 4L Coal Seam indicates the boundary of the metamorphic contact aureole. Demarcation of the spatial shape of the metamorphic aureole in Section 21 is complicated as the sill appears above and below various coal seams.

Table 5.1 Lithological descriptions of the coal seams intersected in Section 21. The red descriptions indicate the influence of the dolerite sill.

SEAM No.	BOREHOLE NUMBERS – GEOLOGICAL CROSS-SECTION 21			
	BNK275	BNK338	BNK346	BNK194
5	Not present.	Not present.	Not present	Coal: soft, highly weathered. Not sampled, core loss (Estimated thickness)
4A	Coal: **burnt, intensely broken, occasional pyrite veins.**	Coal: **pyrite**	Coal: **burnt**	Coal: dull lustrous, **pyrite lenses, calcitic**, 15% bright bands Coal: dull, shaly.
4U	Not present.	Not present.	Coal: **devolatilised, broken core.** Siltstone/Sandstone: carbonaceous. Coal: dull, shaly, **broken core**	No detail descriptions
4L	Coal: **burnt, intensely broken core.** **Oxidised pyrite present.**	Coal: dull lustrous. Coal: dull. Coal: dull lustrous. Coal: dull lustrous. **Slickensided and burnt.** Coal: dull.	Coal: **devolatilised, broken core**, slightly weathered. Limestone: carbonaceous, **pyritic**, strong rock. Coal: **devolatilised, broken core**, slightly weathered.	Coal: dull lustrous. Minor bright bands. 50% coal, 60-90% bright, **calcite on cleats**. 50% coal, dull lustrous. Coal: dull, **blocky, pyrite lenses. Slightly devolatilised?** Limestone: carbonaceous, **calcite on joints. Sub vertical joints**
3	Not present.	Not present.	Coal: **broken**, slightly weathered. Coal: shaly, with bright streaks.	35% coal: dull, shaly. 35% coal: dull lustrous. 30% coal: 40-60% bright.
2	Coal: **burnt, abundant calcite veins.** **Dolerite stringers present.**	Coal: **burnt.** Siltstone, dark grey. Coal: dull. Shale: black, fine grained, coaly, massive. Coal: dull, A few minor bright laminations. Grit: grey, coarse grained, **quartzitic**, coaly, massive. Coal: dull. Grit: white, coarse grained, **quartzitic**, massive. Coal: dull. Coal: mixed, 10-40% bright, **occasional calcite on cleats** Coal: dull lustrous. **Slickensided.** Coal: bright. Coal: dull, **pyritic, abundant pyrite nodules** Siltstone parting. Shale: black, fine grained, massive. Siltstone parting. Coal: dull lustrous.	Coal: mixed, 10-40% bright. Coal: dull, hackly fracture. Coal: dull, with bright streaks. Mudstone: carbonaceous, **pyritic** Coal: mixed, 10-40% bright, **pyrite nodules**. Coal: dull. Coal: mixed, 40-60% bright. Coal: dull, hackly fracture. Coal: dull, with bright streaks, hackly fracture, **pyrite nodules.** Coal: mixed, 10-40% bright. Coal: dull, hackly fracture. Coal: mixed, 10-40% bright, **calcite on cleats**	35% coal: dull. 35% coal: dull lustrous. 30% coal: 40-60% bright, **pyrite lenses, calcite on cleats.** 70% coal: dull., 23% coal: dull lustrous. 7% coal: 40-60% bright, **pyrite lenses, calcite on cleats.** 75% coal: dull. 20% coal: dull lustrous. 5% coal: 40-60 % bright. 80% coal: dull lustrous. Minor bright bands. 20% coal: dull, **pyrite lenses, calcite on cleats**. 65% coal: dull lustrous, **pyrite lenses, calcite on cleats.** 30% coal: dull. 5% coal: 40-60% bright.
1	Not present.	Not present	Coal: shaly. Coal: dull Coal: dull lustrous, hackley fracture. Coal: dull, shaly, **calcite on cleats.** Coal: bright. Coal: shaly. Coal: dull lustrous, hackley fracture. Coal: shaly, **calcite on cleats, pyrite lenses.**	Grit: pebbly, fining up. 50% coal: dull lustrous, pyrite lenses, **calcite on cleats.** 50% coal: dull. Coal: 60-90% bright. Coal: dull lustrous. Siltstone: grey. 90% coal: dull lustrous. 10% coal: dull, **calcite on cleats.** Siltstone: carbonaceous. 75% coal: dull lustrous. Faintly banded in parts. 25% coal: dull, **pyrite lenses.**

a. No. 2 Coal Seam (proximate analyses and RoV max)

Combined graphs (Figures 5.5, 5.6, 5.7, 5.8, 5.9 and 5.10) of the actual relationship between the No.2 Coal Seam, the dolerite sill and various coal parameters are used to quantify dolerite metamorphism. The red arrows on the graphs indicate the distance between the floor elevation of the sill and the No. 2 Coal Seam. In addition, Figure 5.2 depicts the intersection line (apparent strike and dip direction) between the main sill and the No. 2 Coal Seam from which their spatial relationship can be observed. In fact, this map provides the third dimension of the interpreted sill of the two-dimensional geological cross-section. The No. 2 Coal Seam is situated on a valley flank where its thickness varies between 6-8 m (Figures 5.3 A and B).

Ash (Figure 5.5): The No. 2 Coal Seam have lower ash values (boreholes BNK 194 and 346 (bottom)) as opposed to boreholes BNK 275, 338, and the top of borehole BNK346 in Section 21 (Figure 5.5). The ash content ranges from 13.9 to 24.2 (air-dry) in the unaffected coals comparing to those closer to the sill which ranges from 32.4 to 36.8 (air-dry). In Table 5.1 only borehole BNK275 and the top of borehole BNK 338 have been described as “burnt” which are also higher in ash. Both are also low in volatile matter (daf) (Figure 5.9), low in CV MJ/kg (Figure 5.7) and higher in relative density (Figure 5.9) comparing to borehole BNK194. The relationships between ash, CV and relative density could have been expected (compare Figures 5.5, 5.7 and 5.8).

Moisture (ash-free) (Figure 5.6): The coal samples close to the sill have moisture (ash-free) contents of 5.2 and 5.8 as opposed to coal samples further away which have moisture (ash-free) contents ranging between 3.0 and 3.6. This higher moisture content is attributed to the higher micro-porosity of coals affected by intrusions. Hagelskamp (1987) proved that the moisture content is largely dependent on the rank of the coal and is inversely related to vitrinite reflectivity. He also noticed a relationship between moisture content and the type of coal. Inertinite coals have a higher micro-porosity and a higher moisture absorption capacity than vitrinite-rich coals.

VM (daf) (Figure 5.9): The uppermost sample of borehole BNK 346 is anomalously high in VM (daf) compared to the rest of the No. 2 Coal Seam. The most plausible reason for the high VM content is CO_2 that has been derived from carbonate minerals which contaminated the VM content. The coal has been described as mixed; 10-40% bright (dull); hackly fractured with bright streaks; carbonaceous and pyritic (Table 5.1). Provision should be made for the diluting effect of the CO_2.

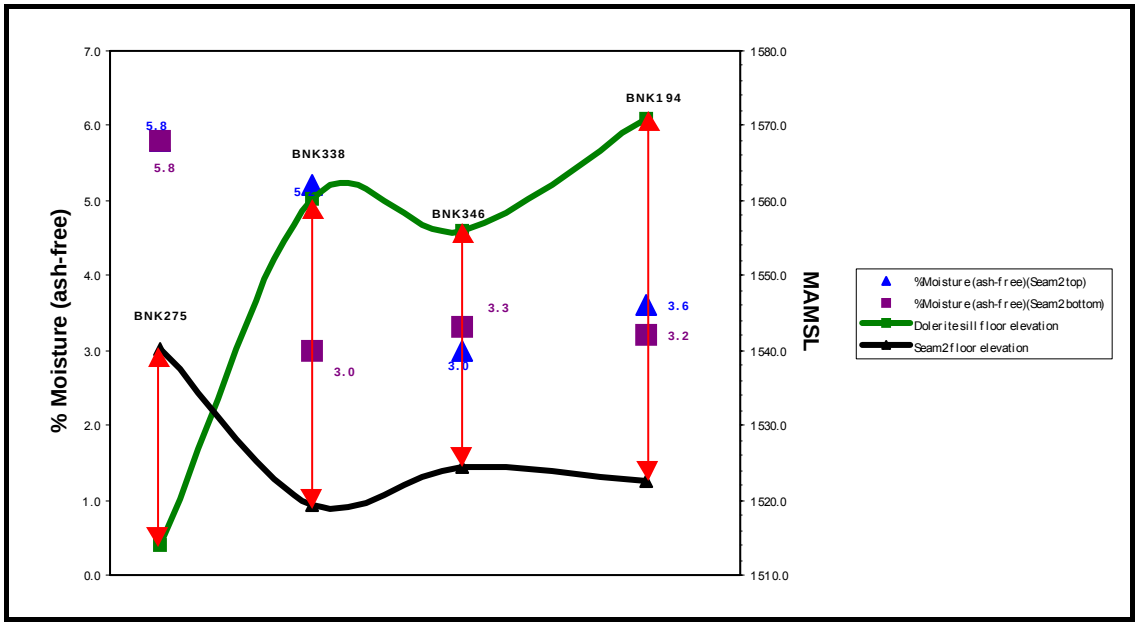

Figure 5.6 *A combined graph of the actual relationship between the No. 2 Coal Seam and the sill, as well as the moisture (ash-free) variation in the top (blue triangles) and bottom (purple squares) of the No. 2 Coal Seam (Section 21). The red lines indicate the vertical distance between the sill and the No. 2 Coal Seam.*

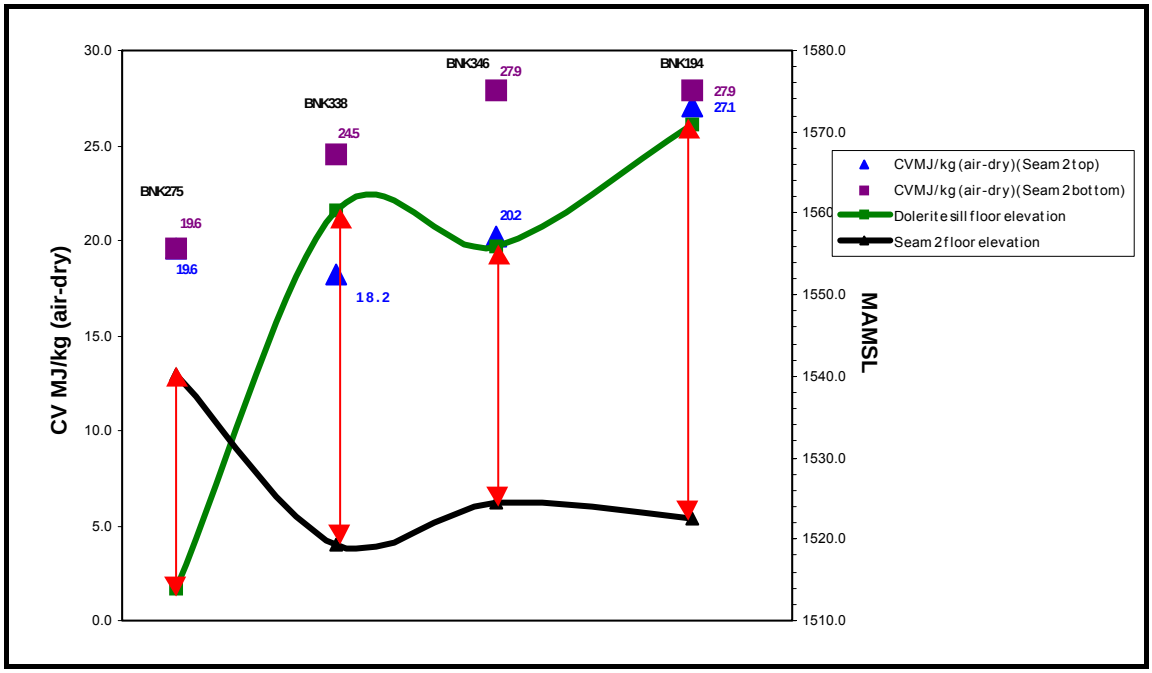

Figure 5.7 *A combined graph of the actual relationship between the No. 2 Coal Seam and the sill, as well as the CV MJ/kg (air-dry) variation in the top (blue triangles) and bottom (purple squares) of the No. 2 Coal Seam (Section 21). The red lines indicate the vertical distance between the sill and the No. 2 Coal Seam.*

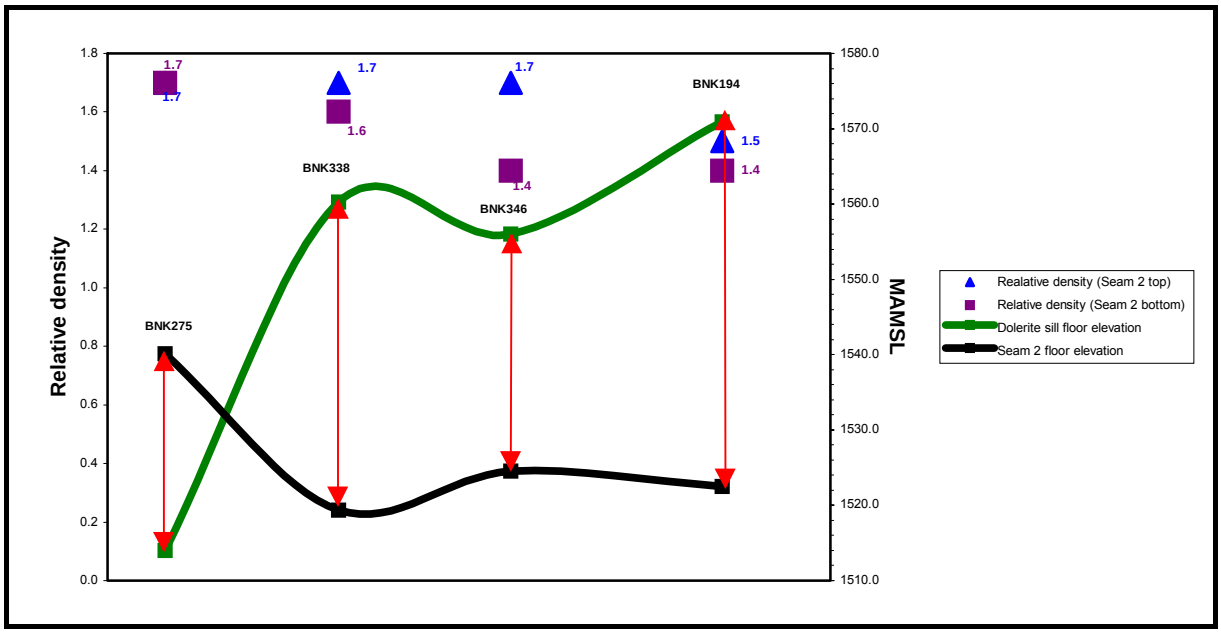

Figure 5.8 *A combined graph of the actual relationship between the No. 2 Coal Seam and the sill, as well as the variation in relative density at the top (blue triangles) and bottom (purple squares) of the No. 2 Coal Seam (Section 21). The red lines indicate the vertical distance between the sill and the No. 2 Coal Seam.*

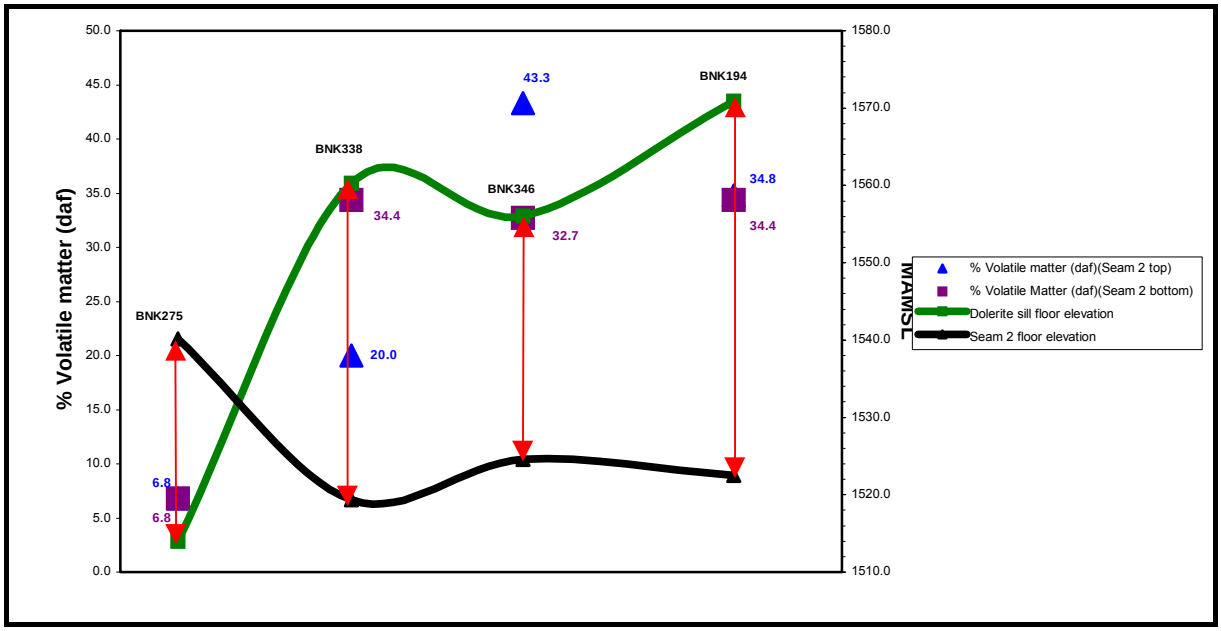

Figure 5.9 *A combined graph of the actual relationship between the No. 2 Coal Seam and the sill, as well as the % volatile matter (daf) variation at the top (blue triangles) and bottom (purple squares) of the No. 2 Coal Seam (Section 21). The red lines indicate the vertical distance between the sill and the No. 2 Coal Seam.*

The correction for CO_2 to the VM and the carbon content derived from carbonate minerals is done according to the following formulae (from British standards 1016 – on the reporting of results):

1. $\%VM_{(daf)} = (\%VM_{(ad)} - \%CO_2) \times (100 \div (100 - \%moisture - \%ash))$

2. $\%C_{(daf)} = (\%C_{(ad)} - 0.273 \times \%CO_2) \times (100 \div (100 - \%moist - \%ash))$

3. $\%C_{(daf)} = (\%C_{(ad)} - 0.273 \times \%CO_2) \times (100 \div (100 - \%moist - \%ash)) \times 100 \div (100 - \%CO_2)$

Equation **2** only takes into account that CO_2 from the carbon determination is contaminated by the CO_2 derived from the carbonate minerals. Therefore it should not only be appropriate to subtract the carbon ratio of the $CO_{2\ (ad)}$ from the $\%C_{(ad)}$ and then normalize to 100 on a dry, ash-free basis. Also provision should be made for the diluting effect of the CO_2 derived from the carbonate minerals on the original coal by applying the modification in equation **3** to equation **2**. Van Vuuren and Quass (1982) reported an enrichment of VM at a certain distance from an intrusion, probably due to the entrapment of volatiles which were distilled off closer to the contact. The coals close to the sill has volatiles in the lower contents ranging from 6.8 to 20 (daf), whereas unaffected coals range from 32.7 to 34.8 (daf).

RoV (max) (Figure 5.10): An average rank of 0.67% RoV has been determined for thermally unaffected coal by Hagelskamp (1987). Reflectivity profiles also showed that the highest values amongst unaffected coals are 0.81% RoV. Up to 8m from a dolerite dyke the rank increased by 1-1.2% RoV. Finally, close to the contact the reflectivity increased above 5.5% RoV_{max}. These cindered coals have an anthracitic and meta-anthracitic character.

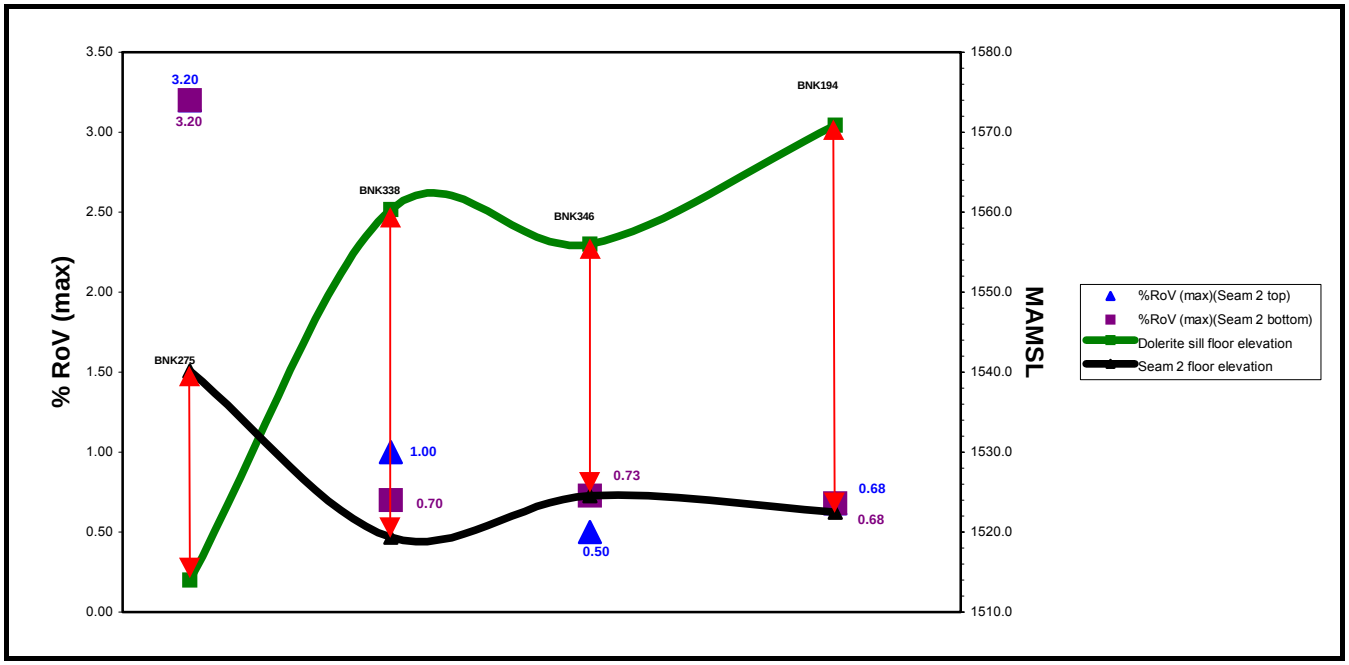

Figure 5.10 A combined graph of the actual relationship between the No. 2 Coal Seam and the sill, as well as the % RoV (max) variation at the top (triangles) and bottom (purple squares) of the No. 2 Coal Seam (Section 21). The red lines indicate the vertical distance between the sill and the No. 2 Coal.

The RoV (max) values (reflectance) in Figure 5.10 were calculated from the Seyler diagram in Figure 5.11 (VM (daf) and CV (daf) were used for the calculation). Borehole BNK 275 has an extremely high reflectance (3.2% RoV (max)) as opposed to the rest of the No. 2 Coal Seam (ranging from 0.5 to 1.0% RoV (max)). Similar observations were reported by Hagelskamp in 1987. His founding was based on actual and not inferred reflectance.

The uplifted and displaced No. 2 Coal Seam in the southern side of Section 21 (Figure 5.4) has undergone the highest degree of metamorphism. Bifurcation of the main sill in this specific area would have explained the spatial behaviour of metamorphism which probably resulted in a bigger contact aureole. It is apparent from the above graphs that the upper part of the in situ No. 2 Coal Seam has also undergone a slight degree of metamorphism.

b. No. 4L Coal Seam (proximate analyses and %RoV max)

The spatial relationship between the sill and the No. 4L Coal Seam is completely different as oppose to the No. 2 Coal seam. It is situated within the metamorphic contact aureole of the sill.

Ash (Figure 5.12): An anomalous high ash content (43.3% ash) at borehole BNK 346 (Figure 5.12) has a low CV (24.62MJ/kg) (Figure 5.14); an extremely high relative density (1.77) (Figure 5.15) and also a high VM (36.6 (daf)) (Figure 5.16). The most plausible reason for such a high VM content has been discussed. It should be mentioned that CO_2 is commonly enriched in proximity to dyke and sill intrusions which result into secondary precipitation of carbonate minerals (Hagelskamp, 1987).

From Section 21, the No. 4L Coal Seam is thinning towards the south. Only a slight variation in ash content prior to the sill intrusion could have been expected. Again, the relationships between ash, CV and relative density remained similar (compare Figures 5.12, 5.14 and 5.15).

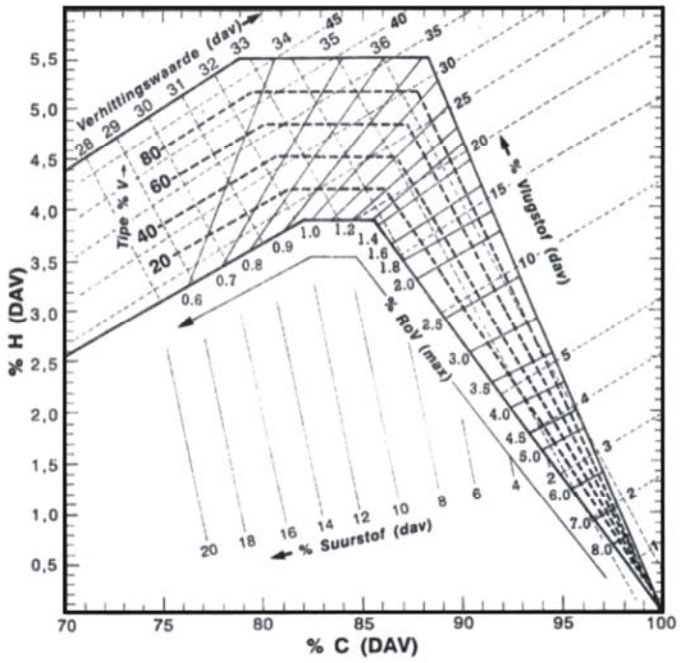

Figure 5.11 A Seyler diagram whereupon rank (%RoV (max)) and type (%V) are indicated (Snyman, 1996).

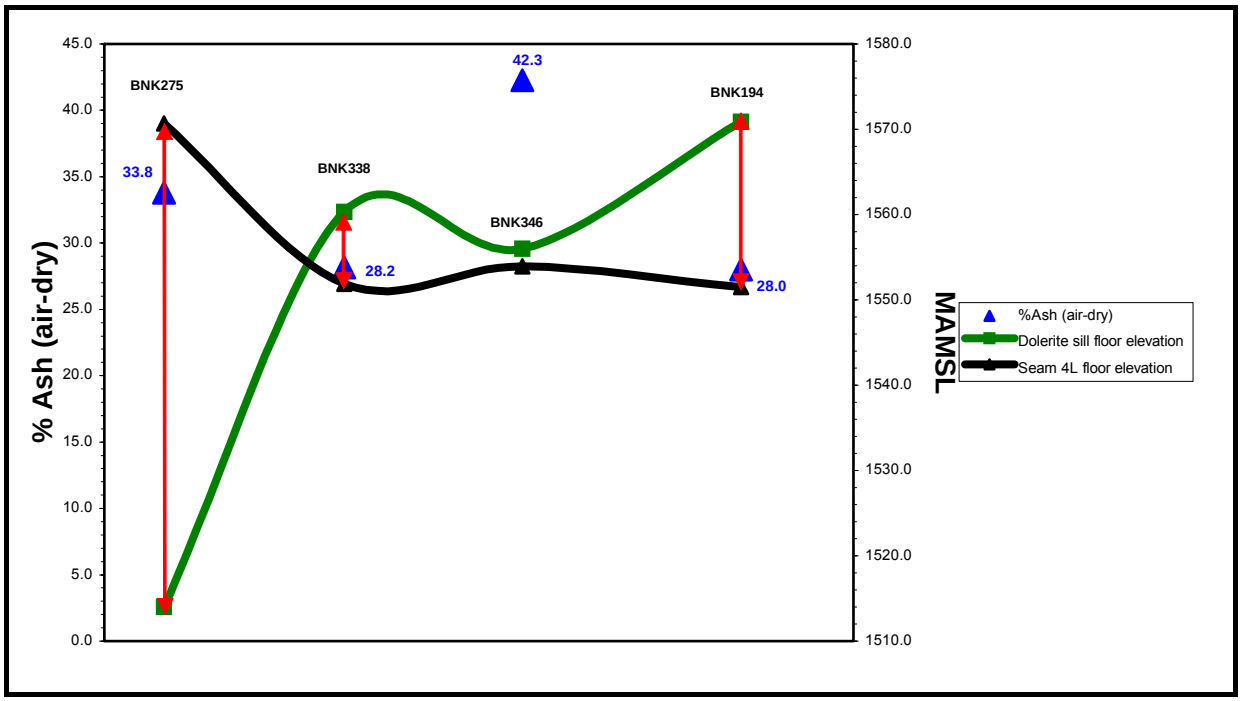

Figure 5.12 A combined graph of the actual relationship between the No. 4L Coal Seam and the sill, as well as the % ash (air-dry) variation (blue triangles) of No. 4L Coal Seam (Section 21). The red lines indicate the vertical distance between the sill and the No. 4L Coal Seam.

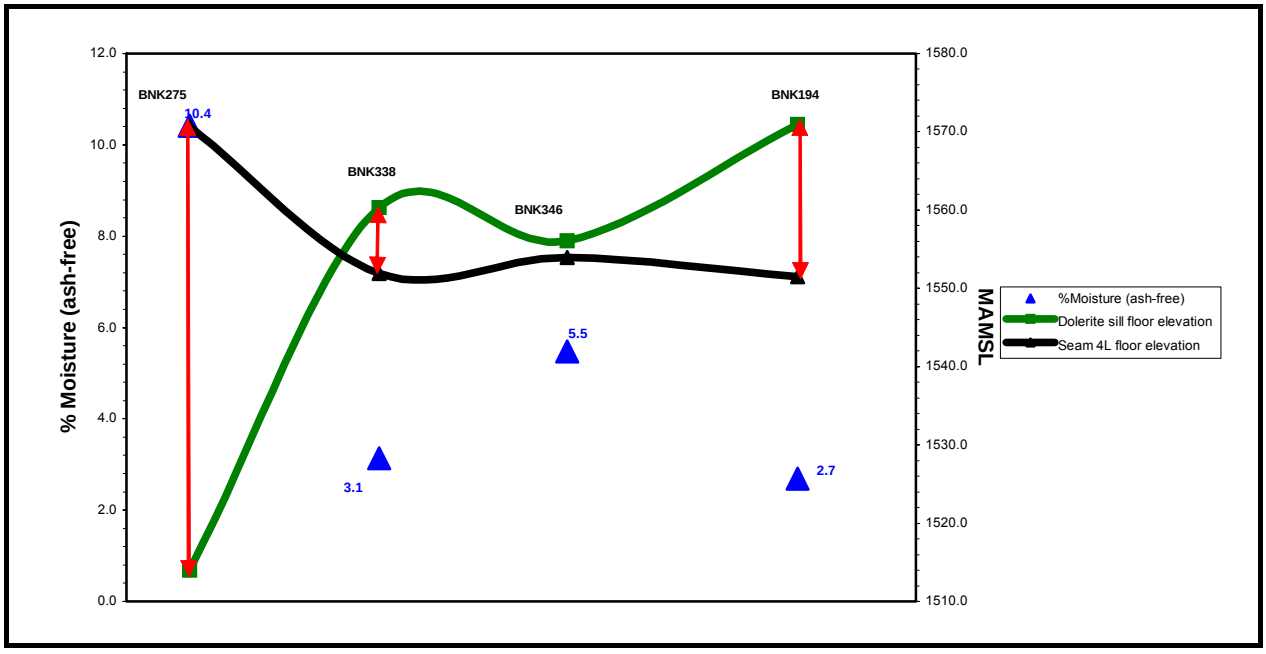

Figure 5.13 A combined graph of the actual relationship between the No. 4L Coal Seam and the sill, as well as the % moisture (ash-free) variation (blue triangles) of No. 4L Coal Seam (Section 21). The red lines indicate the vertical distance between the sill and the No. 4L Coal Seam.

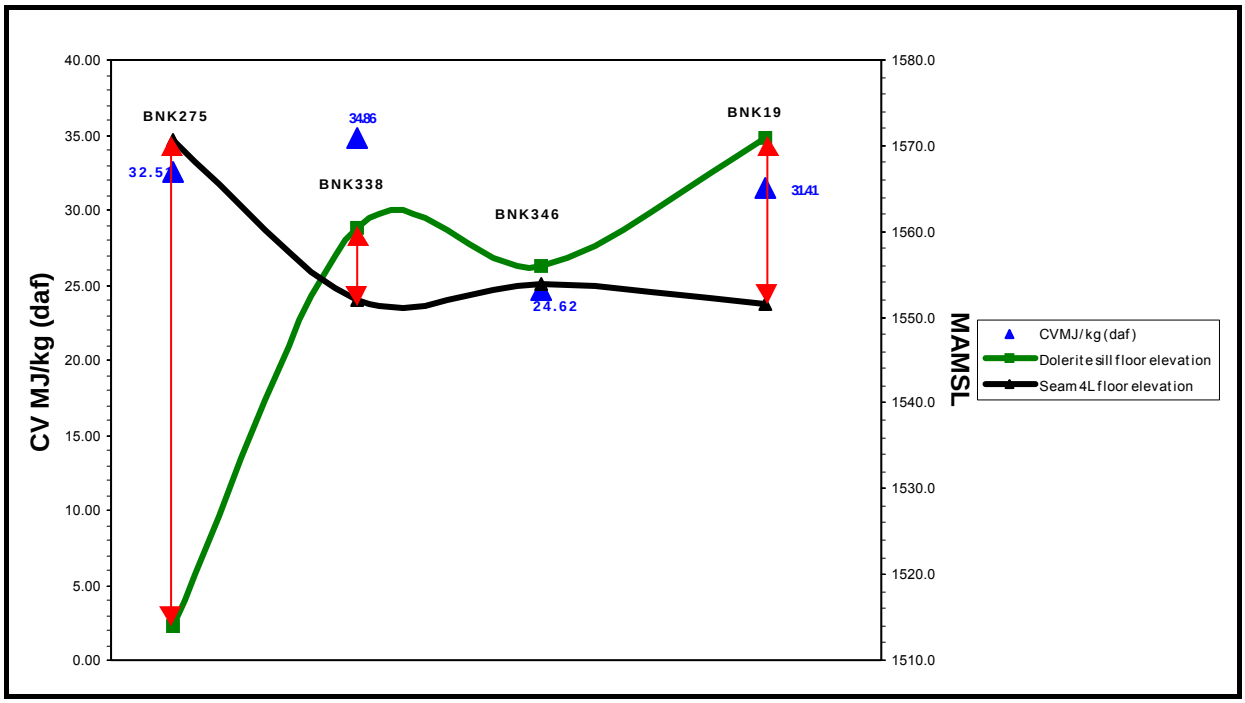

Figure 5.14 *A combined graph of the actual relationship between the No. 4L Coal Seam and the sill, as well as the CV MJ/kg (daf) variation (blue triangles) of the No. 4L Coal Seam (Section 21). The red lines indicate the vertical distance between the sill and the No. 4L Coal Seam.*

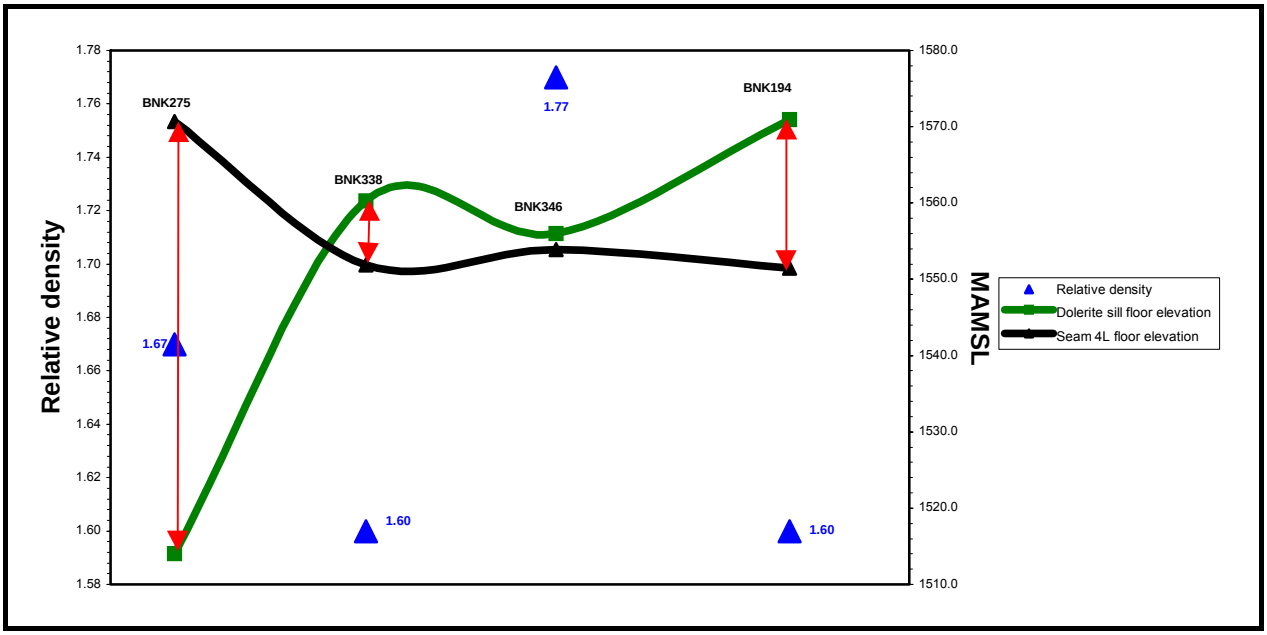

Figure 5.15 *A combined graph of the actual relationship between the No. 4L Coal Seam and the sill, as well as the variation (blue triangles) in relative density of No. 4L Coal Seam (Section 21). The red lines indicate the vertical distance between the sill and the No. 4L Coal Seam.*

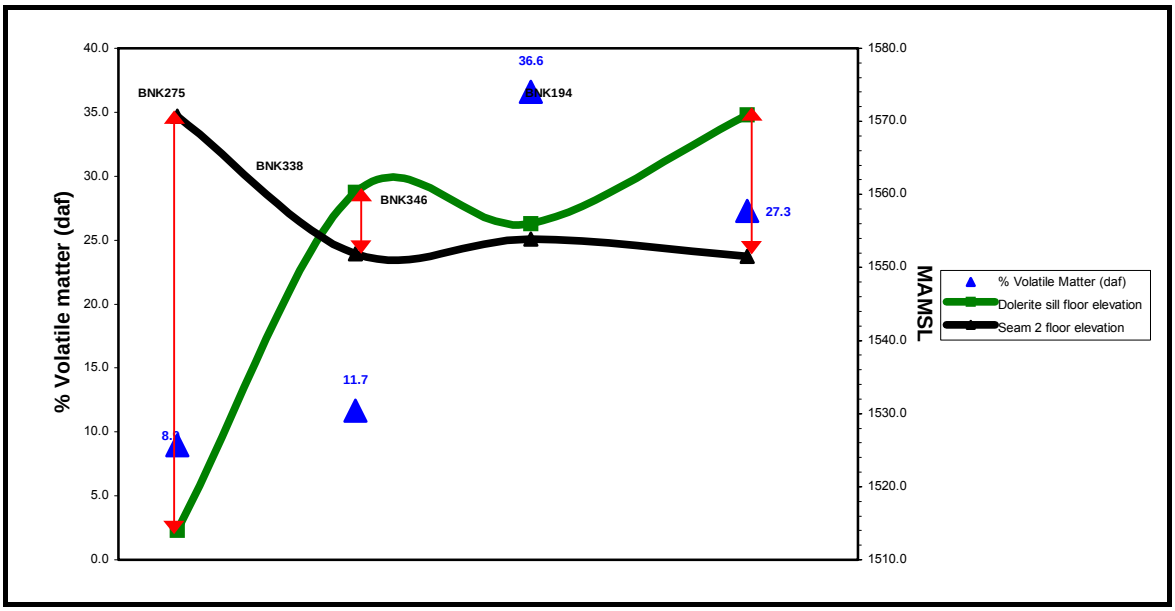

Figure 5.16 *A combined graph of the actual relationship between the No. 4L Coal Seam and the sill, as well as the %VM (daf) variation (blue triangles) of No. 4L Coal Seam (Section 21). The red lines indicate the vertical distance between the sill and the No. 4L Coal Seam.*

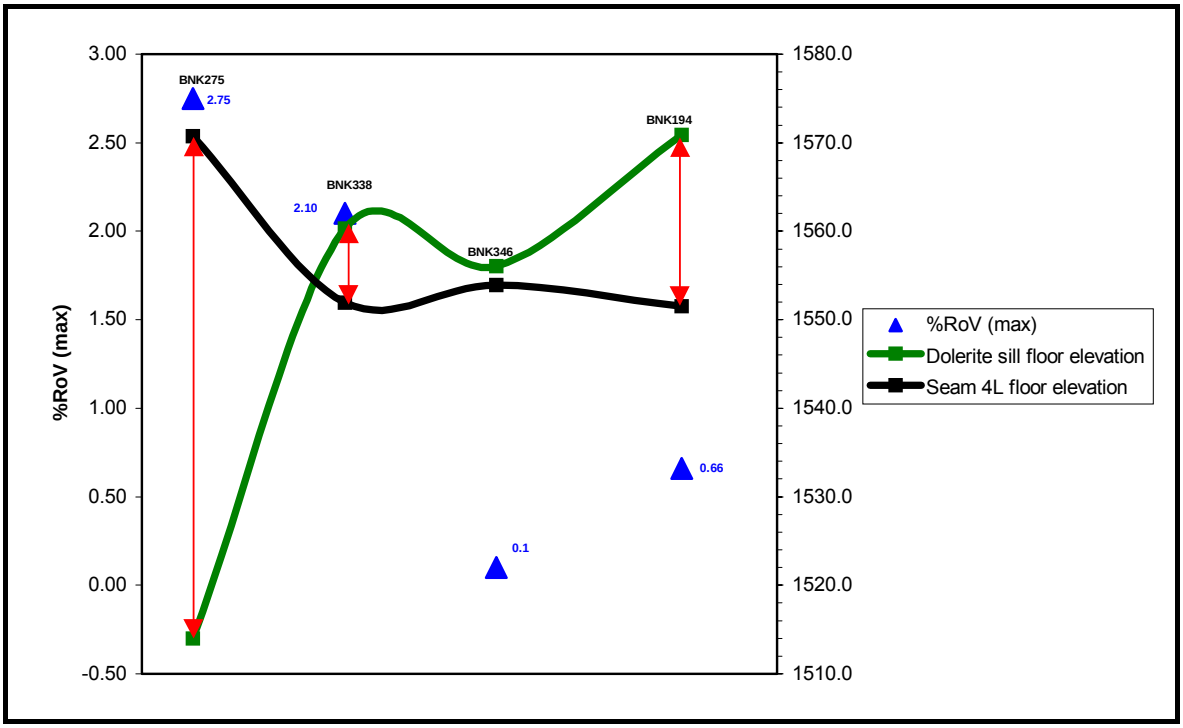

Figure 5.17 *A combined graph of the actual relationship between the No. 4L Coal Seam and the sill, as well as the %RoV (max) variation (blue triangles) of No. 4L Coal Seam (Section 21). The red lines indicate the vertical distance between the sill and the No. 4L Coal Seam.*

Moisture (ash-free) (Figure 5.13): In Figure 5.13 the moisture (ash-free) range from 2.7 to 5.5 in the coal which still remain in situ as opposed to borehole BNK275 which is anomalously high in moisture (ash-free). This trend, however, correlates with the moisture content of the No. 2 Coal Seam. It is apparent that the displaced and uplifted coals in Section 21 contain higher moisture contents as opposed to the coals that still remain in situ. A plausible reason could be the presence of abundant jointing that appears in the sediments above the sill.

VM (daf) (Figure 5.16): The anomalous high VM (daf) content in borehole BNK 346 has been discussed in a previous paragraph. At borehole BNK 275 and 338 the No. 4L Coal Seam have been completely devolatilised by the sill, whereas in borehole BNK194 only slightly. On Average the No. 4L Coal seam has undergone a higher degree of devolatilisation as opposed to the No. 2 Coal Seam as 60% of sill intrusion is in the proximity of the No. 4L Coal Seam (Figure 5.4).

RoV (max): It is apparent that the coal seams contained within the sediments, that have been displaced and uplifted by the sill, have a higher reflectance as opposed to those that still remain in situ. However the very low %RoV (max) value in borehole BNK346 can be ascribed to an enormously high ash value (Figure 5.12) that resulted in a poor CV (Figure 5.14).

To avoid repetition, RoV (max) will not be discussed in the sections that follow.

5.3.1.2 Section HH' EAST (5.18)

In Section HH' EAST borehole BNK263 penetrated the dolerite sill between the No. 2 and 4L Coal Seams and has a thickness of 20m that is regarded as being consistent throughout the section (Figure 5.18). The sill has a characteristic undulating geometry. The elevation difference between boreholes BNK159 and 399 of the coal seams imply a displacement factor that confirmed the interpretation of the sill structure. The sill constitutes a light greyish-blue dolerite and contains abundant calcite veins. No dolerite stringers were observed in the boreholes.

According to the reconstructed isopach and contour maps (Figures 5.3 A and B) of the No. 2 Coal Seam, this area is situated on a palaeo-ridge. The sedimentary environment under which these coals have formed will vary as opposed to those in the palaeo-

valleys. These variations have been discussed in Chapter 3 and need not to be repeated here.

Lithological descriptions of the coal seams in Section HH' EAST are summarised in Table 5.2. Descriptions indicating the metamorphic influence of the sill are shown in red. Metamorphic influenced coal is described as "burnt" or "devolatilised". The altered coal is also to some extent associated with "broken core" which have slickensides on the fracture planes. The slickensides and fracture planes are associated with secondary calcite and pyrite mineralisation. Slickensides and broken core are the result of intrusion by the sill. Coal seams that were intersected in boreholes BNK157 and 159 do not show any thermal effect of the sill. Lithological descriptions of these coal seams and their spatial relationship with the sill, indicate that they lie outside the metamorphic contact aureole.

a. No. 4L Coal Seam

Ash (Figure 5.19): Ash content ranges between 24.5 and 29.7 (air-dry) which compare to unaffected coals of the No. 4L Coal Seam in Section 21. The interpretation of the sill structure in Section HH' EAST implies that the distance between the sill and the displaced No. 4L Coal Seam remains approximately constant as to the red arrows in Figures 5.19, 5.20 and 5.21.

The coals from the No. 4L Coal Seam in boreholes BNK399 and 331 have been described as "burnt" or devolatilised. In Table 5.2 the coal have only negligible higher ash concentrations as opposed to borehole BNK263 which is described as slightly devolatilised.

Moisture (ash-free) (Figure 5.21): A combined graph indicates that all the available moisture (ash-free) data is from the displaced No. 4L Coal Seam. Accordingly values ranging from 4 to 6.9 are indicative of such displaced coal. The scenario in Section 21 (Figure 5.13) regarding the higher moisture (ash-free) distribution associated with the displaced and uplifted coal compares with Section HH' EAST (Figure 5.21)

VM (daf) (Figure 5.20): According to the distance between the sill and the No 4L Coal seam, it is not expected to be situated within the contact aureole. From the VM (daf) values of 11.4 and 14.6 that occur in boreholes BNK399 and 195 respectively, and their lithological descriptions, the uplifted No. 4L Coal Seam is partially situated within

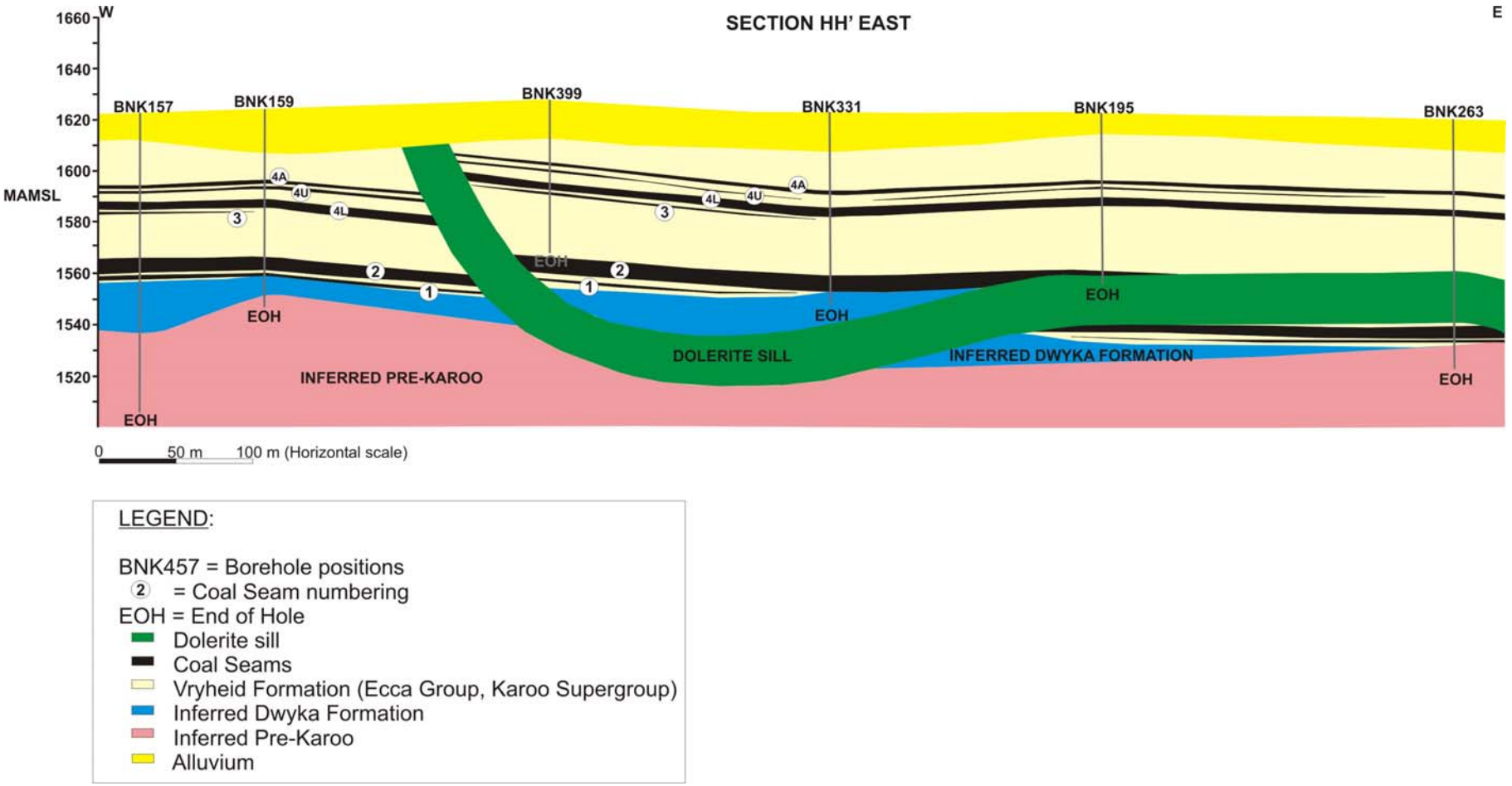

Figure 5.18 A geological cross-section showing the interpretation of a dolerite sill structure (Du Plessis, 2001). See locality of section in Figure 5.1.

the metamorphic contact aureole (Figure 5.20). As to previous occurrences it can be expected that a more extensive contact aureole occurs above the sill as underneath it. However the normal VM (daf) values at boreholes BNK263 and 331 indicate a rather undulating contact aureole.

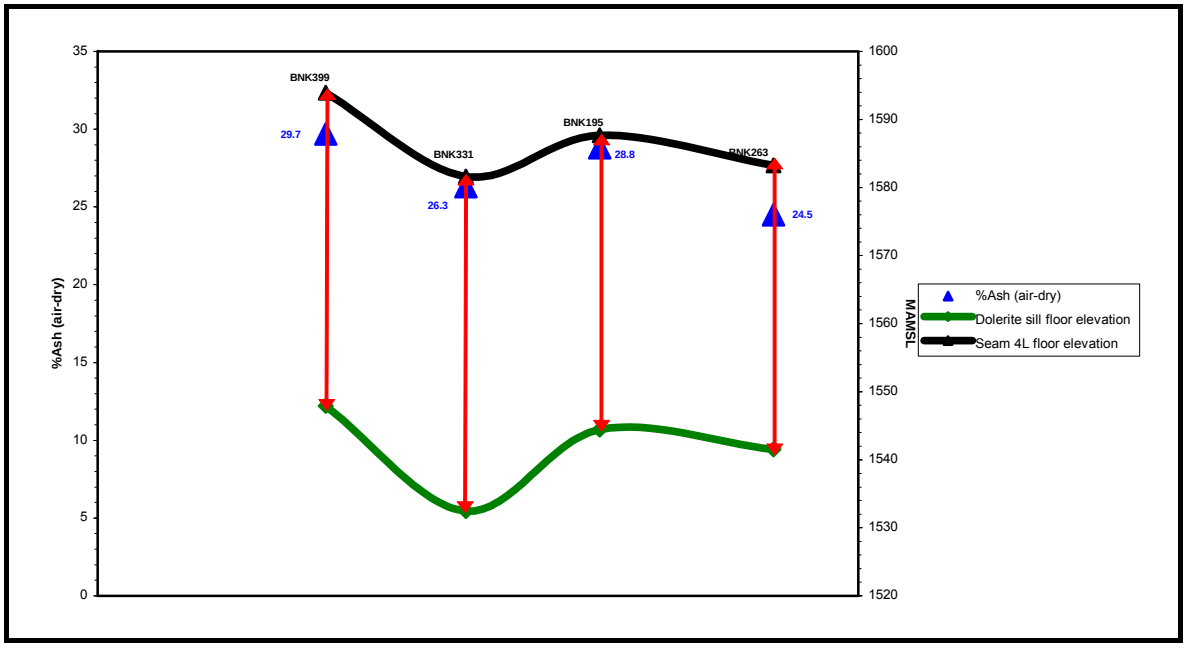

Figure 5.19 ***A combined graph of the actual relationship between the No. 4L Coal Seam and the sill, as well as the % ash (air-dry) variation (blue triangles) of the No. 4L Coal Seam (Section HH'EAST). The red lines indicate the vertical distance between the sill and the No. 4L Coal Seam.***

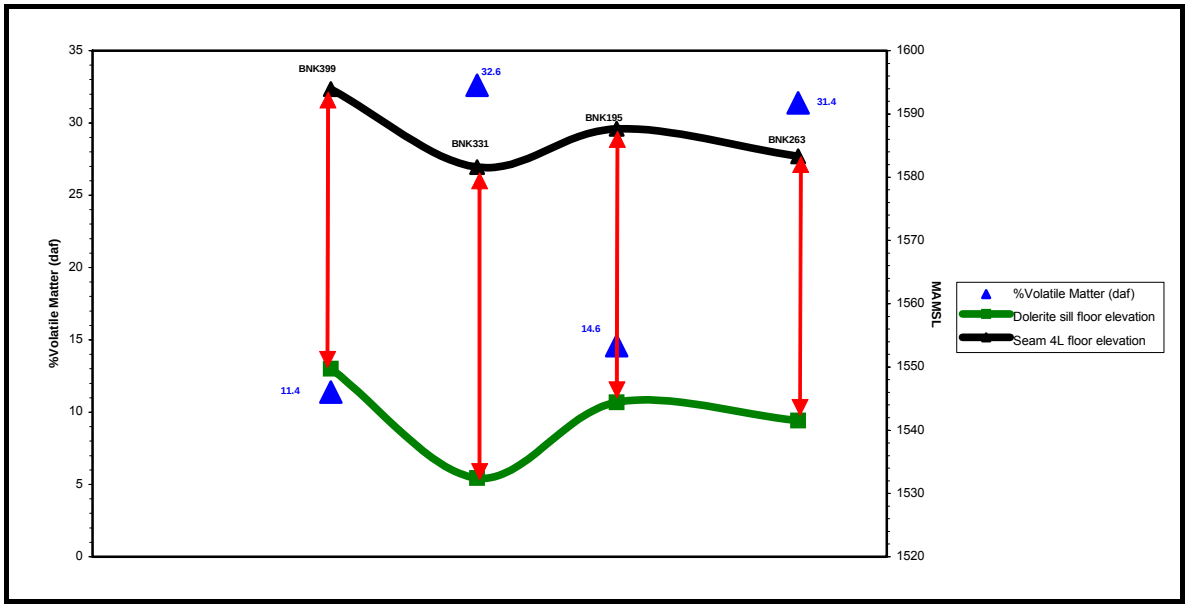

Figure 5.20 ***A combined graph of the actual relationship between the No. 4L Coal Seam and the sill, as well as the % VM (daf) variation (blue triangles) of the No. 4L Coal Seam (Section HH'EAST). The red lines indicate the vertical distance between the sill and the No. 4L Coal Seam.***

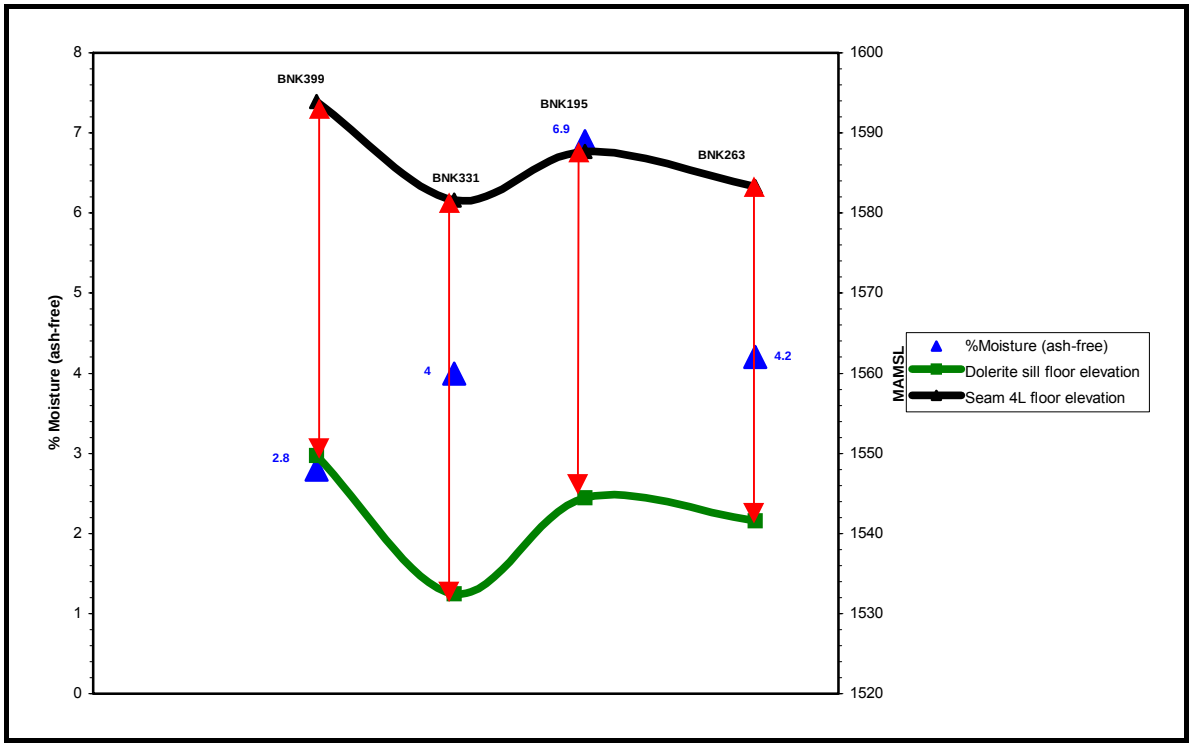

Figure 5.21 ***A combined graph of the actual relationship between the No. 4L Coal Seam and the sill, as well as the % moisture (ash-free) variation (blue triangles) of No. 2 Coal Seam (Section HH'EAST). The red lines indicate the vertical distance between the sill and the No. 4L Coal Seam.***

5.3.1.3 Section HH' WEST (Figure 5.22)

An undulating and bifurcating sill is dealt with in Section HH' WEST. Although borehole BNK297 did not intersect the sill, the elevation difference between the coal seams in boreholes BNK261 and 297 implies a displacement factor which prove the structural interpretation of the sill. According to the rules applied during the interpretation of the sill structure, the 16.2 m thick dolerite intersected in borehole BNK14 had to be a bifurcation from the main sill between boreholes BNK14 and 115. The lithological descriptions (in boreholes BNK14, 115 and 261) indicate that the sill has undergone intensive alteration which generally occurs when dolerites are close to surface.

Table 5.2 Lithological descriptions of the coal seams intersected in Section HH' EAST. The red descriptions the influence of the dolerite sill.

SEAM No.	BOREHOLE NUMBERS – GEOLOGICAL CROSS-SECTION HH' EAST					
	BNK157	**BNK159**	**BNK399**	**BNK331**	**BNK195**	**BNK263**
5	Not present.	Not present.	Not present.	Not present.	Not present.	Not present.
4A	Coal: mixed, ±10% vitrain. Shale: carbonaceous. Coal: dull. Coal: shaly.	No detail descriptions.	**Coal: burnt.**	Coal: dull, shaly. Coal: mixed, <10% bright, **abundant pyrite nodules.** **Coal: dull, intensely broken**.	50% coal: dull lustrous, <10% bright. **Perhaps devolatilised.** 50% coal: dull.	Coal: lustrous, 40-60% bright, thinly laminated. **Few calcite on cleats.** **Occasional pyrite nodules.**
4U	Coal: dull, shaly, **with slickensides**.	No detail descriptions.	**Coal: burnt.** **Dolerite stringer ("white trap").** **Coal: burnt, weathered.**	Not present.	No detail descriptions.	Not present.
4L	Coal: mixed, ±50% vitrain. Grit. Coal: dull. Grit. Coal: mixed. ±30% vitrain. Coal: dull lustrous.	No detail descriptions.	**Coal: burnt.** Remnant bright bands.	Coal: dull lustrous, **occasional calcite on cleats.** Coal: bright, **abundant pyrite nodules.** Coal: dull. Siltstone-shale parting. Coal: dull lustrous	Coal: dull, **burnt (Remnant bright bands)**. 50% coal: dull. 50% coal: dull lustrous, **devolatilised**. Coal: dull, silty, granular, **burnt**. 70% coal: dull. 30% coal: dull lustrous, **devolatilised**.	Coal: lustrous, 40-60% bright, thinly laminated. Rare pyrite laminae, **rare calcite on cleats.** Shale: carbonaceous. Coal: bright, 60-90% bright, blocky, **Abundant calcite on cleats.** Coal: dull lustrous, 40-60% bright, thinly laminated, **Occasional calcite on cleats.** **Slightly devolatilised.**
3	No detail descriptions.	Not present.	**30% coal: burnt**. 70% shale: indurate.	Not present.	Not present.	Not present
2	Coal: mixed. ±20% vitrain. Coal: dull lustrous, slightly shaly. Coal: dull lustrous. Coal: mixed. ±30% vitrain. Coal: dull lustrous. Coal: dull lustrous, **with slickensides**. Coal: mixed. ±10% vitrain. Coal: mixed. ±70% vitrain. Coal: mixed. ±10% vitrain. Coal: bright, slightly shaly.	No detail descriptions.	Not present	Coal: dull, **abundant pyrite nodules.** Coal: dull. Sporadic thin bright bands. Coal: dull lustrous, **abundant pyrite nodules.** **Abundant pyritic bands and slickensided**. Coal: bright, **occasional siderite nodules**. Coal: dull lustrous. Minor bright bands. Coal: dull. Coal: dull lustrous. Coal: mixed, 60-90% bright. **Occasional pyrite bands.** Coal: dull and **slickensided**. Siltstone parting (0.02 m) Coal: bright, **occasional pyrite nodules**. Siltstone parting (0.02 m). Coal: dull lustrous.	**Coal: badly burnt**. Not sampled	Coal: **burnt, broken core.** Shale: carbonaceous. **Coal: burnt.** Shale: carbonaceous, sandy. Coal: **burnt, very broken core.** Shale: carbonaceous, sandy. Coal: **burnt, very broken core**.
1	Coal: mixed. ±20% vitrain.	No detail descriptions.	Not present.	Not present.	Not present.	Coal: dull, <10% bright. Slightly shaly. Coal: lustrous, 40-60% bright, thinly laminated. Slightly **devolatilised**.

According to the reconstructed isopach and contour maps (Figures 5.3 A and B) of the No. 2 Coal Seam (Section HH' WEST) it is located on a palaeoridge (1 to 4m-thick coal) to the west and to the east on a palaeovalley-flank (6 to 8m thick coal). The change in sedimentary environment under which these coals of the No. 2 Coal Seam have formed must be considered when coal parameters are used to define the influence of the sill.

The coal seams in borehole BNK261 are not devolatilised, however according to the secondary mineralisation of calcite and pyrite on cleats and joints associated with slickensides, they were physically influenced as opposed to the coals in borehole BNK297 which have been intensely "burnt" (Table 5.3).

a. No. 2 Coal Seam

Ash content (Figure 5.23): Anomalously high ash values occur at boreholes BNK14 and 297. The discussion on the influence of syngenetic factors on specific ash content in Chapter 3 accordingly proved a negligible increase in ash towards elevated parts of a coal seam. At borehole BNK297 where the No. 2 Coal Seam thins towards the palaeo-ridge higher ash content could have been expected. However, in this case such high ash content (41.2%) is epigenetically related. The extremely high ash at borehole BNK14 could be related to the bifurcation from the sill. From the red arrows in Figures 5.23, 5.24 and 5.25 (boreholes BNK14 and 115) it is evident that the distance between the bifurcation and the No. 2 Coal Seam remains constant. It must be kept in mind that the section views are normally deceiving as to the actual spatial relationship between these dolerites and the coal seams.

VM (daf) (Figure 5.24): The ash content is inversely related to the VM (daf) distribution of the No. 2 Coal Seam (Figure 5.24). VM (daf) values of 19.3 and 15.4 indicate complete devolatilisation. The very low value at borehole BNK297 which is close to the sill and part of the coal (No. 2 Coal Seam) contained within the displaced and uplifted sediments, could have been expected when comparing to borehole BNK14 where the No. 2 Coal Seam appears to be more distant from the bifurcation. As was mentioned in the previous paragraph, in section, the relationship could be deceiving as to the spatial relationship. The undulating geometry of the dolerite sill which could be described as an "egg-box" structure (Figure 5.2) which has a metamorphic contact aureole with similar geometry as the sill. A much more complicated metamorphic contact aureole could have been expected from such an undulating structure as opposed to a sill with a more horizontal geometry.

Moisture (ash-free) (Figure 5.25): Only negligible variations in the moisture (ash-free) content (3.1 to 3.8) indicate a more intermediate micro-porosity throughout the No. 2 Coal Seam in Section HH' WEST (Figure 5.25). Accordingly the sill had only little effect on the No. 2 Coal Seam.

Table 5.3 Lithological descriptions of the coal seams intersected in Section HH' WEST. The red descriptions indicate the influence of the dolerite sill.

SEAM No.	BOREHOLE NUMBERS – GEOLOGICAL CROSS-SECTION HH' WEST			
	BNK14	BNK115	BNK261	BNK297
5	Not present.	No detail descriptions.	Coal: lustrous, 40-60% bright, thinly laminated, **calcitic, occasional pyrite nodules.**	Coal: 60-90% bright, thinly laminated, **blocky**, **broken core**, **rare pyrite veins.**
4A	No detail descriptions.	No detail descriptions.	Coal: dull lustrous, 10-40% bright, thinly laminated. Coal: lustrous, 40-60% bright, thinly laminated, **calcitic**. Coal: dull lustrous, <10% bright, **pyritic**, **occasional calcite on joints**.	Coal: **burnt**, shaly, interlaminated**, scattered pyrite veins.**
4U	Not present.	Not present.	Not present.	Not present.
4L	No detail descriptions.	No detail descriptions.	Coal: dull lustrous, 10-40% bright, thinly laminated. Sandstone: dark grey, medium to fine grained, silty. Coal: dull, <10% bright, **with slickensides**. Coal: lustrous, 40-60% bright, medium laminated. Coal: dull lustrous, 10-40% bright, with **slickensides. Pyrite.** Coal: dull lustrous, 10-40% bright, thinly laminated	Coal: **slightly burnt**, sandy. **Occasional slickensides**, **broken at base**, shaly.
3	Not present.	Not present.	Coal: shaly.	Coal: shaly, lustrous, interlaminated, **occasional calcite on cleats.**
2	No detail descriptions.	No detail descriptions.	thinly laminated. **Pyritic at top**. Inter seam parting: **sideritic and pyritic**. Medium laminated, **occasional calcite on cleats.** Coal: dull lustrous, 10-40% bright. Coal: dull lustrous, 10-40% bright, thinly laminated, **occasional pyrite nodules.** Coal: dull lustrous, 10-40% bright, thinly laminated. Coal: dull lustrous, <10% bright. Coal: dull lustrous, 10-40% bright, thinly laminated. Coal: dull lustrous, 10-40% bright, thinly laminated, **occasional pyrite nodules.**	**Dolerite bearing (mixed with burnt shale), occasional calcite veins.** Shale: dark grey, slightly carbonaceous, coaly, **moderately weak rock.** **Intensely burnt**.
1	Not present.	No detail descriptions.	Not present.	Not present.

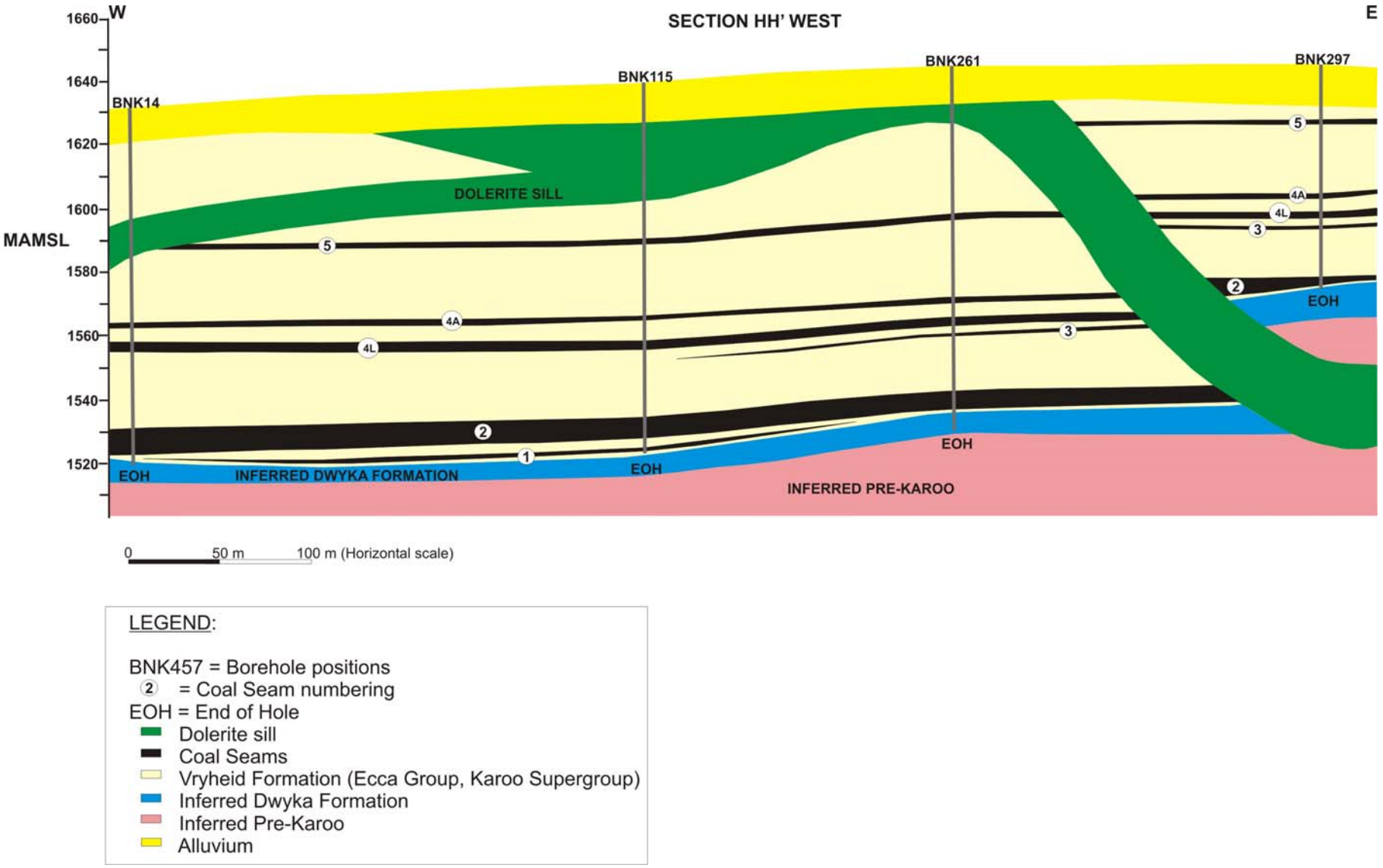

Figure 5.22 A geological cross-section showing the interpretation of a dolerite sill structure (Du Plessis, 2001). See locality of section in Figure 5.1.

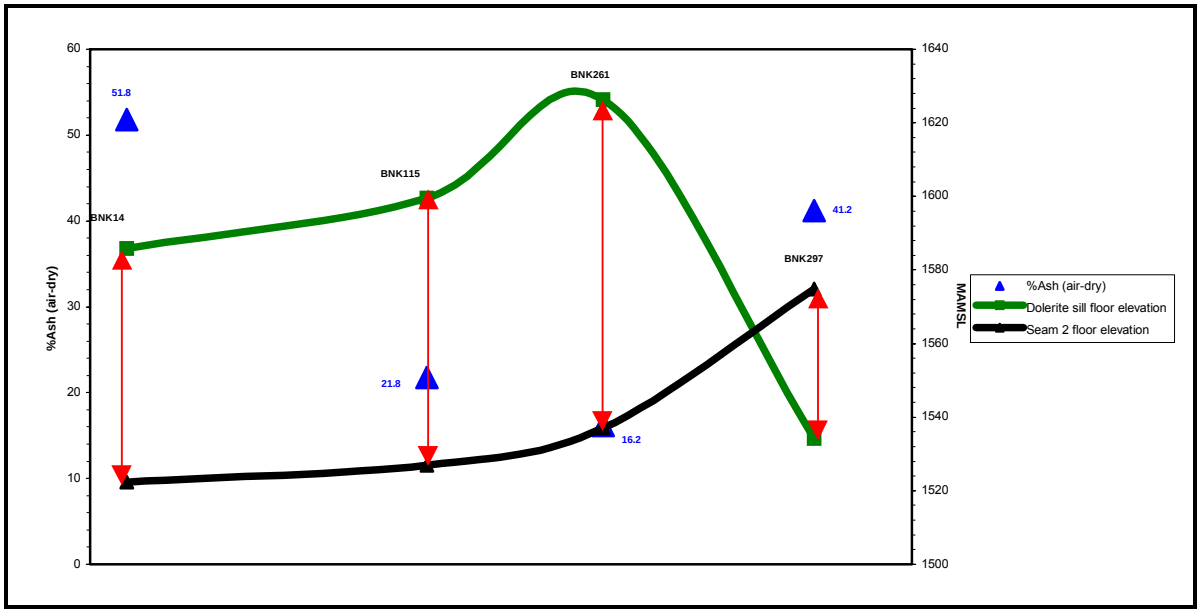

Figure 5.23 A combined graph of the actual relationship between the No. 2 Coal Seam and the sill, as well as the % ash (air-dry) variation (blue triangles) of No. 2 Coal Seam (Section HH'WEST). The red lines indicate the vertical distance between the sill and the No. 2 Coal Seam.

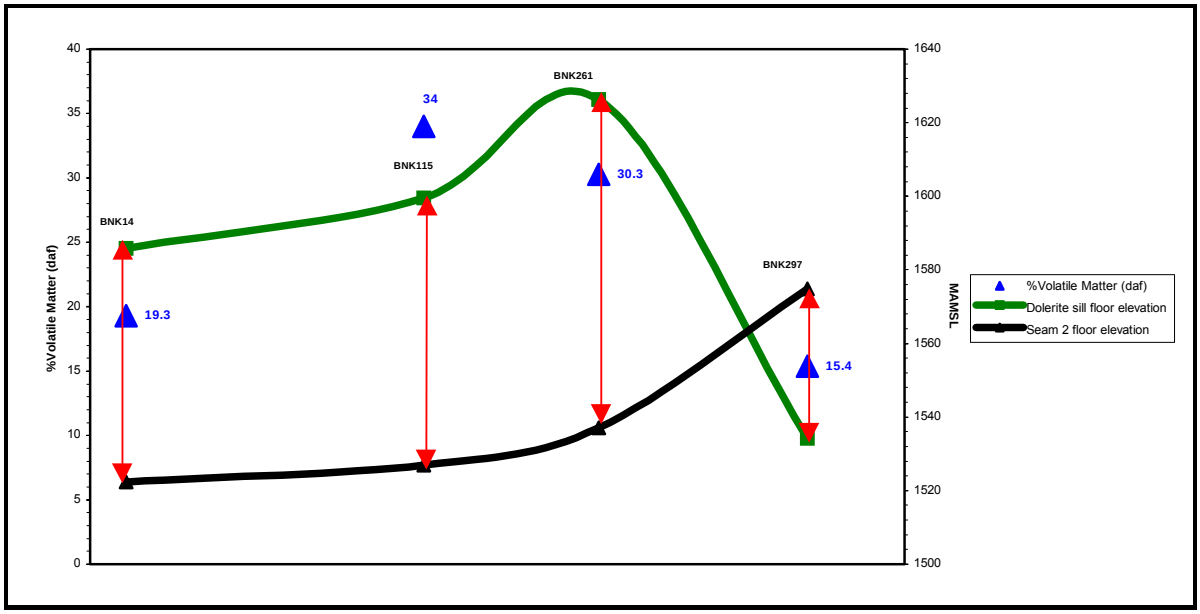

Figure 5.24 A combined graph of the actual relationship between the No. 2 Coal Seam and the sill, as well as the %VM (daf) variation (blue triangles) of No. 2 Coal Seam (Section HH'WEST). The red lines indicate the vertical distance between the sill and the No. 2 Coal Seam measured form the borehole core.

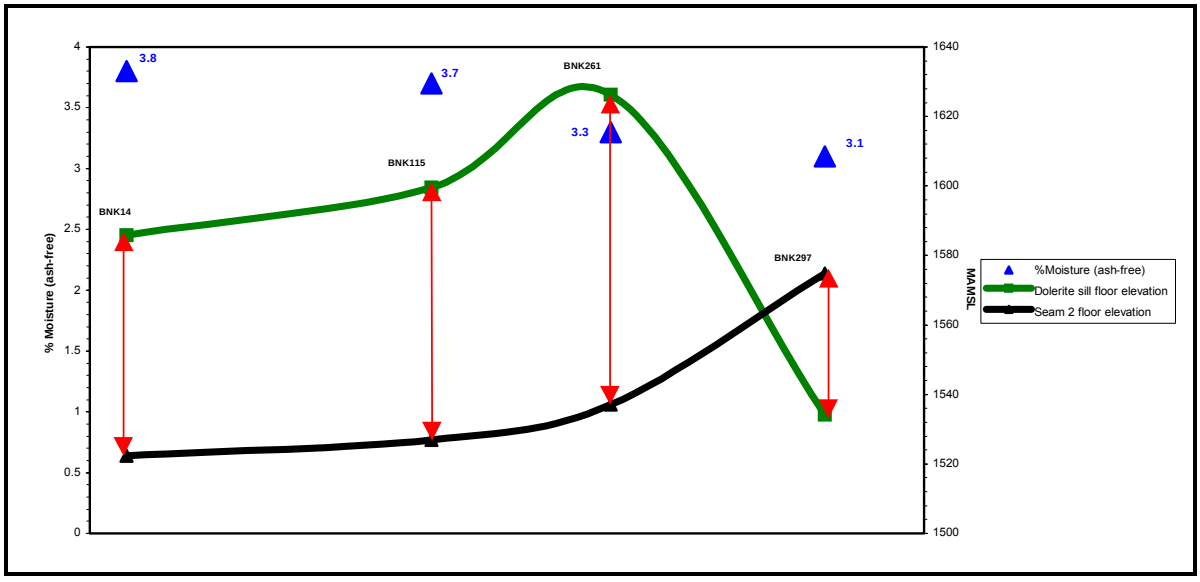

Figure 5.25 ***A combined graph of the actual relationship between the No. 2 Coal Seam and the sill, as well as the % moisture (ash-free) variation (blue triangles) of No. 2 Coal Seam (Section HH'WEST). The red lines indicate the vertical distance between the sill and the No. 2 Coal Seam.***

5.3.1.4 Section GG' (Figure 5.26)

From section GG' it is evident that the 20m thick sill has a transgressive geometry (main sill) and the occurrence of an upper ±9m thick, non-transgressive sill (Figure 5.26). Only remnants of this ±9m thick sill remain throughout the study area.

Steeper intrusion angles adopted by the main sill tend to be associated with bifurcation (as in Section 21) (Figure 5.26). The thicker sill is a light grey, medium grained and siliceous dolerite as opposed to the thinner sill which is a dark green, fine to medium grained dolerite. The bifurcations from the main sill have the same characteristics as the thinner sill even though finely crystalline.

According to the reconstructed isopach and contour maps (Figures 5.3 A and B) the No. 2 Coal Seam (Section GG') is located on a palaeovalley-flank to the east (4 to 6m thick coal) and west on a palaeoridge (1 to 2m thick coal). The change in sedimentary environment under which the coal of the No. 2 Coal Seam have formed needs to be kept in mind when defining the influence of the main sill on the coal.

All the No. 2 Coal Seam intersections show devolatilisation, except for borehole BNK224 which has not been displaced nor intersected by the sill (Table 5.4). Devolatilisation is usually associated with broken core (poor core recoveries) and slickensides. The No's 3, 4L, 4U, 4A and 5 coal seams in borehole BNK417 (Table 5.4) indicate the influence by the sill. The main sill intrusion displaced and uplifted the sediments in this section. Fractures and cracks in the coal seams are associated with pyrite and calcite mineralisation (borehole BNK230, Seam 4A; borehole BNK246, Seam 5; borehole BNK224, Seam 5; borehole BNK260, Seams 5 and 4A and borehole BNK296, Seam5 (Table 5.4)).

a. No. 4L Coal Seam

Ash content (Figure 5.27): The No. 4L Coal Seam thins and eventually pinches out towards the east. Prior to the sill intrusion negligible higher ash values to the east could have been expected (discussion on the influence of syngenetic factors on ash content in Chapter 3). In this section ±80% of the sediments are displaced and uplifted by the major sill. The properties of the coal seams hosted by the surrounding sediments were epigenetic in nature. Only negligible higher ash values occur in boreholes BNK417, BNK246 and BNK260. These higher ash values range between 23.7 and 27.3%. The lower ash values at boreholes BNK230 and 224 range between 19.5 and 21.3%. From the section these latter boreholes with lower ash values are situated further away from the sill.

VM (daf) (Figure 5.28): Only the coals from boreholes BNK224 and 260 indicate complete devolatilisation (23.47 and 24.39 VM (daf) respectively). Boreholes **BNK246** and 230 (28.83 and 28.34 VM (daf) respectively) indicate the boundary of the contact aureole. The higher 31.09 VM (daf) at borehole BNK417 could be ascribed to secondary mineralised carbonate minerals that enhanced the volatiles. Suggestive higher volatiles (daf) at No's 3 and 4A Coal Seams of 41.08 and 31.48 respectively, also prove that volatiles could have had its origin from the nearby sill.

Moisture (ash-free) (Figure 5.29): Only negligible variations in the moisture (ash-free) content (2.1 to 3.49) indicate a much more intermediate micro-porosity. When comparing the moisture (ash-free) values from previous sections (which range between 5 and 6), the values from this section are of a much lower order. A large portion of the No. 4L Coal Seam has been displaced and uplifted by the main sill which caused more intensive joint structures that could have resulted in a porous coal seam.

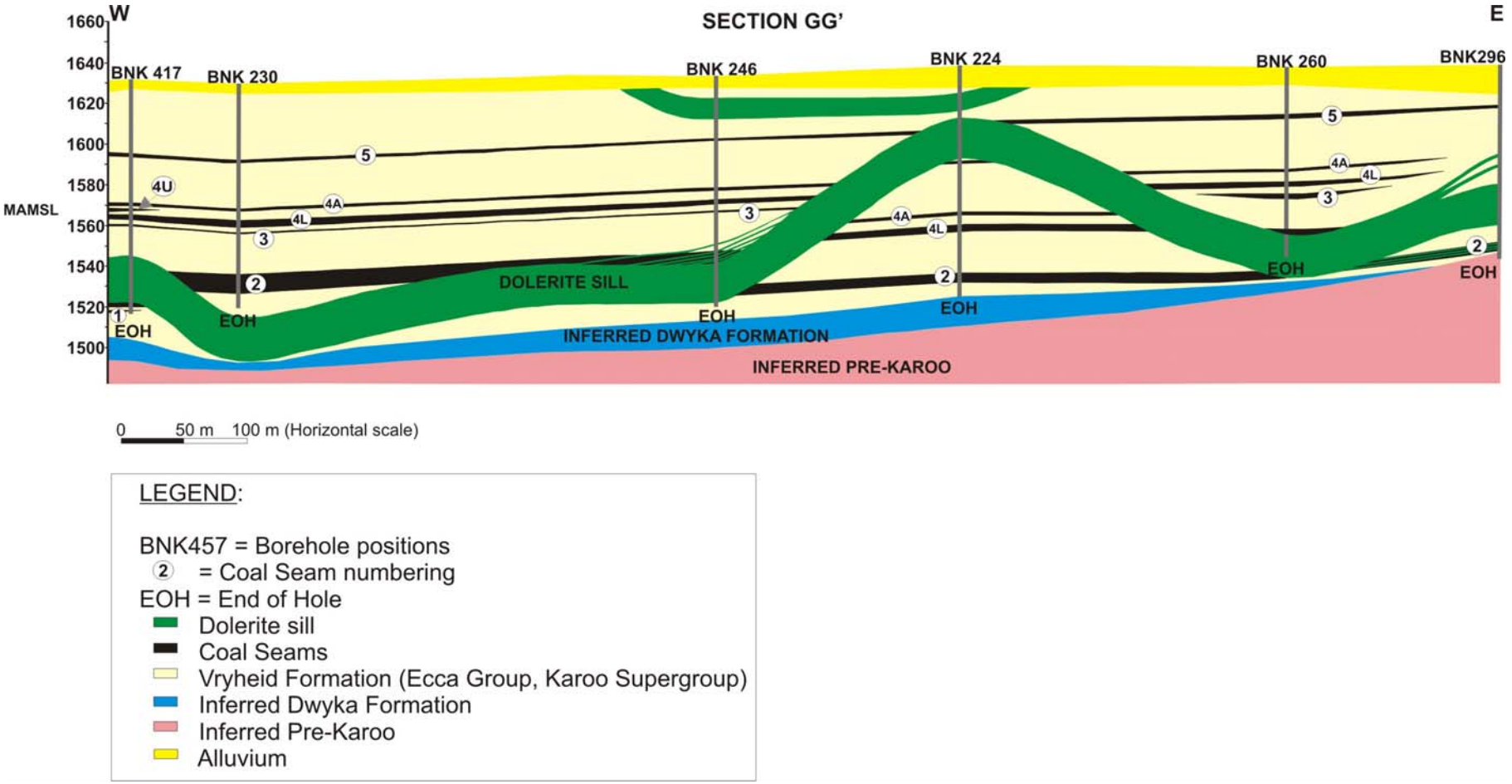

Figure 5.26 A geological cross-section showing the interpretation of a dolerite sill structure (Du Plessis, 2001). See locality of section in Figure 5.1.

Table 5.4 Lithological descriptions of the coal seams intersected in Section GG'. The red descriptions indicate the influence of the dolerite sill on the coal.

SEAM No.	BOREHOLE NUMBERS – GEOLOGICAL CROSS-SECTION GG"					
	BNK417	BNK230	BNK246	BNK224	BNK260	BNK296
5	20% coal, 40-60% bright, **calcite on cleats, pyrite lenses.** 10% coal, 10-40% bright. 70% coal, dull.	No detail descriptions	Coal, dull lustrous, 60-90% bright, thinly laminated. Coal, dull lustrous, 60-90% bright, thinly laminated, **pyrite bearing.** Coal, dull, <10% bright (few bright bands). Coal, dull lustrous, 10-40% bright, thinly laminated.	Coal, dull, <1% bright, **broken core**.	Coal: dull lustrous. **Badly broken, poor recovery**.	**Coal, devolatilised.** **Badly broken.**
4A	5% coal, 40-60% bright, **pyrite lenses, calcite on cleats.** 10% coal, 10-40% bright. 15% coaly shale. 70% coal, dull	Coal, dull lustrous, 10-40% bright, thinly laminated, **abundant calcite on cleats.**	Coal, 10-40% bright, thinly laminated. Coal, 40-60% bright, thinly laminated, calcite bearing. Coal, <10% bright (few bright bands).	No detail descriptions.	Coal: dull lustrous, 10-40% bright, medium laminated. **Occasional pyrite nodules.**	Not present.
4U	50% shale. **Rare pyrite.** 50% coaly shale. 60% coaly shale. 10% coal, 10-40% bright. 30% coal, dull.	Not present.	Not present.	Not present.	Coal, 60-90% bright, thinly laminated. Coal, dull, <10% bright, thickly laminated, silty in places.	Not present.
4L	10% coal, 40-60% bright, **calcite on cleats, pyrite bearing, very broken core.** 15% coal, 10-40% bright. 25% coaly shale. 50% coal, dull. Shale (0.15m) 10% coal, 40-60% bright, **calcite on cleats, pyrite bearing, very broken core.** **Trace devolatilised**. 50% coal, dull lustrous. 40% coal, dull.	Coal, lustrous, 40-60% bright, thinly laminated. Coal, dull lustrous, 10-40% bright. Coal, lustrous, 60-90% bright, thickly laminated. Siltstone. Coal, dull lustrous, 10-40% bright. Coal, dull lustrous, 10-40% bright, thinly laminated.	Coal, dull, <10% bright. Coal, dull lustrous, 40-60% bright, thinly laminated. Coal, dull, <10% bright. Coal, dull, <10% bright.	Coal, dull, <1% bright, thickly laminated. Coal, dull, <1% bright. Coal, dull, <1% bright, with slickensides.		Not present.
3	55% coaly shale, **pyrite lenses**. 10% coal, 10-40% bright. 5% coal, 40%-60% bright. 30% coal, dull.	Coal, 40-60% bright.	Coal, 60-90% bright, dull lustrous, thinly laminated. **Pyrite and calcite bearing.**	Not present.	Coal, dull lustrous, 10-40% bright, thinly laminated.	Not present.
2	**Coal, badly burnt**	Coal, dull lustrous, 10-40% bright (Indurated)	**Coal, dull, devolatilised.** **Dolerite, dark green, fine grained, siliceous, massive.** **Broken contact.** **Coal, dull, devolatilised.** **Dolerite, dark green, massive.** **Coal, dull, devolatilised.** **Dolerite, dark green, massive, slightly siliceous.**	Coal, dull, shaly, <1% bright, **with slickensides**. Coal, dull, <1% bright. Coal, dull, <1% bright.	**Coal, dull, devolatilised.** **Very broken. Poor recovery.** **Sandstone/Siltstone.** **Dolerite, light grey.** **Broken and decomposed (Not sampled).** **Coal, dull, devolatilised.** **Broken core, poor recovery.**	**Coal, burnt, friable.** **Dolerite.** **Coal, devolatilised, broken core.** **Dolerite.** **Coal, devolatilised, broken core.** **Dolerite, coaly, devolatilised, interlaminated.** **Coal, devolatilised, slightly, shaly, rare calcite veins, rare dolerite stringers.** **Dolerite.** **Coal, devolatilised, broken core.** **Slightly shaly at base.**
		Shale, silty, slightly carbonaceous. **Coal, dull burnt, with slickensides.** **Shale.** **Coal, dull, burnt.** Shale (gritty at base).		Siltstone, sandy (Not sampled).		
				Coal, dull, <1% bright. Coal, dull, <1% bright.		
		Coal, dull lustrous, 10-40% bright. Shale, slightly carbonaceous. Coal, dull lustrous, 10-40% bright. Shale, slightly carbonaceous. Coal, dull lustrous, 10-40% bright.	**Coal, dull, devolatilised.** **Dolerite, dark green, massive, Irregular contact.** **Coal, dull, devolatilised.**	Coal, dull, <1% bright. Coal, dull, <1% bright.		
				Torbanite, shaly. Coal, dull, <1% bright.		
1	**Coal, badly burnt**.	Not present.	Not present.	Not present.	Not present	Not present

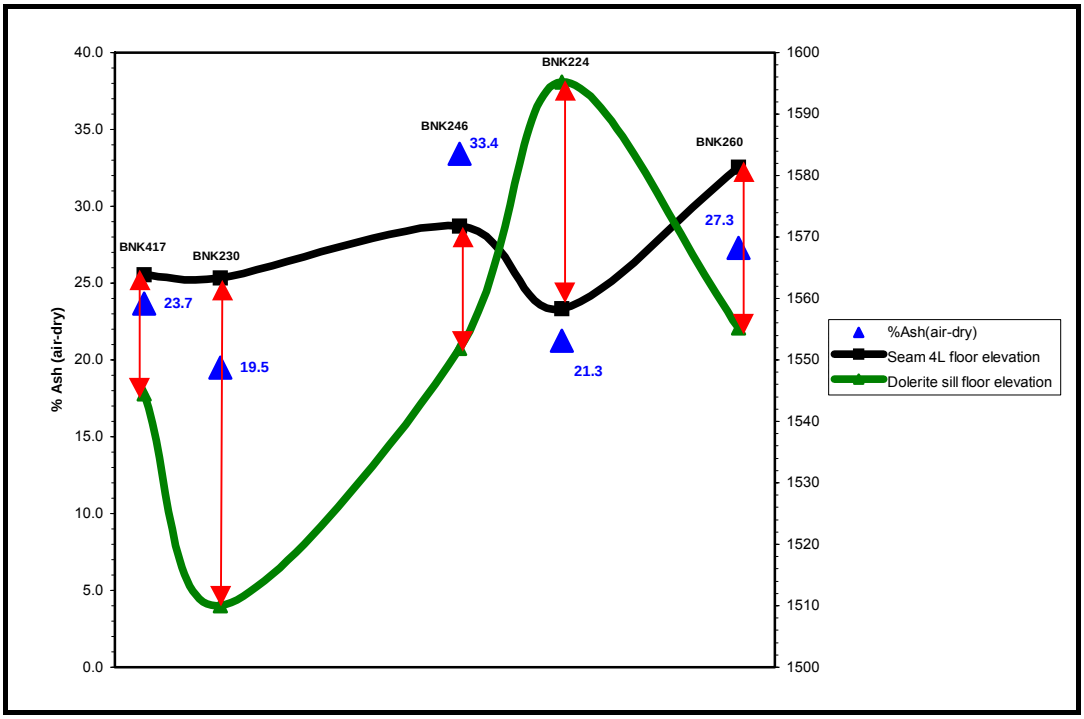

Figure 5.27 *A combined graph of the actual relationship between the No. 4L Coal Seam and the sill, as well as the % ash (air-dry) variation (blue triangles) of No. 4L Coal Seam (Section GG'). The red lines indicate the vertical distance between the sill and the No. 4L Coal Seam.*

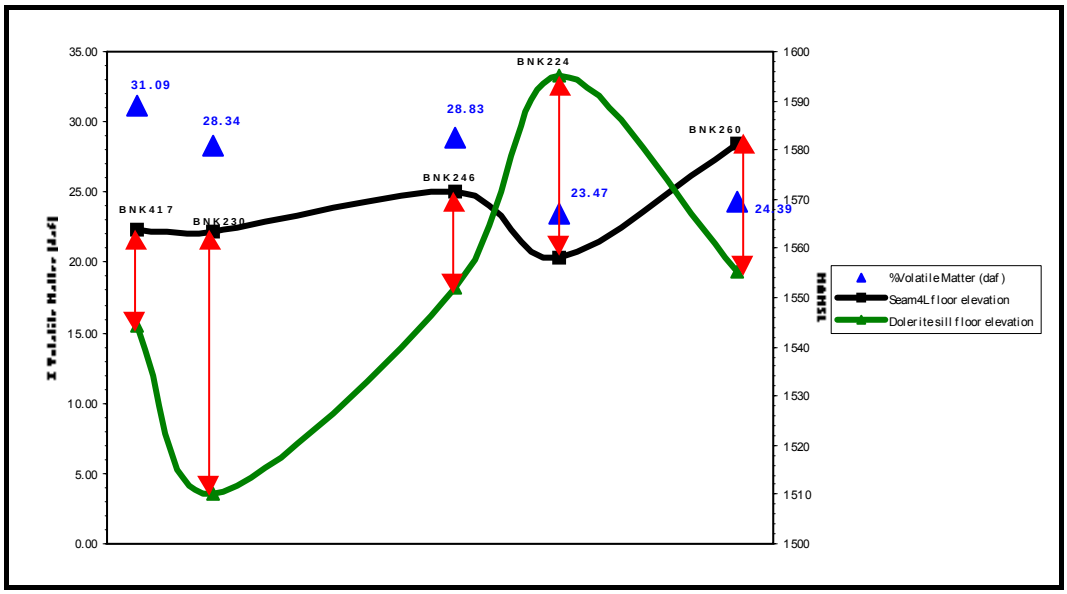

Figure 5.28 *A combined graph of the actual relationship between the No. 4L Coal Seam and the sill, as well as the % VM (daf) variation (blue triangles) of No. 4L Coal Seam (Section GG'). The red lines indicate the vertical distance between the sill and the No. 4L Coal Seam.*

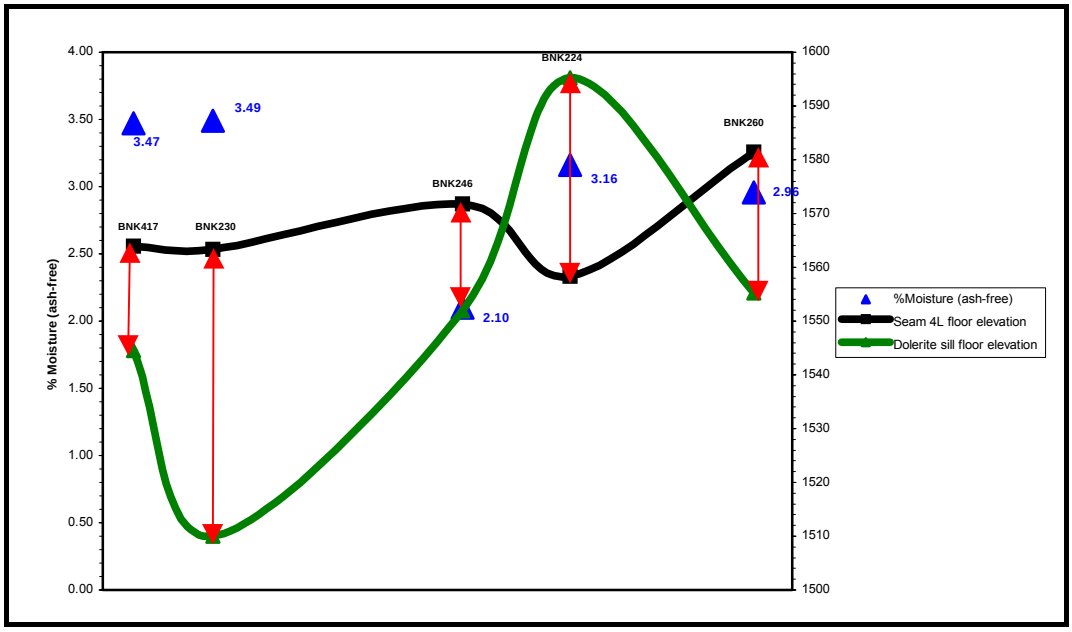

Figure 5.29 A combined graph of the actual relationship between the No. 4L Coal Seam and the sill, as well as the % moisture (ash-free) variation (blue triangles) of No. 4L Coal Seam (Section GG'). The red lines indicate the vertical distance between the sill and the No. 4L Coal Seam.

5.3.1.5 Section 10 (Figure 5.30)

As the dolerite sill was not intersected in boreholes BNK112 and BNK238, the displacement indicated by the elevation difference of the various coal seams between these boreholes confirmed the structural interpretation. The structural interpretation also proved an undulating and transgressive geometry (Figure 5.30).

The sill is dark greenish-grey in colour, medium crystalline and contains abundant calcite veins. The stringer intersected in borehole BNK351 is light grey in colour and finely crystalline.

According to the reconstructed isopach and contour maps (Figures 5.3 A and B) the No. 2 Coal Seam (Section 10) is located on a palaeovalley-flank in the middle of the section (8-9m thick coal) and to the north (6 to 7m thick coal) and south (4 to 6m thick coal) in a palaeovalley (1 to 2m thick coal).

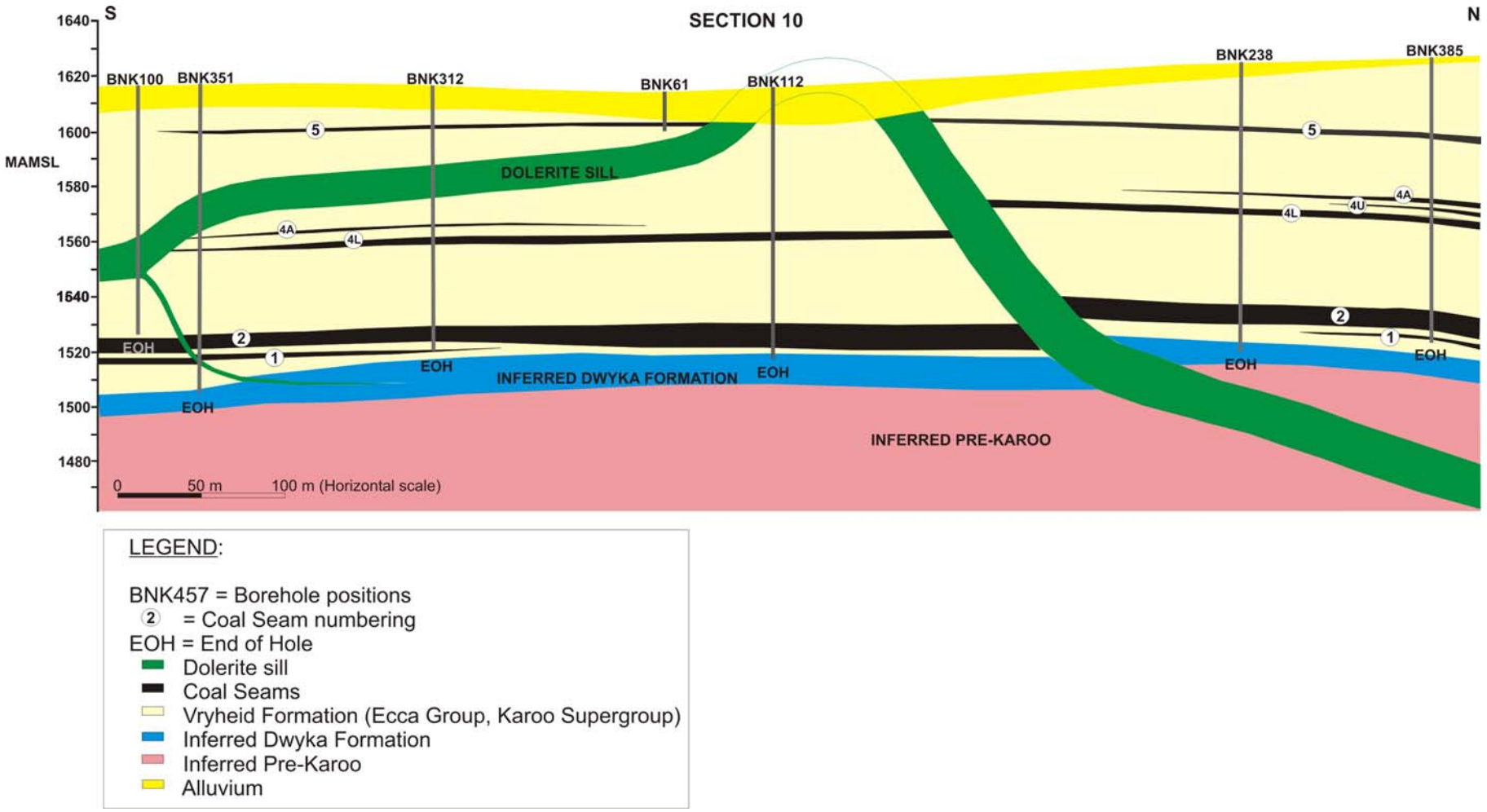

Figure 5.30 A geological cross-section showing the interpretation of a dolerite sill structure (Du Plessis, 2001). See locality of section in Figure 5.1.

Lithological descriptions of the coal seams in Section HH' EAST are summarised in Table 5.5. Accordingly all the coal seams in boreholes BNK100, 351 and 312 show devolatilisation. However the displaced and uplifted coal seams intersected in boreholes BNK238 and 385 show abundant secondary mineralisation of calcite and pyrite on cleats and associated jointed structures. These fracture planes are also associated with slickensides which indicate movement within the sediments that could be related to the intrusion of the sill.

a. No. 2 Coal Seam

Ash content (Figure 5.31): The higher ash values are mainly found in the thicker part of the No. 2 Coal Seam (boreholes BNK112 and BNK238 – both upper and lower samples) which is situated on the palaeo valley-flank. A conspicuous decrease in ash is found in the thinner parts of the seam that are situated in the palaeovalleys to the north and south of the section. Higher ash values would have been expected from the coals deposited in the higher areas according to the work in section 4.2.2.3 which are the scenario in this section, however the thickness distribution of the coals are just the other way round. No significant relationship exist between the ash content (Figure 4.31) and the VM (daf) (Figure 5.32) distribution within the No. 2 Coal Seam.

VM (daf) (Figure 5.32): Coals from boreholes BNK312 and BNK238 are completely devolatilised (both upper and lower samples). The upper sample of borehole BNK112 is devolatilised (25.5% VM (daf)). The bifurcation in the southern side of the section have attributed to the low volatiles in borehole BNK312. Boreholes BNK238 and BNK385 intersected the displaced and uplifted part of the No. 2 Coal Seam. Very low volatiles in borehole BNK238 indicate that the sill could not be very much deeper as to the end of borehole (EOH) BNK238. Higher volatiles in borehole BNK385 indicate that the parting between the sill and the No. 2 Coal seam must be much bigger as opposed to borehole BNK238. There is a good correlation between the volatiles in the top and bottom of the No. 2 Coal Seam.

Moisture (ash-free) (Figure 5.33): Higher moisture values (ranging from 4.2 to 5.0) in the No. 2 Coal Seam occur at the top of boreholes BNK312 and BNK112 and also at the base of borehole BNK238. These coals are lying closest to the sill comparing to the coals with lower moisture contents.

b. No. 4L Coal Seam

Ash content (Figure 5.34): Only negligible higher ash values occur in boreholes BNK351 and 112 which are situated underneath the dolerite sill. Also only a slight decrease in ash occurs in

boreholes BNK238 and 385 (27 and 24.2% respectively) which have been displaced and uplifted. The vague ash distribution throughout this section could be related to both syngenetic and epigenetic factors.

VM (daf) (Figure 5.35): All the boreholes except for BNK385, have been devolatilised by the sill. Boreholes BNK312 and 112 have very low VM (daf) values which indicate complete devolatilisation. In this section the coal underneath the sill tends to be lower in volatiles (daf) as opposed to the displaced and uplifted coals. This is mainly because the vertical distance between the sill and the coal is much smaller where the sill occur above the coal seam (Section 10, Figure 5.30) as opposed to below the coal seam.

Moisture (ash-free) (Figure 5.36): Higher moisture values occur within the coal that still remains in situ as opposed to that part which has been displaced and uplifted. The coal that still remains in situ is situated more within the vicinity of the sill itself (red arrows in Figure 5.36). The sill is the closest to the No. 4L Coal Seam in Borehole BNK351 and 312 where the coal has the highest moisture values and is situated within the contact aureole

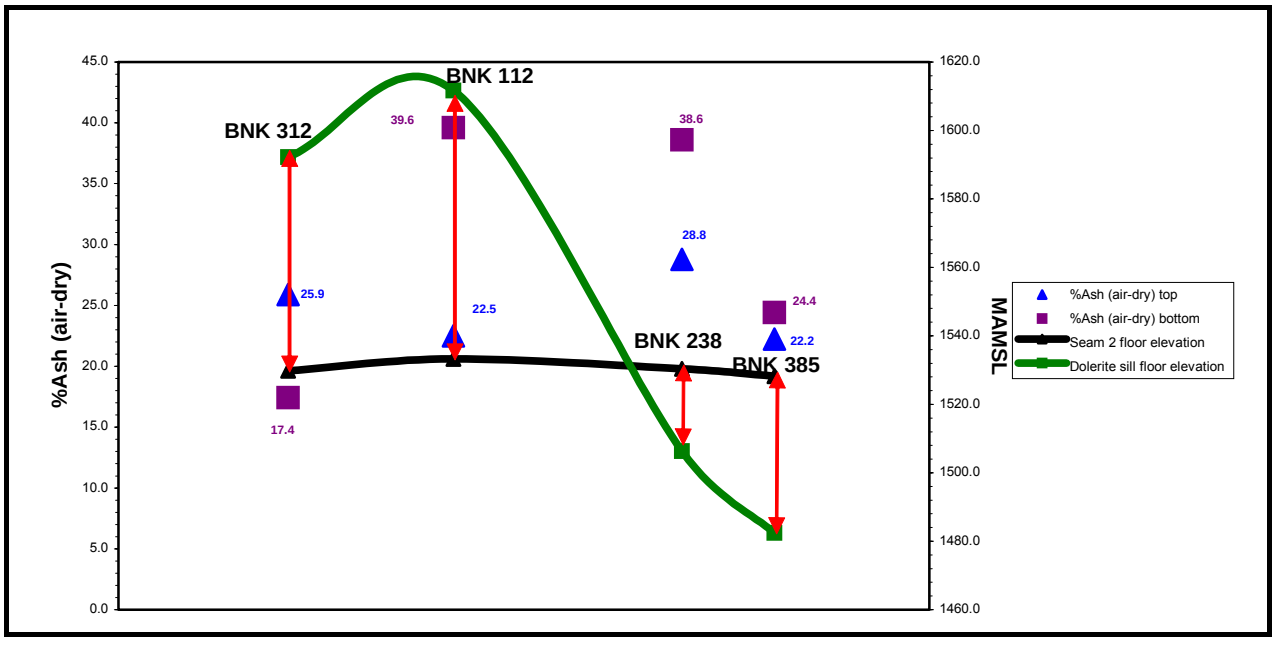

Figure 5.31 ***A combined graph of the actual relationship between the No. 2 Coal Seam and the sill, as well as the % ash (air-dry) variation at the top (blue triangles) and bottom (purple squares) of the No. 2 Coal Seam (Section 10). The red lines indicate the vertical distance between the sill and the No. 2 Coal Seam.***

Table 5.5 Lithological descriptions of the coal seams intersected in Section 10. The red descriptions indicate the influence of the dolerite sill.

SEAM No.	BOREHOLE NUMBERS – GEOLOGICAL CROSS-SECTION 10						
	BNK100	BNK351	BNK312	BNK61	BNK112	BNK238	
5	Not present in borehole	COAL: moderately weathered	COAL: dull lustrous, 40-60% bright 10-40% bright, **broken core**, slightly weathered, **rare calcite on cleats**	No detail geological description	Probably displaced and uplifted by dolerite sill	Coal: Lustrous, 40-60% bright, **rare pyrite on cleats**	65% coal, dull lustrous.
		SANDSTONE: medium grained					15% coal, 10-40% bright.
							10% coal, 10-40% bright.
		COAL: mixed, 10-40% bright					10% coal, dull, **pyrite lenses, calcite on cleats.**
		Weathered to base	BASE OF Hard Weathering				
4A	Not present in borehole	COAL: **burnt**	COAL: dull lustrous, 10-40% bright **abundant calcite on cleats Devolatilised appearance**		Not developed	Coal: dull, <10% cleats bright, **rare pyrite on cleats, Possibly devolatilised**	45% coal, dull lustrous.
							25% coal, dull.
						Coal: Lustrous, 40-60% bright, thinly laminated, **few pyrite on cleats, rare calcite on cleats**	15% coal, 40-60% bright.
							15% coal, 10-40% bright, **pyrite lenses, calcite on cleats.**
						Rare water stains	
4U	Not present in borehole	Not present in borehole	Not present in borehole		Not developed	Not developed	Coaly shale. Dull shaly coal at base.
4	Not present in borehole	COAL: **burnt, broken core**	COAL: dull lustrous, 10-40% bright **abundant calcite on cleats**		No detail geological description	Coal, lustrous, 40-60% bright, thinly laminated. **Abundant calcite on cleats, few pyrite on cleats.** Occasional water stains.	60% coal, dull lustrous.
							25% coal, dull.
							15% coal, 40-60% bright, **pyrite lenses,calcite on cleats.**
			Devolatilised appearance particular basal 2/3 carbonaceous remnants			Coal, bright, 60-90% bright, blocky, occasional calcite on cleats. Rare water stains.	70% coal, dull lustrous.
							25% coal, dull.
						Coal, dull lustrous, 10-40% bright, **abundant calcite on cleats. Rare slickensides.**	5% coal, 40-60% bright, **calcite on cleats.**
							Basal contact at 20°.
3	Not present in borehole	Not present in borehole	Not present in borehole		Not developed	Not developed	Not developed.
2	Not present in borehole	COAL: **burnt, broken core**	COAL: dull lustrous, 10-40% bright **Devolatilised appearance**	Shallow borehole	No detail geological description	Coal: lustrous, 40-60% bright, **very**	50% coal, dull.
		COAL: dull, granular				Coal: dull, <10% bright.	35% coal, dull lustrous.
		COAL: mixed, 40-60% bright, **calcite on cleats**	SHALE: dark grey, carbonaceous, silty			Siltstone: slightly, sandy, gritty.	15% coal, 40-60% bright, **pyrite lenses, calcite on cleats.**
			COAL: dull lustrous, 10-40% bright 40-60% bright.			Coal: dull, <10% bright, friable.	Coal, dull, silty.
						Coal: lustrous, 40-60% bright, thinly	Limestone, carbonaceous.
						Coal: dull, <10% bright, friable.	65% coal, dull.
						Coal: lustrous, 40-60% bright.	35% coal, dull lustrous, pyrite lenses, 10% bright bands.
						Coal: lustrous, 40-60% bright, thinly,	45% coal, dull lustrous.
						Coal: dull lustrous, 10-40% bright, **rare calcite on cleats**	30% coal dull.
						Coal: dull, <10% bright.	15% coal, 10-40% bright.
						Siltstone: shaly, friable.	10% coal, 40-60% bright, pyrite lenses, **calcite on cleats.**
						Coal: dull, <10% bright, **occasional calcite on cleats, rare pyrite on cleats.**	40% coal, dull.
							40% coal, dull lustrous.
							10% coal, 40-60% bright.
						Shale, carbonaceous	10% coal, 10-40% bright, **pyrite**
						Coal, lustrous, 10-40% bright, medium laminated, **rare calcite on cleats.**	60% coal, dull lustrous.
							30% coal, dull.
						Shale, carbonaceous, Rare coaly laminae	10% coal, 10-40% bright, **pyrite lenses**, 4mm grit at top.
						Coal, dull lustrous, 10-40% bright, **few pyrite on cleats**	70% coal, dull.
						Occasional water stains	20% coal, dull lustrous.
						Shale carbonaceous, slightly, sandy.	10% coal, 40-60% bright
						Coal, 60-90% bright, **blocky, rare pyrite on cleats**	50% coal, dull.
						Rare water stains on cleats	15 coal, dull lustrous.
						Coal, lustrous, 40-60% bright, thinly laminated	10% shale, carbonaceous, **pyrite lenses, calcite on cleats**
			COAL: 40-60% bright **Devolatilised appearance**				
1	Not present in borehole	COAL: dull, torbanitic	COAL: lustrous		Not developed	Not developed	75% coal, dull
		COAL: mixed, <10% bright, granular.	COAL: 40-60% bright				15% coal, dull lustrous
		COAL: dull, torbanitic, **calcite on cleats**	COAL: lustrous, slightly, <10% bright.				10% shale, carbonaceous, **pyrite lenses, calcite on cleats**
			SHALE: grey.				
		MUDSTONE: coaly	COAL: dull lustrous, <10% bright.				

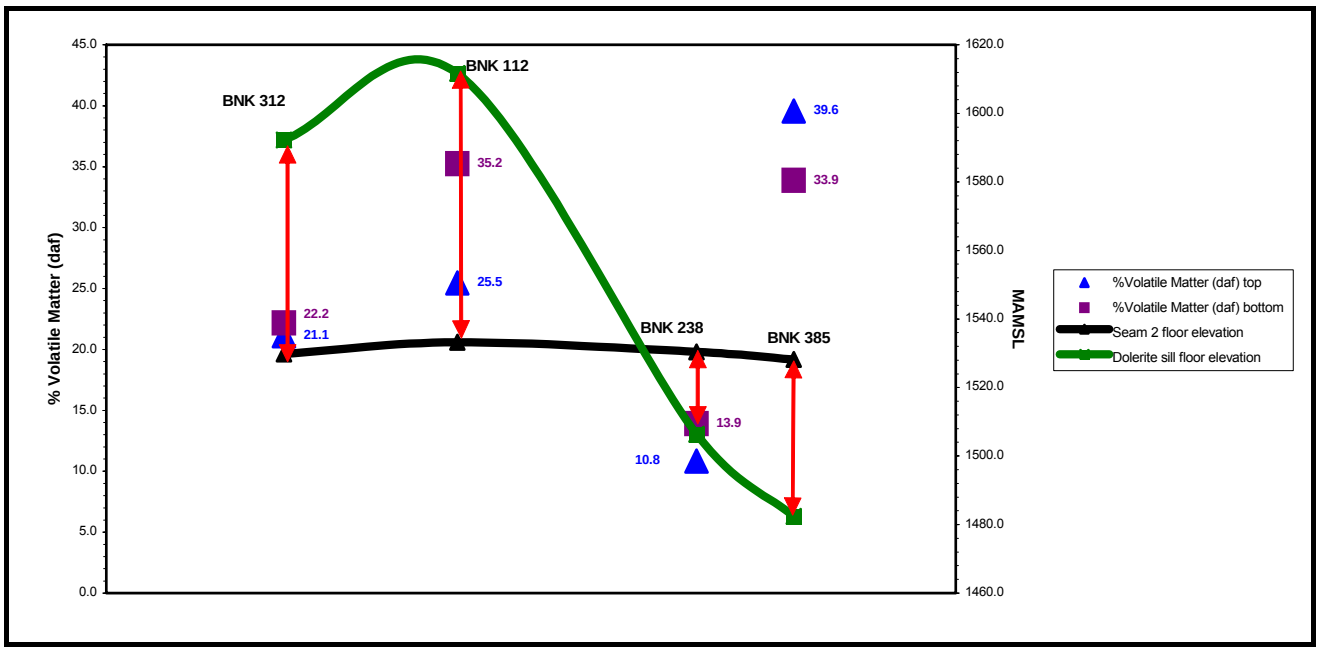

Figure 5.32 A combined graph of the actual relationship between the No. 2 Coal Seam and the sill and also the volatile matter (daf) variation at the top (blue line) and bottom (purple line) of the No. 2 Coal Seam (Section 10). The red lines indicate the vertical distance between the sill and the No. 2 Coal Seam.

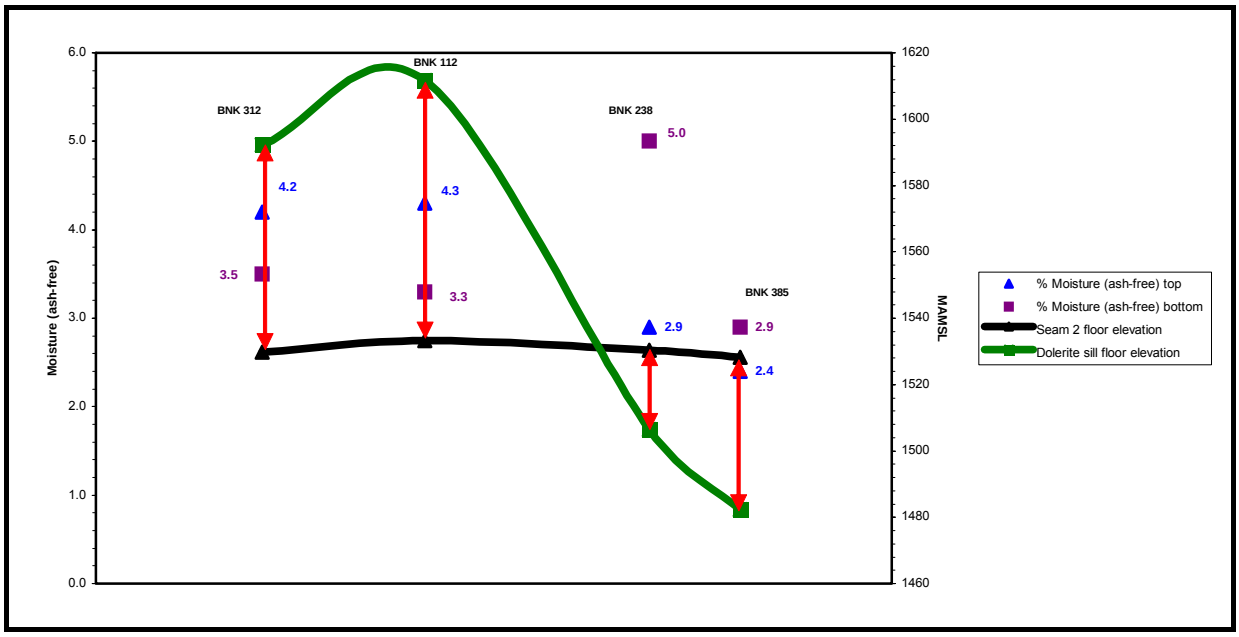

Figure 5.33 A combined graph of the actual relationship between the No. 2 Coal Seam and the sill, as well as the moisture (ash-free) variation in the top (blue triangles) and bottom (purple squares) of the No. 2 Coal Seam (Section 21). The red lines indicate the vertical distance between the sill and the No.2 Coal Seam.

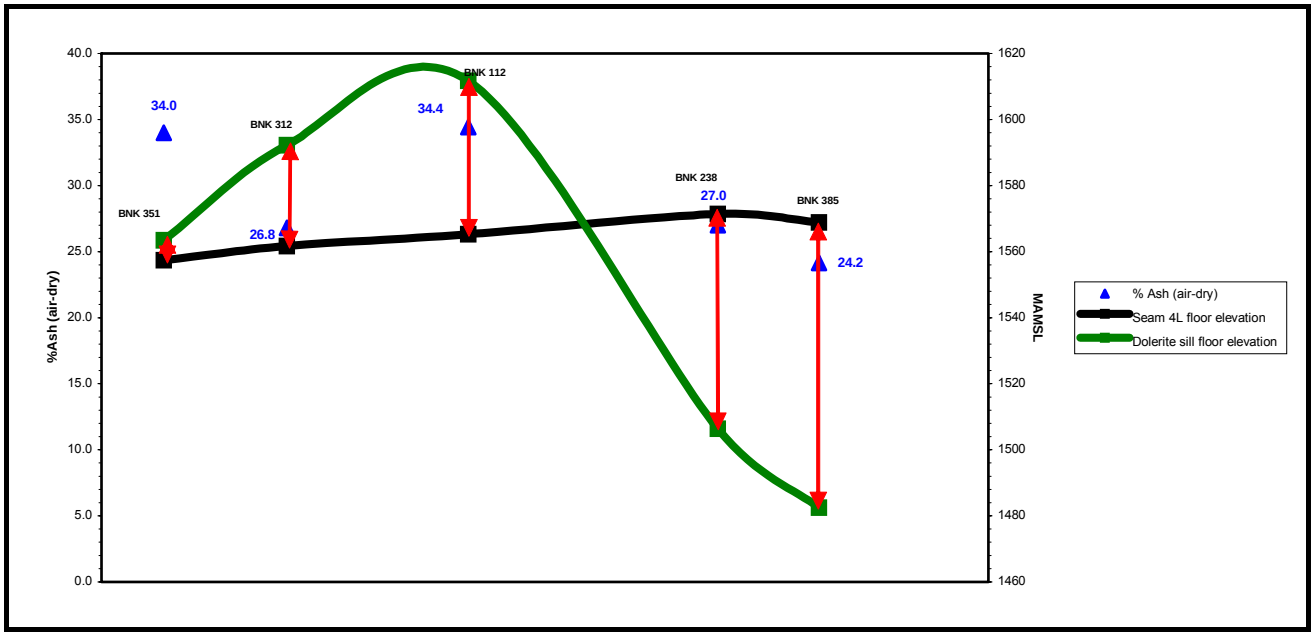

Figure 5.34 ***A combined graph of the actual relationship between the No. 4L Coal Seam and the sill, as well as the % ash (air-dry) variation in the No. 4L Coal Seam (Section 10). The red lines indicate the vertical distance between the sill and the No.4L Coal Seam.***

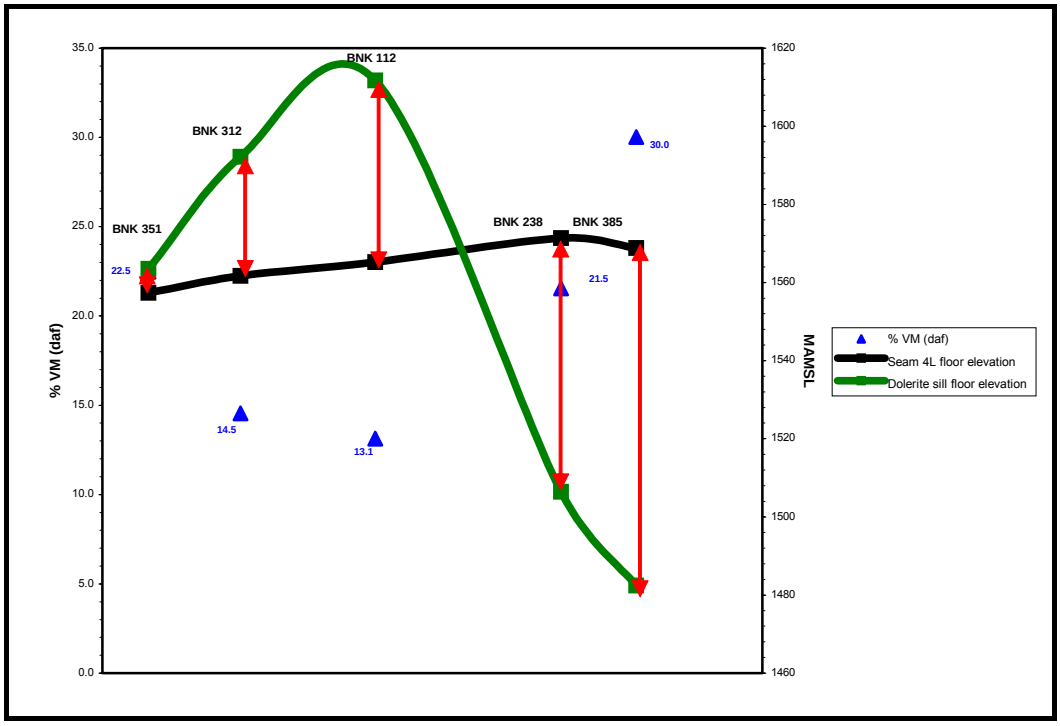

Figure 5.35 ***A combined graph of the actual relationship between the No. 4L Coal Seam and the sill, as well as the % VM (daf) variation (blue triangles) of No. 4L Coal Seam (Section 10). The red lines indicate the vertical distance between the sill and the No. 4L Coal Seam.***

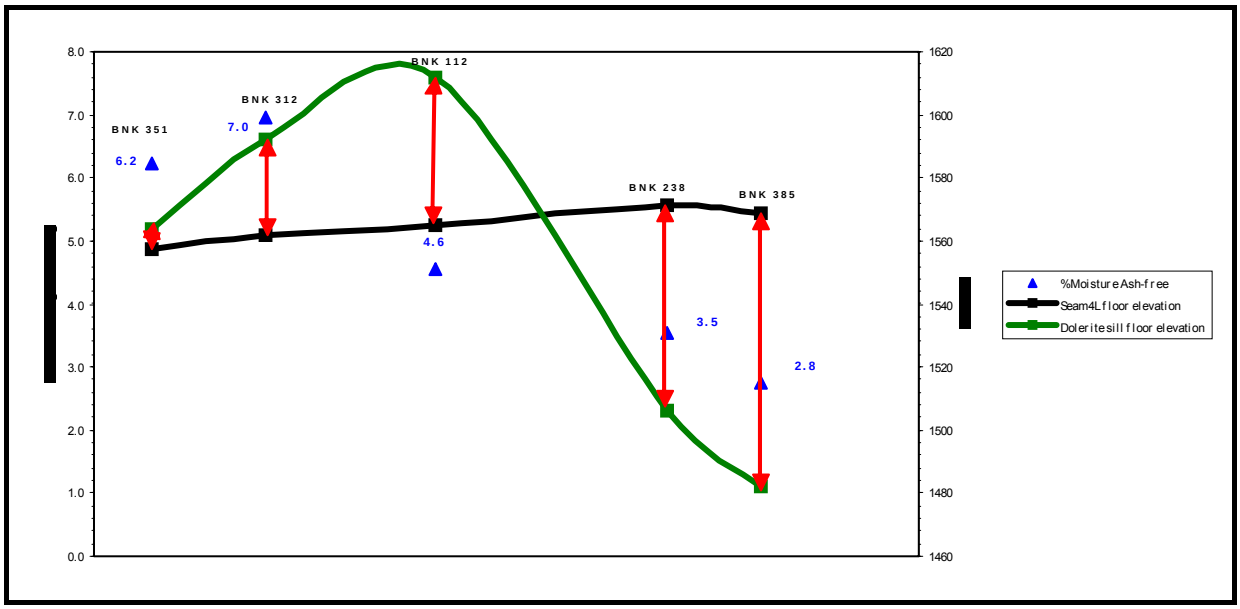

Figure 5.36 *A combined graph of the actual relationship between the No. 4L Coal Seam and the sill, as well as the % moisture (ash-free) variation (blue triangles) of No. 4L Coal Seam (Section 10). The red lines indicate the vertical distance between the sill and the No. 4L Coal Seam.*

5.4 Study area – Goedehoop Colliery

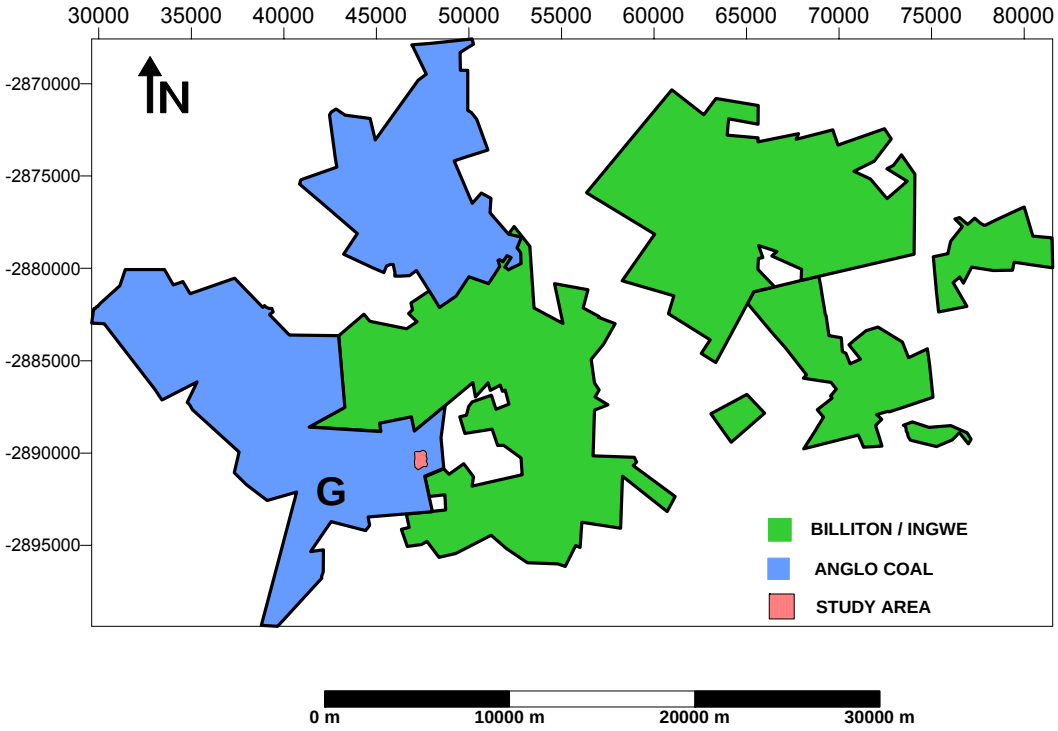

Figure 5.37 *Map of the study area (marked G) at Goedehoop Colliery.*

Coal samples (Figure 5.37) of the No. 2 Coal Seam were obtained from the Goedehoop Colliery (Figure 5.37) where the 20m thick dolerite sill is bifurcating and displacing the Vryheid Formation (No's 2, 3, 4L, 4U, 4A, 4B and 5 Coal Seams).

All the focus is on the No. 2 Coal Seam as Anglo Coal was developing through the sill when the mine was visited. Mine design and planning was executed to develop through the sill and to avoid mining of the metamorphosed and altered coal (Figure 5.37).

Relationships between the various isopleth maps of % volatile matter (daf) (Figure 5.41), CV MJ/kg (daf) (Figure 5.42), % ash (air-dry) (Figure 5.43), % Moisture (ash-free) (Figure 5.44) and the % sulphur (Figure 5.45) were compiled using 31 boreholes from the study area (Figure 5.37) at Goedehoop.

A geological cross-section was drawn through the principal area (Figure 5.38). This cross-section shows the spatial relationship between the sill and the No. 2 Coal Seam (the Goedehoop Section indicated by the blue line in Figure 5.37).

5.4.1 Isopleth maps

Volatile matter (daf) (Figure 5.40):

A distinctive devolatilisation aureole can be recognised from the isopleth map. The area that includes values from 10 to 28% VM (daf) represents the contact zone. This area coincides with the hatched area in Figure 5.40 which high light the boreholes where dolerite bifurcations from the main sill intruded into the No. 2 Coal Seam.

The contact zone can be divided into two sub-zones i.e. **(A)** 10 to 20% VM (daf) and **(B)** 20 to 28% VM (daf) (Figure 5.41). Zone A is represented by a very close spaced borehole pattern which was probably planned due to the intensive devolatilisation influence by the sill. These bifurcations have thicknesses ranging from 0.21m to 3.8m.

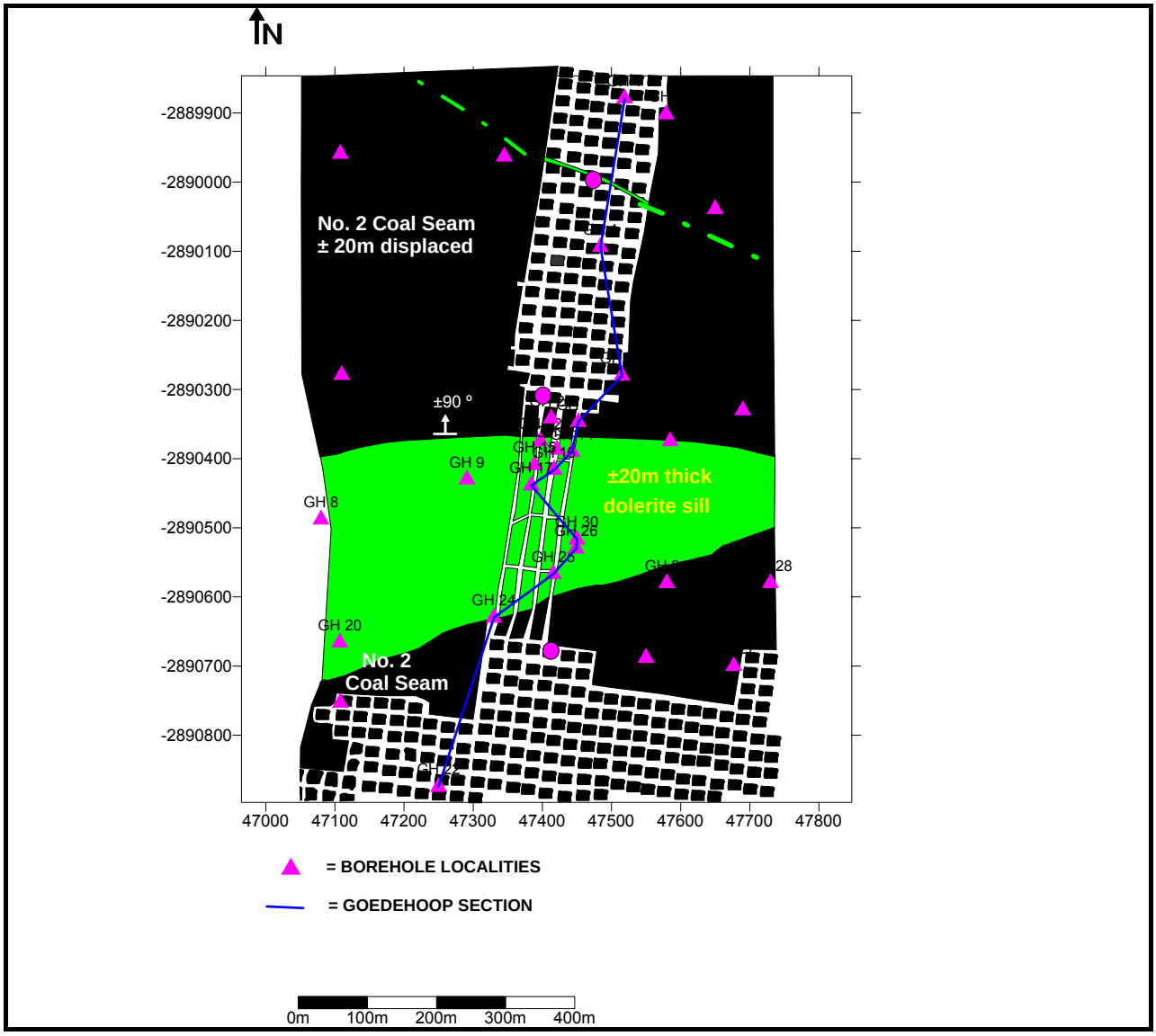

Figure 5.38 A simplified mine plan depicting the boreholes and the Goedehoop section line (See Figure 5.39).

Figure 5.39 A Geological cross-section showing the interpretation of a dolerite sill (Du Plessis, 2001).

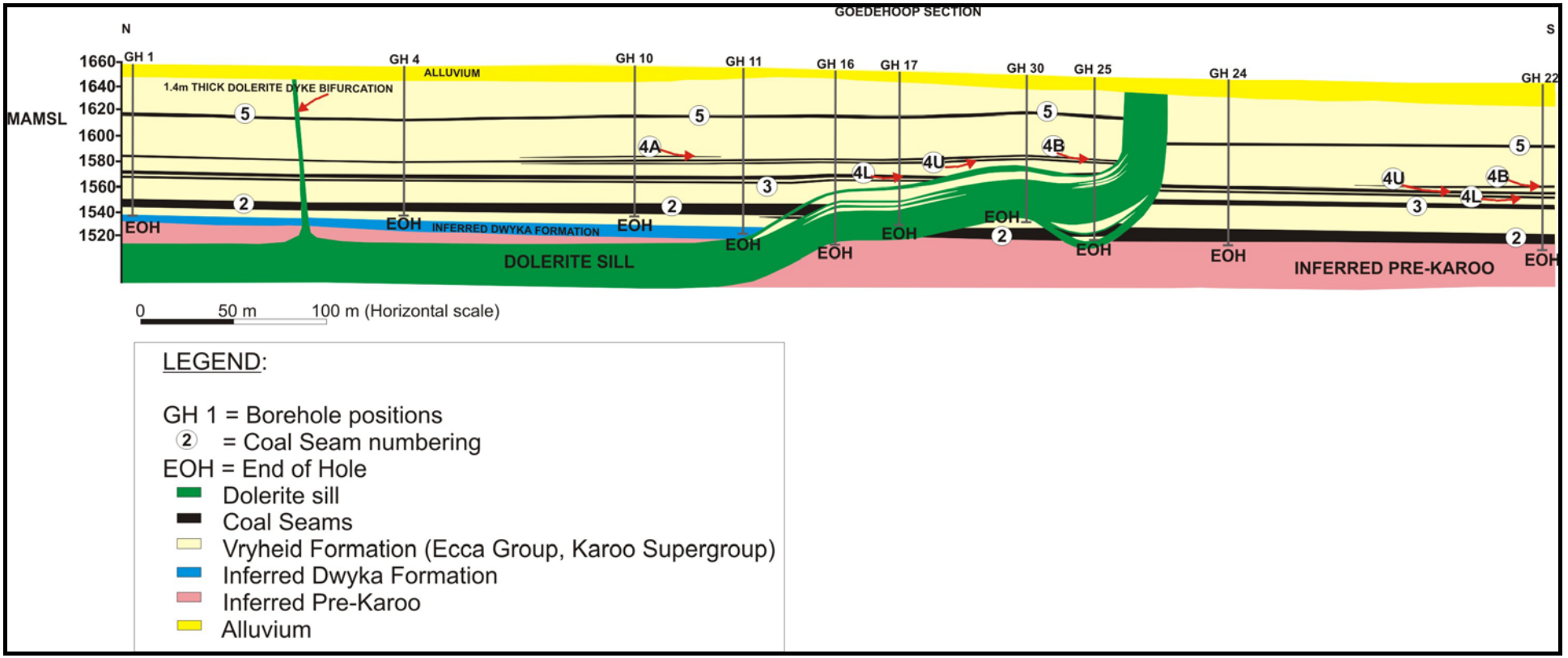

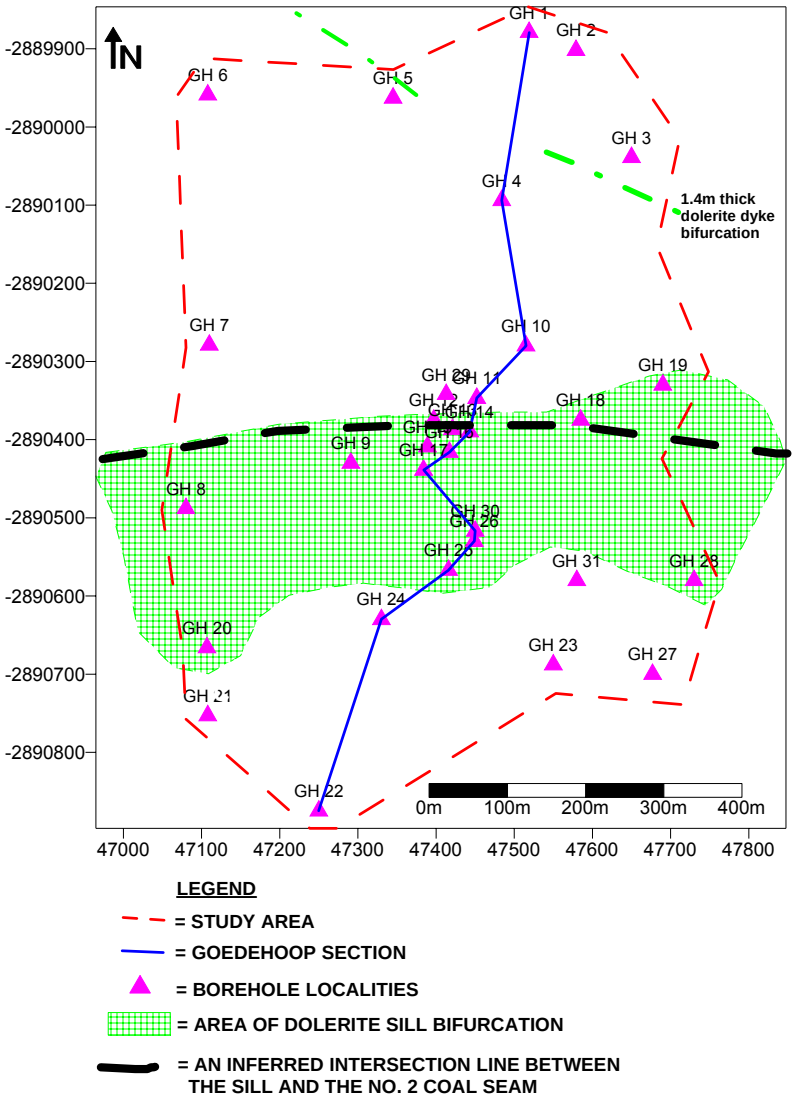

Figure 5.40 ***A map showing all the boreholes (with a # next to the locality) where dolerite bifurcations (or stringers) intruded the No. 2 Coal Seam. The hatched area includes all these boreholes.***

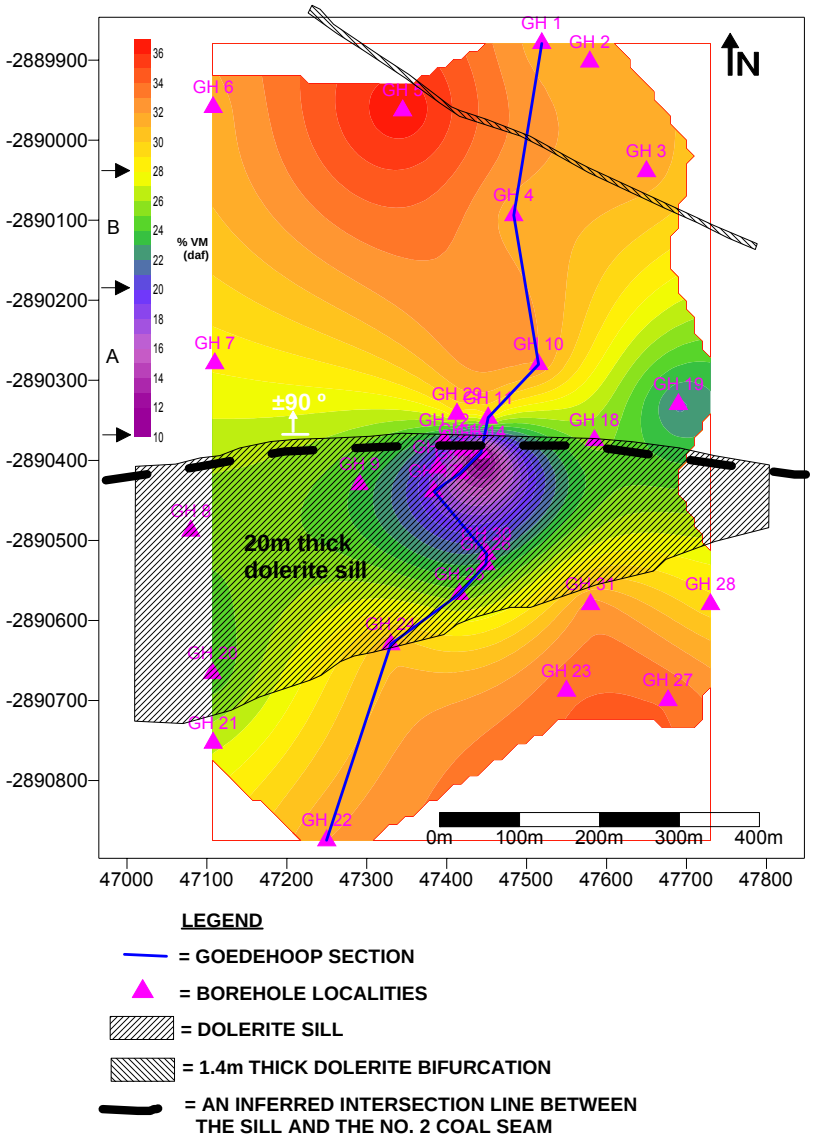

Figure 5.41 Isopleth map of the VM content (daf) of the coal in the No. 2 Coal Seam. Zone A and B are indicated on the vertical color scale bar.

The outer limits of Zone B in Figure 5.41 (the 28% VM (daf) contour line) are showing the size of the contact aureole. It is apparent from Figure 5.38 that the main sill remained for at least 125 m (between boreholes GH 25 and GH 30) above the No. 2 Coal Seam. The sill is situated only a few meters above or below the No. 2 Coal Seam as indicated by the hatched area in Figure 5.40. The sill followed a much deeper plane as soon as it intruded through the No. 2 Coal Seam. Borehole GH 10 in Figure 5.40 is situated on the border between the contact aureole and a more normal VM (daf) content. Boreholes GH 23, GH 27, GH 31, GH 28, GH 10, GH 3, GH 4, GH 1, GH 6, GH 5, and GH 2 indicate that the sill is much further away from the No. 2 Coal Seam comparing to the coal seams. Figure 5.41 provides a good indication of the geometry of the sill.

No specific devolatilisation trend from the 1.4m thick dolerite dyke bifurcation can be observed from the isopleth map (Figure 5.39). A ±3m thick contact zone was identified during an underground visit. Such a zone would therefore not have been detected by the current borehole.

CV MJ/kg (daf) and Ash (air-dry) (Figures 5.42 and 5.43):

The area with lower calorific values (7 to 23 CV MJ/kg) and higher ash values (33 to 59% ash (air-dry)) is situated in the vicinity of the dolerite sill/No. 2 Coal Seam intersection. This area can be divided into sub-zones i.e. **(Zone A)** 7 to 19 CV KJ/kg (daf) in Figure 5.42 / **(Zone A)** 35 to 59% ash (air-dry) in Figure 5.43 and **(Zone B)** 19 to 23 CV MJ/kg (daf) in Figure 5.42 / **(Zone B)** 33 to 35% ash (air-dry) in Figure 5.43.

The boreholes in Zone A and B in Figure 5.42 and 5.43 intersected dolerite sill bifurcations between 1 and 2.5m thickness which cut through the No. 2 Coal Seam.

Zone B is extended over a much larger area as opposed to Zone A and can be classified as an area with more intermediate calorific and ash values (Figures 5.42 and 5.43). A good resemblance can be noted between Zone B and the hatched area in Figure 5.40 that indicates the area where dolerite bifurcations were intersected in the boreholes.

No specific trend in the area close to the 1.4m thick dolerite dyke bifurcation can be seen on the isopleth maps (Figures 5.40 and 5.41). The dolerite dyke bifurcation followed a sub-vertical plain of least resistance that came apart from the main sill (Goedehoop Section in Figure 5.39). This bifurcation did not have any significant metamorphic influence on the No. 2 Coal Seam as it fundamentally filled an open plane.

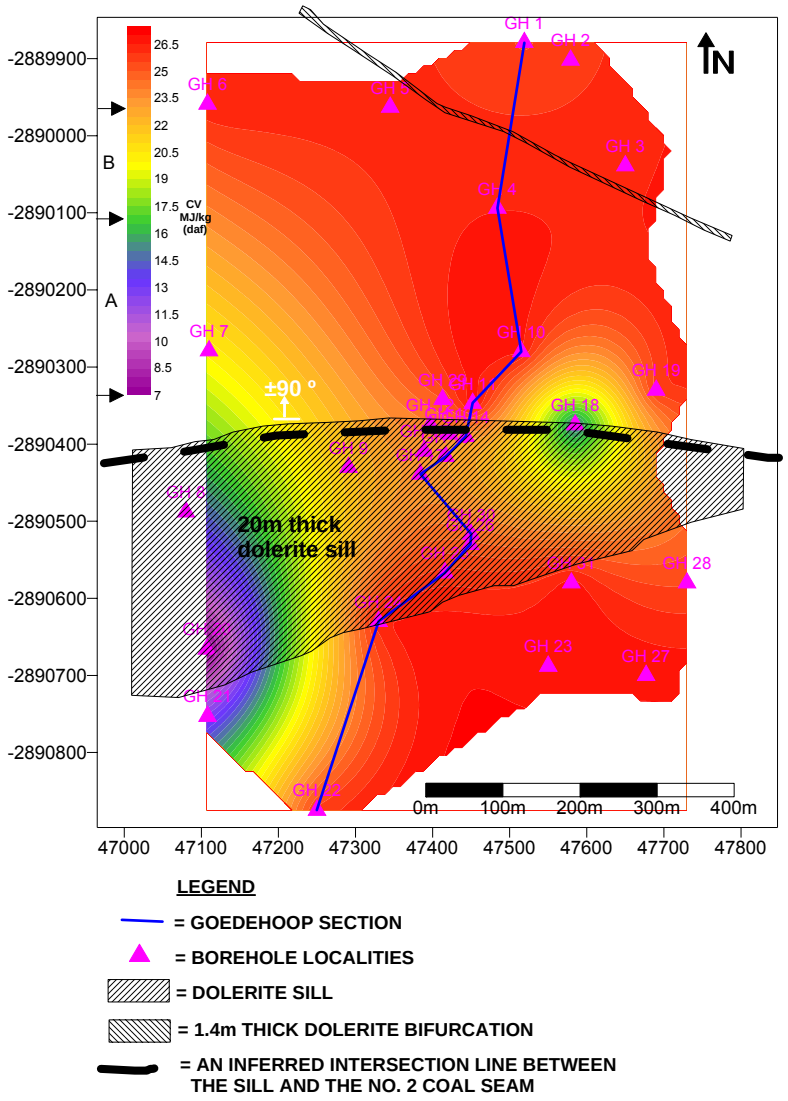

Figure 5.42 Isopleth map of the CV MJ/kg (air-dry) of the coal in the No. 2 Coal Seam. Zone A and B are indicated on the vertical color scale bar

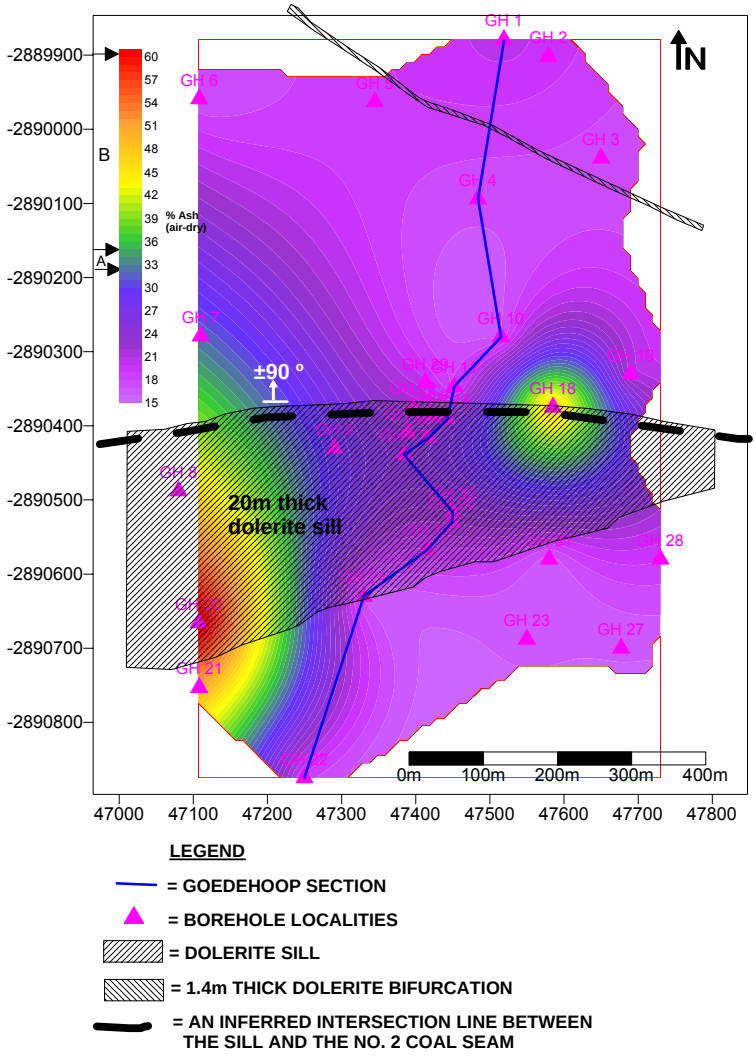

Figure 5.43 Isopleth map of the ash (air-dry) of the coal in the No. 2 Coal Seam. Zone A and B are indicated on the vertical color scale bar

Moisture (ash-free) (Figure 5.44):

There is an anomalous area with higher moisture values in Figure 5.44. This area is located to the south of the sill/No. 2 Coal Seam intersection where the main sill remained for at least 125m (between boreholes GH 25 and GH 17 in Figure 5.39) above the No. 2 Coal Seam. Higher moisture values (ash-free) ranging from 2.5 to 3.8% correspond with the area where the sill bifurcates into the No. 2 Coal Seam. There is no specific trend around the 1.4 m thick dolerite dyke bifurcation could be observed (Figure 5.44).

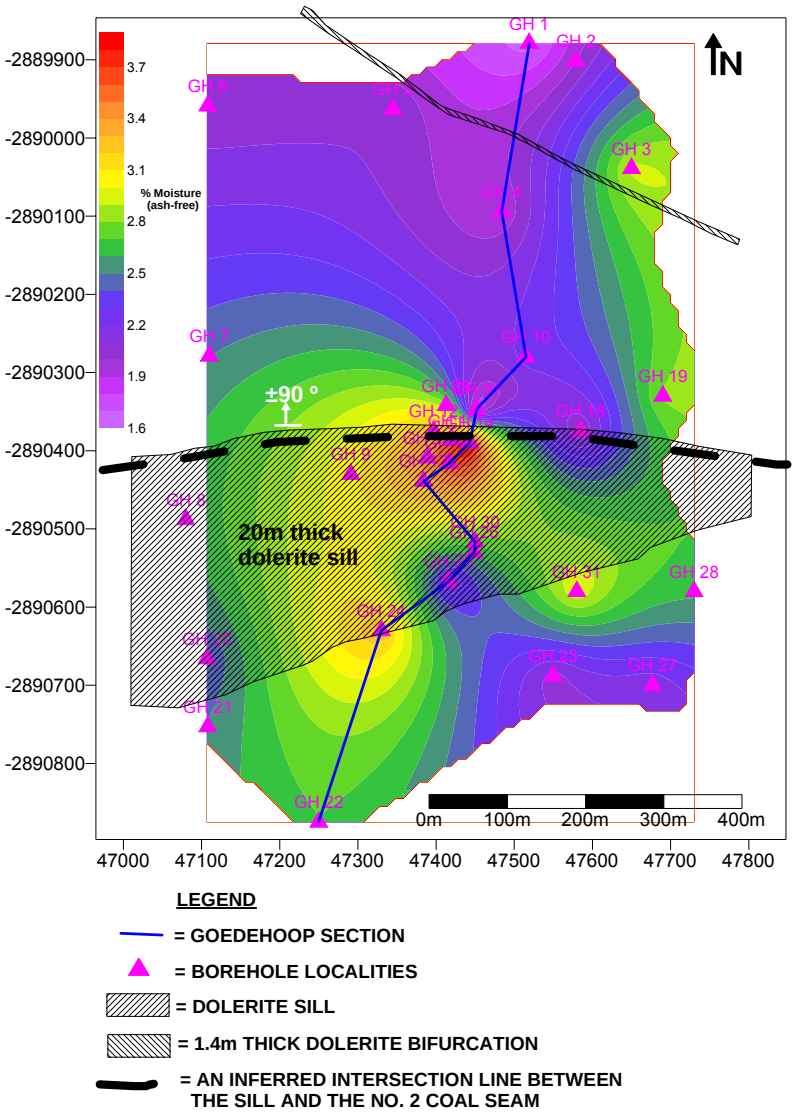

Figure 5.44 Isopleth map of the ash-free moisture content of the coal in the No. 2 Coal Seam.

The Goedehoop Section was drawn through the area with the highest moisture values (from 3.3 to 3.8) which is known for dolerite sill bifurcation. Higher moisture content occurs in micro-porous coal which was caused by the effect of the sill intrusion.

5.4.2 Conclusions.

Dolerite sills and dykes intruded into the coal bearing Vryheid formation in the Witbank Coalfield. Geological cross-sections, isopleth and isopach maps from the Bank study area reveal the relationship between the coal seams and the dolerite intrusions. The dolerite thickness varies in many instances, bifurcations of the dolerite occur. It is associated with ±20m

displacement and metamorphism on coal which is putting major constraints on coal mining in general.

The metamorphic influence of the coal is restricted to the width of the contact aureole. The nature of the aureole depends on the geometry, variation in thickness and bifurcation of the sill. It was also found that the metamorphic contact aureole is much more extensive in the displaced and uplifted coal seams comparing to those beneath the sill.

Moisture (ash-free) of the proximate analyses, volatile matter (daf), CV (daf) and approximated ash yield (AD) isopleth maps show that the dolerite sill caused a localised increase in rank. Areas of high moisture (proximate analyses moisture content) correspond to devolatilised areas, which are higher in ash and lower in CV adjacent to known intrusions.

CHAPTER 6
CONCLUSIONS

Mineralogy of the dolerites.

Involvement of plagioclase in both the Witbank and Sasolburg dolerite fractionation assemblages indicates that the fractionation processes must have occurred within the crust although within different depths. The absence of pyroxene phenocrysts in the B5 sill indicates that the fractionation took place at a pressure significantly higher than that at which the plagioclase and olivine microphenocrysts have formed. The high percentage olivine in the B4 sill indicates that these two sills originated from different magma sources. Plagioclase microphenocrysts in the B5 sill as oppose to the macrophenocrysts of the B4 sill concludes that the fractionation processes of the B5 sill must have happened deeper within the crust.

Both the Ogies Dyke and the Witbank sill are medium crystalline while the B4 sill is coarse and the B5 sill is fine crystalline. This study engage with dolerites that crystallised rapidly, intermediately and slowly as the crystal sizes are directly related to magma cooling. Fine crystalline dolerites like the chilled margins and bifurcations tend to be more susceptible for alteration as opposed to the medium and coarse crystalline dolerites. The 40m thick, fine crystalline B4 sill has undergone the most alteration comparing to the B5 sill, Witbank sill and the Ogies Dyke. The differences identified during this study distinguish the Sasolburg dolerites from the Witbank sill and the Ogies Dyke.

Geochemistry of the dolerites

All the dolerites in this study are falling in the “basic” group. The B4 – Sasol dolerite sll is a high-MgO (picritic) basalt while the rest are basalts. The chilled margins of the bifurcations have an arithmetic mean of 4.89% MgO and the Ogies Dyke has 4.9% MgO. Lower MgO and Ni values are detected in the Witbank bifurcations as oppose to the Witbank sill.

The basaltic and evolved basalts can further be divided into low and intermediate K_2O concentrations. A higher K_2O concentration is placing the Ogies Dyke in the intermediate-K_2O group whilst the Witbank sill (interior and chilled margins), and the Witbank bifurcations (interior and the chilled margins) are all falling in the low-K_2O group. Two of the Witbank bifurcations (interior) having intermediate-K_2O concentrations and are associated with the Ogies Dyke. The picritic B4 sill (Sasol) is also classified as a low- K_2O dolerite.

Considering K_2O and MgO element concentrations the samples are falling in three categories, from evolved to picritic with the majority in the basaltic field.

The influence of syngenetic factors on coal deposition and diagenesis.

The undulated platform onto which the No. 2 Upper Coal Seam formed at the Optimum study area had a major influence on coal grade. Thicker coals were deposited in the lower lying areas while they were thinning towards palaeohigh areas. Significant values indicate that the thinner coals are higher in ash (air-dry), lower in VM (daf), lower in CV MJ/kg (air-dry) and higher in relative density comparing to the coals deposited in the lower lying areas of the palaeovalley.

A decrease in VM to the south and western border of the study area can be associated with the nearby dolerite sill as reported by Smith (1990). According to various authors, the Ogies Dyke is responsible for intense coal devolatilisation; however, in this area it was not found to be the case.

The metamorphic influence of a 20m thick undulating and bifurcating dolerite sill.

Lithological descriptions from boreholes and structural interpretations in geological cross-sections revealed the presence of a green 20m thick, bifurcating dolerite sill that intruded into the Vryheid formation of the Karoo Supergroup. It is associated with ±20m displacement and metamorphism on coal which is putting major constraints on coal mining in general.

The metamorphic influence of the coal is largely restricted to the width of the contact aureole. The nature of the aureole depends on the geometry, variation in thickness and bifurcation of the sill. It is also found that the metamorphic contact aureole is much more extensive in the displaced and uplifted coal seams comparing to those beneath the sill.

Moisture (ash-free) of the proximate analyses, volatile matter (daf), CV (daf) and approximated ash yield (AD) isopleth maps show that the dolerite sill caused a localised increase in rank. Areas of high moisture (proximate analyses moisture content) correspond to devolatilised areas, which are higher in ash and therefore having lower CV's and are adjacent to known intrusions.

ACKNOWLEDGEMENTS

I first of all would like to thank Coaltech 2020 for providing financial backing and support for this project. Furthermore, I've listed the people, companies and organisations that have contributed meaningful suggestions, criticisms with support and enthusiasm. Their input into this work is highly appreciated. I also would like to thank my wife, my twin brother and my parents for encouraging me to complete this study.

Prof. W.A. van der Westhuizen, Late Prof. H. de Bruiyn, and Dr S.W. van der Merwe (UFS)
Dr. R.H. Boer
Mr. M. Grodner, Mrs. L. Jeffrey, Dr. Jochen Schweitzer, Mr. J Beukes (CSIR)
Mr. J. Veldsman, Mr. G. Esterhuizen (SASOL)

Mr. C. van Niekerk, Mr. S. van der Merwe, (Billiton/Ingwe)
Mr. G. Cronje (Billiton/Ingwe)
Mr. B. Schalekamp, Mr. C. Deleporte, Mr. M. Chivasa, Mr. F. Botes (Amcoal)
Prof. C.P. Snyman (UP)
Mr. H. Pinheiro, Mrs. V. du Cann (SABS)

Mr. C. Wessels, Mr. D. Powell (Khanya Laboratories)
Mr. Flip en Mrs. Charlé Opperman (Welverdiend)
Mrs. Rina Immelman (UFS)
Mr. J Choane and Mr. D Radikgomo for assistance in the preparation of thin sections and samples for XRD and XRF analyses (UFS)

REFERENCES

Beukes, J. 2000. Coaltech 2020. *Mining World*, **July**: 19-23.

Blignaut, J.J.G. 1952. Field relationships of dolerite intrusions in the Natal coalfields. *Trans. Geol. Soc. S.Afr.*, 55: 19–31.

Bristow, J.W. and Cox, K.G. 1984. Volcanic rocks of the Lebombo-Nuanetsi-Sabi zone: classification and nomenclature (*In: Erlank, A.J. Petrogenesis of the Volcanic Rocks of the Karoo Igneous Province*. *Spec. Publ. Geol. Soc. S.Afr*.,13: 69 – 75).

BS 1016, 1956. British Standard Methods for the Analyses and Testing of Coal and Coke, Part 16, Reporting of Results.

Cadle, A.B., Cairncross, B., Falcon, R.M.S., Manaczynski, V. and Willis, J. 1989. The characterization of the No. 2 Coal Seam, Witbank Coalfield - a collaborative investigation. Unpublished report. C.S.I.R. Miningtek, Johannesburg, 27-32.

Cadle, A.B., Cairncross, B., Christie, A.D.M. and Roberts, D.L 1990. The Permo-Triassic coal-bearing deposits of the Karoo Basin, Southern Africa. *Economic Geology Research Unit-Information Circular No. 218*: Geology Department, University of the Witwatersrand, 38p.

Cadle, A.B., Cairncross, B., Christie, A.D.M. and Roberts, D.L. 1993. The Karoo basin of South Africa: type basin for the coal-bearing deposits of southern Africa. *Int. J. Coal Geol*., 23: 117–157.

Cairncross, B. and Hobday, D.K. 1985. Depositional environments of the Permo-Carboniferous (Karoo) coals, Van Dyks Drift area, South Africa. *Proceedings of the Compte Rendu, 9th International Congress of Carboniferous stratigraphy and Geology*. Urbana, Illinois, 1985, 4: 223-236.

Cairncross, B. 1986. Depositional environments of the Permian Vryheid Formation in the east Witbank Coalfield; a framework for coal seam stratigraphy, occurrence and distribution. *Ph.D. dissertation*. Johannesburg: University of the Witwatersrand, 232p.

Cairncross, B. and Cadle, A.B. 1987. A genetic stratigraphy for the Permian coal-bearing Vryheid Formation in the east Witbank Coalfield, South Africa. S. Afr. *J. Geol*., 90(3): 219-230.

Cairncross, B. 1989. Paleodepositional environments and tectono-sedimentary controls of the postglacial Permian coals, Karoo Basin, South Africa. *Int. J. Coal Geol.,* 12: 365-380.

Chevallier, L., Goedhart, M and Woodfard, A.C. 2001. The influence of dolerite sill and ring comlplexes on the occurrence of groundwater in Karoo fractured aquifers: a morpho-tectonic approach. *WRC Report No 937/1/01*: Water Research Commission, 146p.

Crelling, J.C. and Dutcher, R.R. 1968. A Petrologic study of a thermally altered coal from the Purgatoire Valley of Colorado. *Geol. Soc. Am. Bull*., 79: 1375–1386.

Crowell, J.C. and Frakes, L.A. 1975. Late Palaeozoic glaciation: Part V, Karoo Basin, South Africa. *Bull. Geol. Soc. Amer*., 83: 2887-2912.

De Oliveira, D.P.S. 1997. The dolerites on Majuba Colliery, south-eastern Transvaal. *M.Sc. thesis*. Johannesburg: University of the Witwatersrand, South Africa., 172p.

Duncan, A.R., Erlank, A.J. and Marsh, J.S. 1984. Regional Geochemistry of the Karoo igneous province. (*In: Erlank, A.J. Petrogenesis of the Volcanic Rocks of the Karoo Igneous Province*. *Spec. Publ. Geol. Soc. S.Afr*.,13:355 – 389).

Duncan, R.A., Hooper, P.R., Ehacek, J., Marsh J.S. and Duncan, R.A. 1997. The timing and duration of the Karoo igneous event, Southern Gondwana. *J. Geophys. Res*., 102: 18127-18138.

Du Plessis, G.P. 2001. Personal communication on the structural interpretations of the ±20m-thick bifurcating dolerite sill in the south-eastern Witbank Coalfield. Vine Yard 2, Rustenburg, South Africa.

Du Toit, A.L. 1954. The Geology of South Africa. Oliver and Boyd, Edinburgh, 611p.

Eales, H.V. Marsh, J.S. and Cox, K.G. 1984. The Karoo Igneous Province: An Introduction. (*In: Erlank, A. J. Petrogenesis of the Volcanic Rocks of the Karoo Igneous Province*. *Spec. Publ. Geol. Soc. S. Afr.,* 13: 1–26.)

Fitch, F.J. and Miller, J.A. 1984. Dating Karoo igneous rocks by the conventional K-Ar and $^{40}Ar/^{39}Ar$ age spectrum methods. *Spec. Publ. geol. S. Afr*., 13, 247-266.

Hagelskamp, H.H.B., 1987. The influence of depositional environment and dolerite intrusions on the quality of coal. *Ph.D. dissertation.* Pretoria: University of Pretoria., 224p.

Harvey, R.D. and Dillon, J.W. 1985. Maceral distribution in Illinois coals and their palaeo-environmental implications. *Int. J. Coal. Geol.*, 5: 141-165.

Helgeson, H.C. 1979. Mass transfer amongst minerals and hydrothermal solutions. *(In: Barnes, H.L., Geochemistry of hydrothermal ore deposits*. Wiley Interscience, p. 568-606).

Henckel, H. 2001. Personal communication on regional scale information of the Witbank Coalfield. CSIR, Miningtek, Auckland Park, Johannesburg, South Africa.

Henning, A. 1995. The Geology, Petrochemistry and genesis of intrusive rocks in the Karoo Supergroup in the vicinity of Speelmanskop, north of Cradock. *M.Sc. dissertation*. Bloemfontein: University of the Free State., 156p.

Kisch, H.J. and Taylor, G.H. 1966. Metamorphism and alteration near an intrusive–coal contact. *Econ. Geol*., 61: 343–361.

Le Blanc Smith, G. 1980. Logical-letter coding system for facies nomenclature: Witbank Coalfield. *Trans Geol. Soc. S. Afr*. 83:301-311.

Le Maitre, R.W., Bateman, P., Dudek, A., Keller, J., Lameyre Le Bas, M.J., Sabine, P.A., Schmid, R., Sorenson, H. Streckeisen, A., Woolle, A.R. and Zanettin, B. 1989. A classification of igneous rocks and glossary of terms. *Blackwell, Oxford*.

Merrit, R.D. 1990. Thermal alteration and rank variation of coals in the Matanuska field, south-central Alaska. *International Journal of Coal Geology*, 14: 255-276.

Meyer, C. and Hemley, J.J. 1967. Wall rock alteration. (*In: Barnes, H.L. Geochemistry of hydrothermal ore deposits*. Holt, Rinehart and Winston, inc. p 166-235).

Norrish, K. and Hutton, J.T. 1969. An accurate X-ray spectrographic method for the analysis of a wide range of geological samples. *Geochim. Cosmochim. Acta*, 33: 431-453.

Richardson, S. H. 1984. Sr, Nd, and O isotope variation in an extensive Karoo dolerite sheet, southern Namibia. *Spec. Publ. geol. Soc. S. Afr*., 13, 289-293.

Rose, A.W. and Burt, D.M., 1979. Hydrothermal alteration. (*In: Barnes, H.L. Geochemistry of hydrothermal ore deposits*. Wiley Interscience).

SACS (South African Committee for Stratigraphy), 1980. Stratigraphy of South Africa, Part I. (*In: L.E. Kent. Lithostratigraphy of the Republic of South Africa, S.W.A./Namibia, and the Republics of Bophuthatswana, Transkei, and Venda. Handb. Geol. Surv. S. Afr*., 8: 690 pp.)

Snyman, C.P. 1996. Geologie vir Suid-Afrika (Volume 2): Departement Geologie, Universiteit van Pretoria, 768p.

Snyman, C.P. 1998. Coal. *In*: Wilson, M.G.C. and Anhaeusser, C.R. (Editors), The Mineral Resources of South Africa, 6th edition, Handbook 16, *Council for Geoscience*, 136-205.

Snyman, C.P. 2001. Personal communication on the influence of dolerite intrusions on coal quality in general. Glenwood weg 33, Pretoria, Souht Africa.

Snyman, C.P. and Barclay, J. 1989. The coalification of South African coal. *Int. J. Coal Geol*., 3: 375–390.

Snyman, C.P., Van Vuuren, M.J.C. and Barnard, J.M. 1983. Chemical and physical characteristics of South African coal and a suggested classification system. National Institute for Coal Research, C.S.I.R., Pretoria, Coal 8306, 110pp.

Smith, J.S. 1990. Koornfontein/Komati life extension project. *Geological report.* Koornfontein and Optimum Collieries.

Smith, D.A.M. and Whittaker, R.R.L.G. 1986. The Springs-Witbank Coalfield. *(In: Anhausser, C.R. and Maske, S. Mineral deposits of Southern Africa* – Volume II: 1969-1994).

Stach, E., Mackowsky, M-th., TeichmÜller, M., Taylor, G.H., Chandra, D. and TeichmÜller, R. 1982. Stach's Textbook of Coal Petrology: 3rd ed., Gebr. Borntraeger, Berlin, 535p.

Stratten, T. 1968. The Dwyka glaciation and its relationship to the pre-Karoo surface. *Ph.D. dissertation*. Johannesburg: University of the Witwatersrand, 196p.

Tankard, A.J., Jackson, M.P.A., Eriksson, K.A., Hobday, D.K., Hunter, D.R. and Minter, W.E.L. 1982. Crustal evolution of South Africa–3.8 billion years of Earth history. Springer Verlag, New York, 523p.

Thorpe, A.N., Senftle, F.E., Finkelman, R.B., Dulong, F.T. and Bostick, N.H. 1998. Change in the magnetic properties of bituminous coal intruded by an igneous dike, Dutch Creek Mine, Pitkin County, Colorado. *International Journal of coal Geology*, 36: 243-258.

Van Vuuren, M.C.J. and Quass, F.W. (1982). What happens to coal when a dyke intrudes? Coal, Gold and Base Minerals, Johannesburg, 30: 143-146.

Varga, E. and Horvath, Z. 1986. Coal petrographical characterization of the Mecsek bituminous coal basin, with special reference to the contact metamorphism of coal seams. *Int. J. Coal Geol*., 6: 381–391.

White, R.S. 1997. Mantle plume origin for the Karoo and Ventersdorp flood basalts, South Africa. *S. Afr. J. Geol.,* 100: 271-282.

Whitelaw, H.T. 1998. Hydrothermal alteration of Pb/Zn mineralisation in the Allanridge Formation, Ventersdorp Supergroup, near Douglas, Northern Cape Province, South Africa. *M.Sc. Dissertation*. Bloemfontein: University of the Free State., 177p.